DOCTOR OF PHILOSOPHY

A functional imaging study of the relationship between the Default Mode Network and other control networks in the human brain

Maxwell, Adele

Award date:
2013

Awarding institution:
University of Dundee

DOCTOR OF PHILOSOPHY

A functional imaging study of the relationship between the Default Mode Network and other control networks in the human brain

Adele Maxwell

2013

University of Dundee

A FUNCTIONAL IMAGING STUDY OF THE RELATIONSHIP BETWEEN THE DEFAULT MODE NETWORK AND OTHER CONTROL NETWORKS IN THE HUMAN BRAIN

Adele M. Maxwell, MA (Hons) MSc (Dist)

A thesis submitted on 30.09.2013 in fulfilment of the requirements for the degree of Doctor of Philosophy in Psychology

School of Psychology
Faculty of Arts and Social Sciences
University of Dundee

DECLARATION

I declare I am the author of this research thesis. Unless otherwise stated, all references cited have been consulted by myself. This thesis is a record of work that I have done, and it has not been previously accepted for a higher degree.

Signed: _____ Adele M. Maxwell

Date: 30.09.2013

CERTIFICATE

I confirm, as research thesis supervisor, that the conditions of the relevant Ordinance and Regulations for the Ph.D. degree have been fulfilled.

Signed: _____ Dr. Douglas D. Potter

Date: 30.09.2013

ACKNOWLEDGEMENTS

This thesis is for my Mum, I think I'll have done her proud.

I thank my Mum for believing I could do this and for making me promise I would finish. I also thank my Dad and my brother, Paul, for their support and encouragement, especially over the last few months. Dad, thanks for taking on Mum's role and putting up with my worrying and 'greeting', it turns out you were right: just a wee bit at a time and I'll get there. Paul, maybe now I'll live up to my 'Brains' nickname but don't be sending Shanna and Iona to me with their homework! I also thank Milly for providing a much-needed distraction (in her own way) almost every day when I was writing, and all the rest of my family.

Thank you to Ross for his support and encouragement, and also for developing his domestic skills through tidying, cleaning and running the flat over the past few weeks. Thank you also for pretending to enjoy almost every ready-meal in existence because I didn't have time to cook whilst writing… What can my excuse be now?

I thank all of my friends (you know who you all are). I especially thank the 'Fifers': Donna, Cat, Jen and Katy for their unwavering support, encouragement and laughs throughout all of my time at University and School. I also thank my academic friends: Juliet, Laura and Shirley, for their advice and support; and I must pay special attention to Matina and Carlos for their help throughout technical development work, and for all of the fun and laughs we had when we were in "lab meetings".

Thank you to the School of Psychology and to SINAPSE for the learning tools and financial support offered to me in the final year of my PhD, I am extremely grateful. And, thank you to everyone at the Clinical Research Centre, Ninewells Hospital, Dundee, for their help, advice and expertise during technical development work. Thank you also to Dr Gordon Waiter, University of Aberdeen, for offering his expert opinion during fMRI preprocessing stages and for providing me with a Matlab routine, and also to John-Henry Bruce for his assistance during EEG preprocessing.

I thank my second supervisor, Astrid, who over the years has offered me invaluable advice, encouragement and much-needed moral support at times. Your friendship has meant (and means) a lot.

And, last (but far from least) I owe a special thanks to my supervisor, Doug, who is one of the most patient, calm and understanding people I have ever met. Your enthusiasm, wisdom and support have played a major part in ensuring my completion of this thesis and I cannot thank you enough for the skills and expertise (and patience!) you have helped me develop over the years. I feel extremely privileged to have worked with you Doug, thanks again.

ABSTRACT

The Default Mode Network (DMN) is a large-scale brain network implicated in the control and monitoring of internal modes of cognition. The aim of this research was to investigate DMN function and its relationship to other large-scale cognitive control networks through functional connectivity analysis and analysis of combined electroencephalographic (EEG) recordings. Data utilised across a series of three experiments were obtained from combined EEG-functional Magnetic Resonance Imaging recordings acquired during technical development of a new scanner in the Clinical Research Centre, Ninewells Hospital, Dundee. Analyses were based on data acquired from neurologically healthy participants while they rested with their eyes-closed for five minutes. Following this, participants completed a 14-minute auditory attention task, designed to engage the dorsal and ventral attention networks. In this task, participants responded to task-relevant stimuli (odd/even numbers) and attempted to inhibit their responses to task-irrelevant 'oddballs' (the number '0') and task-irrelevant/distractor stimuli (environment sounds). Experiment 1 utilised the simultaneous acquired EEG-fMRI resting-state data in order to establish whether EEG frequency content in the beta range (13-30 Hz) was a significant predictor of DMN activity (regions of which were identified on an individual basis using functional connectivity analysis). Results were comparable to existing literature showing there is inconsistency in establishing a reliable electrophysiological signature of the DMN. Experiment 1 also employed region-of-interest (ROI)-to-ROI functional connectivity analysis as a method of exploring the functional relationship between the DMN and: (1) a task-positive resting-state network; (2) other commonly identified DMN regions; and (3) regions covering the whole of the cerebral cortex. Results revealed networks were correlated at a component-based level and

challenged existing literature which appears to over-generalise results from exploration of network interaction. Findings also revealed activation of specific DMN components were coupled with down-regulation of sensory-associated cortical regions. Experiment 2 analysed the fMRI data that were obtained from the auditory attention task in order to: (1) determine whether DMN activity was observed when participants were engaged in an externally-directed task; and (2) explore changes in DMN activity associated with increasing task duration. Results revealed that activation of the DMN was prominent and did not vary over three equal time periods. This supports existing research showing the DMN is a continuously active system (whose activity is modulated based on external-task demands). Results also hinted at the existence of possible relationships between the DMN and components of several other large-scale control networks. Therefore, in Experiment 3 potential interactions were explored using ROI-to-ROI functional connectivity analysis of the whole 14-minute time series. Firstly, functional connectivity within the dorsal/ventral attention, executive/frontoparietal control and salience networks was analysed; secondly, the relationships between putative regions of these networks and the DMN were analysed. Overall, results revealed that networks were functionally connected with one another at a component-based level only. This suggests flexible interaction between several large-scale control networks allows neurologically healthy participants to allocate resources to the simultaneous monitoring of the internal and external worlds.

TABLE OF CONTENTS

LIST OF TABLES

LIST OF FIGURES

CHAPTER 1

The history of the Default Mode Network and its contribution to behaviour

The Default Mode Network (DMN) is a neural system that is predominantly involved in internal modes of cognition. The concept emerged following the discovery of increased levels of activity within a discrete set of brain regions during rest/baseline/passive states (control conditions) versus active states (target/goal-driven conditions). This network was, and is to this day, suggested to signify a cognitive state within which individuals are conscious and vigilant but not actively engaged and/or focussed on the external world.

This chapter begins by providing a brief historical overview of resting state research and the concept of task-induced deactivation. The emergence of the DMN as its own research area is also reviewed, with a focus on the work by Gusnard, Raichle and colleagues who launched the DMN into the scientific mainstream. Individual components of the DMN are then considered, along with the role of the DMN in two forms of spontaneous cognition: stimulus-independent thoughts and momentary lapses in attention. Following on from this, two opposing hypotheses (internal mentation versus sentinel) relating to the function of the DMN are discussed. Finally, concerns about the value, interpretability and utility of studying resting state DMN activity are addressed.

1.1. Early observations that the brain does not 'rest' during rest

The notion that cerebral activity persists in the absence of task demands can be dated back to the electrophysiological work of Berger (1931). Berger examined electrical oscillations in the

human brain using electroencephalography (EEG) in a number of different conditions. One of his most interesting observations was that distinct activity patterns could be observed during mental and physical wakeful rest. This led Berger to propose that the brain is not inactive whilst in a passive state and that activations may reflect internal mentation and cognitive processes (Berger, 1931). This concept was further explored in studies of cerebral circulation and metabolism. Using the kety-schmidt nitrous oxide method, whereby a highly lipid-soluble gas (nitrous oxide) was used as the tracer of cerebral and arterial blood flow, Sokoloff, Mangold, Wechsler, Kennedy and Kety (1955) explored differences in cerebral blood flow (CBF) in a resting versus active condition. Unexpectedly, findings showed that CBF did not vary between conditions. Instead, CBF activity was found to be as robust during rest as it was during the completion of a cognitively demanding task (mental arithmetic problems), therefore supporting the idea that the brain is not idle in passive states. Following on from this, in the 1970s, Ingvar collated evidence which revealed that there were consistent patterns of cerebral activity associated with wakeful resting. In one particular study using the intra-arterial xenon 133 technique, as a method of measuring regional cerebral blood flow (rCBF), Ingvar observed a significantly higher distribution of rCBF in frontal areas compared to central, occipital and temporal areas when participants were resting. Ingvar interpreted these results as the brain anticipating simulation of behaviour whilst in an inactive and undisturbed conscious state, and also proposed that a distinct set of frontal regions may contribute to resting state cerebral activity (Ingvar, 1979, 1985).

Together, these findings suggested the brain was not completely inactive during rest and hinted at the idea that a specific network of regions may be implicated in resting state. In subsequent

years, the advancement in high resolution imaging techniques, e.g. positron emission tomography (PET), led to an increase in the number of studies exploring this issue. Experiments were often designed to include a target condition (e.g. test of attention/memory) as well as a resting state condition to serve as a baseline comparison (control condition). Researchers frequently observed differences in brain activation between these conditions, with regions more active in target conditions (than in resting state) categorised as *activations* and regions less active in target conditions (and comparable to resting state) categorised as *deactivations*.

1.2. A brief history of task-induced deactivation

As stated, regional brain activations and deactivations were frequently observed in early PET research. One particular form of task-induced deactivation, which gained considerable interest, was reduced activity within sensory modalities during tests of attention/memory. A study by Haxby and colleagues (1994) investigated the functional organisation of the extrastriate cortex whilst participants completed tasks of selective attention (face matching and location matching). Whilst task-related increases in rCBF were apparent, findings also revealed reduced rCBF within auditory, auditory association, somatosensory and mid-cingulate areas in both of these tasks, relative to a sensorimotor control task. Similar deactivations were found in a study by Kawashima, O'Sullivan and Roland (1995) that explored the neural correlates of cross-modality inhibition (a phenomenon suggesting that sensory modalities, which are uninvolved in task performance, are inhibited to prevent impaired performance). This was done using two selective attention tasks; roughness discrimination and tactile shape matching. Results showed that there were decreases in rCBF within visual cortices during task completion, irrespective of whether participants had their eyes-open or eyes-closed. Both of these studies are interesting because

they were among the first to show that the *location* of deactivations can be *task-related*; namely, reduced activation of sensory modalities in response to specific target stimuli (see also Amedi, Malach & Pascual-Leone., 2005; Buckner, Raichle, Miezin & Petersen, 1996; Drevets et al., 1995; Somers, Dale, Seiffer, Tootell, 1999).

Another form of task-induced deactivation regularly observed was reduced activity in mid-frontal and mid-posterior regions during target conditions. For example, Ghatan, Hsieh, Wirsen-Meurling, Wredling and Eriksson (1995) investigated patterns of cerebral activation associated with a perceptual maze test (a test of visuospatial skills, general intelligence, motor planning, ability to follow instruction). Findings confirmed predicted task-related activations of the anterior cingulate cortex, prefrontal, premotor, primary sensory and visual areas; however, findings also revealed unanticipated deactivations within medial frontal, temporal, parietal, and posterior cingulate areas. Although difficult to interpret at the time these results are interesting because they show that the *location* of deactivation can also be largely *unrelated* to the target condition content. They were also amongst the first to hint that specific cortical components may be implicated in resting state (see also Baker, Rogers, Owen, Frith & Dolan, 1996; Binder et al., 1999).

1.2.1. Task-induced deactivation and the resting brain

Perhaps one of the most revealing insights into resting state activity was a study by Andreasen and colleagues (1995). The authors explored PET CBF associated with autobiographical memory in three conditions: in a target condition participants completed a focused episodic memory task (recall of past experience); in a control rest condition participants were asked to

engage in random episodic thinking (uncensored thoughts about experiences); and in an active control condition participants completed a semantic memory task (objective memory of the outside world). In order to gain insight into the relationship between anatomical activations and internal cognitive processes, participants were asked to describe their thoughts subsequent to the control rest condition. Overall, results revealed each form of episodic memory (focused/random) shared certain functional components, including medial frontal regions and the precuneus/retrosplenial cingulate cortex. Additional activations of the anterior cingulate cortices, thalamus and cerebellum were apparent in the focused episodic (target) condition, and left/right frontal, angular, supramarginal and posterior inferior temporal areas were activated in the random episodic (control rest) condition (see figure 1.1A). Compared to both of these conditions, the left frontal operculum and Broca's area was activated in the semantic (active target) condition (Andreasen et al., 1995). These activations, along with participants' descriptions of their thoughts, led the authors to form one main conclusion: that greater and more widespread activation in the control rest condition was likely to reflect internal retrieval of past events/experiences and/or planning of the future, along with other personal thoughts/experiences. This outcome is noteworthy for two reasons: firstly, at the time it was one of the first studies to map internal modes of cognition and thought processes onto specific anatomical regions during rest; secondly, it revealed that distinct patterns of activations were associated with rest, particularly within medial frontal and posterior areas which were later to be identified as core regions of the brain's DMN.

A large meta-analysis by Shulman et al. (1997) further established a set of brain regions associated with rest. The authors aggregated data from 132 participants across 9 PET CBF

studies. Studies involved different forms of visual information processing tasks, e.g. same-different discrimination, visual search, spatial attention etc. (target condition). Studies also included one of two control conditions: a passive control in which the same stimuli were presented but participants were not given a task, or a visual fixation control in which participants were required to fixate on a central cross. Shulman and colleagues aimed to identify common functional activations/deactivations by directly comparing target versus control conditions, and also by averaging target minus control CBF across each study. Findings revealed a distinct set of areas showing consistent deactivations in target conditions. These areas included the posterior cingulate/precuneus, left/right inferior parietal cortex, left dorsolateral frontal cortex, left lateral inferior frontal cortex, left inferior temporal gyrus, and portions of medial frontal regions (running along a dorsal ventral axis) and the right amygdala (Shulman et al. 1997). The authors considered a number of possible explanations for these deactivations including cross-modal sensory inhibition, inhibitory effects from increased arousal during task completion and suppression of regulatory and habitual response systems to enhance processing ability. On comparison of CBF between target and control conditions, the authors noted that a set of medial and lateral regions consistently exhibited greater activations during passive viewing/visual fixation (see figure 1.1B). Shulman and colleagues proposed that the activations might be representative of ongoing processes such as: (1) unconstrained verbally mediated thoughts: participants may have been thinking verbally about situations/topics/experiences in the rest conditions unrelated to the target condition causing left hemisphere activations, particularly within the left superior/inferior frontal and inferior temporal cortices; (2) Monitoring of external world: participants may have been in an exploratory state whereby they were monitoring the external world for unanticipated or novel events, causing parietal-occipital activations; (3)

Monitoring of the self/body: parietal changes, particularly within the inferior parietal cortex, could have been due to participants monitoring the position, state and orientation of their body; (4) Monitoring of the emotional state: increased activations in areas including the ventromedial frontal cortex and amygdala might have been due to participants monitoring their current emotional state and sensations (Shulman et al., 1997).

A meta-analysis by Mazoyer et al. (2001) produced similar results to the study by Shulman and colleagues (1997). The authors examined the functional anatomy of resting state from a pool of 63 participants across nine PET studies. Participants completed various tasks within target conditions, including mental calculation, spatial working memory, mental imagery etc. During rest participants had their eyes-closed, were asked to relax/avoid movement and avoid any systematic or structured mental activity, e.g. counting. As with Andreasen et al. (1995) participants were also asked to describe their thoughts, cognitive processes following data acquisition. Mazoyer and colleagues contrasted the target conditions to rest using conjunction analysis, a statistical approach that enables the identification of activations across multiple conditions. Their findings revealed activations within a distinct set of regions during rest in comparison to the target conditions. Regions included the bilateral angular gyrus, left anterior precuneus, posterior cingulate cortex, left medial frontal and anterior cingulate cortex, left superior and medial frontal sulcus, and the left inferior frontal cortex (Mazoyer et al. 2001; see figure 1.1C). From this the authors proposed that a large-scale brain network comprised of frontal and parietal areas was actively involved in wakeful rest. Furthermore, when mapped onto participants' thought reports, Mazoyer et al. (2001) suggested that these areas may represent an episodic working memory fronto-parietal network driven by emotions, recall of past experiences

and future planning, that is supervised by an executive left prefrontal network (Mazoyer et al. 2001).

The meta-analyses by Shulman et al. (1997) and Mazoyer et al. (2001) were two landmark studies in generating a common set of brain regions associated with rest. Resting state regions were consistently identified, irrespective of the diverse range of studies included in each analysis. This strengthened the notion that a specific cortical network is activated during idle and passive states, and also addressed concerns about whether resting state is reliable and specific enough to be a dependable control condition (i.e. Frackowiak, 1991; cited in Buckner & Vincent, 2007; discussed in the upcoming section). The retrieval of participants' thought reports in the study by Mazoyer et al. (2001) also echoed the findings of Andreasen et al. (1995), showing that during rest individuals engage in particular forms of cognition (e.g. episodic recall, future planning etc.). These results therefore supported the existence of a relationship between functional anatomy at rest and internal modes of cognition, suggesting it warranted further investigation.

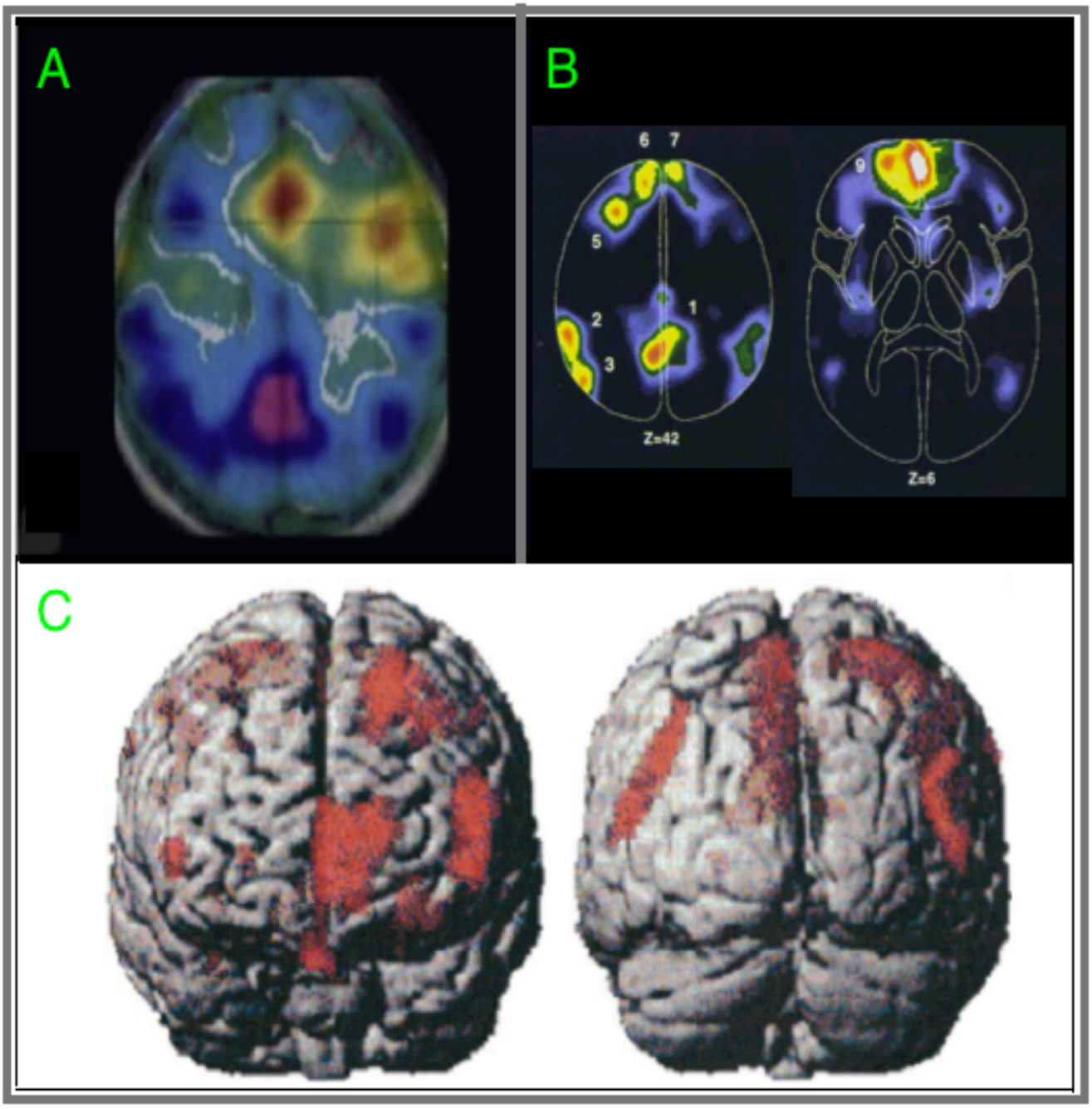

Figure 1.1. Early observed activations during rest. (A) Regions illustrated in blue were activated during a random episodic control rest condition (adapted from Andreasen et al., 1995). (B) Regions active during passive rest states versus target task conditions (adapted from Shulman et al., 1999). (C) 3D renderings of statistical parametric conjunction maps of CBF during resting state (left: front view, right: rear view; adapted from Mazoyer et al., 2001).

1.3. Is resting state an appropriate and reliable control?

Debate over whether resting state should be used as an appropriate control condition was prominent early on within the literature. Many claimed that this cognitive state was far too unrestrained and unspecific to be a reliable control. Hence, brain activations at rest could have been the result of unmeasured cognitive processes, therefore varying unpredictably between participants and reducing its reliability. In a symposium on the exploration of functional anatomy using PET, Frackowiak (1991) summarised concerns by stating: "The best control state is the 'constrained state', which differs from the active state only by the feature you are trying to map. To call a 'free-wheeling' state, or even a state where you are fixating on a cross and dreaming about anything you like, a 'control' state, is to my mind quite wrong" (Frackowiak, 1991; cited in Buckner & Vincent, 2007, p. 1094). Whilst these concerns suggested that researchers should not interpret or deliberate resting state data, others, in particular Raichle (1991), argued that when considered as a baseline, to which other states could be compared, it allowed one to gain perspective and form a complete picture of their data (Raichle, 1991; cited in Buckner & Vincent, 2007; note that modern concerns regarding rest as control/reference data are discussed at the end of this chapter).

1.4. The 'Default mode network' becomes its own research area

In 2001 a series of publications by Gusnard, Raichle and colleagues addressed the debate regarding the use of resting state data as an appropriate control (Gusnard & Raichle, 2001; Gusnard, Akbudak, Shulman & Raichle, 2001; Raichle et al., 2001). In the first of these studies, Raichle et al. (2001) referred to resting state brain activity as a default state, launching the term *default network* into the scientific mainstream. The aim of their study was to define a default

state of the human brain by investigating the uniformity of oxygen extraction fraction (OEF; a quantitative measure of the relationship between oxygen delivery and oxygen utilisation) during wakeful rest. They chose to use average brain OEF as the baseline of activity due to its homogeneity and consistency during wakeful rest, with any deviation signifying changes in neuronal activity; thus, areas exhibiting increased/decreased OEF to average brain OEF were labelled as deactivations/activations respectively. PET metabolic and circulatory measurements were obtained from three participant groups: two groups who rested with their eyes-closed and one group who rested whilst fixating on a central cross. Raichle et al. (2001) predicted that regions previously shown to exhibit reduced CBF in target/task conditions (task-induced deactivated regions identified by Shulman et al., 1997) would show decreases in OEF compared to average OEF, consistent with greater activation during resting state (see figure 1.2 for a schematic representation of this relationship). Findings, however, revealed that the only significant deviations from average OEF were increases in OEF within visual regions when the eyes were closed, consistent with reduced activation of visual areas. Thus, areas identified by Shulman et al. (1997) were not showing greater activation during resting state. From this they concluded that regional decreases in activity typically found in target/task conditions might signify that sustained/on-going activity occurs in the 'default areas' during passive or resting states, and that these decreases become attenuated when resources are temporarily reallocated during goal-directed behaviours. They went on to hypothesise that these 'default' areas are always active when individuals are conscious because they are involved in continuous monitoring of the background or periphery for motivationally significant stimuli.

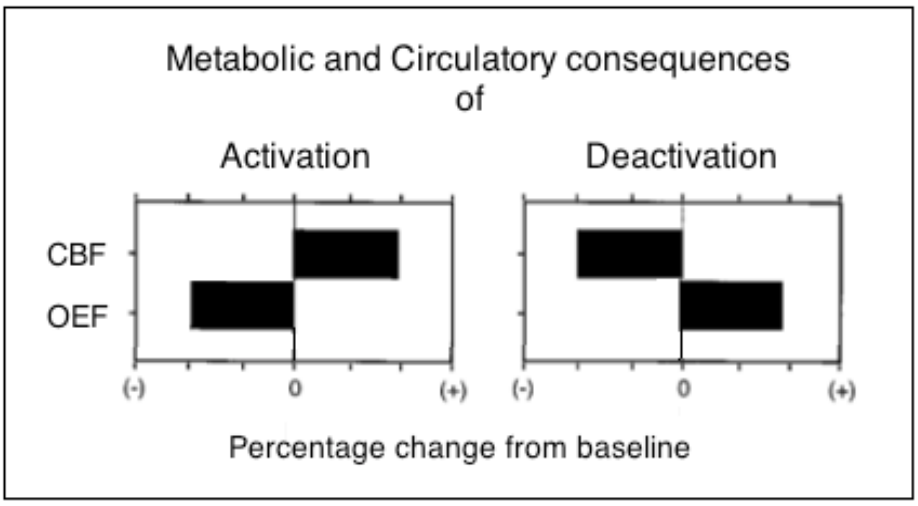

Figure 1.2. Metabolic and circulatory consequences of activation and deactivation from a baseline state. When regions of the brain are activated CBF increases more than oxygen utilisation therefore the OEF decreases (left). When regions of the brain are deactivated oxygen utilisation increases, thus increasing OEF and decreasing CBF (right). Figure modified from Raichle et al. (2001; their figure 3).

In the second of this series of publications, Gusnard et al. (2001) sought to explore the relationship between the medial prefrontal cortex (MPFC), a region shown to be high in metabolic activity at rest (Shulman et al., 1997; Mazoyer et al., 2001) and the DMN. This area was of interest for two reasons: firstly, studies had suggested that the concept of *self* (one's personal awareness of their past, present, and future) is associated with the integrity of the MPFC (e.g. Gallagher, 2000); secondly a wealth of research suggested the existence of a functional distinction between the dorsal and ventral portions of the MPFC (e.g. Ongur & Price, 2000): with the dorsal MPFC implicated in complex cognitive processes, including attention and self-referential/introspectively oriented mental activity; and the ventral MPFC implicated in emotional processes. Using functional magnetic resonance imaging (fMRI), Gusnard and colleagues obtained data from twenty-four participants who completed an attention-demanding self-referential behavioural task. This task involved an internally-cued condition (ICC) in which

participants made judgments towards pleasant vs. unpleasant pictures, and an externally-cued condition (ECC) in which participants judged indoors vs. outdoors pictures. Visual fixation trials were also incorporated into each target condition in order to serve as a control comparison. Overall, findings revealed that increases in activation in the dorsal MPFC in the ICC, was coupled with decreases in activation in the ventral MPFC in both the ICC and ECC. This led Gusnard and colleagues to propose that self-referential mental processes, depicted by increases in dorsal MPFC activity from baseline, represents one of the functions of the default state. In relation to the decreases in activation observed in ventral MPFC, the authors proposed it was consistent with the notion that emotional processing abilities are reduced when participants are required to focus their attention; thus, when completing the self-referential behavioural task. And, from this, whilst acknowledging their findings supported the notion of a dorsal-ventral functional distinction, the authors concluded that both self-referential and emotional processing are two functions subserved by medial prefrontal components of the DMN.

In the final publication by Gusnard and Raichle (2001), the authors reviewed what constitutes a baseline state of the human brain. They attempted to provide an interpretation of what frequently observed brain activations and deactivations might signify in relation to brain function and behaviour (similar to those discussed in this review). They also considered individual components of the DMN and their associated functions, focusing specifically on the medial prefrontal, posterior medial and posterior lateral cortices (reviewed in the upcoming section). Whilst emphasising the value of resting state research, in terms of gaining a better insight into brain function, Gusnard and Raichle also addressed concerns about the unpredictable variation in activity within the resting brain. They proposed that the 'default' functionality of the resting or

baseline state actually constrains brain activity, thus preventing it from varying unpredictably (Gusnard & Raichle, 2001).

Together, this series of publications were the first within the literature to draw attention to the *Default Mode Network* (DMN) and there were several lasting consequences of their work. Firstly, they had collectively distinguished between deactivations specific to the DMN and other commonly observed deactivations (i.e. reductions in sensory modalities during target conditions). Secondly, they had highlighted the value of considering activity in the DMN as a baseline state observed when individuals are conscious, to which other states could be compared, thus enabling researchers to gain better perspective of their data. Thirdly, they addressed the experimental and theoretical implications of studying the DMN, which strengthened the concept that this network exists as a distinct entity and has its own functional and cognitive properties. Fourthly, they had considered what activity within this network of regions might actually represent in terms of the function of the DMN, i.e. the relationship between medial prefrontal regions and self-referential processing (Gusnard et al. 2001): leading to increased interest in the functions subserved by other components of the DMN in order to gain greater insight into this neurobiological system as a whole. And, finally, they had qualified the claim (i.e. Frackowiak, 1991) that resting state brain activity is unpredictable and unrestrained: suggesting that while global activity may be unpredictable, this core network exhibits a consistent regulated pattern of on going activity (Raichle et al., 2001; Gusnard & Raichle, 2001).

1.5. Individual components of the DMN

Although imaging techniques and statistical analyses have varied between studies, a consistent

set of brain regions have been identified as core components of the DMN. Regions broadly include the MPFC and portions of the medial parietal and medial temporal cortices (see figure 1.3). Given that at rest, there is an anatomical connection and interaction between regions, it suggests that the DMN is actually comprised of interacting hubs and subsystems. This view is becoming a prominent feature within the literature and is discussed in more detail in chapter 2; DMN regions as separate entities are discussed in general below. It is important to note that the DMN regions identified in studies of task-induced deactivation will vary depending on the type of experimental task employed. This is because externally-directed goal-driven tasks (i.e. tests of auditory/visual attention) have been shown to elicit more vigorous and widespread task-induced deactivations than internally-directed goal-driven tasks (i.e. introspective thought tasks; see Andrews-Hanna, 2012; Buckner & Carroll, 2007; Spreng, Stevens, Chamberlain, Gilmore & Schacter, 2010 for further discussion).

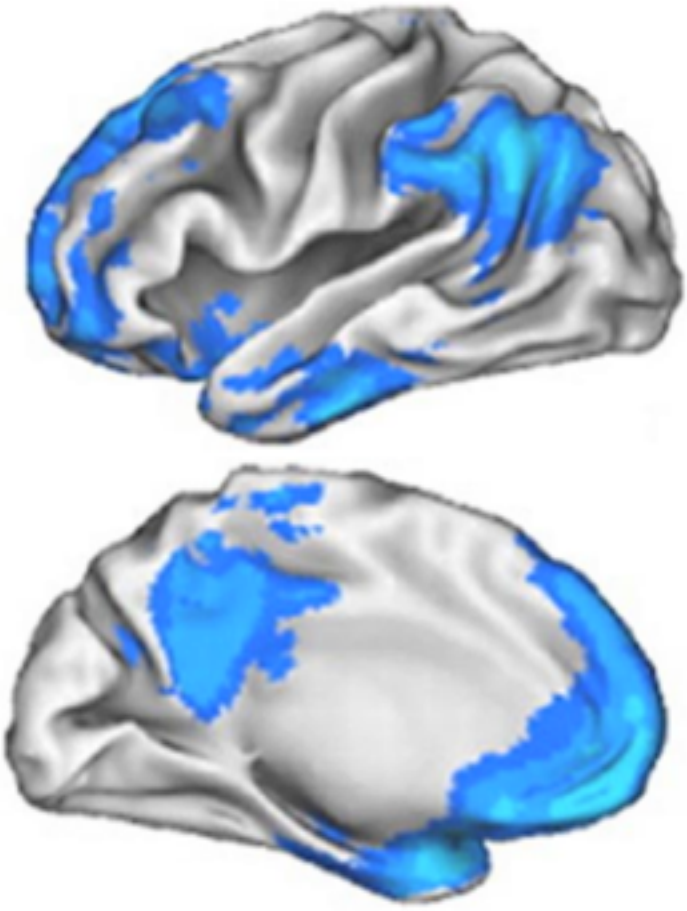

Figure 1.3. Medial and lateral projections of default mode network. Images are based on the reanalysis of Shulman et al's (1997) data by Buckner et al. (2005; adapted by Buckner et al., 2008 where the image is taken from).

1.5.1. Medial Prefrontal Cortex

Widespread activations within the MPFC extending dorsally and ventrally have been implicated in the DMN, with activations encompassing all or parts of Brodmann areas (BAs) 9, 10, 11, 14, 24, 32 (Andrews-Hanna, 2012). Studies have shown that activity within this region of the DMN is highly prominent on tests of self-referential thought and social cognition (e.g. Amodio and Frith, 2006; Benoit, Gilbert, Volle & Burgess, 2010; Gusnard et al., 2001; Knyazev, 2013; Northoff et al., 2006; Sajonz et al., 2010; Whitfield-Gabrieli et al., 2011). Although less

consistently observed, other frontal regions including the inferior, middle, and superior frontal gyri (near BAs 8, 9, 10, 45, 47) have also been identified as portions of the DMN (Andrews-Hanna, 2012).

1.5.2. Medial Parietal Cortex

Medial parietal regions of the DMN include the posterior cingulate cortex (BAs 23, 31) and retrosplenial cingulate cortex (BAs 29, 30; Andrews-Hanna, 2012). At present, there is no agreement about what their precise role in cognition is. However, given they are highly active at rest, particularly the posterior cingulate cortex, it has been suggested that they may be implicated in autobiographical memory or future planning and/or in directing the focus of attention (see Leech and Sharp, 2013 for a review). The precuneus (BA7), intraparietal sulcus, posterior inferior parietal lobule and angular gyrus (near BA 39) also form the parietal portion of the DMN. In some instances the supramarginal gyrus (near BA 40) and temporoparietal junction (near BAs 39, 22), along with areas in close proximity to the middle and inferior temporal gyri, have also been implicated in the DMN (Andrews-Hanna, 2012). Functions associated with activity within these regions generally include self-processing and episodic memory (see Cavanna & Trimble, 2006 for a review).

1.5.3. Medial Temporal Lobe

Hippocampal and parahippocampal regions of the medial temporal lobe have also been implicated with the DMN, with their primary functions being the recollection and formation of new memories (Andrews-Hanna, 2012).

1.6. The role of the DMN in spontaneous cognition (aka mind wandering)

A consistent theme in the literature is the extent to which the DMN is involved in internal modes of cognition. Individuals can focus their attention on an external task (i.e. driving) and can achieve their goal (reaching their destination), but often their mind will have wandered off task several times throughout the process. This is known as *spontaneous cognition/mind wandering* and in fact research suggests that an individual can spend 30-50% of their day engaged in covert thoughts unrelated to the immediate task at hand (Klinger & Cox, 1987; Killingsworth & Gilbert, 2010). Although this may be due to a number of factors, e.g. the monotonous nature of the task, individual differences in brain characteristics etc., it suggests that the mind does not have to be in an undisturbed state (i.e. at rest) for it to engage in spontaneous introspective processes (e.g. daydreaming, episodic thinking, imaginative thoughts etc.). Perhaps as expected, though, the frequency and extent of which the mind engages in these processes increases substantially during rest or low-level attention/passive states. These observations have inspired research into the relationship between the DMN and varying forms of spontaneous cognition.

1.6.1. Two forms of spontaneous cognition and their relationship to the DMN

Over the years a number of experimental approaches have been developed in order to investigate the relationship between spontaneous cognition and the DMN. In target conditions, spontaneous cognitive processes are typically assessed behaviourally through the monitoring of reaction times, response accuracy and/or through self-report measures. Easier and/or practiced tasks in these conditions typically yield a higher percentage of spontaneous thoughts (see Smallwood & Schooler, 2006 for a review) and greater DMN activity (e.g. McKiernan, D'Angelo, Kaufman & Binder, 2006). In rest/passive conditions they are typically assessed retrospectively through the

use of self-report questionnaires (e.g. Delamilliure et al., 2010; for a review of measures see Smallwood & Schooler, 2006). These measures, when used in conjunction with neuroimaging methods, i.e. electroencephalography (EEG) or fMRI, enable insight into when and/or where these processes might occur in the human brain and how they relate to the DMN. The following sections review two forms of spontaneous cognition frequently investigated in the literature: stimulus-independent thoughts, and momentary lapses in attention, with a specific focus on how they are studied, individual differences in tendencies to engage in them, and how they relate to the DMN.

1.6.1.1. Stimulus-independent thoughts

Stimulus-independent thoughts (SITs; also referred to as *task-unrelated thoughts* within the literature) are defined as off-task episodes or covert thoughts about something unrelated to the task at hand/immediate sensory environment (Gilbert, Frith & Burgess, 2005). They are most commonly identified using a probing method, which involves participants signalling when they are experiencing a SIT. This self-report measure requires participants to be highly aware of the content of their internal cognitive experiences; thus prior to participation, they often undergo training to enhance their ability to detect and report SITs. There is, however, a limitation of this measure: that the use of a probe can often interfere and/or halt the SIT (Buckner, Andrews-Hanna & Schacter, 2008). Despite this, a number of researches have shown that these spontaneous thought processes are prominent features of the brain's resting state and thus related to the DMN (e.g. Christoff, Gordon, Smallwood, Smith & Schooler, 2009; Giambra, 1989, 1995; Gusnard et al., 2001; McGuire, Paulesu, Frackowiak & Frith, 1996; Pope and Singer, 1976;

Posner and Rothbart, 1998; Preminger, Harmelech & Malach, 2011; Teasdale, Proctor, Lloyd, Baddley, 1993; Teasdale et al., 1995).

In a series of behavioural studies by Antrobus and colleagues (1966, 1968, 1970) it was found that SITs were prevalent in both passive resting state and target task conditions, including tests of short-term memory, target detection etc. Results also revealed a negative correlation between the occurrence of SITs and task demands, with reductions in the frequency of SIT reports as a function of increasing task demands (see also Andrews-Hanna, Reidler, Huang & Buckner, 2010; Fransson, 2006). Imaging studies have also revealed insight into the relationship between the frequency of SITs and brain activity. For example, an early PET study by McGuire et al. (1996) reported a significant positive correlation between the number of SITs reported and CBF within the MPFC, an identified region of the DMN. Similarly, a series of publications by Binder and McKiernan (Binder et al., 1999; McKiernan et al., 2006; McKiernan, Kaufman, Kucera-Thompson & Binder, 2003) reported a relationship between the frequency of SITs and activity within the DMN, showing that increased SITs were associated with increases in the magnitude of DMN activity across the cortex.

Perhaps one of the most insightful studies into the relationship between SITs and the DMN was a study by Mason et al. (2007). The authors investigated the relationship between the frequency of SITs in different task conditions and their relationship to DMN. They were also interested in individual differences in mind wandering tendencies. Participants were trained on tests of verbal and visuospatial working memory, and the occurrence of SITs reported in this block was compared to a novel variant of the test and also to resting state. Findings revealed participants

reported an increased number of SITs during rest than during the practiced or novel blocks. Participants also reported a significantly higher number of SITs during the practice block, compared to the novel block. In order to determine whether there was a relationship between the DMN and SITs frequency, Mason et al. investigated changes in the fMRI Blood Oxygen Level-Dependent (BOLD) signal (discussed in detail in chapter 2) across blocks (practice/novel/rest). Changes in this signal revealed that the recruitment of DMN areas (most notably the left/right MPFC, left/right superior frontal gyri, anterior/posterior cingulate/precuneus and bilateral areas of the insula), were significantly higher during the resting and practice blocks, in which the highest number of SITs were reported, compared to other the novel block (see figure 1.4A). In addition to exploring this, the authors were also interested in investigating individual differences in tendencies to engage in SITs. They assessed this using a daydream/internal processes frequency scale, in which participants were asked how frequently they tended to daydream, and in what situations etc. Interestingly, results revealed a significant positive correlation between frequency in the occurrence of SITs (as measured by the scale) and the magnitude of activity within the DMN activity (see figure 1.4B). This activity was most pronounced bilaterally across the medial prefrontal cortex, precuneus/cingulate and other DMN areas, with no DMN components showing a negative correlation with SIT frequency scores. Both of these findings supported the role of the DMN in this form of spontaneous cognition respectively.

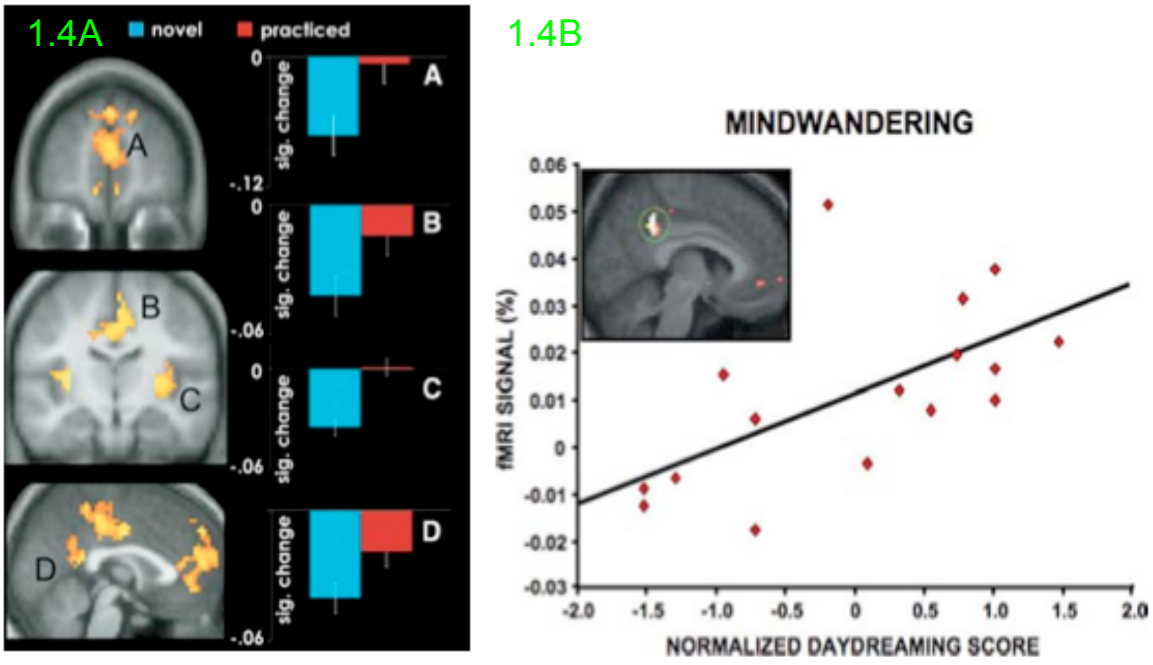

Figure 1.4. Results of Mason et al. (2007). (1.4A) Activation of default mode network regions during practiced versus novel blocks. Graphs shown the mean signal change in DMN regions across participants in practiced (red) compared to novel blocks (blue). (A) Left medial prefrontal cortex (B) Bilateral cingulate (C) Right Insula (D) Left posterior cingulate. Adapted from Mason et al. (2007). (1.4B) The relationship between frequency in SITs and BOLD signal in the posterior cingulate region of the human brain as identified by Mason et al. (2007; adapted from Buckner et al., 2008).

1.6.1.2. Momentary lapses in attention

Momentary lapses in attention (MLA) are another form of spontaneous cognition that have received considerable interest in the literature. The occurrence of these brief 'gaps' in attention is most common when individuals are focussing their attentional resources on the external world. In laboratory settings, they can be measured behaviourally by giving participants an attention demanding task and monitoring their reactions times and/or task performance. They can also be measured neurophysiologically, by looking for changes in stimulus-evoked activity. Recent investigation has given rise to the notion that there is an interaction between internal cognitive

processes (the DMN) and processes implicated in attending to events in the external world (external attention).

It has been proposed that task-induced deactivations in the DMN are associated with the reallocation of processing resources toward behaviourally relevant stimuli (McKiernan et al., 2003). A number of researches suggest that DMN activity is attenuated rather than diminished during the transition of states (i.e. the shift in the monitoring of the internal vs. external world), and also that activity within some portions of the DMN (albeit at a lower magnitude) is observed alongside task-specific activations (e.g. Fransson, 2006; Greicius, Krasnow, Reiss & Menon, 2003; McKiernan et al., 2003; Raichle et al., 2001). A particularly informative fMRI study by Greicius and Menon (2004) explored DMN activity during rest and a low-level attention task. In their study, participants completed a task consisting of seven rest epochs in which they were required to fixate on a central cross (measure of DMN); and six sensory epochs of auditory and visual stimuli in which they were required to concentrate on the stimuli (measure of attention). Greicius and Menon hypothesised that, given the low-level attentional demands of the sensory epochs, activity within the DMN would not be interrupted. Findings confirmed this hypothesis, showing that in the majority of participants DMN activity persisted in both the epochs of the task. Furthermore, findings also revealed that sensory-evoked responses were attenuated in participants with the strongest DMN activity. These results supported the proposals that the DMN is constantly active, and infer that there is an interaction between internal cognitive processes and processes implicated in attending to events in the external world.

Leading on from the study by Greicius and Menon (2004), Weissman, Roberts, Visscher and

Woldorff (2006) aimed to investigate the brain mechanisms involved in MLA. Brain activity was measured using event-related fMRI (discussed in chapter 2) and the occurrences of MLA were measured by monitoring participants' reaction times on a global/local selective-attention task (whereby MLA were defined as slow reaction times towards behaviorally relevant stimuli). Findings revealed that a reduction in activity within anterior cingulate and right prefrontal regions was observed just prior to the occurrence of MLA. Results also showed that during MLA increases in activity within DMN regions (including frontal, parietal and posterior cingulate areas) were apparent (see figure 1.5). Not only are these results interesting because they provided insight into patterns of brain activity associated with MLA, particularly within the DMN; they also suggested that MLA involve a shift in attention from the external to the internal world (see also Li, Yan, Bergquist & Sinha, 2007).

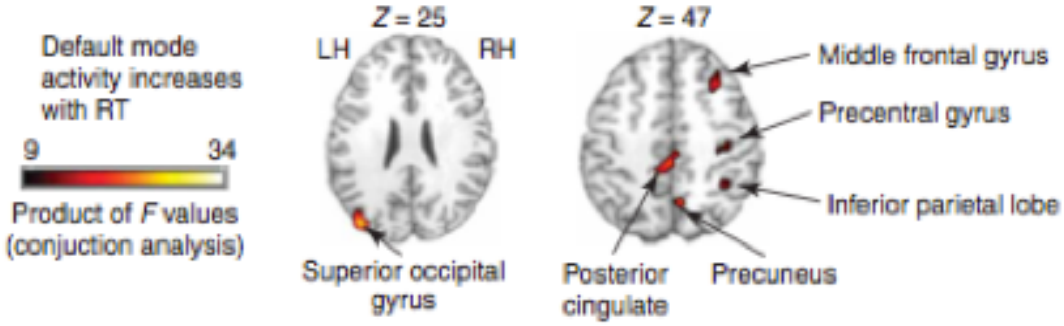

Figure 1.5. Statistical map showing regions of the default mode network that are active during momentary lapses in attention. Adapted from Weissman et al. (2006).

1.7. The function of the default mode network: Two competing hypotheses

As shown thus far, activity within the DMN is most apparent during rest/passive states. The fact that brain activations within the DMN remain, albeit at lower levels during goal-directed tasks,

suggests that this system is not simply 'switched off' when processing demands increase. Instead, it infers that activity within the DMN is *modulated*. Whilst this provides insight into the neurobiology of the DMN during internal-/external-directed states, it does not aid understanding of the *function* of the DMN. A review article by Buckner and colleagues (2008) sought to address this by formulating two opposing hypotheses outlined in the following sections (*1.7.1-1.7.2*).

1.7.1. The sentinel hypothesis

The *sentinel hypothesis* proposes that the DMN maintains a general low-level focus of attention in order to monitor the external environment for significant and/or unpredictable events (Buckner et al., 2008; Gilbert, Dumontheil, Simons, Frith & Burgess, 2007; Gilbert, Simons, Frith & Burgess, 2006; Hahn, Ross & Stein, 2007). It has been argued that DMN activity associated with SITs might not necessarily represent periods of mind wandering and instead may represent the capture of attention from events occurring in the external world (Gilbert et al., 2007). Hence, in this instance, the DMN could be considered as a low-level attention system. It has also been argued that studies reporting increased activity within some or all DMN regions during externally-directed goal-driven tasks support the role of the DMN in the monitoring of the external world. For example, Shulman et al. (1997) as previously discussed, noted that task-induced deactivations were prominent when target conditions involved the processing of visual stimuli. Similarly, a study by Gilbert and colleagues (2007), which aimed to discriminate between brain activity associated with stimuli-oriented thoughts (cognitive processes provoked by stimuli) and stimulus-independent thoughts, revealed that increases in MPFC activity were correlated with reduced reaction times on a trial-by-trial basis. These findings were echoed by

Hahn et al. (2007) who reported that increases in activity within DMN regions, including the posterior cingulate cortex and superior temporal gyrus, were correlated with enhanced performance on target detection trials in which target stimuli were presented in unexpected locations compared to predictable locations. It has also been shown that increased levels of activity within the DMN can be observed following brief projections of task-unrelated stimuli during the maintenance period on tests of working memory (e.g. Anticevic, Repovs, Shulman & Barch, 2010). Each of these results lend support to the role of the DMN in the monitoring and processing of the external world; thus concurring with the sentinel hypothesis of DMN function.

1.7.2. The internal mentation hypothesis

The *internal mentation* hypothesis suggests that the DMN supports internal mentation alone and is largely detached from the external world (Buckner et al. 2008). In comparison to the sentinel hypothesis, a greater wealth of research appears to support this hypothesis, with evidence coming largely from two sources: firstly, studies investigating the role of the DMN in spontaneous cognition have shown that it is particularly active when participants engage in SITs and MLAs (see section *1.6.1* for previous discussion); secondly, studies investigating the neurobiology of internally-directed mental processes and social cognition have reported overlap between regions implicated in each of these processes and regions of the DMN. These processes, including autobiographical memory, theory-of-mind, envisioning the future and moral decision-making (see figure 1.6), are considered in turn below.

Autobiographical memory is the recollection of episodes from past experiences. It encompasses a complex set of operations, some of which include episodic memory, self-reflection, emotion,

attention and executive functions (Svoboda, McKinnon, Levine, 2006; Tulving, 1985). The results of the study by Andreasen et al. (1995), previously discussed in section *1.2.1*, were the first to highlight a relationship between autobiographical memory and the DMN, revealing that greater activation of DMN regions was associated with episodic memory compared to semantic memory. In 2009, a meta-analysis by Spreng, Mar and Kim further established this relationship. Their analysis included several PET and fMRI studies, all of which had measured brain activity during tests of autobiographical memory. Findings revealed a network of regions that overlapped significantly with DMN regions, including the MPFC, dorsal/ventral prefrontal cortex, medial parietal regions, hippocampal formation and several other regions. More recently, Ino, Nakai, Azuma, Kimura and Fukuyama (2011) reported that regions showing increased and decreased activation on tests of autobiographical memory (relative to rest) corresponded significantly with several portions of the DMN (see also Addis, Wong & Schacter, 2007 (figure 1.6A); Andrews-Hanna et al., 2010a; Hayes, Salat, Verfaellie, 2012; Sestieri, Corbetta, Romani & Shulman, 2011; Svoboda et al., 2006).

Theory-of-mind relates to the ability to understand and manipulate the beliefs and intentions of others, in order to predict their actions (Spreng et al., 2009). A study by Saxe and Powell (2006) showed that DMN regions, including the left and right temporoparietal junction and posterior cingulate cortex, responded selectively to stories about a character's thoughts, but not when the stories involved other socially relevant information about the character. Results also revealed that the MPFC elicited the same activation response to all story conditions (see also Saxe, Carey & Kanwisher, 2004). These findings supported previous results revealing that the MPFC (specifically the dorsal MPFC), posterior cingulate cortex/retrosplenial cortex and a region in

close proximity to the temporoparietal junction (again DMN regions) were active whilst participants encountered a story about an event based on a character's beliefs, in comparison to a story about events captured by a camera (Saxe & Kanwisher, 2003; see figure 1.6B; see also Dodell-Feder, Koster-Hale, Bedny & Saxe, 2011; Hagmann et al., 2008; Lombardo et al., 2010; Rabin, Gilboa, Stuss, Mar & Rosenbaum, 2010; see meta-analysis by Spreng et al., 2009; see Mars, 2012 for a review).

Studies measuring cognitive and the neural correlates of envisioning the future have shown that during these tasks participants often form personally-related scenarios that contain sensorial and emotional content (D'Argembeau & Van der Linden, 2004). And, that neural substrates associated with this form of cognition (overlapping with DMN regions) can include the anterior prefrontal cortex, ventral medial prefrontal cortex, medial temporal lobe and posterior cingulate cortex (Addis et al., 2007: see figure 1.6C; D'Argembeau et al., 2010; Okuda et al., 2003; Race, Keane & Verfaellie, 2011; Schacter and Addis, 2009; Szpunar, Watson & McDermott, 2007; Verfaellie, Race & Keane, 2012). Although research pertaining to the role of the DMN in moral dilemmas/decision making is somewhat sparse, studies have shown that when participants are required to make *personal* moral judgments, activations within the anterior medial prefrontal cortex, dorsolateral prefrontal cortex and posterior cingulate cortex, are apparent, thus suggesting some involvement of the DMN (Greene & Haidt, 2002; Greene, Sommerville, Nystrom, Darley

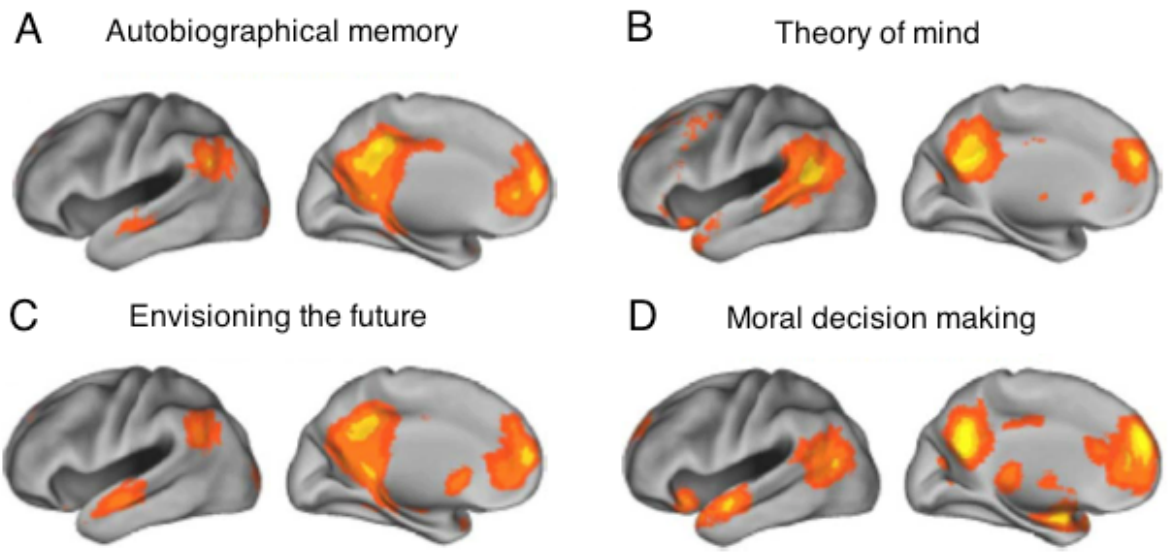

Figure 1.6. Default mode network regions implicated in autobiographical memory, theory of mind, envisioning the future and moral decision-making. (A) Autobiographical memory. (B) Theory of mind. (C) Envisioning the future. (D) Moral decision-making (all images are adapted from Buckner et al., 2008). Data shown in A and C are from Addis et al. (2007; adapted by Buckner et al., 2008). Data in is from an analysis using a paradigm from Saxe and Kanwisher (2003; adapted by Buckner et al., 2008). Data in D is from Greene et al. (2001; adapted by Buckner et al., 2008).

& Cohen, 2001: see figure 1.6D; Moll, Zahn, de Oliveira-Souza, Krueger & Grafman, 2005; Reniers et al., 2012) which in turn suggests a role of the DMN in this domain of social cognition.

1.7.3 Are the sentinel and internal mentation hypotheses really mutually exclusive?

Whilst the sentinel and internal mentation hypotheses suggest two competing functions of the DMN, an emerging literature has sought to investigate whether these two hypotheses are as mutually exclusive as they appear.

A study by Andrews-Hanna et al. (2010b) aimed to disambiguate between the internal mentation and sentinel hypotheses by contrasting DMN activity across three conditions. Conditions varied in the direction (internal/external) and scope of attention (focal/broad). Thus, in conditions designed to provoke external attention, participants passively viewed a central cross and

responded when a brief flicker was detected in either central (focal) or peripheral (broad) locations. In contrast, in a rest condition, designed to provoke spontaneous cognition, participants passively viewed a central cross. Results revealed increased fMRI BOLD signal across multiple regions within the DMN, including the anterior MPFC and posterior cingulate cortex in the rest condition compared to the other conditions. In a second experiment the authors sought to explore the content of participants' spontaneous thoughts. They did this by analysing responses from a post-scanning questionnaire which participants were unaware of prior to participation. Results revealed that half of the allotted time during the rest condition was spent thinking about one's personal past and future. Together, both of these results lend support to the internal mentation hypothesis only, showing that activity within the DMN is largely associated with internally-directed processes.

Contradictory findings, offering support to both of theses hypotheses, were found in a recent study by Stawarczyk, Majerus, Maquet and D'Argembeau (2011). The authors investigated the neural correlates of various forms of internal mental experiences occurring during a sustained attention to response task (SART). This task (also known as a go/no go task) involved participants responding to numerical stimuli (go) and withholding their response when the number 3 was presented (no go). During task completion participants were required to report their internal mental experiences, in terms of task-relatedness and stimulus-independency, through the use of thought probes. Four categories of internal mental processes were possible: (1) task-related and stimulus-dependent (the participant's attention was focused on the task and the stimuli); (2) task-related and stimulus-independent (the participant was thinking about other aspects of the task, i.e. their performance, and not directly on the stimuli); (3) task-unrelated and

stimulus-dependent (the participant's attention was focused on the external experimental environment (i.e. lighting/temperature) but not on the task; (4) task-unrelated and stimulus-independent (the participant was experiencing thoughts unrelated to the task; Stawarczyk et al., 2011). Results revealed that activations within DMN regions varied with respect to the internal mental process reported: activations of the MPFC, posterior cingulate cortex/precuneus, and posterior inferior parietal lobe, were correlated with reports task-unrelated thoughts; and midline components revealed an increase in activity when stimulus-independent thoughts were reported. Most interesting was that, in addition to showing an increase in response to both the task-unrelated and stimulus-independent dimensions, MPFC and PCC also exhibited an increase when task-related and stimulus-dependent processes were reported. This led the authors to conclude that these midline portions of the DMN are implicated in both internally- and externally-directed processes in different ways; thus suggesting the internal mentation and sentinel hypotheses are, in fact, not mutually exclusive.

1.8. An argument against the study of resting state DMN

Other than dated caveats surrounding the study of resting state (i.e. Frackowiak, 1991; cited in Chadwick & Whelen, 1991), a commentary by Morcom and Fletcher (2007) is one of the few papers within the literature that expresses concern about the value, interpretability and utility of studying resting state DMN. They suggest that observation and inference made from resting-state research has no privileged status as a measure of brain functioning, a proposal they base on two main arguments. Firstly, if consistent patterns of brain activity are identified as being associated with rest, it does not automatically infer that individuals are in a 'default' mode, because there is no explicit task to measure this. This is to an extent a valid point, and it is

important to note that most researches report correlational relationships between psychological processes (i.e. resting state cognition) and brain activity. Thus, it does not mean that the activity is causally or directly related to behaviour; instead, perhaps a small number of neurone may generate thoughts that may be undetectable. Secondly, Morcom and Fletcher (2007) argue that a sufficient insight into the processing functions of specific brain regions, in order to understand the relationship between brain and behaviour, can be gained through experimental task manipulation alone rather than the study of rest. One would argue, however, that given individuals spend a lot of their time directed away from the external environment and engaged in their internal world (i.e. autobiographical recall, envisioning the future etc.), the analysis of resting-state DMN brain activity may provide a greater insight into these processes as compared to strict experimental control. Furthermore, as discussed throughout, several studies have provided insight into types of internal cognition (e.g. self-referential mental thoughts/autobiographical recall) that is associated with activation of the DMN, and also in some instances subcomponents of the DMN (see also Buckner & Vincent, 2007; Raichle & Snyder, 2007).

CHAPTER 2

Measuring the Default Mode Network

The previous chapter focused on the history and functions associated with the Default Mode Network (DMN). It showed that the concept of the DMN, and subsequent research into it, emerged following controversy over what a control or resting state was. Chapter 1 also concentrated on the repeated observation that frontal, medial parietal and medial temporal regions were consistently identified in studies of task-induced deactivation, and also in studies of resting state brain activity. This led to the characterisation of these regions as belonging to the DMN, which in turn allowed for inference to be made about the functions of DMN and its contribution to behaviour.

2.1. Overview of aims of chapter

This chapter reviews the multiple approaches that have been used to study the anatomy, metabolic activity and interplay between DMN regions. It begins by briefly addressing the use of blocked and event-related designs in defining the anatomy of DMN. The characterisation of the DMN through spontaneous low frequency neuronal oscillations is then addressed and followed by discussion of the proposal that the DMN is a *task-negative* network, which shows temporal anti-correlation to a *task-positive* network. Functional connectivity measures of the DMN are then considered and following on from this, two methods that are commonly employed within the literature, as means of analysing the DMN using the blood-oxygen-level dependent response, are discussed. These include independent component analysis and region-of-interest

seed-based correlation. Understanding the DMN through electrophysiological measures, i.e. electroencephalography, and the integration of this technique with functional magnetic resonance imaging, is then reviewed. Finally, the measures employed in this research thesis are addressed.

2.2. Measuring the anatomy of the DMN: Blocked and event-related designs

As stated in chapter 1, initial investigation into the DMN was predominantly done using positron emission tomography (PET). The advantage of this technique was that it provided an absolute measure of oxygen consumption and cerebral blow flow. However, limitations of it were its low resolution, short half-life of radioactive tracers and that it only allowed for the measurement of the DMN in *blocked* designs. In blocked design studies, data from extended blocks of active tasks are compared to data from extended blocks of passive tasks/resting state. A measure of task-induced deactivation/DMN activity is then obtained by averaging across blocks respectively. This design has a number of advantages: firstly, averaging across a number of blocks attains an adequate signal-to-noise ratio; secondly, it is suited for the detection of regions-of-interest in particular tasks (see Petersen & Dubis, 2011 for a review). The meta-analyses by Shulman et al. (1997) and Mazoyer et al. (2001), along with the study by Raichle et al. (2001; as discussed in chapter 1), were among the first to provide insight and initial interpretation into the anatomy and tonic state of DMN structures based on the analyses of *blocked* PET measures.

The anatomy of the DMN has also been defined by analysing the brain's response to individual stimuli or 'events'. In *event-related* functional magnetic resonance imaging (fMRI) studies, stimuli can be presented rapidly, at random time intervals and in a random intermixed order. Subsequently, measures of task-induced deactivation in response to stimuli, and/or the

magnitude of DMN activity occurring during inter-stimulus rest periods, are obtained. Interestingly, there is similarity between approaches (blocked versus event-related) in defining the anatomy of the DMN using fMRI; figure 2.1 shows similar deactivations of frontal, posterior and parietal nodes of the DMN in an experiment utilising a blocked design (figure 2.1A) and an experiment employing an event-related design (figure 2.1B). Overall, this is noteworthy as it demonstrates that neuroimaging techniques (PET and fMRI), along with experimental design (blocked and event-related), are comparable on their estimates of the anatomy/neural regions implicated in the brain's DMN.

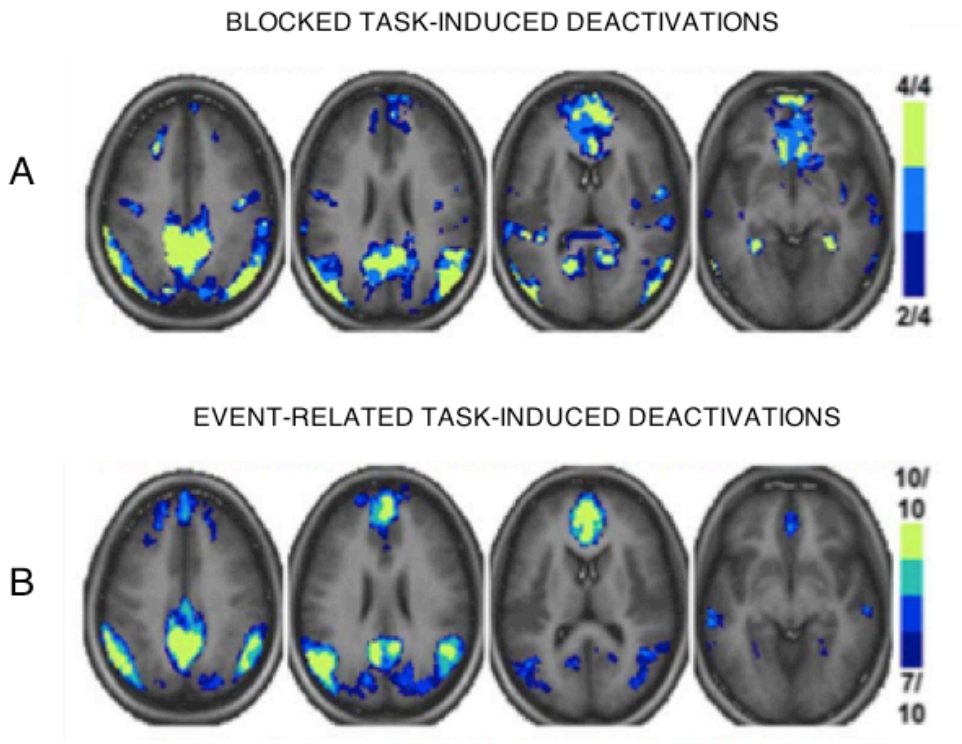

Figure 2.1. The default mode network defined by blocked and event-related fMRI task-induced deactivations. (A) Meta-analysis of blocked fMRI data originally adapted from Shannon (2006) by Buckner et al. (2008), revealing frontal, medial and parietal deactivations during a blocked-design active visual task. (B) Meta-analysis of event-related fMRI data by Shannon (2006), adapted by Buckner et al. (2008), showing similar deactivations in an event-related design. The colours (scales to the right) reflect the number of data sets showing the significant effects within each image (Images adapted from Buckner et al., 2008).

It should be noted that the DMN can also be measured by analysing interleaved resting epochs from mixed blocked/event-related designs. Studies have reported qualitative and quantitative similarities between the functional connectivity of the DMN in resting epochs from mixed designs to residuals derived from continuous resting state data (e.g. Fair et al., 2007). However, certain caveats are associated with this: firstly, if rest periods are relatively short in duration, there may be limitations in the range of frequencies that can be used to extract information for certain analyses (i.e. functional connectivity analysis); secondly, resting state activity within blocked conditions/epochs of the design may be affected by previous task states (see Fair et al., 2007 for further discussion; see Petersen & Dubis, 2011 for a review of designs).

2.3. Resting state fMRI

Resting state fMRI (rs-fMRI), as the name suggests, is the functional imaging of the brain at rest using fMRI. Due to the high spatial and temporal resolution of fMRI, this technique has proven valuable in the localisation and separation of the DMN from other networks that are apparent in the resting brain (discussed in section *2.3.2*). One of the main objectives of rs-fMRI is to obtain a measure of synchronous neuronal activity. This is done by measuring oscillatory activity and common variance of the fMRI blood oxygen level-dependent (BOLD) signal in different regions of the brain (the BOLD signal is an indirect measure of regional brain activity based on the interplay between neuronal oxygen consumption and blood flow; see Buxton, 2009 for a comprehensive review). One of the main assumptions of rs-fMRI is that temporal similarity between BOLD signals demonstrates they are constantly in communication with one another, and therefore form a functional network (Murphy, Birn, Bandettini, 2013). Subsequently, in the resting brain, rs-fMRI has been used to measure: spontaneous low frequency (<0.1 Hz)

fluctuations in the BOLD signal; the relationship between resting state networks; and connectivity strength and patterns between brain regions. These measures are considered in turn below.

2.3.1. Spontaneous low frequency fluctuations in the BOLD signal

The BOLD signal has been extensively used to investigate how task performance modulates brain activity. However, this type of analysis largely ignores the fact that the brain maintains a constant level of activity at rest, as shown by low frequency oscillations in the BOLD signal (<0.01 Hz). These fluctuations are particularly evident across regions that show a temporal synchrony to one another. They are thought to represent activations that are intrinsically generated by the brain, which are not attributable to any input/output, and are also independent of cardiac and respiratory processes. Subsequently, the term *spontaneous low frequency (SLF) fluctuations*, has been coined in reference to the presence of these unprompted/unconstrained BOLD signal oscillations during rest (see Fox & Raichle, 2007 for a review).

Biswal and colleagues (1995) were the first to investigate SLF fluctuations in the BOLD signal at rest. Using a blocked-design, the authors acquired data whilst participants took part in a bilateral finger tapping condition and a resting state condition, in which they were instructed to refrain from performing any cognitive, language or motor tasks. The authors identified a seed region within the left somatomotor cortex and then calculated the correlation coefficient between the BOLD time course of this seed to regions covering the whole of the cortex (the BOLD time course refers to a single seed/voxel's response signal over time). Findings revealed during rest there was a high level of temporal correlation between time courses of SLF BOLD signals,

revealing that the left somatomotor cortex was highly positively correlated with homologous areas in the contralateral hemisphere. These results were interesting at the time because they were among the first to reveal that functionally related brain regions exhibit synchronous and correlated SLF fluctuations at rest. Since its publication, the existence of synchronous SLF fluctuations has been confirmed and extended to other sensory systems, including visual, auditory and higher order somatosensory processing areas (e.g. De Luca, Beckmann, De Stefano, Matthews & Smith, 2006; Greicius et al., 2003; Smith et al., 2009; Van de Ven, Formisano, Prvulovic, Roeder & Linden, 2004: Yeo et al., 2011). Researchers have also shown that correlated SLF fluctuations can also be observed in areas known to support attention function during active tasks (i.e. frontal and parietal regions; Laufs et al., 2003b) and in regions which typically show task-induced deactivation, e.g. medial prefrontal, and posterior regions (Greicius et al., 2003; Greicius & Venon, 2004).

2.3.1.1. The DMN characterised by spontaneous low frequency fluctuations in BOLD signal

As discussed in chapter 1, in positron emission tomography (PET) significant deviations from mean oxygen extraction fraction suggests that the DMN is the baseline state of the human brain (Raichle et al., 2001). In fMRI the DMN is characterised by SLF BOLD signal fluctuations in a group of anatomically distinct, but operationally synchonised, areas (Fox et al., 2005; Fox, Snyder, Zacks, Raichle, 2006a; Fransson, 2005, 2006). Figure 2.2 illustrates an example of this within two components of the DMN: the medial prefrontal cortex (MPFC) and the posterior cingulate cortex (PCC), over a 5-minute eyes-open visual fixation rest period. As shown, there is spontaneous modulation of the BOLD signal in each region over time. This measure of the DMN has proven useful in exploring the relationship between the DMN and other networks that

are active in the resting brain (discussed in the upcoming section). Furthermore, it has also allowed for investigation into functional connectivity; that is the pattern/strength of correlated activity between DMN regions over time (discussed in section *2.3.4*).

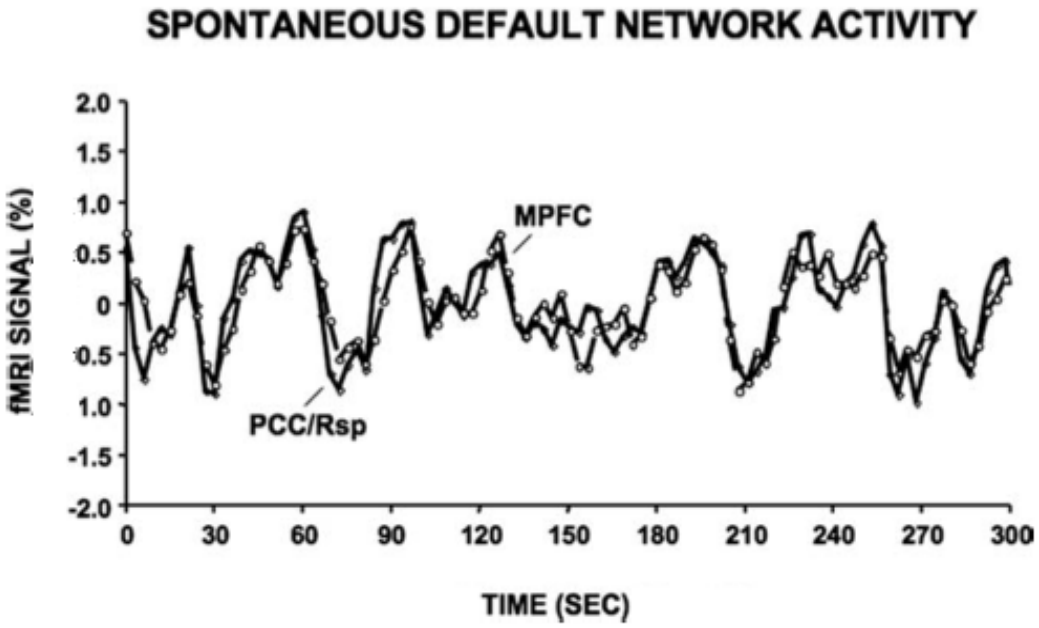

Figure 2.2. Spontaneous low frequency fluctuations in the Blood Oxygen-Level Dependent signal within the medial prefrontal cortex and posterior cingulate cortex components of the default mode network in a 5-minute resting state condition. This illustration is based on data published in Fox et al. (2005) that was adapted by Buckner et al. (2008), and reveals that spontaneous increases and decreases in activity are correlated between these two DMN regions (adapted from Buckner et al., 2008)

2.3.2. SLF BOLD fluctuations reveal that the DMN is a 'task-negative' network

As reviewed in chapter 1, during attention-demanding tasks DMN regions, including the MPFC, PCC, and medial and lateral parietal areas, are deactivated. Conversely, a distinct set of frontal and parietal regions, whose precise location and magnitude of activation depends on the type of task, are activated (Andreasen et al., 1995; Mazoyer et al., 2001; Shulman et al., 1997). Based on this task-related dichotomy between networks in active conditions, and that correlated SLF

fluctuations are observed in task-related and unrelated areas at rest (e.g. Laufs et al., 2003; Greicius et al., 2003; Greicius & Venon, 2004), researchers have sought to investigate the extent to which a task-related dichotomy is apparent in the resting brain.

A particularly insightful rs-fMRI study by Fox and colleagues (2005) examined correlations in SLF BOLD fluctuations in six predefined regions-of-interest (ROIs). BOLD signal was obtained across three different rest conditions: visual fixation on a crosshair; eyes-closed; eyes-open with no visual fixation. ROIs were chosen based on their activation response during attention-demanding tasks; they included three regions that typically exhibit task-induced activation, and three regions that typically exhibit task-induced deactivation. The authors labeled these regions as *task-positive* (activations) and *task-negative* (deactivations) respectively. Task-positive regions included the intraparietal sulcus (IPS), frontal-eye-field (FEF) regions of the precentral sulcus and the middle temporal region (MT+); and task-negative regions included the MPFC, PCC and the lateral parietal cortex. In their analysis, correlation coefficients between the BOLD signal time course for each seed and all other brain voxels were computed; this was done on a single participant basis. This allowed for the measure of positive and negative correlations between each seed and the rest of the brain (see figure 2.3A). Correlation coefficients for each participant were then converted to *z-scores* in order to combine results across the participant group and assess statistical significance. This enabled the authors to determine regions that were significantly correlated or anti-correlated to each of the six seed regions (see figure 2.3B). Finally, using conjunction analysis, the six correlation maps were combined in order to determine the common pattern of BOLD response across participants. Overall, findings revealed that SLF fluctuations in the BOLD signal were correlated between regions within each network

(task-positive/task-negative). Findings also revealed that the task-positive and task-negative networks were anti-correlated with one another, and that these results were apparent in each condition (eyes-open visual fixation, eyes-closed, eyes-open no fixation). These results supported the notion that the task-related dichotomy between networks, observed in attention-demanding tasks, is also represented intrinsically in the resting brain (figure 2.3C). This study is interesting for a number of reasons: firstly, it revealed a dynamic interplay between two spatially distributed networks in the brain that are differentially implicated in behaviour; secondly, it extended the concept of the DMN to be considered as a *task-negative* network; thirdly, it showed that regions within each network are correlated, despite being supplied by different vascular territories and anatomically distant from one another; and finally, it showed additional networks are observed in the brain at rest, thus spurring research to investigate the existence and functionality of other networks.

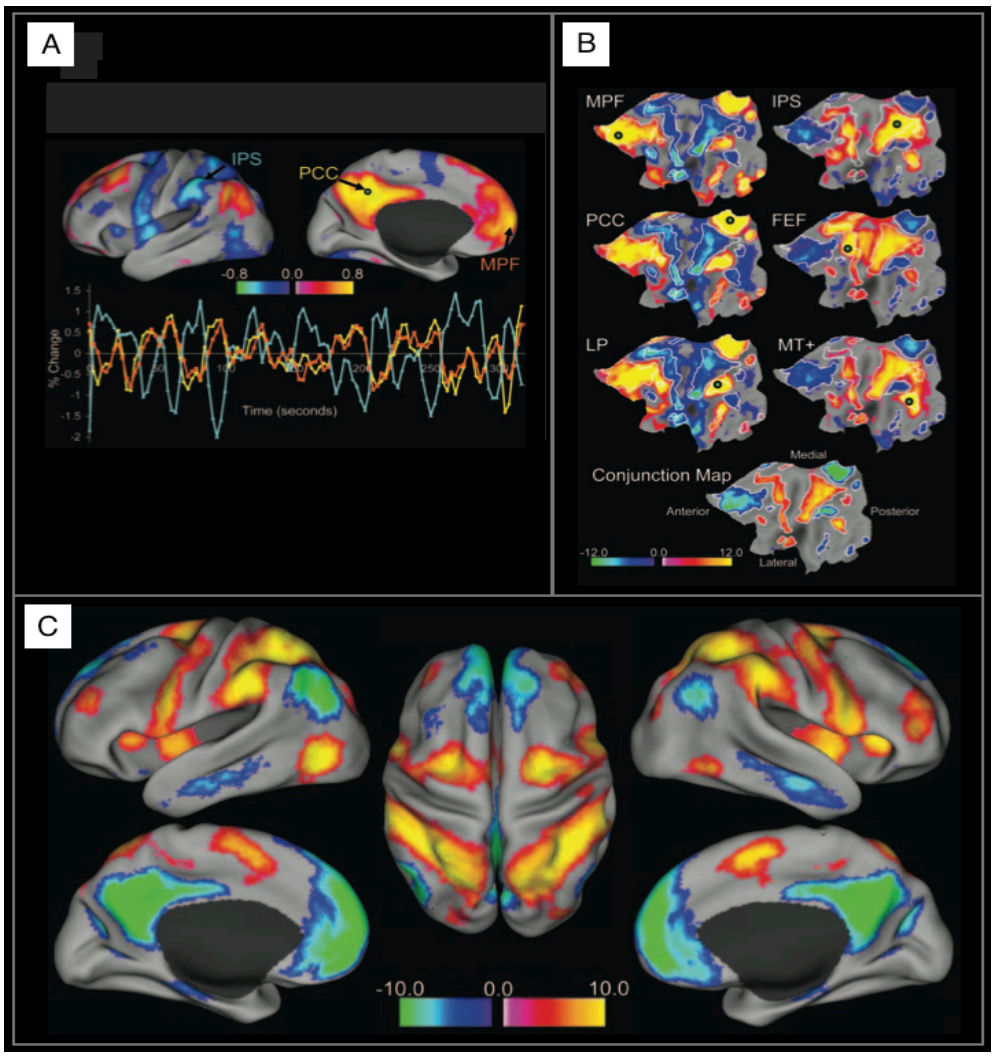

Figure 2.3. Analysis results of Fox et al. (2005). (A) Intrinsic correlations between the task-negative seed region PCC and all other brain voxels; revealing that a region positively correlated with PCC is MPFC (task-negative region, illustrated in orange), and a region negatively correlated with PCC is IPS (task-positive region). (B) Population based z-score maps showing regions significantly positively or negatively correlated with seed ROIs. Task-negative ROIs are displayed on the left and task-positive ROIs are on the right. The lower conjunction map (lower map) is an average, this included regions that were significantly (anti/)correlated with five out of the six ROIs. (C) Anti-correlated networks in the resting brain. Task-positive ROI are significantly anti-correlated with task-negative ROI, illustrations are lateral and medial views of the left-hemisphere (left) and right-hemisphere (right) and a dorsal view (centre). Adapted from Fox et al., 2005.

The existence of a task-positive network in the resting brain has been proposed to reflect extroceptive attentional orienting during rest. Similar to the functions associated with the DMN

in terms of the sentinel hypothesis (as discussed in chapter 1), activity within the task-positive network is thought to reflect the maintenance of attention in order to monitor and respond to significant and/or unpredictable events in the external world. This has led to the functional relationship between the two networks being described as low frequency toggling between externally-directed and internally-directed attentional processes at rest. Thus, increasing levels of activity in one network, as determined by SLF BOLD fluctuations, is coupled with down-regulation of the other; therefore varying the degree of attention focus (Fransson, 2005; see figure 2.4 for an idealised illustration of this relationship). A second proposal by Sonuga-Barke and Castellanos (2007) is that the temporal linkage between the task-positive and task-negative networks suggests they could be two components of a single more complex network. However, this concept, which the authors do not develop in their paper, has been overlooked within the literature and as such researchers appear to consistently discuss them as being pseudo-independent of one another.

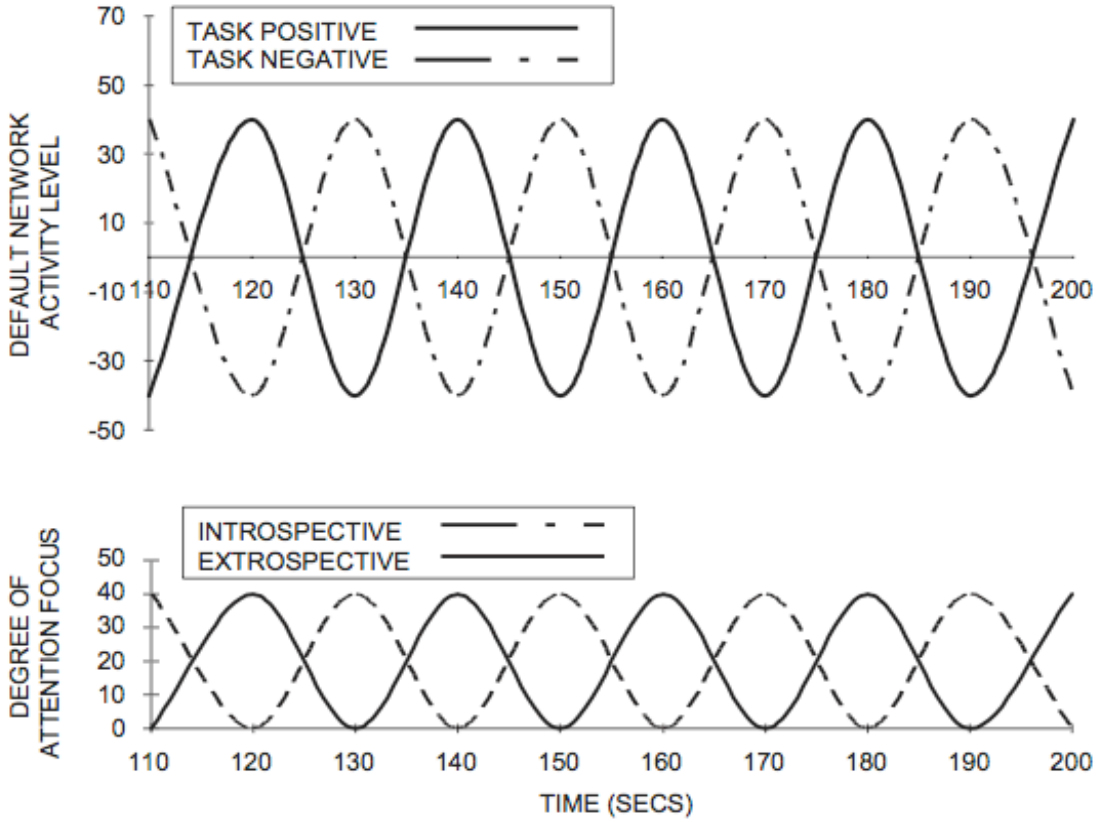

Figure 2.4. An idealised representation of the anti-correlated task-positive and task-negative/default mode networks. The illustration reflects the low frequency toggling between internally- externally-directed attentional modes and was adapted from Sonuga-Barke & Castellanos (2007). As shown, increase in the task-positive network is associated with a decrease in the task-negative network from baseline; this is reflected in the lower image, which shows suppression in introspective/internally-directed processes as a function of increased extrospective/externally-directed processes. The authors assumed that cycles of activity within the networks were 0.05 Hz, thus the inter-peak gaps between each network was 10s. The units of activity and extent of external/internal focus was arbitrary (adapted from Sonuga-Barke & Castellanos, 2007).

2.3.3. An important note on anti-correlated SLF BOLD fluctuations between networks

Although briefly addressed in chapter 1, it is important to re-emphasise here that despite saying that networks are *anti-correlated* with one another, this does not mean that activity in one network is associated with a complete 'shut down' of the other network. Instead, activity is *modulated* as a function of changes in SLF BOLD signal fluctuations between networks. This is the case for the study of differences in BOLD signal fluctuations in networks in rs-fMRI (i.e.

comparing resting state task-positive and task-negative networks, Fox et al., 2005) and task-based (i.e. comparing the task-positive/negative networks in active and resting state conditions, Fransson, 2006).

Fransson (2006) highlighted the *modulatory* effect of one network on the other by acquiring fMRI data from a 10-minute eyes-open visual fixation condition (resting state data) and also from a sequential two-back verbal working memory task. Of particular interest was whether directing the brain's resources towards a goal-directed attention-demanding task would attenuate intrinsic activity in the DMN. Further to this, Fransson explored the effects of task performance on the two anti-correlated networks in the brain, as identified by Fox et al. (2005). The spatial and temporal characteristics of SLF BOLD signal fluctuations associated with each condition were assessed using three analyses. Firstly the patterns and strength of correlated activity within and between the task-positive and task-negative networks were assessed using region-of-interest correlational analysis approach (see section *2.4.3* for description of this method). Two sample t-tests were then used to compare intrinsic activity between conditions. Secondly, power spectral densities were computed as estimates of the amount of BOLD signal fluctuation within the DMN: power spectral densities are computations of the average power in a signal over a particular frequency band; in this instance the frequency interval of interest was 0.012-0.15 Hz. Finally, independent component analysis (see section *2.4.2*) was employed to compare intrinsic DMN activity between the two conditions. Overall, findings from the three different analysis approaches were consistent in showing that SLF fluctuations in the BOLD signal in DMN regions were apparent in the active condition, albeit *down-regulated* compared to the resting state condition. Analysis of the behavioural data also revealed that high accuracy rates on the

active task, coupled with low ratings on the presence of stimulus-independent thoughts, were concurrent with this finding. Not only are these results interesting because they complement previous studies showing the relationship between attention-demanding tasks and task-induced deactivation (as discussed in chapter 1), they are key in demonstrating that intrinsic activity in the brain (as depicted by SLF BOLD signal fluctuations) is not completely shut down and abolished during task completion, and is instead *modulated*.

2.3.4. Functional connectivity and the DMN

Functional connectivity has been defined as the synchronisation of neurophysiological events in two or more spatially remote anatomical regions (Friston, Frith, Liddle & Frackowiak, 1993). Understanding the interplay between brain regions and how they are connected functionally has provided insight into the relationship between the brain and behaviour. In functional connectivity studies, measuring the temporal correlation between SLF BOLD signal fluctuations in discrete anatomical regions (see figure 2.5) has not only aided understanding of the DMN and the architecture of the healthy brain (Martuzzi, Ramani, Oiu, Rajeevan, Constable, 2010; Gillebert & Mantini, 2013), it has also revealed that the brain is organised into distinct, correlated, functional-anatomic networks, that often mimic task-induced patterns of activity (i.e. the task-positive network; Fox et al., 2005; Fox and Raichle, 2007; Smith et al., 2009).

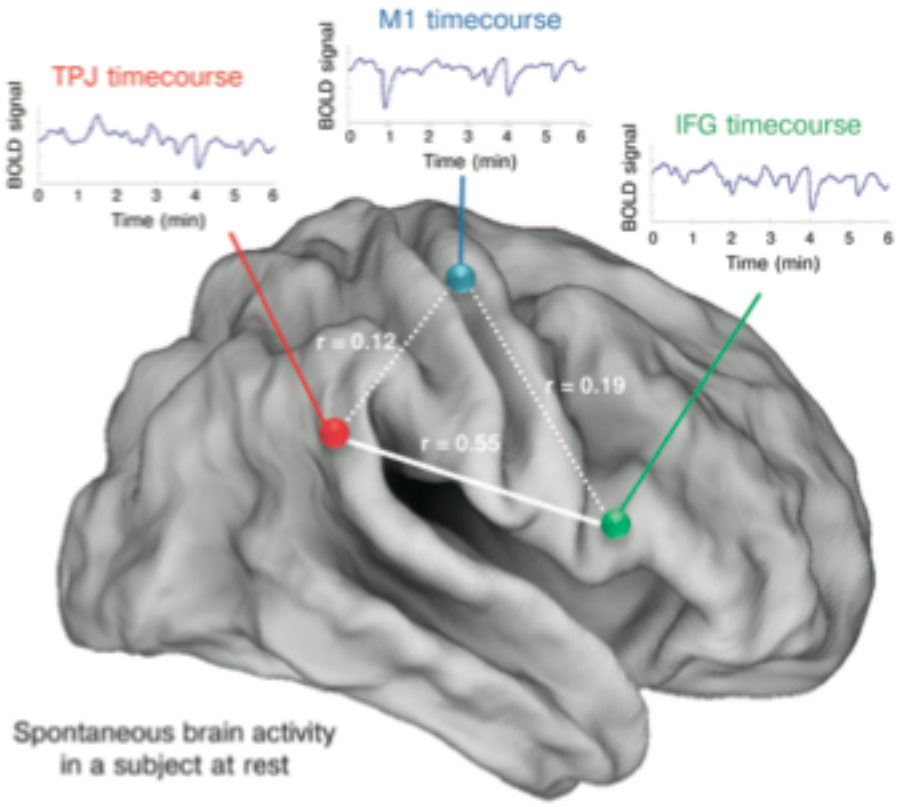

Figure 2.5. The basic principles of resting-state fMRI functional connectivity. SLF BOLD signals are compared between multiple brain regions. Assessing the BOLD time course by temporal correlation can be significant ($p<.05$; solid white line) or not significant ($p>.05$; dashed white line). Selective correlations can be used to determine how different brain networks (i.e. DMN and task-positive network) are related to each other. For illustration purposes only, the example above shows that the right temporoparietal junction (TPJ) and right inferior frontal gyrus (IFG) are significantly correlated with each other; but neither region is correlated to the primary motor cortex (M1). Adapted from Gillebert and Mantini (2013).

Greicius and colleagues (2003) were the first to apply resting state functional connectivity to the DMN. Based on functional imaging studies that had revealed insight into the anatomy and activity of specific DMN regions, the authors were particularly interested in three issues: (1) the functional connectivity between DMN regions; (2) cognitive processes subserved by the DMN; and (3) whether DMN activity was modulated during simple sensory processing tasks. In order to address each of these questions, Greicius et al acquired fMRI data whilst participants

completed three conditions in a standard blocked design. Conditions included a visuospatial working memory task, in order to define task-induced deactivated regions; a visual processing task, which involved passive viewing of a checkerboard; and a face-processing task, which the authors chose not to include in their analysis. Participants also completed an eyes-closed 4-minute resting state condition in which they were instructed not to think of anything in particular. The authors hypothesised that resting-state connectivity should reveal at least one component of the DMN, which in turn should be connected (or partially connected) to other DMN regions. A second hypothesis was that DMN connectivity should be similar in the resting and passive viewing conditions. And, thirdly Greicius et al proposed if the active condition provoked suppression in DMN activity, then DMN regions would be anti-correlated with regions showing task-induced activations. ROIs were identified based on their activation/deactivation during the working memory task. Subsequently, task-related ROIs included the left and right ventrolateral prefrontal cortices (VLPFC) and the right dorsolateral prefrontal cortex (DLPFC) and DMN ROIs included the posterior cingulate cortex (PCC) and ventral anterior cingulate cortex (vACC). Overall, findings revealed that the vACC was significantly positively correlated to two DMN regions, including the MPFC and the PCC. Findings also revealed that the PCC was positively correlated to eight DMN regions identified in the meta-analysis by Shulman et al. (1997). Given that in 2003 the DMN was a relatively new research area, these results provided convincing evidence for the existence of the DMN. Furthermore, results revealed that connectivity maps for the PCC (DMN region) and vACC (task-related region) were almost identical in the resting state and passive viewing conditions; suggesting that the DMN is unaffected by low-level attending demanding tasks. Finally, it was found that each of the three task-related ROI (left/right VLPFC, right DLPFC) were anti-correlated with the PCC during rest.

Together, these findings are interesting not only because at the time they provided evidence for the existence of a tonically active DMN, but because they were among the first to show that the DMN is comprised of several functionally correlated areas, showing a temporal anti-correlation to regions that are typically active during active task conditions.

The initial study of resting-state functional connectivity in normal populations (e.g. Greicius et al., 2003), coupled with the fact that resting state has no behavioural demands, has generated interest into to the exploration of functional connectivity of the DMN in the ageing and the developing brain (i.e. Damoiseaux et al., 2008; see Power, Fair, Schlaggar & Petersen, 2010 for a review), in cases of neurological damage (e.g. Carter et al., 2010; Vanhaudenhuyse et al., 2010) and in several psychiatric and neurological disorders (see Broyd et al., 2008; Buckner et al., 2008; Zhang & Raichle, 2010 for reviews). Furthermore, as briefly mentioned in chapter 1, resting-state functional connectivity studies in normal populations have also revealed the DMN is intrinsically organised into several distinct subsystems that converge on hubs (Buckner et al., 2008). To illustrate this, Buckner et al. (2008) plotted the overlap of functional correlations across three separate DMN seed regions using data from Andrews-Hanna et al. (2007). Seed regions included the dorsal and ventral medial prefrontal cortices (dMPFC/vMPFC) and the hippocampal formation (HF+). As shown in figure 2.6A, the posterior cingulate cortex (PCC), vMPFC and intraparietal sulcus (IPS) show a complete overlap across the map, suggesting these regions are best described as anatomical hubs to which all other DMN regions are correlated. Figure 2.6A also illustrates that the HF+ and dMPFC are correlated to the hubs but not to one another, suggesting they form independent subsystems within the DMN and may be responsible for different forms of DMN-associated cognition, i.e. autobiographical recollection (Buckner et

al., 2008; see also Buckner et al., 2009; Hagmann et al., 2008; Vincent et al., 2006).

More recently, a study by Andrews-Hanna et al (2010a) explored the functional architecture of the DMN by examining intrinsic connectivity and clustering properties of eleven midline and lateral DMN regions. Consistent with previous findings, and based on having the highest graph analysis measures (see Lee et al., 2012b for a review of graph-analysis and clustering techniques), the authors identified a core set of hubs, including the PCC and aMPFC, to which all other DMN regions were functionally correlated. The authors then applied hierarchical clustering analysis to the remaining nine DMN regions, revealing that regions could be separated into two anatomically distinct subsystems. Subsystems included a dMPFC subsystem, comprised of the dMPFC, temporoparietal junction, lateral temporal cortex, and the termporal pole; and, the MTL subsystem, which included the vMPFC, posterior inferior parietal lobule, retrosplenial cortex, parahippocampal cortex and the HF+ (see figure 2.6B). Furthermore, results revealed a dissociation between DMN subsystems and cognition; with the dMPFC subsystem implicated in self-referential thoughts, i.e. when participants were considering their present mental states; and the MTL subsystem associated with using episodic memory in order to construct a mental scene (see also Uddin, Kelly, Biswal, Castellanos & Milham, 2009). These results are noteworthy because they suggest the DMN can be functionally segregated into distinct subsystems, which in turn, can allow for the disentanglement of certain cognitive processes associated with the DMN into specific component processes.

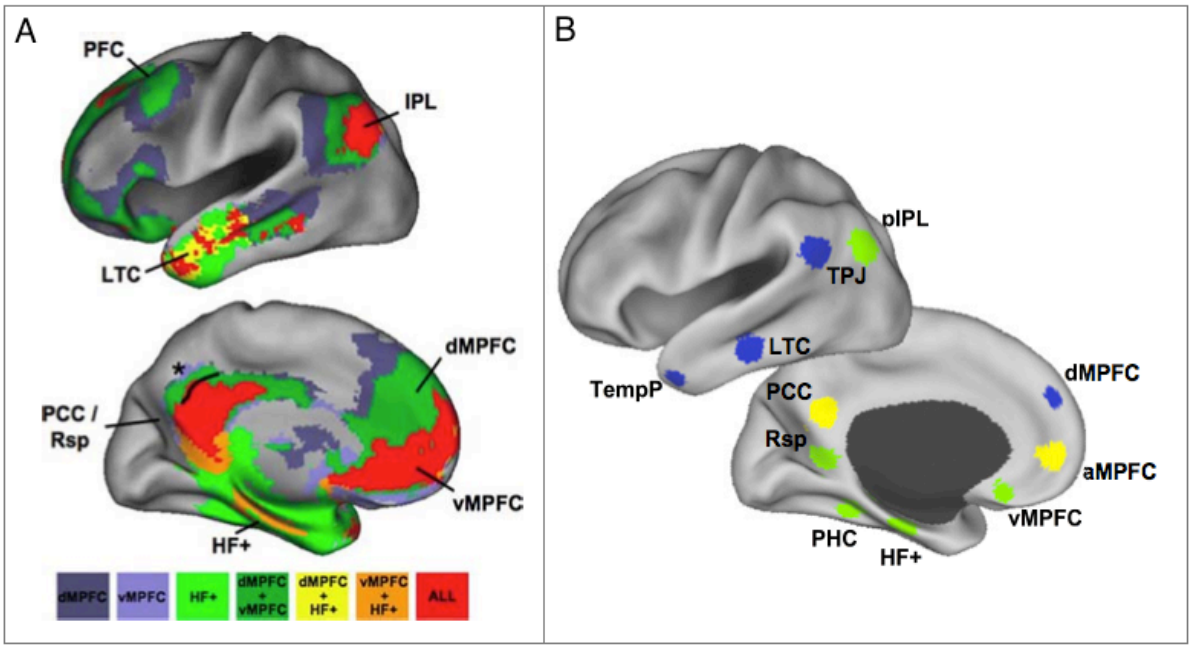

Figure 2.6. Hubs and subsystems within the default mode network identified using functional connectivity analysis. (A) Anatomical subsystems and hubs as identified by Buckner et al., (2008). The map was produced by seeding three separate regions of the DMN and plotting the overlap of functional correlations (threshold for each map is r = .07). The authors point out that in this analysis the precuneus does not appear as part of the DMN in this analysis (represented by the asterisk; adapted from Buckner et al., 2008). (B) DMN hubs and subsystem areas projected onto a surface template. Areas in yellow represent to two anatomically distinct hubs; areas in blue form the dMPFC subsystem; and areas in green form the MTL subsystem. Adapted from Andrews-Hanna et al. (2010).

2.4. Analysing the functional connectivity of the DMN using the BOLD response

Thus far, this chapter has defined functional connectivity in terms of how it has provided an insight into the DMN and behaviour, and how this has been used to assess the architecture of the DMN. This section discusses how functional connectivity within the DMN is analysed. It focuses on two distinct methodological approaches that are commonly employed in the literature: independent component analysis and region-of-interest seed based correlations.

2.4.1. A short note of the importance of preprocessing

BOLD signal preprocessing typically aims to correct for slice-dependent time shifts, eliminate

systematic odd-even slice intensity differences (due to interleaved acquisition without gaps) and correct for movement and other nuisance regressors (Lee, Smyser & Shimony, 2012b). Nuisance regressors are typically related to cardiac or respiratory processes, which, when corrected for, improves the signal- (i.e. BOLD fluctuations) to-noise (i.e. head movement, scanner artifact etc.) ratio. Addressing BOLD signal noise is crucial for functional connectivity analysis in order to avoid obtaining spurious correlations that are based on non-neuronal events. Inadequate or partial removal of noise significantly decreases the validity of the analysis and thus increases the probability of making a type 1 error (incorrect rejection of a true null hypothesis; Whitfield-Gabrieli & Nieto-Castanon, 2012). Both whole-brain regression (as employed by Fox, Zhang, Snyder & Raichle, 2009) and component-based noise correction (employed by Chai, Nieto-Castanon, Ongur & Whitfield-Gabrieli, 2012) have been shown to be reliable methods for reducing noise and increasing specificity of correlations. In whole-brain regression, the average time-course of the entire brain is regressed out; in component-based noise correction voxel-specific noise effects are estimated from the variability in BOLD responses within noise ROIs and then regressed out (Whitfield-Gabrieli & Nieto-Castanon, 2012). In addition to this, spurious correlations, as a result of inadequate head motion correction, has also been shown to affect the reliability and validity of functional connectivity measures, leading to new strategies being introduced to account for such effects (Power, Barnes, Snyder, Schlaggar, & Petersen, 2012).

2.4.2 Independent component analysis

Independent component analysis (ICA) is a model-free data-driven approach to analysing functional connectivity of the DMN, which, unlike other techniques, is not reliant on a priori

predictions. Thus, although ICA is useful for exploratory analyses, it is not suitable for hypothesis-driven analyses. ICA works by analysing the entire set of fMRI BOLD signals and then decomposing data into spatially/temporally independent components. In turn, these components represent the spatiotemporal signatures contained in the data (Lee et al., 2012b). This approach has proven useful in revealing that in addition to the DMN, several other networks exist in the resting brain (i.e. Beckmann, De Luca, Devlin & Smith, 2005; Damoiseaux et al., 2006; De Luca, Beckmann, De Stefano, Matthews & Smith, 2006).

2.4.3. Region-of-interest seed-based analysis

In comparison to ICA, region-of-interest (ROI) seed based analysis is reliant on a priori predictions; it is a hypothesis-driven approach. It involves extracting the BOLD signal-intensity time course from a seed region and correlating the average time course of voxels within that seed to those of all other brain voxels (e.g. Biswal et al., 1995; Fox et al., 2005; Greicius et al., 2003). Using a probability threshold (i.e. <0.05) then determines voxels that are significantly positively/negative correlated with that seed (Ganzetti & Mantini, 2013). This approach has proven useful in assessing the pattern and strength of correlation within and between resting-state brain networks (Fox et al., 2005; Fransson, 2005, 2006).

2.4.4. Convergence across methods

Despite differences in each approach (ICA versus ROI seed-based analysis) direct comparison has revealed they are consistent in identifying regions of the DMN. For example, Long and colleagues (2008) compared the use of ICA, ROI correlation analysis and regional homogeneity analysis (evaluation of synchronisation between the BOLD signal time course of a voxel and its

neighbours; see Zang et al., 2004 for a review) in identifying DMN activity in eyes-closed resting-state data. The authors were also interested in validating components of the anti-correlated task-positive network as identified by Fox et al. (2005). Overall findings revealed convergence across approaches in identifying the MPFC, PCC and bilateral inferior parietal cortex components of the DMN, as well as regions within its anti-correlated task-positive network (see also Bluhm et al., 2008; Greicius, Srivastava, Reiss & Menon, 2004; Rosazza, Minati, Ghielmetti, Mandelli, & Bruzzone 2012; Van Dijk et al., 2010).

2.5. Electrophysiological measures

In recent years there has been increased electrophysiological exploration into the DMN using electroencephalography (EEG). EEG's sub-millisecond temporal resolution allows for the detection of spontaneous changes in electrical activity across different neuronal populations in the brain (see Jorge, van der Zwagg & Figueiredo, 2013 for a review of EEG). Subsequently, this technique has been used to examine DMN activity in terms of very slow EEG frequencies (Helps et al., 2008; Vanhatalo et al., 2004) and traditional bands of EEG frequencies. In particular, Chen, Feng, Zhao, Yin & Wang (2008) compared the spatial distribution (the spread of electrical potential over the head) and spectral power (the strength of signal across different frequencies) of eyes-closed and eyes-open resting state EEG data. In their study participants were asked to relax and keep their eyes-closed for 3-minutes, followed by their eyes-open for 3-minutes (this order remained constant across participants): during this time EEG was recorded from 128 scalp sites. The authors reported low-frequency prefrontal delta (0.5–3.5 Hz) was enhanced in the eyes-closed state compared to eyes-open. Reductions in EEG field power were reported for frontocentral theta (4-7 Hz), anterior-posterior alpha-1 (7.5–9.5 Hz), and posterior

alpha-2 (10–12 Hz), along with posterior beta-1 (13-23Hz) between the eyes-closed to the eyes-open state. In comparison, high frequency prefrontal beta-2 (24-34 Hz) and prefrontal gamma (35-45 Hz) exhibited a similar distribution of EEG field power and showed no change between eyes-closed to eyes-open. Correlational analyses, in order to determine the relationship between spectral field powers and condition (eyes-closed versus eyes-open), revealed there was a significant association between conditions for the delta and theta bands only. This study is interesting as it reveals that EEG can be used to observe a distinct distribution of regional and frequency specific activity that is associated with the DMN (see also Chen, Zhao & Feng, 2008, Li, 2009).

More recently, Knyazev, Slobodskoj-Plusnin, Bocharov and Pylkova (2011) aimed to explore EEG correlates of the DMN by employing analysis techniques commonly used in fMRI studies to EEG data. In their study participants completed two explicit emotion judgment tasks and a 6-minute resting state condition which involved alternating two-minute epochs of eyes-open and eyes-closed. Following this, participants were instructed to complete a questionnaire detailing their mental state and thought processes during rest; this was designed to measure variation in the degree of self-referential thought between participants. EEG was recorded across 32 scalp sites and the authors aimed to explore the degree of task-relatedness of each condition to spatial patterns identified in traditional EEG frequency bands. Compared to fMRI, which localises brain activity in a 3D volume, EEG only provides a 2D representation. Thus, Knyazev and colleagues applied a low-resolution brain electromagnetic tomography technique (sLORETA; see Pascual-Marqui, 2002) in order to obtain a 3D distribution of the neuronal activity. The authors then applied ICA to the 3D EEG data in order to determine whether it reproduced DMN

features typically shown in fMRI studies. This also allowed them to explore the relationship between task-relatedness and spatial patterns of EEG frequency bands, and to examine oscillatory responses in response to stimuli presented in the active conditions. One of the most interesting findings of their study was that only alpha band frequencies showed a high positive correlation with presumed DMN functions (as measured using the self-referential questionnaire) in the posterior region of the DMN; this activity was then disrupted during the active conditions. This study is interesting as it reveals specific EEG frequencies, in this case alpha oscillations, may be mapped on to DMN-associated processes, in this case self-referential thought.

2.6. Understanding the DMN using combined EEG and fMRI

A number of researches have sought to investigate the DMN by using EEG and fMRI combined (EEG-fMRI). The integration of these two techniques allows for simultaneous measurement of when (high temporal resolution of EEG) and where (high spatial resolution of fMRI) neuronal activity occurs in the brain (see Jorge, van der Zwagg & Figueiredo, 2013 for a review EEG-fMRI). To date, a number of resting-state EEG-fMRI studies have aimed to establish electrophysiological signatures of DMN activity by investigating the relationship between high frequency fluctuations in EEG signal and SLF fluctuations in the fMRI BOLD signal. However, variation in the findings obtained suggests evidence is somewhat inconsistent in allowing for the formulation of specific hypotheses to be made, with correlations reported between the DMN and alpha (negative: Laufs et al., 2003a, 2003b, 2006; positive: Jann et al., 2009; Jann, Kottlow, Dierks, Boesch & Koenig, 2010; Mantini, Perrucci, Del Gratta, Romani & Corbetta, 2007), theta (negative: Meltzer, Negishi, Mayes & Constable, 2007; Scheeringa et al., 2008), beta (positive: Jann et al., 2010; Laufs et al., 2003b; Mantini et al., 2007) and gamma (positive, but weak:

Mantini et al., 2007) frequency bands.

A particularly insightful study by Mantini et al. (2007) aimed to explore the relationship between electrophysiological oscillations in different frequency bands and fMRI BOLD signal oscillations. In their study EEG (32 channels) and fMRI were simultaneously recorded from participants in a 4-minute eyes-closed resting state. The authors hypothesised that the DMN, along with other networks that are active in the resting brain, would exhibit electrophysiological oscillations in multiple frequency bands; in turn, these frequency bands would be coupled to facilitate cognitive processes/behaviour. By applying ICA to the fMRI data the authors identified independent spatiotemporal patterns in the BOLD signal that corresponded with the DMN, along with five other widely distributed resting state networks. Mantini and colleagues then estimated the similarity between the EEG waveforms and BOLD signal time courses of each of the resting state networks, with findings revealing each of the resting state networks were associated with a specific combination of EEG oscillations. The DMN in particular was strongly associated with beta and alpha power and showed a weak relationship to gamma (see figure 2.7). These findings are noteworthy for a number of reasons: firstly, they were among the first to identify EEG signatures of the DMN; secondly, they suggest that electrophysiological oscillations in multiple frequency bands are implicated in the DMN (in this case beta and alpha in particular), suggesting researchers should not limit their study to a particular frequency band; and finally they offered support for the existence and activity of multiple networks in the resting brain (see also Jann et al. 2010).

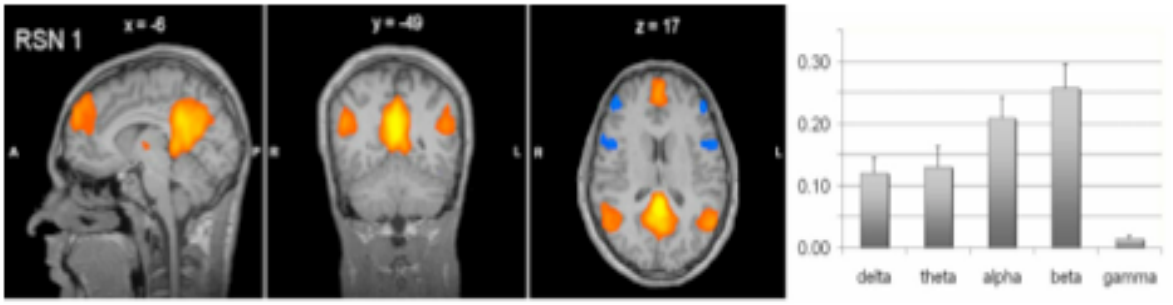

Figure 2.7. Relationship between electroencephalographic rhythms and the fMRI default mode network. Sagittal, coronal, and axial spatial maps of the six RSNs (left). Bar plots of the average correlations between the EEG oscillatory activity in the delta, theta, alpha, beta, and gamma bands, and the DMN time course (right). Adapted from Mantini et al. (2007).

A similar study by Scheeringa et al. (2008) aimed to explore the relationship between spontaneous electrophysiologial fluctuations in frontal theta power and fMRI BOLD signals. The authors were particularly interested in this frequency band due to its prominence across midline frontal areas during tasks of working memory, mental arithmetic etc. Thus, if this frontal theta is positively correlated with attention-demanding cognitive processes, it should be negatively correlated with the DMN. In their study, participants passively viewed a central cross for 10-minutes whilst EEG over 29 scalp sites and fMRI was recorded simultaneously. ICA was applied to band-pass filtered (2-9 Hz) EEG data in order to obtain an estimate of frontal theta power. On a single participant basis, the authors then selected out the component that was the most representative of the frontal theta rhythm, to which they applied time-frequency analysis. This allow Scheeringa and colleagues to obtain a frequency bin with the highest power, which in turn would form a regressor that modeled SLF fluctuations in frontal theta (Scheeringa et al., 2008). Overall, findings revealed no significant positive correlation between this regressor (frontal theta) and the fMRI BOLD signal. However, findings did reveal significant negative correlations in DMN regions, including the MPFC, PCC, inferior frontal, inferior parietal,

middle temporal regions and the cerebellum; thus suggesting that frontal theta can be considered as an electrophysiological signature of the DMN.

More recently, in comparison to exploring the relationship between EEG frequency and the fMRI BOLD signal, researchers have attempted to relate levels of EEG power to the functional connectivity within the DMN. For example, Hlinka, Alexakis, Diukova, Liddle and Auer (2010) found EEG band powers explained 70% of the variance in functional connectivity in the DMN. In their study, participants rested with their eyes-closed for 15-minutes whilst EEG (across 30 scalp sites) and fMRI were simultaneously recorded. EEG band power was calculated using a Fast Fourier Transform and functional connectivity within the DMN was assessed using ROIs including MPFC, PCC and the left/right temporoparietal cortex. The relationship between EEG power and DMN functional connectivity was then analysed using multiple linear regression, where the predictor variables were EEG band powers, and the dependent variable was functional connectivity within the DMN. Overall, findings revealed beta power (13-30 Hz) was significantly positively correlated with functional connectivity in the DMN, whilst delta power (1-4 Hz) was significantly negatively correlated with DMN functional connectivity. This study is noteworthy as it demonstrates an alternative approach to investigating the relationship between EEG and fMRI measures of the DMN. Furthermore, it revealed that beta might be considered as a reliable EEG signature of DMN activity.

2.7. Measures employed in this research thesis

The measures employed in this research thesis in order to investigate the functional connectivity of the DMN, along with its relationship to the task-positive network (as identified by Fox et al.,

2005) and other brain regions, are outlined below. These measures were also used: (1) to explore the functional connectivity within other large-scale brain networks (dorsal/ventral frontoparietal attention, executive/frontoparietal control and salience networks); (2) to determine how these networks were related to other brain regions; and (3) to explore their functional relationship to the DMN.

2.7.1. Combined EEG-fMRI

Resting state and active data were acquired using combined EEG-fMRI. This method was chosen based on an initial aim of this thesis: to explore the relationship between high frequency EEG signal fluctuations and SLF BOLD signals in the fMRI. Thus, of particular interest was whether EEG recordings could provide an effective measure of DMN fluctuations at lower cost than fMRI and with higher temporal resolution. This was especially of interest in relation to the use of resting state differences as possible markers of psychological or neurological abnormality. However, as shown in chapter 4, no significant EEG predictor of DMN activity was found. Therefore a shift in the emphasis of this thesis resulted in fMRI data only being used to complete subsequent analyses (chapters 5 and 6). EEG-fMRI was also chosen because these two techniques had not previously been integrated for experimental purposes within the School of Psychology, University of Dundee.

2.7.2. ROI seed-based correlation analysis

A ROI seed-based correlation approach was selected as a method of analysing fMRI data in this thesis, and was chosen for three reasons. Firstly, it allowed for the assessment of functional connectivity of the DMN and other large-scale brain networks, as well as their relationship to

each other and other brain regions. Secondly, in comparison to ICA (a purely data-driven approach: see section *2.4.2*), specific a priori predictions were made for each analysis (hence, specific relationships between networks were hypothesised). Finally, no one in the School of Psychology, University of Dundee, had attempted to investigate the DMN or any other brain network using this approach before.

2.7.2.1. CONN toolbox

Functional connectivity within the DMN and other large-scale brain networks was analysed using the MATLAB toolbox *CONN* (www.nitrc.org/projects/conn). This was chosen as it provides estimations of functional connectivity in terms of: region of interest (ROI)-to-ROI (connectivity between multiple ROIs), seed-to-voxel (connectivity between one/multiple seeds to regions covering the whole brain) and voxel-to-voxel (connectivity of the whole brain exclusive of a priori defined ROIs/seed). Subsequently, this enabled DMN areas (as identified by Fox et al., 2005) and user-specified regions (i.e. dorsal/ventral attention regions) to be compared to defined and/or all other voxels in the brain. This toolbox was also chosen on recommendation by Dr. Gordon Waiter, University of Aberdeen, as no one in the School of Psychology, University of Dundee, had used it before.

CHAPTER 3

Other large-scale brain networks and their relationship to the Default Mode Network

Thus far, this thesis has predominantly focused on the Default Mode Network (DMN), largely ignoring the fact that other large-scale brain networks exist. Chapter 1 focused on the history of the DMN, its implicated regions and contribution to behaviour. Chapter 2 focused on the study of the anatomy, metabolic activity and interplay between DMN regions. It showed that at rest the DMN is characterised by spontaneous low frequency (SLF) fluctuations in the blood oxygen level-dependent (BOLD) signal. It also considered the way in which this signal has been used to characterise the DMN as a *task-negative* network and to explore its *functional connectivity* (typically measured using independent component analysis or region-of-interest seed based correlation analysis). Chapter 2 also reviewed electrophysiological studies that have aimed to examine the relationship between specific electroencephalographic (EEG) frequency bands and DMN activity. Finally, it showed that studies integrating this technique with functional magnetic resonance imaging (fMRI) have produced relatively inconsistent results in establishing electrophysiological signatures of DMN activity.

3.1. Overview of aims of chapter

This chapter reviews other large-scale networks within the brain (also referred to as *control* networks due to the control they exert over cognitive processes and/or other networks). It focuses on their neurobiology, function and contribution to behaviour, as well as their relationship to the DMN. It begins by providing a short overview of attention and three

networks that are thought to contribute to it: alerting, orienting and executive control. Based on this theory, two networks that contribute to the orienting of attention in particular are discussed; these include the dorsal frontoparietal network (goal-driven network), and the ventral frontoparietal network (stimulus-driven network). Following on from this, the executive control network is considered in more detail, followed by a description and discussion of studies that have focused on the salience and frontoparietal control networks.

3.2. A short history of attention

Paying attention is the process of concentrating on a particular aspect of something in order to achieve a goal. It is controlled by top-down factors such as knowledge and expectation, and bottom-up factors such as sensory stimulation. Whilst initially assumed to be a property of the brain as a whole, Posner and Petersen (1990) were among the first to propose that three networks: *alerting*, *orienting* and *executive control*, perform interrelated functions and contribute to it. The alerting network involves increasing and maintaining sensitivity/response readiness towards anticipated or unanticipated stimuli. The orienting network concerns information scanning and selection from sensory input, and the executive control network involves the monitoring and control of conflict between internal processes (i.e. thoughts/feelings) and responses (Posner & Rothbart, 2007). A neuroanatomical illustration of these networks is shown in figure 3.1.

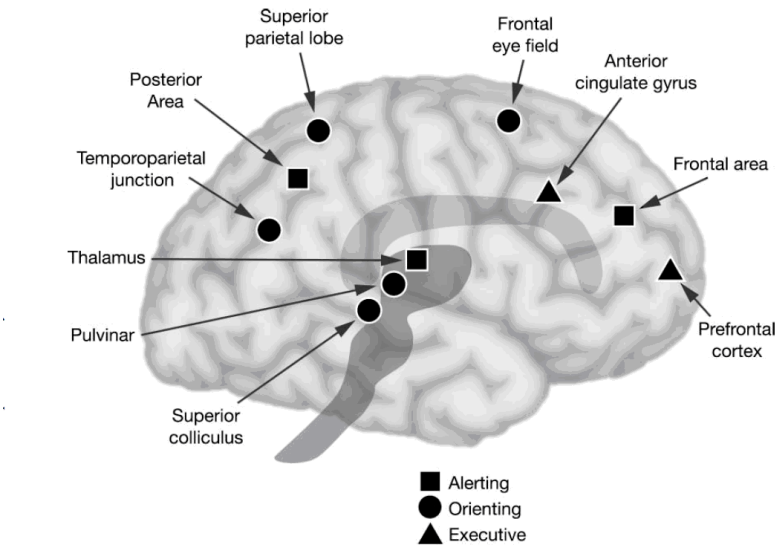

Figure 3.1. Neuroanatomical layout of networks contributing to attention. Alerting (squares), orienting (circles) and executive control (triangles) networks. Adapted from Posner and Rothbart (2007).

3.2.1. Alerting network

Researches into the *alerting* network have shown that *alertness* can be categorised into two forms. *Tonic alertness*, also known as *intrinsic alertness* or *vigilance,* is related to wakefulness and arousal, and involves maintaining brain activity over time. It can be measured using continuous performance tasks whereby participants are required to maintain attention to target stimuli whilst either inhibiting responses or detecting unrelated/novel stimuli; or, by rapid visual information-processing (RVIP) tasks, in which participants are instructed to detect target sequences during rapid stimuli presentation (e.g. Coull, Frith, Frackowaik & Grasby, 1996). Conversely, *phasic alertness* is related to increased response readiness towards target stimuli. It can be measured by assessing the influence of warning cues on reaction times, with studies suggesting that these cues suppress on-going thought processes in order to make a rapid response (Posner, 2008). Studies have shown the alerting function is associated activations of frontal,

posterior and thalamic regions respectively (Fan, McCandliss, Fossella, Flombaum & Posner, 2005; Coull, Nobre & Frith, 2001; Sturm & Willmes, 2001; see Posner & Rothbart, 2007 for a review).

3.2.2. Orienting network

The *orienting* of attention involves three basic processes: disengaging attention from its existing focus; shifting attention to a new target/event; and engaging attention in the new target/event (Posner, Walker, Friedrich & Rafal, 1984). Researches have shown this network is reliant on the frontal eye fields, superior and inferior parietal lobule, temporoparietal junction, superior colliculus, pulvinar and thalamic regions (Corbetta, Kincade, Ollinger, McAvoy & Shulman, 2000; Corbetta & Shulman, 2002; Posner & Rothbart, 2007). These regions play a differential role in the act of orienting, depending on whether it is *exogenous*, i.e. when an unexpected stimulus attracts attention to its location, or *endogenous*, i.e. planned search for a target stimulus (Fan et al., 2009). In laboratory settings this network is typically studied using target detection tasks, whereby a valid (true target location) or an invalid (false target location) cue/stimulus is presented thus provoking participants to direct/relocate their attention (e.g. Corbetta et al., 2000).

3.2.3. Executive control network

Regions that make up the *executive control network* include the lateral prefrontal cortex, basal ganglia, midline frontal areas and the anterior cingulate cortex (Posner & Rothbart, 2007). This network can be measured through conflict monitoring tasks, such as the flanker task (e.g. Botvinick, Nystrom, Fissell, Carter, & Cohen, 1999; Fan, Flombaum, McCandliss, Thomas & Posner, 2003) and the stroop task (e.g. Botvinick, Cohen & Carter, 2004; Fan et al., 2003; Liu,

Banich, Jacobson & Tanabe, 2004). In the flanker task participants are required to respond to a target stimulus whilst it is surrounded by non-target congruent/ incongruent or neutral stimuli. In the Stroop task participants are required to report on one dimension of stimuli, whilst it is presented in a conflicting dimension. These tasks measure the efficiency of the executive control network as they involve conflict amongst elements of stimuli, which in in turn provokes conflict between processing resources in the brain.

3.3. Attention control networks involved in the orienting of attention

Based on attention-orienting in particular, rapid adjustments in behaviour in response to novel or unanticipated stimuli have been characterised as *reorienting responses* (Corbetta & Shulman, 2002). Reorienting can occur between two or more external stimuli; for example, whilst reading this text the telephone may ring, thus causing the reader to reorient his/her attention. It can also occur between external stimuli (i.e. reading this text) and internally-directed processes, i.e. stimulus-independent thoughts/daydreaming. Recent behavioural and anatomical evidence suggests that the adaptation of behaviour and response, as a consequence of attention-(re)orienting, is dependent on the interaction of two distinct cortical networks: the dorsal frontoparietal (goal-driven) network; and the ventral frontoparietal (stimulus-driven) network (Corbetta & Shulman, 2002; Corbetta, Patel & Shulman, 2008).

3.3.1. Dorsal frontoparietal network: Goal-driven network

The goal-driven network (GDN) is controlled by top-down mechanisms and its core regions include the dorsal frontal cortex, dorsal parietal cortex (particularly the intraparietal sulcus and superior parietal lobule), along with the precentral sulcus (in close proximity to the frontal eye

field; Corbetta et al., 2008; see figure 3.2). This network is primarily associated with the selection of sensory stimuli from the external world, based on an individual's internal goals, existing knowledge and expectations (Corbetta & Shulman, 2002). The functions of the GDN have been validated by studies that have shown pre-activation of GDN regions is apparent when stimuli are presented in expected locations (Corbetta et al., 2000; Shulman et al., 1999), and also when specific planned responses are required towards stimuli (Connolly, Goodale, Menon & Munoz, 2002). This anticipatory pre-activation effect has also been shown to predict behavioural performance on a variety of tasks (Pessoa, Gutierrez, Bandettini & Ungerleider, 2002; see Corbetta et al., 2008 for a review).

3.3.2. Ventral frontoparietal network: Stimulus-driven network

The functionally distinct stimulus-driven network (SDN) is controlled by sensory bottom-up signals. Its core regions include the temporoparietal junction cortex (defined as the posterior region of the superior temporal sulcus/gyrus and ventral part of the supramarginal gyrus), along with the frontal operculum, ventral frontal cortex, regions of the middle frontal gyrus, inferior frontal gyrus, and anterior insula (Corbetta et al., 2008; see figure 3.2). This network is involved in detecting and responding to events that are not in the current focus of attention, and was proposed to represent exogenous orienting (Posner & Cohen, 1984). However, since this original proposal research has shown that the SDN responds together with the GDN in order to detect goal-relevant stimuli (Corbetta & Shulman, 2000), with enhanced activation in the SDN in particular if stimuli are salient but not relevant to the current goal e.g. if they appear in unanticipated locations, or if they appear at infrequent time intervals (Arrington, Carr, Mayer &

Rao, 2000; Bledowski, Pryulovic, Goebel, Zanella & Linden, 2004; Corbetta et al., 2000; Kincade, Abrams, Astafiev, Shulman & Corbetta, 2005).

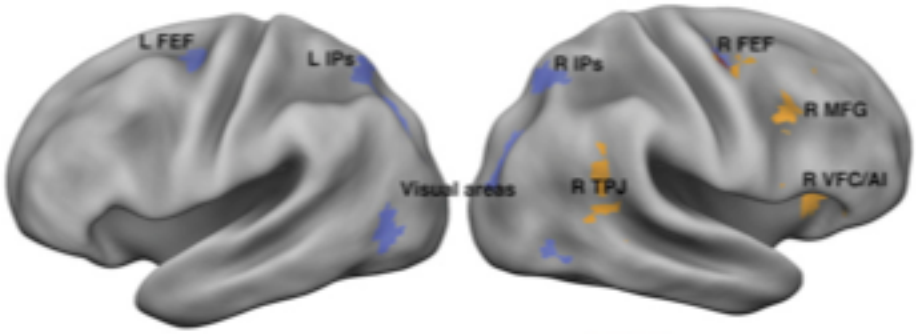

Figure 3.2. The goal-driven and stimulus-driven attention networks in the human brain. Results from a meta-analysis of activation data by Corbetta et al., 2008, revealing that, goal-driven regions (blue) are activated by central cues, indicating where a stimulus will appear or what is the feature of an upcoming object. Stimulus-driven regions (orange) are activated when attention is reoriented to unanticipated but behaviourally relevant stimuli. Adapted from Corbetta et al. (2008).

3.3.3. The interaction between the goal-driven and stimulus-driven networks

Findings have revealed that in the resting brain, the GDN and SDN are functionally distinct (Corbetta et al., 2008; Fox, Cobetta, Snyder, Vincent & Raichle, 2006b; He et al., 2008; Mantini et al., 2007; see figure 3.3). Research also suggests when attention is focussed there is functional interplay between networks: the SDN is suppressed by the GDN in order to reduce the chance of reorienting to distracting stimuli, and therefore prevent interference with internal goals/task performance (Corbetta & Shulman, 2002; Shulman et al., 1999; Todd, Fougnie & Marois, 2005). The extent to which this suppression occurs, however, is largely dependent on the task at hand, with studies revealing that during target-detection tasks both the GDN and SDN respond rapidly towards target stimuli (Corbetta et al., 2000; Shulman et al., 1999). The interaction and activity

of these networks is therefore commonly studied using the *Posner Spatial Cueing Paradigm*, in which participants respond to targets that appear in expected/unexpected locations (e.g. Arrington et al., 2000; Kincade et al., 2005; Vossel, Thiel & Fink, 2006; Vossel, Weidner, Thiel & Fink, 2009). *Oddball paradigms* are also commonly used, in which participants are required to detect/ignore oddball stimuli that appear infrequently within a series of standard frequent stimuli (e.g. Bledowski et al. 2004; Bradzil et al., 2005). For example, participants may be required to discriminate between aurally presented odd/even numbers (GDN engaged), whilst ignoring task-relevant/irrelevant (oddball) novel sounds (SDN engaged). Subsequently, behavioural (i.e. reaction time), and/or electrophysiological (event-related potential), and/or fMRI (neuronal activation) measures are analysed, allowing for the characterisation of behavioural/neural responses to oddball stimuli (relative to standard frequent stimuli). Although multiple variants of this task exist, i.e. using auditory (Brazdil et al., 2005) or visual (Bledowski et al., 2004) stimuli, findings are relatively consistent in observing oddball-related activations particularly within the SDN's temporoparietal junction (TPJ) and prefrontal regions. Activation within the GDN's frontal and parietal regions are also commonly observed, which are proposed to reflect the shift in focus of attention (Brazdil et al., 2005; Linden et al., 1999; Bledowski et al., 2004; Fichtenholtz et al., 2004).

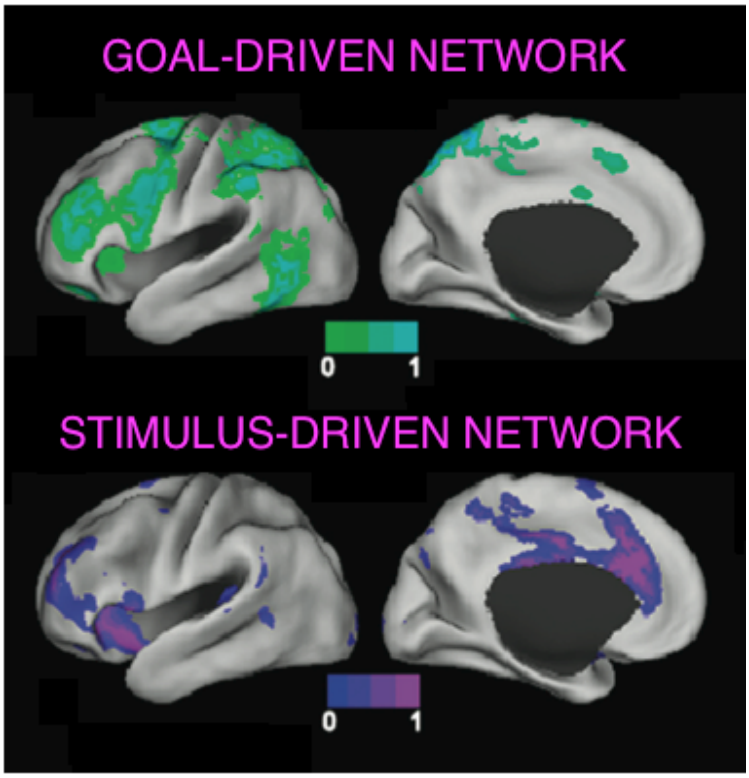

Figure 3.3. Surface plots of the GDN and SDN in the resting brain. Adapted from Lee et al. (2012a).

3.3.4. The interaction between the attention-orienting networks and the DMN

As discussed in chapters 1 and 2, deactivation of the DMN is commonly observed during goal-directed tasks (Shulman et al., 1997; Mazoyer et al., 2001). Furthermore, functional connectivity studies have revealed that the DMN is anti-correlated to a task-positive network, whose core regions are implicated in goal-directed tasks (Fox et al., 2005; Fransson, 2005, 2006). Together, these findings have provided a valuable insight into the relationship between the DMN and GDN, suggesting that when the GDN is engaged, the DMN is suppressed/down-regulated.

In comparison, the relationship between the DMN and SDN is somewhat complicated and brings into question the function of the DMN. For example, as discussed in chapter 1, Hahn et al., (2007) reported that increased activity within DMN regions was correlated with enhanced performance on a target detection task. Most interestingly was that one of the DMN regions, the superior temporal gyrus, located in the vicinity of the TPJ, was particularly active during trials in which target location was unpredictable. Given the overlap of this region between networks, it suggests that the DMN may adopt a similar role to the SDN in the monitoring of the external environment: thus supporting the sentinel hypothesis of DMN function. Alternatively, studies have reported reductions in DMN activity are associated with enhanced task performance on stimulus-driven tasks. For example, Shulman, Astafiev, McAvoy, d'Avossa and Corbetta (2007) investigated fMRI BOLD task-evoked signals from a task in which participants were required to detect a target within a rapid serial visual presentation task. Findings revealed activity in the right supramarginal gyrus, a region in close proximity to the TPJ, showed greater suppression in activity when a target was correctly identified than when it was missed (GDN engaged). Again, this infers the DMN and SDN may assume similar roles during active task conditions, and also suggests that the GDN suppresses activity within each network respectively (see also Daselaar, Prince & Cabeza, 2004).

A more recent functional connectivity study by Anticevic et al. (2010) investigated the role of the TPJ in a delayed working memory task. This task contained two levels of working memory load and three potential distractor types that were presented during the maintenance period. One distractor in particular was expected to engage the TPJ due to its task-relatedness in visual appearance, whilst the other two were unrelated. Of particular interest was whether the

magnitude of TPJ deactivation during the working-memory encoding phase would be predictive of task performance. Furthermore, in order to disentangle the relationship between the TPJ as part of the SDN versus DMN, the authors were interested in activation and correlation pattern between the TPJ and other DMN regions. Overall, findings revealed greater TPJ deactivation during encoding was associated with better task performance. Findings also revealed that the relationship between the TPJ and DMN changed over task duration. During the encoding phase, TPJ was positively correlated to several components of the DMN (see figure 3.4A) and negatively correlated to the GDN. Conversely, in the maintenance phase (in which distractors were presented) this pattern remained, but at an attenuated level (see figure 3.4B). In addition, comparison of trial-based functional connectivity of the TPJ and DMN between the encoding and maintenance/distractor phase revealed reduced connectivity (see figure 3.4C), suggesting the TPJ had, in fact, de-coupled from the DMN in this phase. This study is interesting for a number of reasons: firstly, it shows the functional importance of suppression of the TPJ and DMN in terms of cognitive performance; secondly, it enhances understanding of the function of the TPJ, showing that it is more responsive to distractor stimuli than the DMN, thus disentangling the role of the TPJ in the SDN and the DMN; finally, it suggests there is a greater flexible interaction between the SDN and DMN, unlike the relationship between the GDN and DMN.

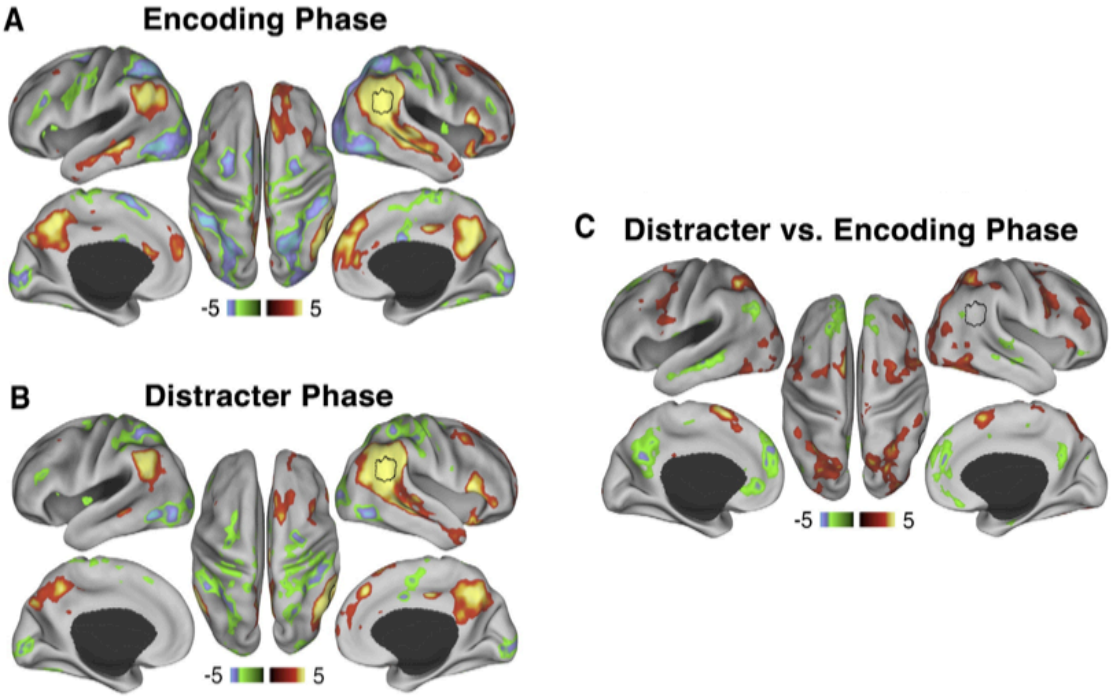

Figure 3.4. Relationship between TPJ and DMN. (A) During the encoding phase TPJ is positively correlated with components of the DMN (yellow/red) and negatively correlated with components of the GDN (green/blue). (B) A similar pattern is observed during the distractor phase, albeit attenuated (C) Results of a paired t-test, which compared TPJ trial-based connectivity during distractor versus encoding phase, shows where correlations with the TPJ seed increased between phases (yellow/red), and where correlations with this seed decreased (green/blue), suggestive of de-coupling activity with the DMN. TPJ represented in the black border outline). Adapted from Anticevik et al. (2010).

3.4. A little more on the executive control network

As previously discussed (section *3.2.3*), the executive control network (ECN) is defined with respect to brain mechanisms implicated in the monitoring and control of thoughts, feelings and responses (Posner & Rothbart, 2007). It has been proposed that in some circumstances, this network modulates activity in the orienting networks by acting directly on the GDN in order to maintain and adjust goal-driven attention for current task demands (Corbetta, Patel & Shulman, 2008). Furthermore, experimental manipulation has revealed activity within the anterior cingulate cortex, a putative region of the ECN, is more pronounced when some form of response

conflict occurs during task completion of external goal-directed tasks (i.e. the flanker task; Botvinick et al., 1999; Botvinick et al., 2004). Research has also shown that the prefrontal cortex is a key associate in the optimal functioning of this network (Elliot, 2003; Kane & Engle, 2002; see Verhaeghen & Cerella, 2002 for a review). Given the vast and complex architecture of this region, and the number of processes that the ECN is implicated in, literature suggests the ECN can be functionally segregated into hierarchically ordered control processes, and, in turn, these processes can be mapped on to specific frontal regions (Koechlin and Summerfield, 2007). Furthermore, as with the GDN, SDS and DMN, the ECN has also been identified as a resting-state network, in absence of stimulation (Lee et al., 2012a; Weissman-Fogel, Moayedi, Taylor, Pope & Davis, 2010; Woodward, Rogers & Heckers, 2011).

3.4.1. The executive control network and the DMN

Goal-driven tasks that require some form of executive control, i.e. working memory tasks, have been shown to suppress activity and reduce functional connectivity within the DMN (e.g. McKiernan et al., 2003; Fransson, 2006; see chapters 1 and 2 for a review). This suggests that when the ECN is engaged in externally-directed processes, the DMN is down-regulated. However, given the ECN is also implicated in the control and monitoring of internal modes of cognition, it brings to the forefront questions regarding the relationship between this network and the DMN.

A particularly insightful fMRI study by Christoff et al. (2009) aimed to establish the extent to which the ECN is implicated in mind wandering, an internally-directed DMN-associated process (see chapter 1 for a review). The authors were interested in this network based on evidence

from experience sampling studies (e.g. Smallwood & Schooler, 2006) suggesting mind wandering involves complex mental processes: inferring the ECN may participate in this form of cognition (experience sampling is similar to the stimulus-independent thought probing method discussed in chapter 1, whereby participants are probed to self-report their current thought content/mental state). The authors were also interested in the extent to which the DMN engaged in periods of mind wandering and the relationship between brain activity and *meta-awareness*: the phenomenon that individuals vary in their awareness of their thought content (see Schooler & Schreiber, 2004 for a review). In their study, participants completed a sustained attention to response task (go/no go task), throughout which they were also presented with thought probes. These probes explored participants' thought content immediately prior to presentation of the probe, and asked (1) whether their attention was task focused/unfocused; and (2) whether or not they were aware of what their attention was focused on. Overall, findings revealed a core set of DMN regions (medial prefrontal, posterior cingulate/precuneus and temporoparietal regions) were active during periods of mind wandering in which participants exhibited reduced meta-awareness, compared to when they were aware of their thought content. Interestingly, results also revealed that activation within the dorsal anterior cingulate and dorsolateral prefrontal cortices, two putative regions of the ECN, increased substantially during mind wandering without meta-awareness, suggesting the existence of a relationship between this form of cognition and the ECN. The authors interpreted this relationship as reflective of (1) multitasking between external task-performance and internally-directed processes; (2) conflict monitoring between internal and external modes of attention; and (3) conflict monitoring of specific thoughts/feelings occurring during mind wandering. These results are interesting as they reveal an overlap between putative regions of the DMN and ECN. They also support the role of the

ECN in the control, management and 'paying attention' to internal cognitive processes. Given these internal cognitive processes (mind-wandering) are commonly mapped onto DMN regions, the results also infer the existence of a functional relationship between these networks.

A more recent study by Gerlach, Spreng, Gilmore and Schacter (2011) explored the co-activation of the DMN and ECN during goal-directed mental simulations. This was of interest based on (1) the overlap between ECN and DMN regions; (2) previous findings implicating the DMN in imagining/planning/envisioning the future (see chapter 1 for discussion); and (3) the role of the ECN in the control and monitoring of internal/external thought processes. In their study, fMRI data were obtained whilst participants read a number of scenarios and related problems, during which they were instructed to imagine themselves being *in* the scenario and actively solving the problem (*goal-directed mental simulation*). Cues were provided in order to assist participants in forming plans, thus encouraging mental simulation. As a comparison control task, participants were presented with a word and asked to silently generate words that were semantically associated. The authors hypothesised that the posterior cingulate cortex (DMN region) would be active due to the internal-directed nature of the task. And, also that activation within the dorsolateral prefrontal cortex (ECN region) would be apparent given its role in the maintenance and control of goal-directed processes. Interestingly, findings revealed that relative to the semantic association task, goal-directed mental simulation was associated with recruitment of medial prefrontal and posterior cingulate portions of the DMN (see figure 3.5A), along with the dorsolateral prefrontal cortex component of the ECN (See figure 3.5B). Further to this, findings from task-related functional connectivity revealed the posterior cingulate cortex and dorsolateral prefrontal cortex were functionally connected to each other and to several other regions across

the cortex, implicated in the DMN and ECN. These results are interesting as they echo the findings of Christoff et al. (2009), revealing that the DMN and ECN are functionally related, suggesting both networks are implicated in the control and simulation of internal goal-directed behaviour. In some ways, these results also call into question the relationship between the DMN and the *task-positive* network, as discussed in chapter 2: this is because as the findings show, the ECN is implicated in goal-directed tasks, inferring that it is a task-positive network. Given this, along with the ECN's functional relationship to the DMN, it suggests the DMN and the task-positive network might not be as *anti-correlated* as first believed.

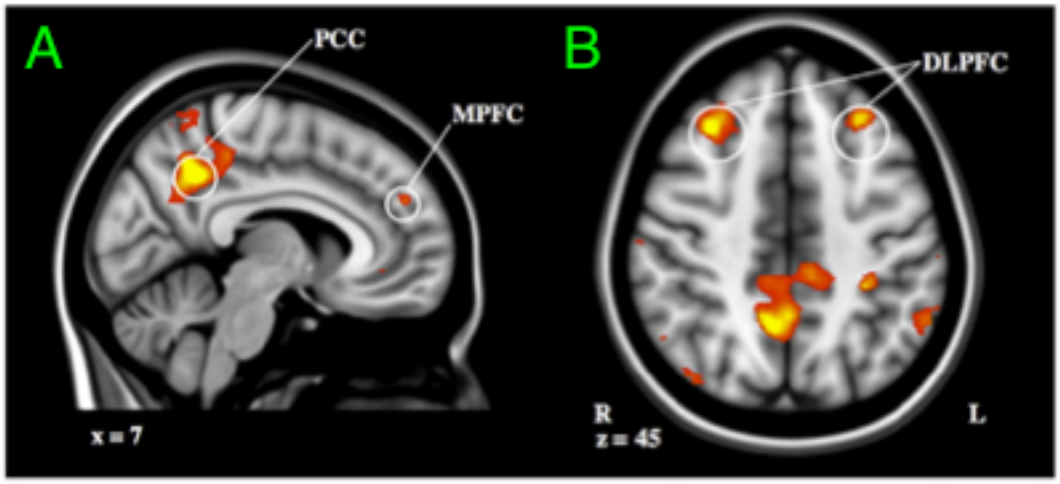

Figure 3.5. Default mode and executive control regions active during goal-directed mental simulation (A) DMN regions medial prefrontal cortex and posterior cingulate cortex. (B) Bilateral dorsolateral prefrontal cortex. Adapted from Gerlach et al. (2011).

3.5. The salience Network

The existence of an additional network involved in the monitoring of internal processes and the detection of external salient events has received considerable interest in recent years. Referred to as the salience network (SN), this network is involved in the switching between brain networks when an externally salient event is detected, and guiding the appropriate behavioural response(s)

towards the event (Menon & Uddin, 2010). Research shows this network is apparent in the resting brain (Weissman-Fogel et al., 2010) and that cortical regions implicated in the SN overlap with those involved in the orienting networks and the ECN (Seeley et al., 2007). Regions include the ventrolateral prefrontal cortex, anterior cingulate cortex and the fronto-insular cortex (also referred to as the anterior insula; Sridharan, Levitin, & Menon, 2008). The fronto-insular component of this network in particular has received considerable interest throughout the literature, with research suggesting that, given its anatomical position between networks, it may be regarded as the facilitator/mediator in the changeover between externally- and internally-directed processing (Menon & Uddin, 2010).

3.5.1. The salience network and the DMN

Research has shown that in some instances (i.e. task-free resting conditions) activation in the SN is coupled with down-regulation of activity in DMN components (i.e. the posterior cingulate cortex; Seeley et al., 2007). The functional relationship between these networks is further supported by studies suggesting that damage to the structural connectivity of the SN has a detrimental effect on regulation of DMN activity. This is apparent in traumatic brain injury, whereby patients fail to deactivate DMN regions during tasks of inhibitory control (Bonnelle et al., 2012) and in neurodegenerative disease (i.e. frontotemporal dementia), in which the SN is disrupted resulting in enhanced DMN activation (Zhou et al., 2010).

In the healthy brain, based on the functions of the SN, research has concentrated on its involvement in the transition between cognitive states, focussing on the operation of the SN in the dynamic control of activity between networks. A particularly insightful study by Sridharan,

Levitin and Menon (2008) studied the brain mechanisms implicated in switching between the ECN (which they term as the central executive network) and the DMN. The authors were particularly interested in the role of the frontal insular and anterior cingulate components of the SN, hypothesising that these regions facilitate the switching between networks during tasks varying in difficulty and differing in content (thus engaging the ECN/DMN respectively). They acquired fMRI data from three experimental conditions: an active auditory event segmentation task, in which participants listened to classical music whilst salient-orienting events occurred; an active visual oddball task; and a rest state. Overall findings revealed during the auditory task activations within the ECN and SN were coupled with deactivation of DMN regions. The authors confirmed the response of these regions using independent component analysis (to ensure that they were not merely isolated regional responses), from which they concluded the existence of statistically independent networks (see figure 3.6A). Latency analysis also revealed event-related fMRI BOLD signals within SN components temporally preceded activity in ECN and DMN components (see figure 3.6B). Finally, the authors applied Granger causality analysis (a technique which assesses the directional influence of signal change between brain regions) to the data in order to examine the influence of the SN components on other brain regions. Findings revealed the right frontal insular cortex exhibited significantly high net casual outflow connections in comparison to components of the ECN and DMN (see figure 3.6C), leading the authors to propose that this region plays a key role in activating the ECN and deactivating the DMN. And, interestingly, findings converged when the analysis techniques were applied to the other experimental conditions. These findings are noteworthy for a number of reasons: firstly, they support the notion of a functional relationship between large-scale brain networks; secondly, they suggest a role for the frontal insular component of the SN in the switching

between networks, suggesting this region has 'hub-like' properties; finally, the application of analysis techniques across task paradigms and stimulus-modalities, revealing consistent results for the role of the right frontal insular cortex, strengthens the functional role of the SN in cognition and behaviour.

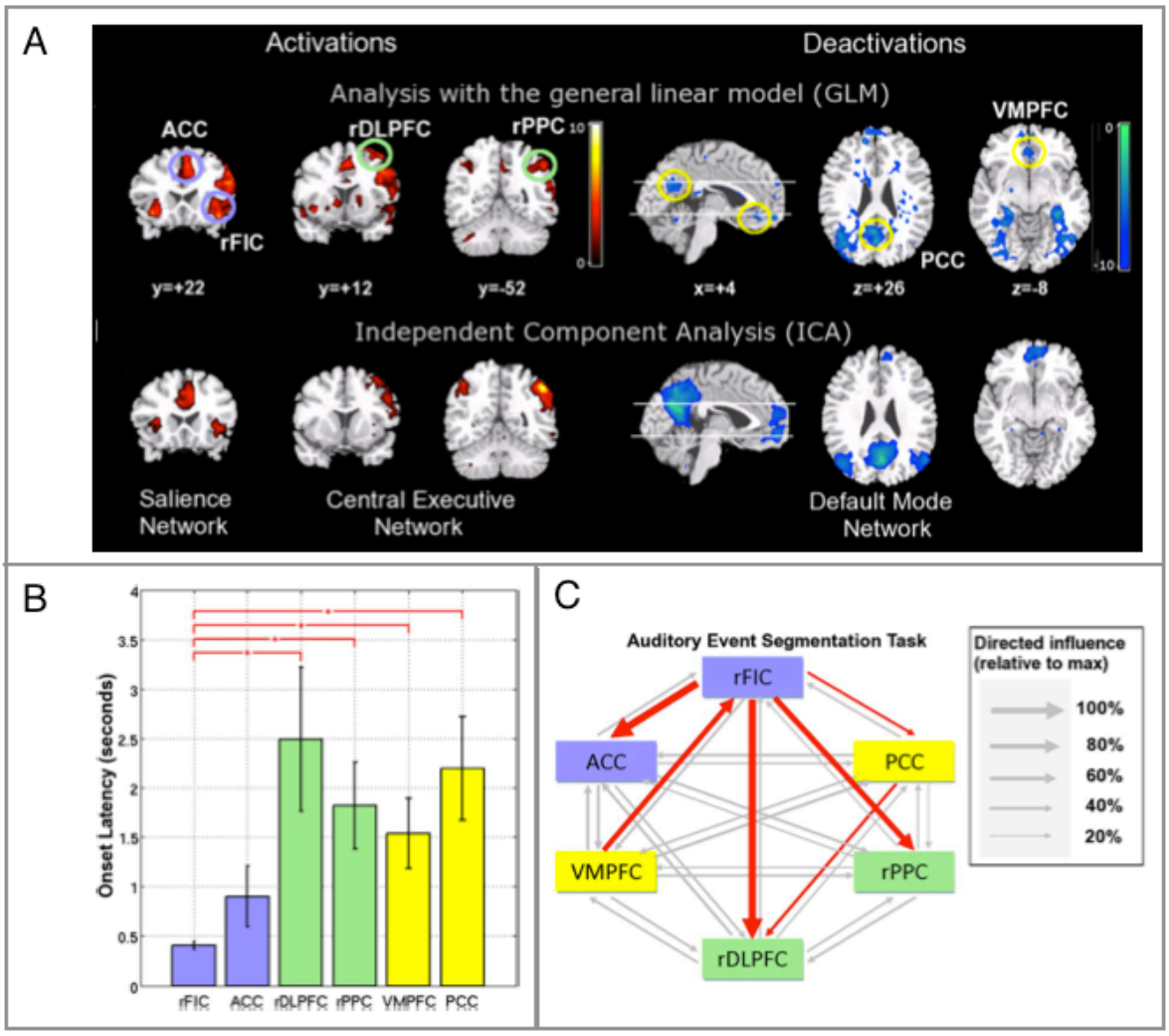

Figure 3.6. The salience, executive control and default mode networks and the role of the right fronto-insular cortex in switching between networks. (A) Activations of the SN and ECN and deactivation of the DMN during an active auditory task. Analysis results from general linear model (upper figure), ICA results revealing that these networks are spatially distinct (lower figure). (B) Onset latencies for components of the SN (purple), ECN (green) and DMN (yellow). (C) Granger causality analysis components of the SN (purple), ECN (green) and DMN (yellow), revealing significant causal outflow from the right fronto-insular cortex. The thickness of arrows corresponds to the strength of connection (20-100%). Adapted from Sridharan et al. (2008).

3.6. The frontoparietal control network and its relationship to the DMN

Thus far, it is apparent that the DMN is implicated in internal-modes of cognition (i.e. envisioning the future) and that the GDN is implicated in external modes of cognition. Furthermore, the studies by Christoff et al. (2009) and Gerlach et al (2011; as discussed in section *3.4.1*) suggest the ECN and DMN are functionally related, thus questioning the anti-correlated relationship between the DMN and all task-positive networks. Given goal-driven cognition can have an internal focus (as shown by the aforementioned studies), it has been proposed that a third network, the frontoparietal control network (FCN), may facilitate the functional interplay between the 'internal' GDN and the DMN. It should be noted that the FCN is a relatively new network within the literature, with some anatomical regions and associated functions overlapping with those of the ECN.

Whilst individual nodes of the FCN have been identified in studies of attention control (Cabeza et al., 2008; Corbetta et al., 2008) its functional anatomy was not fully established until the publication of a resting-state functional connectivity study by Vincent, Kahn, Snyder, Raichle and Buckner (2008). In this study, the authors were particularly interested in the interaction between the DMN and task-positive network (Fox et al., 2005) in the resting brain, speculating that a control system may regulate activity and integrate information between networks. Vincent et al. selected seed regions of interest (ROIs) implicated in the GDS and DMN based on previous research, and included the middle temporal area (MT+; GDN; Fox et al., 2005) and the hippocampal formation (HF; DMN; Buckner et al., 2008). The anterior prefrontal cortex (aPFC) was selected as a seed region for the potential FCN, based on research implicating this region in tasks of decision making and cognitive control (Buckner, 2003; Ramnani & Owen, 2004). Using

a similar procedure to Fox et al. (2005; see chapter 2 for a description), Vincent and colleagues analysed the correlations between SLF fluctuations in the BOLD signal between ROIs and regions covering the rest of the cortex. Functional correlations maps were then computed in order to determine the functional connectivity of the regions correlated to the GDN, DMN and the FCN respectively. Overall, one of the most interesting findings was that the FCN was anatomically interposed between regions of the GDN and DMN, with findings revealing it was comprised of the rostrolateral prefrontal cortex, middle frontal gyrus, anterior insula, anterior cingulate cortex, precuneus and the inferior parietal lobule (Vincent et al., 2008; see figure 3.7). Based on its position and correlated activity across the brain, and the control-type processes associated with the aPFC, the authors concluded that the FCN is implicated in the facilitating and controlling the integration of information between the GDN and DMN.

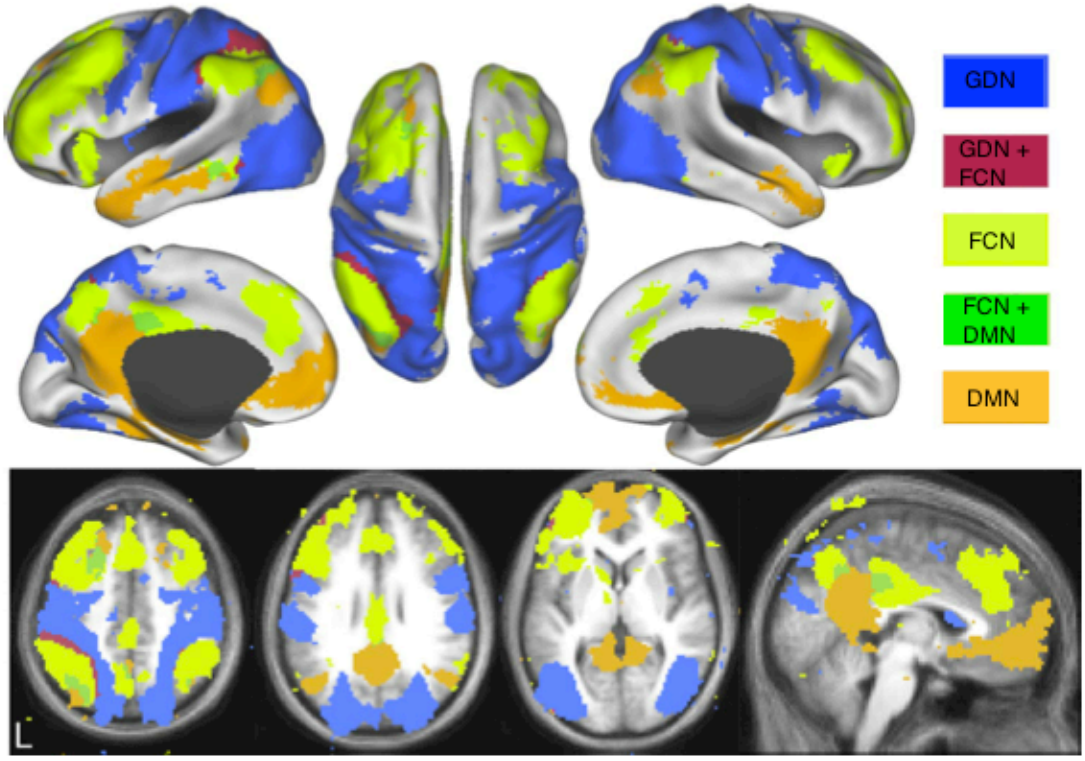

Figure 3.7. The goal-driven, frontoparietal control and default mode networks in the resting brain. Voxels correlated with the goal-driven network (GDN) are shown in blue; frontoparietal control network (FCN; light green); default mode network (DMN; orange). Voxels correlated with the GDN and FCN are shown in red. Voxels correlated with the DMN and FCN are shown in dark green. Adapted from Vincent et al. (2008).

A more recent study by Spreng et al. (2010) aimed to investigate the functional relationship between the FCN, DMN and GDN. Based on the functions associated with nodes of the FCN (i.e. memory/attention), and its anatomical position between the GDN and DMN (see figure 3.7), the authors hypothesised this network would couple with either the GDN or DMN during externalised and internalised goal-directed cognition. In their study participants completed two tasks; the first of which was the Tower of London task, an externally-directed neuropsychological test of visuospatial planning, thus engaging the GDN. The second task was an internally-directed autobiographical planning task, which required participants to plan for

external world personal goals, thus engaging the DMN. The authors hypothesised that activation of the FCN would be apparent in both of these tasks respectively. Overall, results from a task-related functional connectivity analysis revealed that, both tasks engaged the relevant associated network (GDN/DMN) respectively; and, that this task-related functional connectivity mimicked their functional independence during resting-state (as shown by connectivity maps obtained during rest). Findings also revealed activity within the GDN and DMN was coupled with activity in the FCN in each task: FCN and GDN during visuospatial planning; FCN and DMN during autobiographical planning. These results infer that the DMN can be implicated in typically 'external-type' goal-directed cognition when it is united with activity in the FCN. The results also suggest the FCN can be considered as a facilitator in linking internally and externally directed processes from each domain. Thus, again calling into question the perceived anti-correlated relationship between the DMN and task-positive networks, and in some ways challenging the notion put forward by Fox et al. (2005) that the DMN is a *task-negative* network.

3.7. Conclusions

The studies addressed in this chapter have shown there is functional interplay between the DMN and several other large-scale control networks within the brain. Each of the networks considered appear to have a modulatory effect on DMN activation: enhancing/down-regulating activity respectively (see figure 3.8 for an interpretation of these relationships). As discussed, externalised goal-directed tasks, provoking activity within the GDN, are associated with suppression of DMN activity. Activity in nodes of the SDN (e.g. TPJ) has, however, raised questions regarding the function of the DMN, inferring it may play a sentinel role in the monitoring of the external environment (thus supporting the sentinel hypothesis of DMN

function; discussed in section *1.7.1*, chapter 1). Furthermore, the relationship between the ECN and DMN suggest that when goal-directed tasks have an internalised focus to them, there is overlap in ECN and DMN regions that are active. Finally, the role of the salience and frontoparietal networks as switcher/modulatory networks suggest they are also implicated in the functional interplay between networks, which, in turn, suggests that they facilitate the switching between internally- and externally-directed cognitive states.

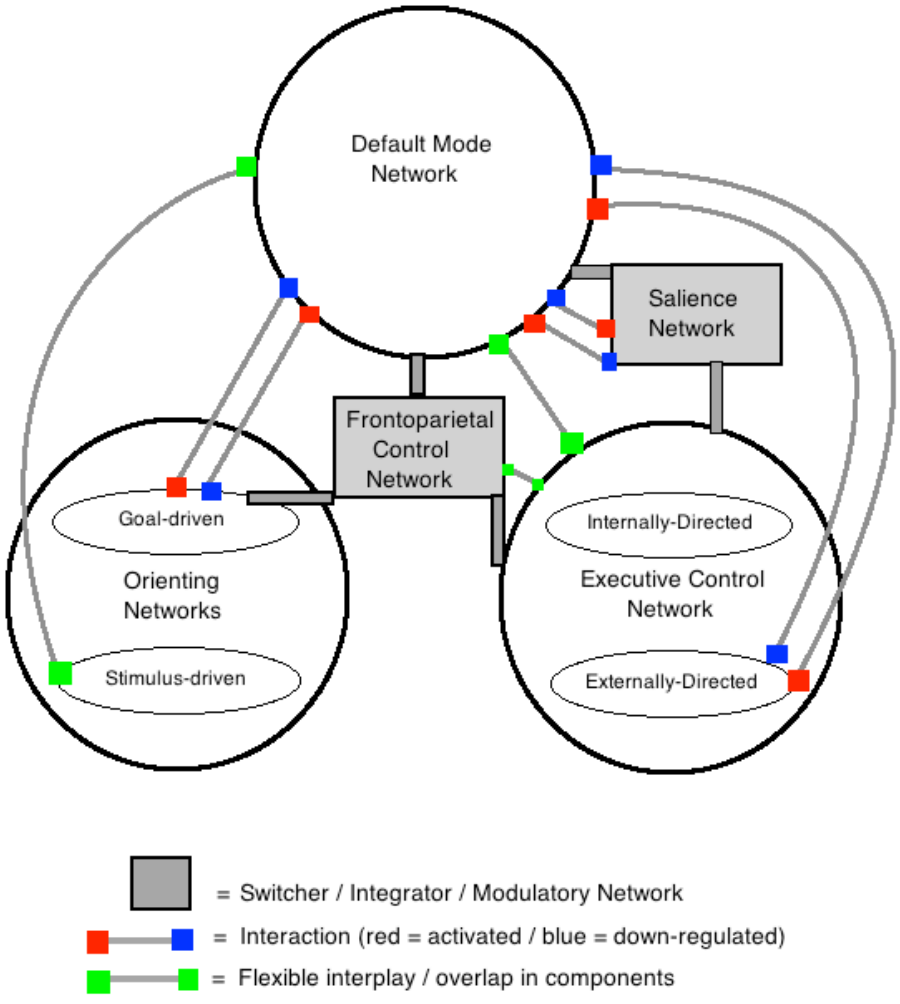

Figure 3.8. Proposed relationships between the default mode network and several other large-scale control networks. As shown, each network related to the default mode network, in terms of their modulatory effect, and/or flexible interplay, and/or overlap in implicated brain regions. Note that these relationships are based on what is discussed in this chapter only and does not take into account the relationship between the executive and stimulus-driven network for example

3.8. Overview and aims of thesis

The overall aim of this thesis was to attempt to gain a better understanding of the function of the Default Mode Network (DMN) by exploring the relationship between the DMN and other large-scale cognitive control networks. This was done by utilising resting-state and active task data from integrated EEG-fMRI technical development work.

Experiment 1 (reported in chapter 4) explored functional connectivity of the DMN during task-free resting-state. Of particular interest was the relationship between the DMN and: (1) the *task-positive* network identified by Fox et al. (2005); (2) other common DMN regions defined by Buckner et al. (2008); and (3) regions covering the whole of the cerebral cortex. After identifying putative regions of the DMN in this analysis, beta frequency (13-30 Hz) was selected for exploration as a potential electrophysiological correlate of fMRI DMN activity. Beta frequency was selected because previous studies have shown a positive correlation between this band and DMN activity (e.g. Hlinka et al.,2010; Laufs et al., 2003; Mantini et al., 2010; see chapter 2), and also because a previous pilot study exploring delta frequency (0.5-3.5 Hz; in line with Chen et al., 2008) failed to produce a significant result (discussed in detail in section *4.1.2* in chapter 4).

Having investigated the relationship between EEG and fMRI markers of the DMN with minimal success in experiment 1, it was decided that a shift in the emphasis of this thesis would be to explore DMN activity (in the same group of participants) in an active auditory attention task in experiment 2 (reported in chapter 5). In line with previous studies exploring task-related activations within the DMN (e.g. Fransson et al., 2006; Greicius & Menon, 2004; Hahn et al.,

2007), it was predicted that strong functional connectivity between DMN regions would be observed. This experiment also explored potential changes in DMN activation across task duration: firstly, by analysing reaction times as a behavioural index of DMN activity (in line with Smallwood & Schooler, 2006; Weissman et al., 2006); and secondly, by investigating changes in the strength and number of functionally correlated DMN regions over time.

Having demonstrated in experiment 2 that DMN activity was present in the active auditory task and with results hinting at the existence of relationships between the DMN and components of several other large-scale control networks, experiment 3 (outlined in chapter 6) investigated these relationships further. In line with the large-scale networks discussed in this chapter and because the auditory attention task was designed to engage activity in several brain networks, functional connectivity within the GDN, SDN, ECN/FCN and SN were explored using the same method of analysis as experiments 1 and 2. The relationship between components of these networks and DMN regions identified by Fox et al. (2005) was also investigated.

Implications and conclusions of each experiment, along with their contribution to existing DMN literature, are summarised in the General Discussion of this thesis (chapter 7).

CHAPTER 4

Experiment 1: Resting-state functional connectivity and electrophysiological investigation of the Default Mode Network

4.1. Aim of experiment

Resting-state data reported in this experiment were obtained during combined electroencephalographic (EEG)-functional Magnetic Resonance Imaging (fMRI) technical development work. The overall aim was to develop a suitable analysis strategy to investigate the relationship between EEG signal fluctuations and spontaneous low-frequency (SLF) fluctuations in the fMRI blood oxygen level-dependent (BOLD) signal within Default Mode Network (DMN) regions (identified on an individual basis using functional connectivity analysis). Region-of-Interest (ROI)-to-ROI functional connectivity analysis was carried out on five minutes of eyes-closed resting-state fMRI data (analysis 1). Simultaneously recorded EEG was then analysed using wavelet analysis, with EEG frequency content in the beta range (13-30 Hz) selected as a potential predictor of DMN activity (analysis 2).

4.1.1. Analyses 1a-1c: Rationales and hypotheses

As discussed in chapter 2, Fox and colleagues (2005) examined SLF fluctuations in the fMRI BOLD signal in the resting brain. The authors identified the existence of two cortical networks, whose anatomical regions and patterns of activity at rest mimicked their response during externally-directed tasks. These networks included the DMN, which Fox et al. termed as a *task-negative* network (a group of regions commonly deactivated during goal-directed tasks), and a

task-positive network (a group of regions typically activated during goal-directed tasks). Further to this, using ROI/seed-driven functional connectivity analysis, Fox et al. (2005) revealed that these networks were anti-correlated with one another; inferring that when the DMN is engaged, the *task-positive* network is down-regulated and vice versa (see also Fransson, 2005, 2006).

As proof of concept and also in order to identify a suitable analysis strategy for measuring DMN connectivity in five-minutes of eyes-closed resting-state fMRI data, analysis 1a aimed to replicate the findings of Fox et al. (2005). In comparison to their study, which investigated the functional relationship between networks in three conditions: eyes-closed, eyes-open with/without visual fixation (revealing consistent results across conditions); the current experiment explored functional connectivity of the DMN in an eyes-closed condition only. The rationale behind this was: (1) to increase the signal from the DMN, as shown in previous comparisons of eyes-open and eyes-closed connectivity analyses (2) original studies of the DMN implemented an eyes-closed design (e.g. Raichle et al., 2001); and (3) previous research has reported increased mean activity in specific EEG frequency bands with eyes-closed versus eyes-open resting-state (e.g. Barry, Clarke, Johnstone, Magee & Rushby, 2007). It should also be noted that the duration of *5-minutes* resting-state data acquisition was based on: (1) previous research identifying DMN connectivity in as little as 4-minutes of data (e.g. Greicius et al., 2003; see section *2.3.4* in chapter 2); and (2) time constraints during technical development work allowed for this duration only to be incorporated into the overall experimental design (see method section *4.2.1* for a description of technical development work). In line with Fox et al. (2005) it was hypothesised that the DMN (task-negative/internally-directed network) would be negatively correlated with the task-positive (externally-directed) network.

In addition to DMN regions identified by Fox et al. (2005), several other regions have been identified as core components of the DMN. According to Buckner et al. (2008) these regions, typically observed in studies of resting-state brain activity/task-induced deactivation, include: the ventral medial prefrontal cortex; posterior cingulate/retrosplenial cortex; inferior parietal lobule; lateral temporal cortex; dorsal medial prefrontal cortex and the hippocampal formation. In order to gain greater insight into this network as a whole, the functional relationship between DMN regions identified by Fox et al. (2005) and DMN regions identified by Buckner et al. (2008) was analysed (analysis 1b). It was hypothesised that these two sets of DMN regions would be positively correlated with one another.

Finally, in order to explore the way in which the DMN interacts with the rest of the brain, correlations between DMN regions identified by Fox et al. (2005) and regions covering the whole of the cortex were examined (analysis 1c). As this analysis was exploratory no predictions were made.

4.1.2. Analysis 2: Rationale and hypotheses

As discussed in chapter 2, resting-state EEG-fMRI has been used to explore electrophysiological signatures of DMN activity by correlating high frequency fluctuations in EEG signal to SLF fluctuations in the fMRI BOLD signal. However as previously addressed, variation in findings from combined EEG-fMRI studies and from those utilising EEG data only, are somewhat inconsistent in linking fluctuations in DMN activity with fluctuations in a specific EEG frequency band (see section *2.6* in chapter 2). In the current analysis electroencephalographic

frequency content in the beta (13-30 Hz) range was selected as a potential predictor of DMN activity; with reasons pertaining to the selection of this frequency outlined below.

Firstly, a previous attempt to explore frequency and regional activity associated with the DMN failed. EEG data used in this pilot study were from an eyes-closed 15-minute pre-pulse inhibition (PPI) task (initially collected for a different purpose). It seemed feasible that inference could be drawn about the DMN in this task, consistent with the view that the DMN is constantly active and its activity is modulated in response to specific task demands (Raichle et al., 2001). Therefore, based on: (1) the notion that the DMN is characterised by very low frequencies (e.g. Helps et al., 2008); (2) the results of Chen et al. (2008) who observed widespread delta (0.5 – 3.5 Hz) frequency across frontal regions (discussed in section *2.5*, chapter 2); and (3) that frontal regions are implicated in the brain's DMN (i.e. Gusnard et al., 2001); delta frequency (0.5-3.5 Hz) was investigated across frontal scalp sites as a potential electrophysiological signature of DMN activity. Findings, however, revealed no significant relationship between this frequency range and localised prefrontal brain activity. Given this result could have been due to the task employed (engaging the stimulus-driven orienting network, measuring inhibitory control/startle response), and that PPI tasks have been shown to evoke oscillatory activity in the gamma (30-48 Hz) range across frontal and temporal sites (e.g. Kedzior, Koch & Basar-Eroglu, 2007), it was decided that this analysis would not be pursued and that instead, higher-frequency correlates of DMN activity from resting-state data would be investigated.

The second reason for selecting beta frequency was based on previous resting-state studies reporting a relationship between this frequency range and SLF fluctuations in the fMRI BOLD

signal within DMN regions. For example, having subdivided the beta range into three bands (beta-1: 13-16 Hz; beta-2: 17-23 Hz; beta-24-30 Hz), Laufs et al. (2003) observed significant positive correlations between beta-2 power (17-23 Hz) and SLF fluctuations in the fMRI BOLD signal in a number of DMN regions including: the left/right dorsal medial prefrontal and posterior cingulate cortices; precuneus; and left/right temporoparietal areas. In addition, findings also revealed alpha frequency (8-12 Hz) showed no relationship to DMN regions, and was instead significantly negatively correlated with SLF fluctuations in the fMRI BOLD signal in frontal and parietal regions that are commonly implicated in attention function. Beta frequency has been further established as an electrophysiological signature of the DMN in studies linking particular resting state networks (i.e. the DMN, dorsal attention (goal-driven) network etc.) with specific combinations of EEG oscillations (e.g. Jann et al., 2010; Mantini et al., 2007; although it should be noted that these studies also reported positive correlations between the DMN and alpha frequencies); and also in studies showing that beta power (13-30 Hz) is significantly positively correlated with functional connectivity in the DMN (e.g. Hlinka et al., 2010; see section *2.6* in chapter 2 for reviews of these studies).

In line with the findings discussed above, it was hypothesised that beta frequency (13-30 Hz) would be significantly positively correlated with SLF fluctuations in the fMRI BOLD signal in DMN regions, identified on an individual basis using functional connectivity analysis (i.e. medial prefrontal, posterior cingulate and parietal regions).

4.2. Method

4.2.1. Technical development work

Data reported in this experiment were obtained from an eyes-closed resting-state measure (5 minutes). This was incorporated into a series of technical development studies as a baseline condition. Additional technical development work included an eyes-open visual N-Back task (10 minutes); an eyes-closed auditory odd/even number decision task (14 minutes); and an eyes-open visual pavlovian conditioning working memory task (10 minutes). Data from the eyes-closed auditory odd/even number decision task are reported in experiments 2 (chapter 5) and 3 (chapter 6). Data from the other two tasks are not reported in this thesis.

4.2.2. Participants

Twelve participants (5 male, 7 female) took part in this study (mean age = 29.08, SD = 6.76, range = 18-41). Data from two participants were excluded: one due to an insufficient number of fMRI volumes available, and the other due to excessive head movements during scanning; data from ten participants are therefore included in this analysis (4 male, 6 female; mean age = 28.9, SD = 7.46). Participants had no history of neurological or psychiatric illness or any other medical conditions that may have affected their participation. Participants also had no known history of claustrophobia, metal implants, and had normal or normal-to-corrected vision and hearing. Prior to EEG/fMRI acquisition and scanning, each participant provided written informed consent in accordance with ethical guidelines and approval of the Tayside Committee for Medical Research Ethics; and also completed an MRI safety questionnaire in accordance with guidelines set out by the Clinical Research Centre, Ninewells Hospital, Dundee.

4.2.3. Resting-state data acquisition

Participants were instructed to remain as motionless as possible with their eyes-closed for 5-minutes. No instruction or thought probe was given to participants regarding what they should think about during this time.

4.2.4. Electrophysiological recordings

Scalp EEG was recorded at 64 scalp sites using a Brain Cap MR compatible cap (EasyCap, Herrsching, Germany). Electrocardiographic data was recorded using an electrode positioned on the back and referenced to Cz. EEG Electrodes were equipped with an additional 5 kΩ in series-resistor and impedances were kept below 20 kΩ. A band-pass filter (0.05 to 250 Hz) was applied and the EEG was sampled continuously at 5 kHz with sensitivity of 0.25 microvolts, referenced to Cz. Data was acquired using Brain Amp MR+ amplifiers (Brainproducts, Munich, Germany; http://www.brainproducts.com) which were positioned approximately 20 cm outside the bore of the scanner and sampling of EEG was synchronized to the scanner clock. The EEG signal was transmitted via fibre optic cables to Brain Vision Recorder software (Brainproducts, Munich, Germany; http://www.brainproducts.com) available on a computer situated in the scanner control room.

4.2.5. Electroencephalography preprocessing

In order to test whether beta frequency was a significant predictor of SLF fluctuations in the fMRI BOLD signal, several preprocessing steps were conducted offline using Brain Analyzer 2 (Brainproducts, Munich, Germany; http://www.brainproducts.com). Preprocessing steps were as follows: (1) *Scanner Artifact Correction*: in order to detect and correct for artifacts associated with changes in the magnetic field in the scanner. (2) *Pulse Artifact Correction*: allowing for the

correction of cardioballistic (CB) artifacts; this was done in semiautomatic mode, using the range of 50 pulses per minute as the minimal pulse rate and 120 pulses per minute as the maximal pulse rate. (3) A separate CB *Segmentation*: allowing the subdivision of EEG into 1000ms epochs, this step was not essential at this point but it was conducted in order to determine how well the pulse artifact correction had worked. (4) *Edit Markers*: changing the fourth volume to the start marker and last volume to the end marker. (5) 5 minute *Segmentation:* this was based on the newly defined 'start' and 'end' markers. (6) *Continuous Wavelet Transform*: this was done using frequency parameters of: minimal frequency = 0.5 Hz; maximal frequency = 40 Hz in 10 frequency bands. (7) *Wavelets Layer Extraction*: allowing for the extraction of the layer representative of beta frequency (13-30 Hz). (8) Application of a filter (*Filters*): applied to the beta frequency amplitude measure to remove any spurious short interval changes in the EEG signal (this varied between 1-5 Hz across participants). (9) *Level trigger*: setting threshold markers (varying between channels and participants) on channels of interest (Fz, Cz, Pz in this experiment) in order detect regions of peak beta frequency. (10) *Export Markers:* this allowed for the exportation of peak timing information for the later first-level analysis in SPM8 (http://www.fil.ion.ucl.ac.uk/spm/). (11) *Segmentation:* this was based around the newly defined markers (+/- 200ms) (12) Peak Information Export: Peak amplitude measures were exported and combined with peak timing information for use as a parametric predictor in the first-level analysis stage in SPM8 (outlined in section *4.2.6*). Note that visual illustrations of the outcomes of key preprocessing steps for one participant are available in appendix A.

4.2.6. SPM8 setup for determining EEG predictors of fluctuations in fMRI BOLD signal

SPM8 was used in order to determine whether beta-frequency (13-30 Hz) was a significant predictor of SLF fluctuations in the fMRI BOLD signal. Key first-level setup steps included: (1) *Units for design*: scans; (2) *Interscan interval (TR)*: 2.5s; (3) *Microtime resolution*: 16 (this was the default setting in SPM8); (4) *Microtime onset*: 1 (this was the default setting in SPM8). Data and design setup steps were as follows: (1) *Scans*: 120 preprocessed fMRI scans (note that fMRI preprocessing is outlined in section *4.2.8*); (2) *Predictor onsets*: (A) Timing of Beta frequency amplitude peaks; *Predictor magnitudes*: (B) Corresponding amplitude measures of peak beta power; (3) Regressors: Movement parameters: x, y, z, pitch, roll, yaw (obtained from SPM8 preprocessing stage: outlined in section *4.2.8*). All other first-level settings were default settings within SPM8.

4.2.7. Functional magnetic resonance imaging acquisition

Data was acquired on a 3T Trio MR scanner (Siemens, Erlangen, Germany) using a transmit body coil and a 12-channel receive-only head coil and the head was secured using foam pads. A T1-weighted sagittal MPRAGE structural image was obtained prior to the acquisition of functional images (176 slices). 124 functional images were acquired using a BOLD contrast sensitive gradient echo echo-planar sequence (TE = 30ms; TR = 2500ms; FOV = 240mm; matrix size = 64x64).

4.2.8. Functional magnetic resonance imaging preprocessing

In order to reduce the effects of confounding measurement variables on neuronal activity measures and to facilitate across subject comparisons, several preprocessing steps were conducted using Statistical Parametric Mapping software (SPM8;

http://www.fil.ion.ucl.ac.uk/spm/). Note that whilst 124 functional images were acquired, the first four volumes of fMRI data were discarded to allow for magnetic saturation effects; preprocessing steps then performed were as follows: (1) *Realignment* (estimate and reslice), in order to remove movement related artifact, and also to produce a time series of translations and rotations for possible use as a covariate in subsequent analyses. (2) *Co-registration* (estimate only) of the mean functional image to the T1-weighted sagittal MPRAGE structural image. (3) *Segmentation* of the T1-weighted sagittal MPRAGE structural image using the grey and white matter and cerebral spinal fluid probability maps as priors. (4) *Spatial Normalisation* (Normalise Write) of the co-registered functional images to the MNI template using parameters from segmentation and coregistration. (5) *Non-spatial Normalization* (using a MATLAB routine provided by Dr Gordon Waiter, University of Aberdeen), whereby the signal in each functional image was normalised to a whole brain mode range of 1000. In addition this toolbox calculated a mean global signal for each time point that was used in the General Linear Model in the CONN preprocessing stage. (6) *Spatial smoothing* of the normalised and realigned images, where full Width at Half Maximum (FWHM) was changed from [8 8 8] to [6 6 6] in order to enhance signal detail for subsequent correlation analyses.

4.2.9. ROI seed based functional connectivity analysis using 'conn' toolbox

Functional connectivity was assessed using the MATLAB (http://www.mathworks.co.uk/products/matlab/) toolbox *CONN* v.12.i (http;//www.nitrc.org/projects/conn). Bivariate correlations were conducted as a method of investigating the pairwise connectivity between each ROI to other voxels within the brain. CONN set-up steps, including task related information are available in appendix B.

4.2.10. Selection of ROIs

4.2.10.1. DMN (task-negative) seed ROIs based on Fox et al. (2005)

Four primary seed regions that typically show deactivation during attention demanding tasks were included in this analysis. The regions were the left lateral parietal area (LLP; -42, -68, 38), medial prefrontal cortex (MPFC; 0, 54, -8), posterior cingulate cortex (PCC; 0, -56, 28) and the right lateral parietal area (RLP; 48, -60, 38). These regions, also referred to as *task-negative* regions, were functionally defined as 10mm spheres centred at the locations reported in Fox et al. (2005). Whilst Fox and colleagues identified several additional task-negative/DMN regions, in the current series of experiments, LLP, MPFC, PCC and RLP were selected due to: (1) being representative of frontal, midline and parietal portions of the DMN; and (2) existing as predefined ROIs within the CONN toolbox.

4.2.10.2. Task-positive ROIs based on Fox et al. (2005)

As previously stated according to Fox et al. (2005) task-positive regions, typically active during attention-demanding tasks, include the frontal eye fields (FEF, BA6), intraparietal sulcus (BA7) and middle temporal cortex (MT+; BA37). Note that Fox et al. did in fact identify several additional task-positive regions, but restricted their analyses to these three regions: the current experiment therefore employs a similar design). Furthermore, there was some disparity between the identification of BAs and their cortical areas proposed by Fox et al. (2005) and those produced using the CONN toolbox in the current study. Whereas Fox and colleagues defined BA6 as the FEFs, here BA6 is referred to more broadly as the premotor cortex; BA7 as the somatosensory cortex; and BA37 as the fusiform gyrus.

4.2.10.3. Additional ROIs implicated in the DMN based on Buckner et al. (2008)

As previously stated according to Buckner et al. (2008) DMN regions include the ventral medial prefrontal cortex, posterior cingulate/retrosplenial cortex, inferior parietal lobule, lateral temporal cortex, dorsal medial prefrontal cortex and the hippocampal formation. As with Fox et al. (2005) there was some disparity between the regions identified by Buckner et al. (2008) and those produced in the CONN toolbox. Thus, DMN regions included: the anterior prefrontal cortex (BA10) ventral/dorsal anterior cingulate cortices (BA24, BA32), retrosplenial cingulate cortex (BA29), cingulate cortex (BA30), ventral/dorsal posterior cingulate cortices (BA23, BA31), angular gyrus (BA39), supramarginal gyrus (BA40), middle temporal gyrus (BA21) and the parahippocampal cortex (BA36)

4.3. Results

4.3.1. Analysis 1a: The relationship between the DMN (also known as the task-negative network; Fox et al., 2005) and the task-positive (attention-associated/externally directed) network

The correlations between DMN regions and task-positive regions are shown in figure 4.1. Tables 4.1.1-4.1.4 illustrate connectivity areas (as produced by the CONN toolbox), Brodmann area (BA) labels, the strength of connectivity (*Beta (B)* value) and the significance (*p* value). Note that *B* values represent Fisher-transformed correlation coefficient values; and also that significant ($p<.05$) correlations only are reported within figures and tables. In both the figures

and tables, positive correlations are shown in red text and negative correlations are shown in blue, and DMN seed regions (Fox et al., 2005) are displayed in *italics*.

Table 4.1.1. Connectivity between the left lateral parietal (LLP) region of the DMN and task-positive regions defined by Fox et al. (2005).

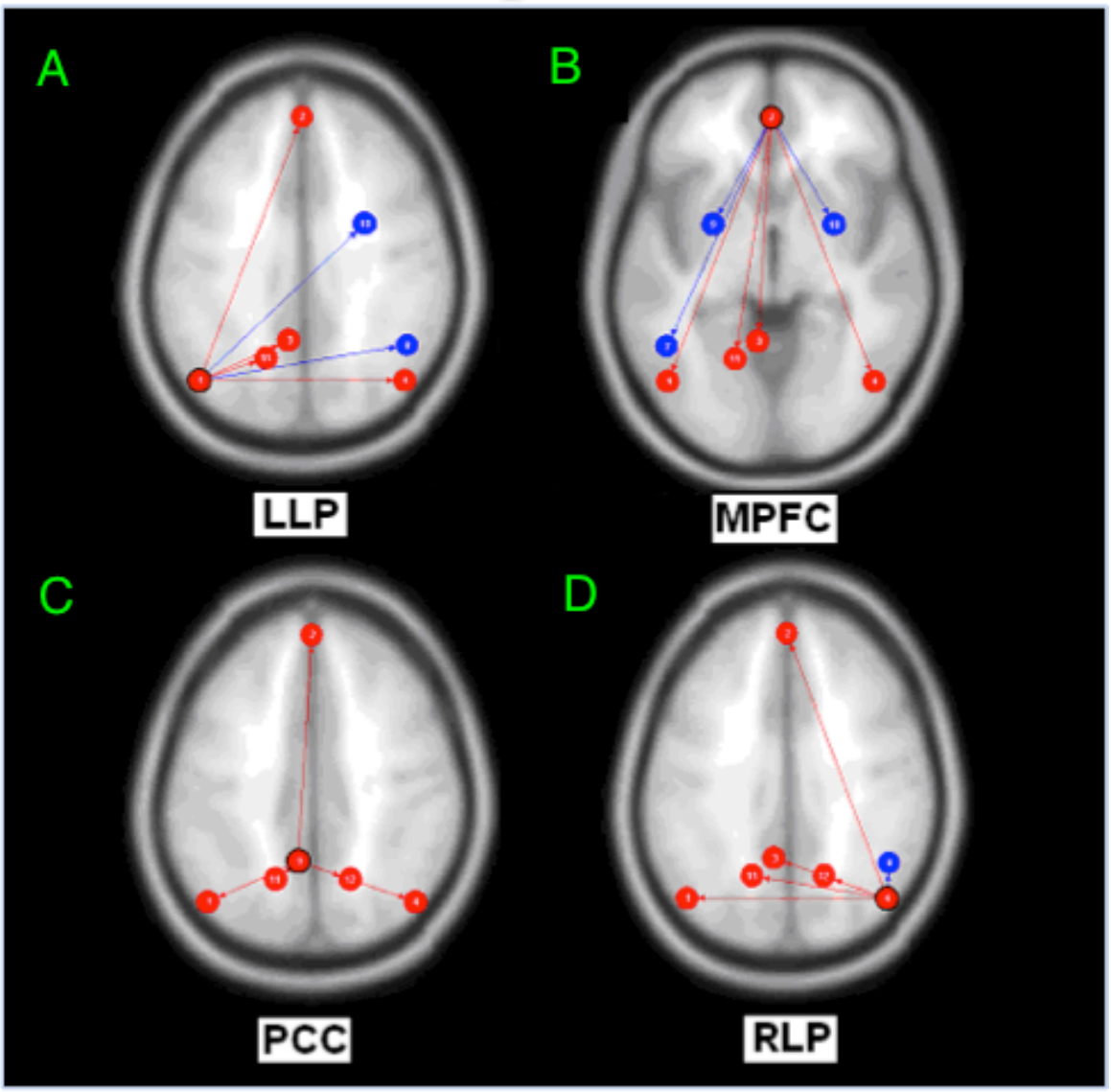

Figure 4.1. Relationship between DMN and task-positive regions as defined by Fox et al. (2005). (A) Connectivity between LLP and task-positive regions (B) Connectivity between MPFC and task-positive regions (C) Connectivity between PCC and task-positive regions (D) Connectivity between RLP and task-positive regions.

Connectivity area	Brodmann area	Brain region	*B*	*p*	Correlation (+/-)

(2)	*Seed ROI*	*Medial prefrontal cortex*	*0.42*	*0.008*	+
(3)	*Seed ROI*	*Posterior cingulate cortex*	*0.50*	*0.003*	+
(4)	*Seed ROI*	*Right lateral parietal*	*0.58*	*<0.001*	+
(8)	37 (R)	Fusiform gyrus	-0.16	0.027	-
(10)	6 (R)	Premotor Cortex	-0.20	0.042	-
(11)	7 (L)	Somatosensory Association cortex	0.32	0.008	+

As shown in table 4.1.1 and figure 4.1A, there were significant positive correlations between DMN regions LLP and MPFC, PCC and RLP. Unexpectedly, LLP was also positively correlated to the task-positive region representing the intraparietal sulcus (left somatosensory association cortex; BA7) commonly implicated in the brain's dorsal attention (goal-driven) network. As predicted, significant negative correlations were observed between the LLP and a task-positive region representing the middle temporal cortex (right fusiform gyrus; BA37) and between the LLP and a region representing the frontal eye fields (right premotor cortex; BA6). No significant correlations were observed between LLP and left BA6, right BA7, or left BA37.

Table 4.1.2. Connectivity between the medial prefrontal cortex (MPFC) region of the DMN and task-positive regions defined by Fox et al. (2005).

Connectivity area	Brodmann area	Brain region	*B*	*p*	Correlation (+/)
(1)	*Seed ROI*	*Left lateral parietal*	*0.42*	*0.011*	+
(3)	*Seed ROI*	*Posterior cingulate cortex*	*0.39*	*0.008*	+
(4)	*Seed ROI*	*Right lateral parietal*	*0.33*	*0.011*	+
(7)	37 (L)	Fusiform gyrus	-0.13	0.011	-
(9)	6 (L)	Premotor cortex	-0.16	0.011	-
(10)	6 (R)	Premotor cortex	-0.28	0.011	-
(11)	7 (L)	Somatosensory Association cortex	0.14	0.011	+

Table 4.1.2 and figure 4.1B illustrates the significant positive correlations between the MPFC and the other DMN areas as defined by Fox et al. (2005). As predicted, significant negative correlations were observed between the MPFC and the left fusiform gyrus (BA37) and the left/right premotor cortices (BA6). Unexpectedly there was a significant negative correlation

between the MPFC and the left somatosensory association cortex (BA7; as previously stated representing the task-positive *intraparietal sulcus*). No significant correlations were observed between MPFC and right BA7 or right BA37.

Table 4.1.3. Connectivity between the posterior cingulate cortex (PCC) region of the DMN and task-positive regions defined by Fox et al. (2005).

Connectivity area	Brodmann area	Brain region	*B*	*p*	Correlation (+/-)
(1)	*Seed ROI*	*Left lateral parietal*	*0.50*	*0.002*	+
(2)	*Seed ROI*	*Medial prefrontal cortex*	*0.39*	*0.002*	+
(4)	*Seed ROI*	*Right lateral parietal*	*0.32*	*0.006*	+
(11)	7 (L)	Somatosensory Association cortex	0.60	<0.001	+
(12)	**7 (R)**	**Somatosensory Association cortex**	**0.37**	**0.001**	**+**

Table 4.1.3 and figure 4.1C, illustrate that unexpectedly, PCC was positively correlated to the left and right somatosensory association cortices (BA7). However, no significant correlations were found between this seed and task-positive left/right premotor cortex (BA6) or the fusiform gyrus (BA37).

Table 4.1.4. Connectivity between the right lateral parietal (RLP) region of the DMN and task-positive regions defined by Fox et al. (2005).

Connectivity area area	Brodmann area	Brain region	*B*	*p*	Correlation (+/-)
(1)	*Seed ROI*	*Left lateral parietal*	*0.58*	*<0.001*	+
(2)	*Seed ROI*	*Medial prefrontal cortex*	*0.33*	*0.011*	+
(3)	*Seed ROI*	*Posterior cingulate cortex*	*0.32*	*0.010*	+
(8)	37 (R)	Fusiform gyrus	-0.19	0.024	-
(11)	7 (L)	Somatosensory Association cortex	0.26	0.034	+
(12)	7 (R)	Somatosensory Association cortex	0.41	0.003	+

Table 4.1.4 and figure 4.1D, show the significant positive correlations between the RLP and other DMN regions. Unexpectedly, RLP was also positively correlated with the task-positive left/right somatosensory cortices (BA7). However a negative correlation was observed between the RLP and the right fusiform gyrus (BA37). No significant correlations were observed

between RLP and task-positive left/right premotor cortex (BA6) or the left fusiform gyrus (BA37).

4.3.1.1. Summary of results of analysis 1a: Is the DMN (task-negative/internally-directed network) negatively correlated with the task-positive (externally-directed) network?

In summary, the results of analysis 1a confirm the strategy employed as a method of measuring the functional connectivity of the DMN. Results also support the widely reported notion that the DMN is active during task-free rest, revealing DMN ROIs: LLP, MPFC, PCC and RLP, were strongly positively correlated with each other in 5-minutes of resting-state fMRI data. It should be noted that not all DMN regions were negatively correlated to all task-positive regions identified by Fox et al. (2005). Instead, only individual components of each network were correlated with each other: LLP, MPFC and RLP were negatively correlated with the task-positive fusiform gyrus (BA37; representing the *middle temporal cortex*); LLP and MPFC were negatively correlated with the task-positive premotor cortex (BA6; representing the *frontal eye field*); and PCC showed no relationship to these regions. Furthermore, each DMN ROI was positively correlated with the left and/or right task-positive somatosensory association cortex (BA7), representing the *intraparietal sulcus* (an area commonly implicated in the dorsal attention (goal-driven) network). Overall, these results only partially support the prediction that the DMN would be negatively correlated with the task-positive (attention-associated/externally directed) network as identified by Fox et al. (2005); this is because only individual nodes of each network were anti-correlated with each other. Discussion of these results is presented in section *4.4.1.2*.

4.3.2. Analysis 1b: The relationship between DMN regions identified by Fox et al. (2005) and those identified by Buckner et al. (2008).

Analysis 1b sought to investigate the direction and strength of correlation between DMN regions (LLP, MPFC, PCC, RLP; Fox et al., 2005) and regions commonly identified during studies of resting-state brain activity/task-induced deactivation as defined by Buckner et al (2008). This allowed for the generation of a larger set of regions implicated in the brain's DMN thus providing greater insight into this network as a whole. Correlations between these regions are displayed in figure 4.2 and tables 4.2.1-4.2.4. Again, note that only significant correlations ($p<.05$) are reported; in both the figures and the tables, positive correlations are shown in red text and negative correlations are shown in blue; and, within tables, seed regions are displayed in *italics*.

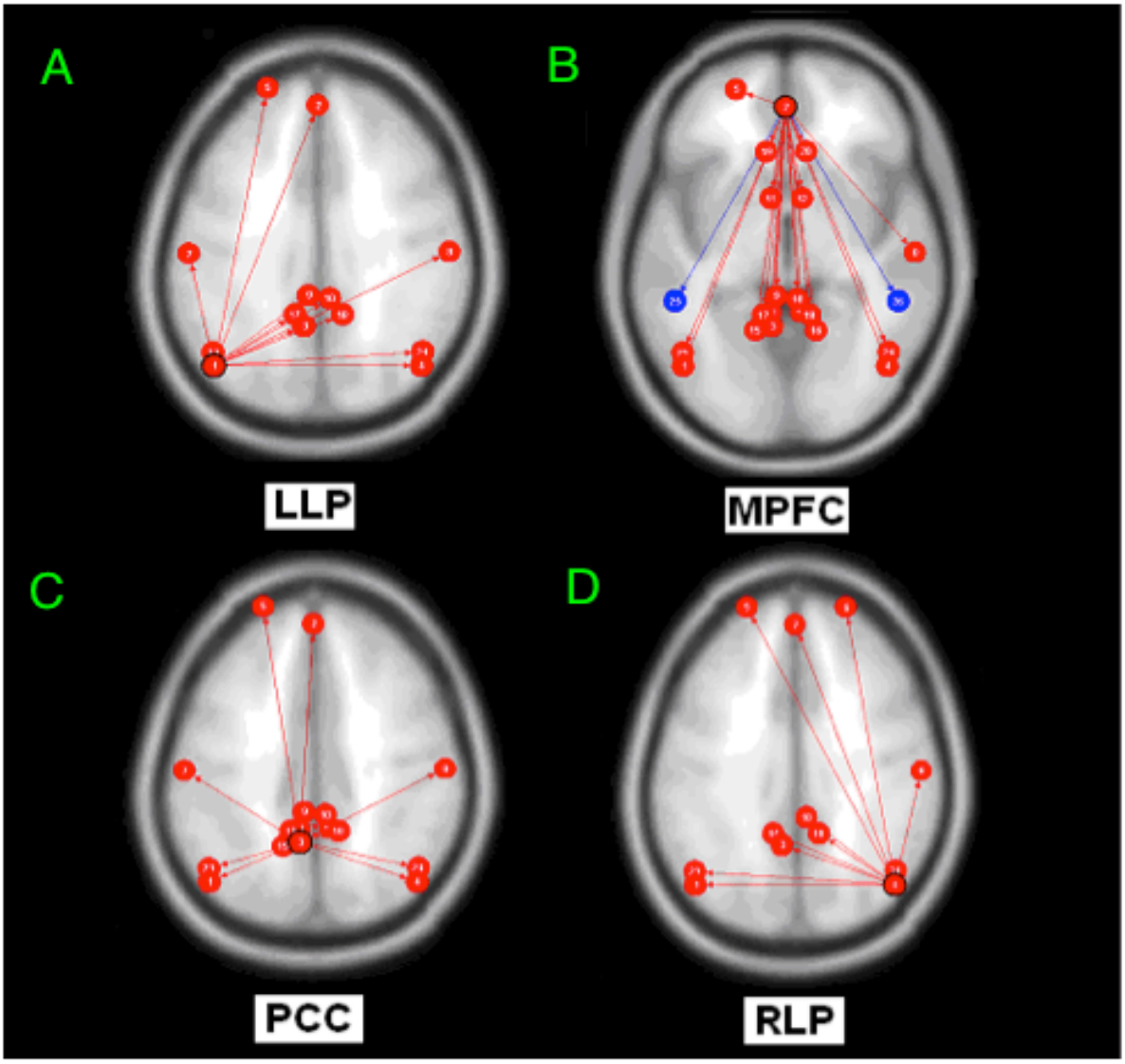

Figure 4.2. Relationship between DMN regions (Fox et al., 2005) and areas defined as the DMN by Buckner et al. (2008). (A) LLP connectivity to Buckner et al. defined areas (B) MPFC connectivity to Buckner et al. defined areas (C) PCC connectivity to Buckner et al. defined areas (D) RLP connectivity to Buckner et al. defined areas.

Table 4.2 1. Connectivity between the left lateral parietal (LLP) region of the DMN (Fox et al., 2005) and DMN regions defined by Buckner et al. (2008).

Connectivity area	Brodmann area	Brain region	*B*	*p*	Correlation (+/-)
(2)	*Seed ROI*	*Medial prefrontal cortex*	*0.42*	*0.007*	+
(3)	*Seed ROI*	*Posterior cingulate cortex*	*0.50*	*0.002*	+
(4)	*Seed ROI*	*Right lateral parietal*	*0.58*	*<0.001*	+
(5)	10 (L)	Anterior prefrontal cortex	0.37	0.001	+
(7)	21 (L)	Middle temporal gyrus	0.27	0.002	+
(8)	21 (R)	Middle temporal gyrus	0.29	0.005	+
(9)	23 (L)	Ventral posterior cingulate cortex	0.22	0.002	+
(10)	23 (R)	Ventral posterior cingulate cortex	0.16	0.012	+
(17)	31 (L)	Dorsal posterior cingulate cortex	0.50	<0.001	+
(18)	31 (R)	Dorsal posterior cingulate cortex	0.27	0.018	+
(23)	39 (L)	Angular gyrus	1.10	<0.001	+
(24)	39 (R)	Angular gyrus	0.56	<0.001	+

Table 4.2.1 and figure 4.2A show there were significant positive correlations between LLP and a number of DMN regions identified by Buckner et al. (2008), including: the left anterior prefrontal cortex (BA10); and the left/right middle temporal gyri (BA21), ventral and dorsal posterior cingulate cortices (BA23, BA31) and the angular gyri (BA39).

Table 4.2.2. Connectivity between the medial prefrontal cortex (MPFC) region of the DMN (Fox et al., 2005) and DMN regions defined by Buckner et al. (2008).

Connectivity area	Brodmann area	Brain region	*B*	*p*	Correlation (+/-)
(1)	*Seed ROI*	*Left lateral parietal*	*0.43*	*0.005*	+
(3)	*Seed ROI*	*Posterior cingulate cortex*	*0.39*	*0.002*	+
(4)	*Seed ROI*	*Right lateral parietal*	*0.33*	*0.007*	+
(5)	10 (L)	Anterior prefrontal cortex	0.30	0.001	+
(8)	21 (R)	Middle temporal gyrus	0.22	0.009	+
(9)	23 (L)	Ventral posterior cingulate cortex	0.34	<0.001	+
(10)	23 (R)	Ventral posterior cingulate cortex	0.33	<0.001	+
(11)	24 (L)	Ventral anterior cingulate cortex	0.28	0.005	+
(12)	24 (R)	Ventral anterior cingulate cortex	0.20	0.008	+
(13)	29 (L)	Retrosplenial cingulate cortex	0.30	0.001	+
(14)	29 (R)	Retrosplenial cingulate cortex	0.28	0.002	+
(16)	30 (R)	Cingulate cortex	0.30	0.007	+
(17)	31 (L)	Dorsal posterior cingulate cortex	0.57	<0.001	+
(18)	31 (R)	Dorsal posterior cingulate cortex	0.43	0.001	+
(19)	32 (L)	Dorsal anterior cingulate cortex	0.53	<0.001	+
(20)	32 (R)	Dorsal anterior cingulate cortex	0.39	<0.001	+
(23)	39 (L)	Angular gyrus	0.28	0.011	+

(24)	39 (R)	Angular gyrus	0.35	0.001	+
(25)	40 (L)	Supramarginal gyrus	-0.32	<0.001	-
(26)	40 (R)	Supramarginal gyrus	-0.29	0.025	-

Table 4.2.2 and figure 4.2B show in addition to a number of the areas positively correlated with the LLP, MPFC was also positively correlated with the left/right ventral anterior cingulate cortex (BA24), retrosplenial cingulate cortex (BA29), dorsal anterior cingulate cortex (BA32) and the right cingulate cortex (BA30). Unpredicted, there were significant negative correlations between MPFC and the left and right supramarginal gyrus (BA40).

Table 4.2.3. Connectivity between the posterior cingulate cortex (PCC) region of the DMN (Fox et al., 2005) and DMN regions defined by Buckner et al. (2008).

Connectivity area	Brodmann area	Brain region	*B*	*p*	Correlation (+/-)
(1)	*Seed ROI*	*Left lateral parietal*	*0.50*	*0.002*	+
(2)	*Seed ROI*	*Medial prefrontal cortex*	*0.39*	*0.002*	+
(4)	*Seed ROI*	*Right lateral parietal*	*0.32*	*0.007*	+
(5)	10 (L)	Anterior prefrontal cortex	0.29	0.007	+
(7)	21 (L)	Middle temporal gyrus	0.19	0.039	+
(8)	21 (R)	Middle temporal gyrus	0.31	0.002	+
(9)	23 (L)	Ventral posterior cingulate cortex	0.47	<0.001	+
(10)	23 (R)	Ventral posterior cingulate cortex	0.41	0.001	+
(13)	29 (L)	Retrospenial cingulate cortex	0.26	0.027	+
(14)	29 (R)	Retrospenial cingulate cortex	0.21	0.025	+
(15)	**30 (L)**	**Cingulate cortex**	**0.29**	**0.012**	**+**
(17)	31 (L)	Dorsal posterior cingulate cortex	0.89	<0.001	+
(18)	31 (R)	Dorsal posterior cingulate cortex	0.56	<0.001	+
(23)	39 (L)	Angular gyrus	0.56	0.002	+
(24)	39 (R)	Angular gyrus	0.43	0.003	+

Table 4.2.3 and figure 4.2C show there were significant positive correlations between PCC and the left anterior prefrontal cortex (BA10), left/right middle temporal gyri (BA21) ventral/dorsal posterior cingulate cortices (BA23, BA31), retrosplenial cingulate cortex (BA29) and angular gyri (BA39). PCC was also positively correlated with the left cingulate cortex (BA30).

Table 4.2.4. Connectivity between the right lateral parietal (RLP) region of the DMN (Fox et al., 2005) and DMN regions defined by Buckner et al. (2008).

Connectivity area area	Brodmann area	Brain region	*B*	*p*	Correlation (+/-)
(1)	*Seed ROI*	*Left lateral parietal*	*0.58*	*<0.001*	+
(2)	*Seed ROI*	*Medial prefrontal cortex*	*0.33*	*0.011*	+
(3)	*Seed ROI*	*Posterior cingulate cortex*	*0.32*	*0.01*	+
(5)	10 (L)	Anterior prefrontal cortex	0.20	0.023	+
(6)	10 (R)	Anterior prefrontal cortex	0.26	0.003	+
(8)	21 (R)	Middle temporal gyrus	0.24	0.010	+
(10)	23 (R)	Ventral posterior cingulate cortex	0.23	0.017	+
(17)	31 (L)	Dorsal posterior cingulate cortex	0.40	0.002	+
(18)	31 (R)	Dorsal posterior cingulate cortex	0.44	0.001	+
(23)	39 (L)	Angular gyrus	0.38	<0.001	+
(24)	39 (R)	Angular gyrus	0.99	<0.001	+

Table 4.2.4 and figure 4.2D show that there were significant positive correlations between the RLP and the right middle temporal gyrus (BA21) and ventral posterior cingulate cortex (BA23). RLP was also significantly positively correlated to the left/right anterior prefrontal (BA10) and dorsal posterior cingulate cortices (BA31) and angular gyri (BA39).

4.3.2.1. Summary of results of analysis 1b: Are regions of the DMN identified by Fox et al. (2005) positively correlated to those identified by Buckner et al. (2008)?

Analysis 1b revealed individual DMN ROIs defined by Fox et al. (2005) were significantly positively correlated to a number of DMN regions identified by Buckner et al. (2008); offering support to the hypothesis that these two sets of DMN regions would be functionally connected. Unpredicted was that the MPFC was negative correlated with parietal left/right supramarginal regions (BA40) and furthermore, no DMN region specified by Fox et al. was correlated with the parahippocampal cortex (BA36), a putative DMN region defined by Buckner and colleagues. Results also revealed a left/right dichotomy in the spread of regions that LLP/RLP were

correlated to, with both parietal regions showing an ipsilateral bias in lateralisation. Discussion of these results is presented in section *4.4.1.3*.

4.3.3. Analysis 1c: An exploration of the relationship between DMN regions as identified by Fox et al. (2005) and regions covering the whole of the cerebral cortex

Of final interest, analysis 1c aimed to explore the direction and strength of correlation between primary DMN ROIs (LLP, MPFC, PCC, RLP; Fox et al., 2005) and regions covering the whole of the cerebral cortex; thus providing insight into the way in which the DMN interacts with the rest of the brain. Figure 4.3 and tables 4.3.1-4.3.4 illustrate the results of this exploratory analysis. The surrounding text in figure 4.3 details regions that were negatively correlated to the corresponding seed and lists some of their associated functions. Again, note that only significant correlations ($p<.05$) are reported; in both the figures and the tables, positive correlations are shown in red text and negative correlations are shown in blue; and within tables seed regions are displayed in *italics*.

L/R insular cortex *(emotion, perception, self-awareness etc.)*
R fusiform gyrus *(face, body, word processing/ recognition)*
R primary auditory cortex *(processes auditory information)*
L/R IFC pars opercularis *(language production)*

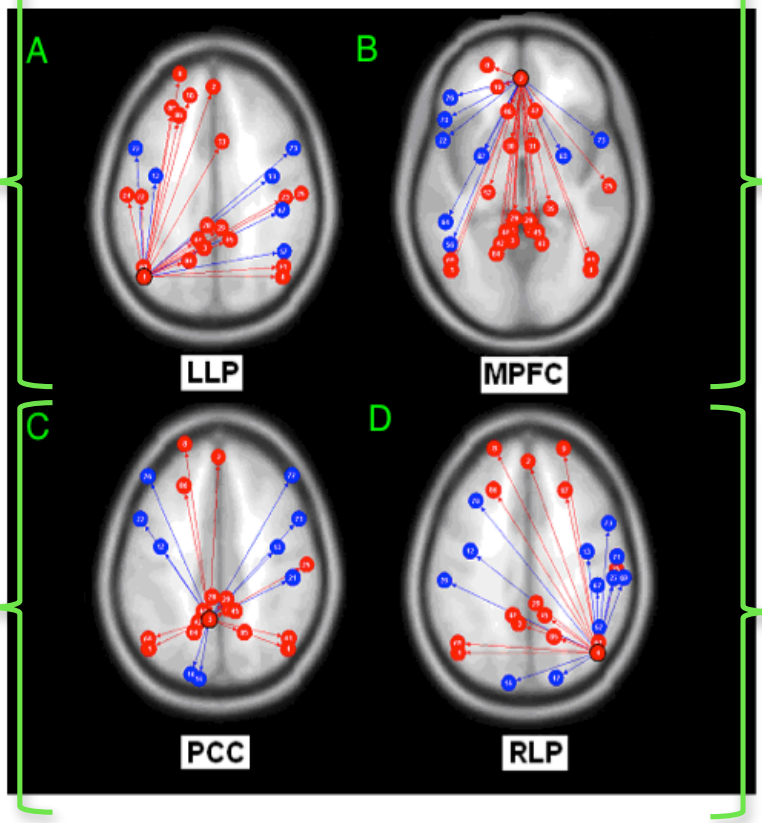

L fusiform gyrus
L supramarginal gyrus *(Phonological processing, spatial orientation, semantic representation)*
L/R IFC pars opercularis
L IFC pars triangularis
L dorsolateral PFC
L/R premotor cortex *(Storage of motor patterns, voluntary activities)*

L/R insular cortex
L primary visual cortex *(processes visual information)*
L secondary visual cortex
R primary somatosensory cortex *(sensory modalities: touch, temperature etc.)*
L/R IFC pars opercularis
L/R dorsolateral PFC *(working memory, planning, decision making)*

L/R insular cortex
L primary visual cortex
R secondary visual cortex
L/R superior temporal gyrus *(emotion perception)*
R fusiform gyrus
R primary auditory cortex
R subcentral area
R IFC pars opercularis
L inferior prefrontal gyrus *(language production/ comprehension)*

Figure 4.3. Relationship between DMN regions (Fox et al., 2005) and regions covering the whole of the cerebral cortex. (A) LLP connectivity to all other brain regions (B) MPFC connectivity to all other brain regions (C) PCC connectivity to all other brain regions (D) RLP connectivity to all other brain regions. The surrounding text illustrates negatively correlated regions to each seed and details some of their associated functions (L = left/ R= right).

Table 4.3.1. Connectivity between the left lateral parietal (LLP) region of the DMN (Fox et al., 2005) and regions covering the whole of the cortex.

Connectivity area	Brodmann area	Brain region	*B*	*p*	Correlation (+/-)
(2)	*Seed ROI*	*Medial prefrontal cortex*	*0.42*	*0.015*	+
(3)	*Seed ROI*	*Posterior cingulate cortex*	*0.50*	*0.004*	+
(4)	*Seed ROI*	*Right lateral parietal*	*0.58*	*<0.001*	+
(8)	10 (L)	Anterior Prefrontal Cortex	0.37	0.004	+
(10)	11 (L)	Orbitofrontal Cortex	0.19	0.008	+
(12)	13 (L)	Insular Cortex	-0.34	0.004	-
(13)	13 (R)	Insular Cortex	-0.38	0.001	-
(22)	20 (L)	Inferior Temporal Gyrus	0.16	0.031	+
(23)	20 (R)	Inferior Temporal Gyrus	0.12	0032	+
(24)	21 (L)	Middle Temporal Gyrus	0.27	0.004	+
(25)	21 (R)	Middle Temporal Gyrus	0.29	0.011	+
(28)	23 (L)	Ventral Posterior Cingulate Cortex	0.22	0.006	+
(29)	23 (R)	Ventral Posterior Cingulate Cortex	0.16	0.023	+
(33)	25 (R)	Subgenual cortex	0.09	0.023	+
(44)	31 (L)	Dorsal Posterior Cingulate Cortex	0.50	0.001	+
(45)	31 (R)	Dorsal Posterior Cingulate Cortex	0.27	0.032	+
(57)	37 (R)	Fusiform gyrus	-0.16	0.044	-
(60)	39 (L)	Angular gyrus	1.10	<0.001	+
(61)	39 (R)	Angular gyrus	0.56	0.001	+
(67)	41 (R)	Primary Auditory Cortex	-0.15	0.029	-
(72)	44 (L)	IFC pars opercularis	-0.25	0.010	-
(73)	44 (R)	IFC pars opercularis	-0.32	0.009	-
(84)	7 (L)	Somatosensory Association Cortex	0.32	0.016	+
(86)	8 (L)	Dorsal Frontal Cortex	0.43	0.004	+
(88)	9 (L)	Dorsolateral Prefrontal Cortex	0.25	0.017	+

Table 4.3.1 and figure 4.3A show that there were significant positive correlations between LLP and the left anterior prefrontal cortex (BA10), orbitofrontal cortex (BA11), somatosensory association cortex (BA7), dorsal frontal cortex (BA8), dorsolateral prefrontal cortex (BA9) and the right subgenual cortex (BA25). LLP was also positively correlated with the left/right inferior temporal gyri (BA20), middle temporal gyri (BA21), ventral/dorsal posterior cingulate cortices (BA23, BA31) and angular gyri (BA39). Significant negative correlations were observed between LLP and the left/right insular cortex (BA13) and IFC pars opercularis (BA44); along with the right fusiform gyrus (BA37) and right primary auditory cortex (BA41).

Table 4.3.2. Connectivity between the medial prefrontal cortex (MPFC) region of the DMN (Fox et al., 2005) and regions covering the whole of the cortex.

Connectivity area	Brodmann area	Brain region	*B*	*p*	Correlation (+/-)
(1)	*Seed ROI*	*Left lateral parietal*	*0.42*	*0.010*	+
(3)	*Seed ROI*	*Posterior cingulate cortex*	*0.39*	*0.006*	+
(4)	*Seed ROI*	*Right lateral parietal*	*0.33*	*0.018*	+
(8)	10 (L)	Anterior Prefrontal Cortex	0.30	0.007	+
(10)	11 (L)	Orbitofrontal Cortex	0.20	0.011	+
(25)	21 (R)	Middle Temporal Gyrus	0.22	0.022	+
(28)	23 (L)	Ventral Posterior Cingulate Cortex	0.34	0.001	+
(29)	23 (R)	Ventral Posterior Cingulate Cortex	0.33	0.001	+
(30)	24 (L)	Ventral Anterior Cingulate Cortex	0.28	0.013	+
(31)	24 (R)	Ventral Anterior Cingulate Cortex	0.20	0.020	+
(35)	27 (R)	Piriform Cortex	0.14	0.006	+
(38)	29 (L)	Retrosplenial Cingulate Cortex	0.30	0.004	+
(39)	29 (R)	Retrosplenial Cingulate Cortex	0.28	0.006	+
(42)	30 (L)	Cingulate Cortex	0.38	0.020	+
(43)	30 (R)	Cingulate Cortex	0.30	0.019	+
(44)	31 (L)	Dorsal Posterior Cingulate Cortex	0.57	0.001	+
(45)	31 (R)	Dorsal Posterior Cingulate Cortex	0.43	0.005	+
(46)	32 (L)	Dorsal anterior Cingulate Cortex	0.53	<0.001	+
(47)	32 (R)	Dorsal anterior Cingulate Cortex	0.39	0.001	+
(52)	35 (L)	Perirhinal cortex	0.14	0.030	+
(56)	37 (L)	Fusiform gyrus	-0.13	0.020	-
(60)	39 (L)	Angular gyrus	0.28	0.026	+
(61)	39 (R)	Angular gyrus	0.35	0.005	+
(64)	40 (L)	Supramarginal Gyrus	-0.32	0.001	-
(72)	44 (L)	IFC pars opercularis	-0.31	0.006	-
(73)	44 (R)	IFC pars opercularis	-0.35	0.011	-
(74)	45 (L)	IFC pars triangularis	-0.14	0.037	-
(76)	46 (L)	Dorsolateral Prefrontal Cortex	-0.21	0.020	-
(82)	6 (L)	Premotor Cortex	-0.16	0.022	-
(83)	6 (R)	Premotor Cortex	-0.28	0.017	-
(84)	7 (L)	Somatosensory Association Cortex	0.14	0.019	+

Table 4.3.2 and figure 4.3B show that there were significant positive correlations between MPFC and the left anterior prefrontal cortex (BA10), orbitofrontal cortex (BA11), perirhinal cortex (BA35) and the somatosensory association cortex (BA7); along with the right middle temporal gyrus (BA21) and piriform cortex (BA27). MPFC was also positively correlated with the left/right ventral posterior/anterior cingulate cortices (BA23, BA24), dorsal posterior/anterior cingulate cortices (BA31, BA32) and angular gyri (BA39). Significant negative correlations were observed between MPFC and the left fusiform gyrus (BA37), the supramarginal gyrus

(BA40), IFC pars triangularis (BA45), dorsolateral prefrontal cortex (BA46); along with the left/right premotor cortex (BA6) and IFC pars opercularis (BA44)

Table 4.3.3. Connectivity between the posterior cingulate cortex (PCC) region of the DMN (Fox et al., 2005) and regions covering the whole of the cortex.

Connectivity area	Brodmann area	Brain region	*B*	*p*	Correlation (+/-)
(1)	*Seed ROI*	*Left lateral parietal*	*0.50*	*0.004*	+
(2)	*Seed ROI*	*Medial prefrontal cortex*	*0.39*	*0.005*	+
(4)	*Seed ROI*	*Right lateral parietal*	*0.32*	*0.015*	+
(8)	10 (L)	Anterior Prefrontal Cortex	0.29	0.028	+
(12)	13 (L)	Insular Cortex	-0.28	0.005	-
(13)	13 (R)	Insular Cortex	-0.31	0.005	-
(14)	17 (L)	Primary Visual Cortex	-0.15	0.05	-
(16)	18 (L)	Secondary Visual Cortex	-0.14	0.28	-
(21)	2 (R)	Primary Somatosensory Cortex	-0.22	0.05	-
(25)	21 (R)	Middle Temporal Gyrus	0.31	0.005	+
(28)	23 (L)	Ventral Posterior Cingulate Cortex	0.47	0.001	+
(29)	23 (R)	Ventral Posterior Cingulate Cortex	0.41	0.002	+
(39)	29 (R)	Retrosplenial Cingulate Cortex	0.21	0.05	+
(42)	30 (L)	Cingulate Cortex	0.29	0.024	+
(44)	31 (L)	Dorsal Posterior Cingulate Cortex	0.89	<0.001	+
(45)	31 (R)	Dorsal Posterior Cingulate Cortex	0.56	<0.001	+
(60)	39 (L)	Angular gyrus	0.56	0.004	+
(61)	39 (R)	Angular gyrus	0.43	0.007	+
(72)	44 (L)	IFC pars opercularis	-0.27	0.005	-
(73)	44 (R)	IFC pars opercularis	-0.27	0.005	-
(76)	46 (L)	Dorsolateral Prefrontal Cortex	-0.22	0.04	-
(77)	46 (R)	Dorsolateral Prefrontal Cortex	-0.22	0.022	-
(84)	7 (L)	Somatosensory Association Cortex	0.60	<0.001	+
(85)	7 (R)	Somatosensory Association Cortex	0.37	0.002	+
(86)	8 (L)	Dorsal Frontal Cortex	0.26	0.021	+

Table 4.3.3 figure 4.3C reveal PCC was significantly positively correlated with left cingulate cortex (BA30) and dorsal frontal cortex (BA8). PCC was also positively correlated with the right middle temporal gyrus (BA21) and retrosplenial cingulate cortex (BA29); along with the left/right ventral/dorsal posterior cingulate cortices (BA23, BA31), angular gyri (BA39) and somatosensory association cortices (BA7). Significant negative correlations were observed

between the PCC and the left primary/secondary visual cortices (BA17, BA18), right primary somatosensory cortex (BA2), and the left/right insular cortices (BA13), IFC pars operculari (BA44), and dorsolateral prefrontal cortices (BA46).

Table 4.3.4. Connectivity between the right lateral parietal (RLP) region of the DMN (Fox et al., 2005) and regions covering the whole of the cortex.

Connectivity area	Brodmann area	Brain region	*B*	*p*	Correlation (+/-)
(1)	*Seed ROI*	*Left lateral parietal*	*0.58*	*<0.001*	+
(2)	*Seed ROI*	*Medial prefrontal cortex*	*0.33*	*0.023*	+
(3)	*Seed ROI*	*Posterior cingulate cortex*	*0.32*	*0.018*	+
(8)	10 (L)	Anterior Prefrontal Cortex	0.20	0.041	+
(9)	10 (R)	Anterior Prefrontal Cortex	0.26	0.007	+
(12)	13 (L)	Insular Cortex	-0.28	0.008	-
(13)	13 (R)	Insular Cortex	-0.34	0.007	-
(14)	17 (L)	Primary Visual Cortex	-0.11	0.048	-
(17)	18 (R)	Secondary Visual Cortex	-0.17	0.025	-
(25)	21 (R)	Middle Temporal Gyrus	0.24	0.019	+
(26)	22 (L)	Superior Temporal Gyrus	-0.22	0.003	-
(27)	22 (R)	Superior Temporal Gyrus	-0.15	0.048	-
(29)	23 (R)	Ventral Posterior Cingulate Cortex	0.23	0.030	+
(44)	31 (L)	Dorsal Posterior Cingulate Cortex	0.40	0.004	+
(45)	31 (R)	Dorsal Posterior Cingulate Cortex	0.44	0.003	+
(57)	37 (R)	Fusiform gyrus	-0.19	0.042	-
(60)	39 (L)	Angular gyrus	0.38	0.001	+
(61)	39 (R)	Angular gyrus	0.99	<0.001	+
(67)	41 (R)	Primary Auditory Cortex	-0.12	0.045	-
(69)	42 (R)	Primary Auditory Cortex	-0.15	0.032	-
(71)	43 (R)	Subcentral Area	-0.22	0.009	-
(73)	44 (R)	IFC pars opercularis	-0.29	0.027	-
(78)	47 (L)	Inferior Prefrontal Gyrus	-0.13	0.028	-
(85)	7 (R)	Somatosensory Association Cortex	0.41	0.006	+
(86)	8 (L)	Dorsal Frontal Cortex	0.18	0.014	+
(87)	8 (R)	Dorsal Frontal Cortex	0.37	0.004	+

Table 4.3.4 and figure 4.3D show that there were significant positive correlations between RLP and the left/right anterior prefrontal (BA10), dorsal posterior cingulate (BA31) and dorsal frontal (BA8) cortices, and the angular gyri (BA39). RLP was also positively correlated with the right ventral posterior cingulate cortex (BA23), somatosensory association cortex (BA7) and middle

temporal gyrus (BA21). Significant negative correlations were observed between RLP and the left primary visual cortex (BA17) and inferior prefrontal gyrus (BA47); along with the right secondary visual cortex (BA18),), fusiform gyrus (BA37), primary auditory cortex (BA41, 42), subcentral area (BA43), and IFC pars opercularis (BA44) and the left. RLP was negatively correlated with the left/right insular cortices (BA13), superior temporal gyri (BA22)

4.3.3.1. Summary of results of analysis 1c: An exploration of the relationship between DMN regions as identified by Fox et al. (2005) and regions covering the whole of the cerebral cortex

The results from this analysis show that during rest, several frontal, posterior and parietal regions are strongly positively correlated. These areas are in line with commonly identified DMN regions outlined in the introductory chapters. As shown in figure 4.3, each DMN seed region was strongly positively correlated with a number of regions surrounding the PCC, including the left/right ventral/dorsal posterior cingulate cortices (BA23, BA31). Furthermore, LLP exhibited correlated activity somewhat lateralised to the left-hemisphere; and, similarly the RLP showed correlated activity lateralised to the right-hemisphere. Individual nodes of the DMN were also negatively correlated to insular (BA13) primary/secondary visual (BA17, BA18), primary auditory (BA41, BA42) and the premotor cortices (BA6), along with the dorsolateral prefrontal cortex (BA46). Whilst the text surrounding each seed in figure 4.3 details some of the functions associated with these negatively-correlated regions, consideration of the functional implications for these findings are outlined in the upcoming section (*4.3.3.2*) and are further addressed in the discussion of this experiment (section *4.4.1.4)*.

4.3.3.2 Whole brain contrasts of the relationship between DMN regions as identified by Fox et al. (2005) and regions covering the whole of the cerebral cortex

Due to the above analysis (which compared DMN ROIs to regions across the whole of the

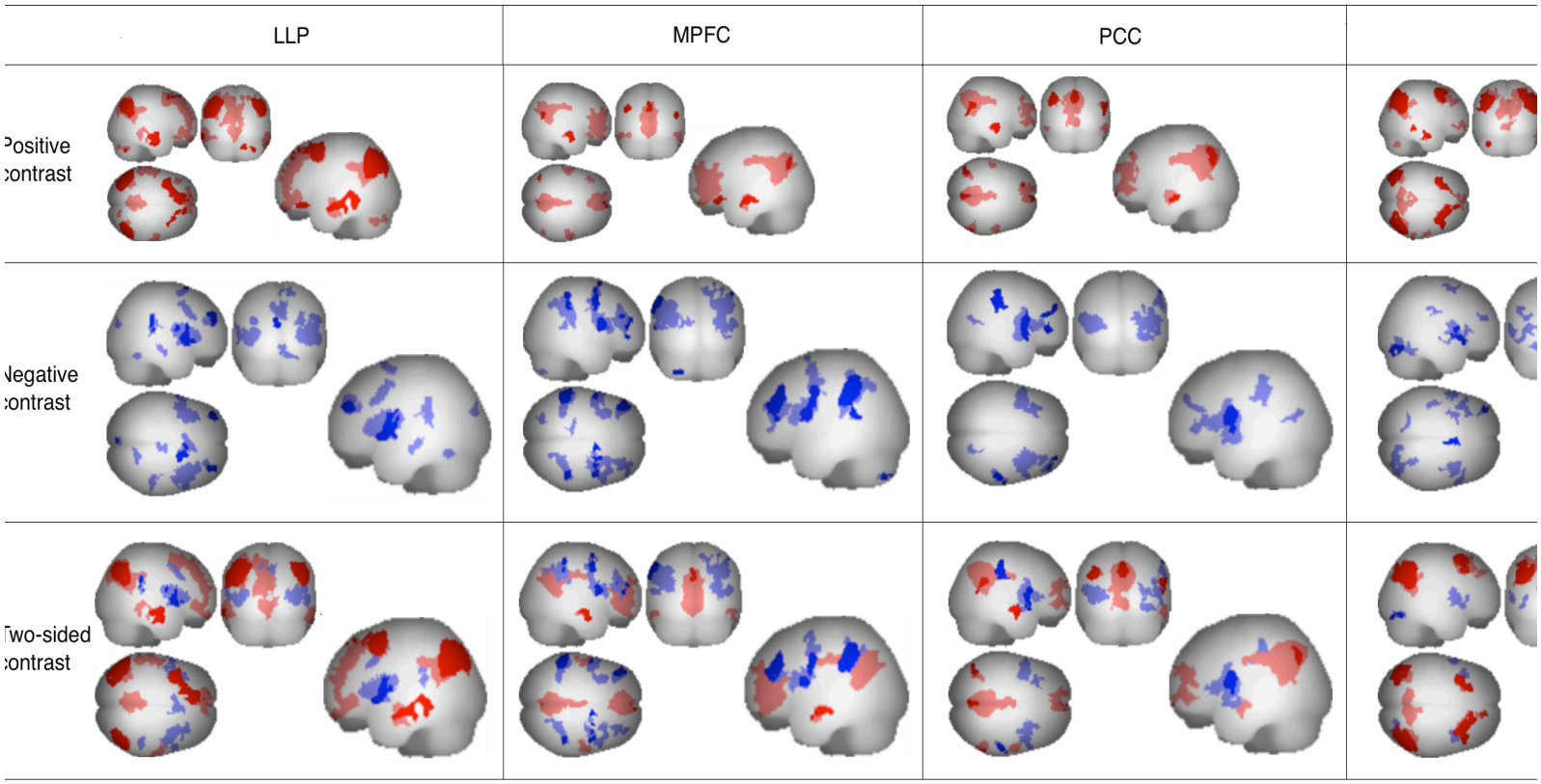

Figure 4.4. Whole brain positive, negative and two-sided maximum intensity projection maps for DMN seed regions in a 5-minute resting-state lateral parietal: LLP; medial prefrontal cortex: MPFC; posterior cingulate cortex: PCC; right lateral parietal: RLP (height (voxel-level) threshold (cluster-level) threshold: p=.05) Top images represent positive contrasts; middle images are negative contrasts; and lower images are two-side (positive/negative) contrasts displayed on the same map.

cortex) possibly being constrained by the use of Brodmann area (BA) definitions, whole brain positive/negative/two-sided maximum intensity projection maps were generated; allowing for a further exploration of the extent of correlated activity in the current population. Positive, negative and two-sided contrasts maps for each seed region are shown in figure 4.4 on the next page.

As shown in figure 4.4, whole brain positive contrast maps (top row of images) confirm the pattern of connectivity observed between DMN ROIs and the rest of the cerebral cortex, showing activations across frontal, posterior and parietal regions commonly implicated in the brain's DMN. Negative contrasts maps (middle row of images) reveal that each DMN component (LLP, MPFC, PCC, RLP) is coupled with down-regulation of activity in regions within (or in close proximity to) the temporal lobe. Whilst down-regulation of auditory, motor and some somatosensory regions was perhaps expected, given that participants were not actively processing auditory information and were asked to remain motionless, this finding raises questions about the functional relationship between these regions and the DMN. For example, it could be that the DMN suppresses activity in these regions in order to prevent information from the external world (received through the sensory modalities) interfering with the engagement in internal mental processes. Similarly participants could be focusing their attention on their 'internal' world to such an extent that regions implicated in the processing of external sources are down-regulated. Alternatively, auditory areas could in fact become habituated to background scanner noise, thus showing decreases in activity as the task progresses. Results might also be explained in terms of the support they offer to the existence of additional low-frequency networks in the resting brain; with the down-regulation in auditory and superior temporal regions observed here mapping on to an *auditory-phonological* low-frequency resting state network (RSN) found by Mantini et al. (2007; although it should be noted that studies exploring RSNs commonly employ independent component analysis; see Lee et al. 2012a for a review). The two-sided contrast maps (lower images; showing positive/negative contrasts in single maps) illustrate functional interactions between the DMN (frontal/posterior/parietal regions shown in red) and other brain regions. Clusters of activity in regions in the vicinity of, and overlapping

with, other neuronal networks (i.e. dorsal frontal regions implicated in the dorsal attention (goal-driven) network) also raise questions about the interaction between internally- and externally-directed control networks.

4.3.4. Analysis 2: Does electroencephalographic frequency content in the beta range (13-30 Hz) predict spontaneous low-frequency (SLF) fluctuations in DMN regions?

Continuous wavelet analysis of the 5 minute resting state data in the beta frequency range at electrode sites Fz, Cz and Pz was calculated to determine whether fluctuations in power in this frequency range was a significant predictor of fluctuations in the BOLD signal within DMN regions. The selection of these channels was based on: (1) that they allowed beta frequency to be analysed at frontal (Fz), central (Cz) and parietal (Pz) regions; and (2) they appeared to be most representative of beta signal across all other channels.

First-level findings in SPM8 revealed that across participants, when beta power was regressed against the fMRI BOLD signal, fluctuations in EEG beta frequency (13-30 Hz) did not significantly predict signal changes in the fMRI BOLD signal within frontal, parietal and lateral DMN regions at the 0.05 (FWE) significance threshold (see figure 4.5). When the significance level was changed to 0.001 (uncorrected) the resulting SPM maps revealed spurious surface activations that appeared to represent uncorrected residual movement artifact (see figure 4.6). It should be noted figures 4.5 and 4.6 illustrate results from one participant only and that data from an additional five participants was analysed, with comparable non-significant results obtained.

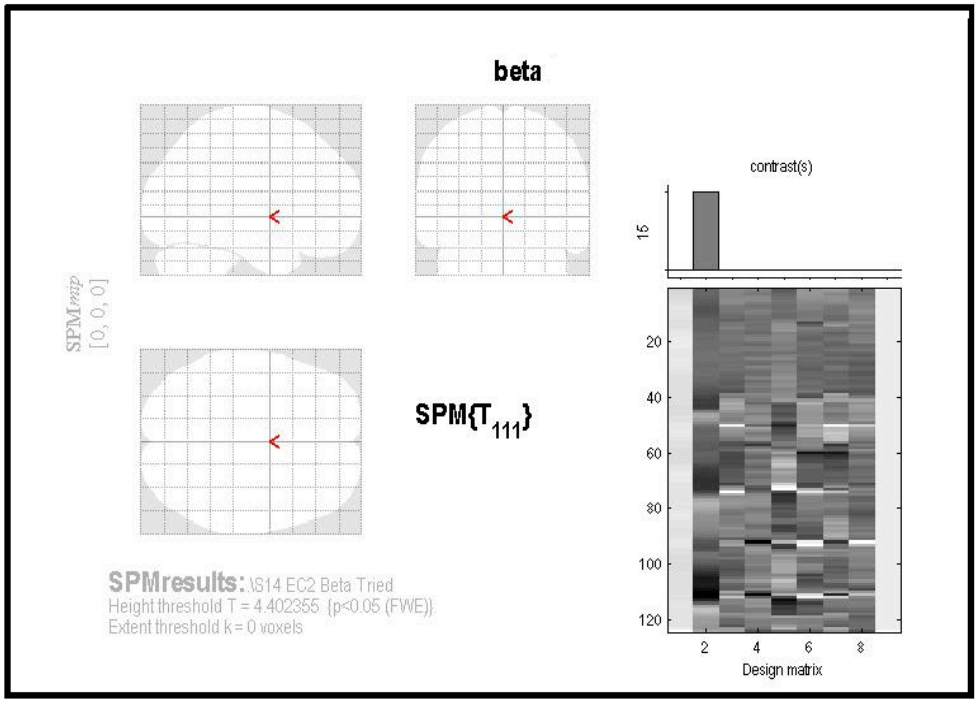

Figure 4.5. Resulting SPM maps for one participant, showing that beta frequency was not a significant predictor of SLF fluctuations in fMRI BOLD signal (p<0.05;

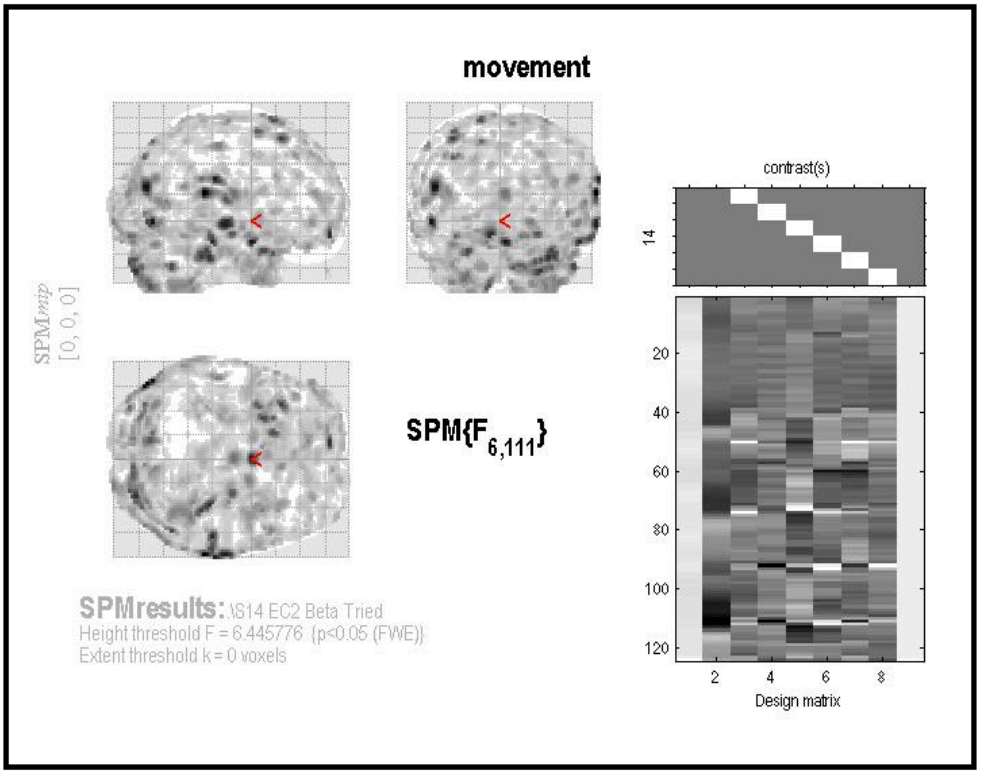

Figure 4.6. Resulting SPM maps for one participant, showing movement related artifact

4.4. Discussion of experiment 1

As previously stated, the overall aim of this experiment was to develop a suitable analysis strategy for the investigation of the relationship between EEG signal fluctuations and SLF fluctuations in the fMRI BOLD signal in DMN regions. Discussion of results is outlined below.

4.4.1. Exploring the DMN using resting-state functional connectivity analysis

In the current experiment, resting-state functional connectivity was assessed using the MATLAB toolbox *CONN*. As previously described in chapter 2 (section *2.7.2.1*) CONN provided an estimation of connectivity in terms of ROI-to-ROI correlations (connectivity between multiple ROIs) and seed-to-voxel relationships (connectivity between one/multiple seeds to regions covering the whole brain). As shown by the results of analyses 1a-1c, a ROI-to-ROI approach proved reliable in determining functional connectivity of the DMN, showing LLP, MPFC, PCC and RLP ROIs were significantly positively correlated with one another. ROI-to-ROI analyses were also reliable in calculating the strength and direction of correlations between DMN ROIs (defined by Fox et al., 2005) and: (1) task-positive regions proposed by Fox et al. (2005); (2) DMN regions identified by Buckner et al. (2008); (3) all other regions of the cerebral cortex. These results are each discussed in turn.

4.4.1.1. Confirmation that the DMN is active in a 5-minute resting state fMRI data

DMN ROIs (LLP, MPFC, PCC, RLP; Fox et al., 2005) were found to be significantly positively correlated with one another (analysis 1a) and to a number of other DMN regions defined by Buckner et al. 2008 (analysis 1b). These results support previous resting-state functional connectivity studies showing that correlated fluctuations in the fMRI BOLD signal within frontal

posterior and parietal regions are prominent when participants are asked to rest with their eyes-closed (e.g. Fox et al., 2005; Fransson, 2005, 2006; Greicius et al., 2003; previously reviewed in chapters 1 and 2 of this research thesis).

4.4.1.2. The relationship between the DMN and the task-positive network

It was hypothesised that during rest the DMN would be anti-correlated to a network of regions that typically exhibit task-related activations (the task-positive/externally-directed network). This prediction was based on the findings of Fox et al. (2005) who reported the existence of, and anti-correlation between, these two low-frequency networks in multiple rest conditions (eyes-closed, eyes-open without/without visual fixation). Results obtained in the current experiment, however, only partially supported this hypothesis: they revealed only individual components of the DMN were negatively correlated to individual components of the task-positive network. As previously stated: MPFC and L/RLP DMN regions were negatively correlated with a region representing the middle temporal cortex; MPFC and LLP were negatively correlated with a region representing the frontal eye field; and PCC showed no relationship to these regions. In addition, an unpredicted finding was that each frontal, posterior and parietal DMN region was positively correlated with the left and/or right task-positive intraparietal sulcus (an area commonly implicated in the dorsal attention (goal-driven) network). The result is suggestive of communication between nodes of internally- and externally-directed control networks perhaps in the generation/modulation of stream of thought, this along with the response of PCC in particular, is considered further in the general discussion of this thesis (chapter 7).

Whilst the CONN toolbox was reliable in measuring the strength of correlated activity between network components, a fundamental issue that could have influenced this result was the disparity between the identification of task-positive regions by Fox et al. (2005) and the definition and position of these BAs produced in CONN. Thus, whereas Fox and colleagues defined BA6 as the frontal eye fields, in CONN BA6 represented the premotor cortex; BA7 (the intraparietal sulcus; Fox et al.) represented the somatosensory cortex; and BA37 (the middle temporal cortex; Fox et al.) represented the fusiform gyrus. Therefore, it is feasible to assume if this analysis was to be replicated, selection of task-positive regions based on alternative criteria, i.e. neighbouring regions rather that BAs, may in fact yield different results.

Whilst one may also question the effects of a small sample size and 5-minute fMRI data acquisition time as factors contributing to the partial results obtained here, it is unlikely that these were problematic. This is because in line with Fox et al. (2005) 10 participants took part in the current experiment, and further, spontaneous low-frequency resting-state networks have been previously successfully identified in as little as 4-minutes of fMRI data (e.g. Mantini et al., 2007) and in as little as 3-minutes of EEG data (e.g. Chen et al., 2008; note that Fox et al. investigated this relationship in conditions lasting 5.5-minutes each).

4.4.1.3. Generation of a further set of regions implicated in the brain's DMN

A secondary hypothesis of analysis 1 (analysis 1b) proposed DMN regions identified by Fox et al. (2005) would be positively correlated with DMN regions identified by Buckner et al. (2008). Results revealed multiple positive correlations between these two sets of regions, therefore

generating a further set of DMN regions implicated in the 5-minute resting-state condition and showing the vast extent to which this system is engaged during task-free rest.

Although detracting from the initial aim of this analysis, no measure of participants' thought processes during the rest condition was obtained; also no thought probe(s) was presented prior to/during scanning. The incorporation of this measure could have offered insight into: (1) variation in the spread of correlated activity, i.e. the same-side hemispheric bias of regions that LLP/RLP were positively correlated with; and (2) the difference in the number of functional relationships that each ROI exhibited, i.e. more correlated activity observed between MPFC and other DMN regions in comparison to PCC and other DMN regions. Presentation of a thought probe prior to/during scanning could have also enabled the mapping of specific thought processes (i.e. self-referential thought) onto specific DMN components and aided understanding of subsystems within the DMN: a trend that is becoming prominent in the literature (i.e. Andrews-Hanna et al., 2010a; Uddin et al., 2009; see section *2.3.4* in chapter 2 for a review of DMN fractionation into subsystems).

An unpredicted finding of analysis 1b was that no DMN ROI specified by Fox et al. (2005) showed a functional relationship to the parahippocampal cortex (BA36): a putative DMN region defined by Buckner et al. (2008). The functions associated with this region and the underlying hippocampal formation have been shown to overlap with the DMN in terms of activation at rest (Andrews-Hanna et al., 2010a) and associated cognitive processes (i.e. recollection of one's past; Andreasen et al., 1995). It should be noted: it is possible that activation of the hippocampal formation was apparent but undetectable due to: (1) signal loss in areas that are adjacent to air

spaces in the skull; or (2) overlying cortex and its deep/embedded anatomical position within the cortex: an assumption which is based on the limited and restrictive nature of using Brodmann areas (BAs) in the CONN toolbox. This is also plausible based on the outcome of the whole-brain maximum intensity projection contrasts, which removed the restriction of BAs to reveal that there were activations within medial temporal regions.

4.4.1.4. How the DMN interacts with regions covering the rest of the cerebral cortex

As a final exploration of the fMRI data in the current experiment, DMN seed ROIs (Fox et al., 2005) were compared to regions covering the whole of the cerebral cortex (analysis 1c). This analysis provided insight into the functional relationship between the DMN and the rest of the brain during eyes-closed resting state. Results based on BA definitions (summarised in the results section *4.3.3.1*) echoed one of the findings obtained in analysis 1b: showing LLP exhibited a pattern of correlated activity largely lateralised to the left-hemisphere; and RLP demonstrated a pattern lateralised to the right-hemisphere, raising questions about component functions of the DMN. For example, it is possible this component may be implicated in proposed sentinel functions of the DMN to a greater extent than LLP, a notion based on the fact that RLP showed strong connectivity to left/right dorsal and anterior prefrontal regions and that the right hemisphere is implicated in attention function.

Results of analysis 1c also revealed individual nodes of the DMN were negatively correlated with insular, primary/secondary visual, primary auditory and premotor cortices; also shown in the whole brain maximum intensity projection contrasts (see results section *4.3.3.2*). Whilst suppression of activity in these areas was perhaps expected given participants were lying

motionless and not actively processing/responding to external stimuli, as previously discussed, it is possible that the DMN was provoking down-regulation of these regions in order to prevent external sensory information interference with internal thought processes. This, however, is merely speculation and will be considered further in the general discussion of this thesis (chapter 7). The location of these regions showing suppression in activity also supports this existence of additional resting-state networks (RSNs) in the brain, i.e. the *auditory-phonological* low-frequency RSN identified by Mantini et al. (2007). However, as previously stated, it is important to note that RSNs are commonly investigated using independent component analysis (ICA); therefore inference about the existence of additional RSNs in the current data set is based on the anatomical overlap with previously identified RSNs only.

4.4.2. Exploring electrophysiological signatures of the DMN

As previously stated, this experiment also aimed to determine whether electroencephalographic frequency content in the beta range (13-30 Hz) was a significant predictor of SLF fluctuations in the fMRI BOLD signal in DMN regions (analysis 2). However, results revealed that when beta frequency peak amplitude information was extracted and used as a predictor in the current model, no significant results were obtained.

Whilst beta frequency seemed like a reasonable selection based on the reasons outlined in the introductory section of this chapter (e.g. the outcome of a previous pilot study; results of Laufs et al., 2003; Hlinka et al., 2010; Mantini et al., 2007), as previously addressed, the existing literature is somewhat inconsistent in linking the DMN with a specific EEG frequency band. The results of the current analysis are therefore not completely unanticipated and one could

argue that they might have benefited from adopting a similar approach to Laufs et al. (2003) in which the beta range was subdivided into three bands (beta-1: 13-16 Hz; beta-2: 17-23 Hz; beta-24-30 Hz), with significant positive correlations observed between beta-2 power (17-23 Hz) and SLF fluctuations in the fMRI BOLD signal. Future analysis of the current data set might also benefit from employing a similar data driven ICA approach to that of Mantini et al. (2007); thus not restricting the analysis to a specific EEG frequency band (see also Jann et al., 2010).

4.4.3. Conclusions and future directions

To conclude, through the use of a ROI seed-based functional connectivity approach, the current experiment was successful in determining that the DMN was active in a 5-minutes eyes-closed resting-state condition. As discussed, findings revealed that a core set of DMN ROIs (identified by Fox et al., 2005) were strongly positively correlated with one another and to several other putative regions of the DMN defined by Buckner et al. (2008). Results also revealed down-regulation of several brain regions implicated in the processing of sensory information from the external world and also hinted at the fact DMN components may be anti-correlated to regions implicated in other large-scale brain networks (i.e. the dorsal (goal-driven) attention network). Based on the fact no significant electrophysiological correlate of the DMN was found, an obvious next step was to investigate activation and functional connectivity of the DMN, along with its relationship to other large-scale brain networks in other task conditions; thus utilising other data obtained from technical development work. These investigations (in an active auditory attention task) are reported in experiments 2 and 3 (chapters 5 and 6) respectively.

CHAPTER 5

Experiment 2: Exploring the Default Mode Network (DMN) in an active auditory attention task and determining whether changes in DMN activity are observed across task duration

5.1. Aim of experiment

The main aim of this experiment was to determine whether DMN activity was observed in an active auditory attention task that was designed to systematically modulate activity in the goal- and stimulus-driven attention networks (analysis 1). Based on the outcome of analysis 1, a secondary aim was to investigate whether DMN activity increased over task duration, consistent with participant reports of increasing difficulty in maintaining concentration in the latter part of this task (analysis 2). This was explored in terms of: (1) increasing reaction times towards goal-driven stimuli (as a behavioural indicator of DMN activity); and (2) increases in the functional connectivity of the DMN over time. In view of the fact no significant EEG correlate of DMN activity was found in experiment 1 (chapter 4) this experiment focuses on fMRI data only.

5.1.1. Analysis 1: Rationale and hypotheses

As discussed in chapter 1, Raichle et al. (2001) were among the first to hypothesise that the DMN is constantly active when individuals are awake/conscious. The authors suggested neuronal activity associated with the DMN reflects continuous monitoring of the background or periphery for motivationally relevant stimuli, and that DMN activity is not abolished but *attenuated* when resources are temporarily reallocated during goal-directed behaviours. Since the work of Raichle et al. (2001) several studies have supported this view, revealing DMN

activity is observed (albeit at lower levels compared to rest) in target detection tasks (Hahn et al., 2007), simple and/or practiced tasks (Smallwood & Schooler, 2006), low-level attention-demanding tasks (Greicius & Menon, 2004), and working memory tasks (Fransson, 2006; see chapters 1 and 2 for reviews).

As proof of concept, the aim of analysis 1 was to investigate whether DMN activity was observed in an active auditory oddball task designed to induce activity in the goal- and stimulus-driven attention networks. This was done by investigating functional connectivity between DMN regions identified by Fox et al. (2005) and regions covering the whole of the cerebral cortex; allowing for: (1) the testing of the hypothesis that DMN regions (left lateral parietal area: LLP; medial prefrontal cortex: MPFC; posterior cingulate cortex: PCC; right lateral parietal area: RLP; Fox et al., 2005) would be significantly positively correlated with one another (suggesting the DMN was active); and (2) exploration of the interaction between the DMN and several other brain regions.

5.1.2. Analysis 2: Rationale and hypotheses

As previously discussed in chapter 1, Weissman et al. (2006) reported increases in the occurrence of momentary lapses in attention (indicative of DMN activity) were positively correlated with increases in reaction times towards behaviourally relevant stimuli (see section *1.6.1.2*, chapter 1; see also McKiernan et al., 2006). This infers reaction times can be considered as a behavioural index of enhanced or attenuated activity in the DMN (see Smallwood & Schooler, 2006 for a review of behavioural measures of the DMN).

Furthermore, as addressed in chapter 1 (see section *1.6*) individuals can focus their attention on an external task and achieve their goal but often their mind will have wandered off-task several times, thus modulating activity in the DMN (Klinger & Cox, 1987; Killingsworth & Gilbert, 2010). Whilst tendencies to engage in internal modes of cognition can be due to individual differences in brain characteristics etc., Mason et al. (2007) showed that a practiced version of a monotonous task was positively correlated with increased activity in the DMN, which in turn was positively correlated with increased reports of engaging in periods of mind wandering (previously discussed in section *1.6.1.1*, chapter 1). These results infer that during a lengthy task, which is consistent in level of difficulty, DMN activity may increase as participants become familiar with/skilled/habituated to task demands. Thus, the extent to which individuals engage in *internal* modes of cognition may increase as a function of reduced allocation of attention resources to (and engagement in) the external world.

Based on the above and on the outcome of analysis 1 (investigating DMN activity in an *active* task), analysis 2 sought to establish whether DMN activity increased as a function of increasing task duration. This was firstly investigated through the analysis of reaction times towards behaviourally relevant goal-driven stimuli, consistent with the notion that reaction times provide an indirect measure of DMN activity (Weissman et al., 2006; Smallwood & Schooler, 2006), and secondly by exploring changes in functional connectivity of the DMN over time. Both of these explorations were conducted by subdividing the active auditory task data (840s) into three equal portions lasting 280s each (thus containing 112 fMRI volumes each).

It was hypothesised that if DMN activity increases over task duration, consistent with participant reports, then reaction times towards behaviourally-relevant stimuli should be slower in the latter portions of the task.

5.2. Method

5.2.1. Participants

Twelve participants (5 male, 7 female) took part in this study (mean age = 29.08, SD = 6.76, range = 18-41). Data from three participants were excluded; this was due to an insufficient number of fMRI slices available (2 participants) and excessive head movements during scanning (1 participant). Data for nine participants (4 male, 5 female; mean age = 30, SD = 7.31) are therefore included in this analysis. Matching the criteria of experiment 1, participants had no history of neurological or psychiatric illness, or any other medical conditions, which may have affected their participation. Participants also had no known history of claustrophobia or metal implants and had normal or normal-to-corrected vision and normal hearing. Prior to EEG/fMRI acquisition and scanning, each participant provided written informed consent in accordance with ethical guidelines and approval of the Tayside Committee for Medical Research Ethics; and completed an MRI safety questionnaire in accordance with guidelines set out by the Clinical Research Centre, Ninewells Hospital, Dundee.

5.2.2. Auditory odd/even number decision task

An auditory odd/even number decision task with incorporated oddball stimuli was used in this experiment. Goal stimuli were 250 number items in the range of 2-9 as well as 50 simultaneous

goal and irrelevant novel stimuli. For these stimuli, participants were instructed to respond to odd numbers (3, 5, 7, 9) using their index finger, and respond to even numbers (2, 4, 6, 8) using their middle finger; all responses were made with the right hand. In addition, 50 non-goal stimuli (the number '0': task-relevant oddball) and 50 novel stimuli (environmental sounds: task-irrelevant oddballs) were included in the sequence. Participants were instructed to respond to all stimuli containing the numbers 2-9 and inhibit a response to all other stimuli. The presentation time of goal and non-goal number stimuli was 300ms per item and novel stimuli lasted between 100-135ms. Stimuli were presented at a variable inter-stimulus interval of 1900-2100ms (random 500ms steps). Onset of presentation software was synched to MR volume signals. Coded stimulus presentation markers (number/novel sound), participant responses and scanner volume triggers were logged in EEG recordings. An MR-compatible button response box (Current Designs, PA, USA) was used to record responses to stimulus presentation. The duration of this task was 840s (14 minutes). Following completion, participants were asked how they felt they had performed throughout the task, and whether they experienced a lack of concentration at any point: all participants reported difficulties in maintaining their response towards stimuli in the latter stages of the task.

5.2.3. Functional data acquisition

During scanning participants were instructed to remain as motionless as possible and keep their eyes closed. As stated in section *4.2.1* in chapter 4, participants completed three additional EEG/fMRI tasks prior to and subsequent to the auditory task; these included the resting state condition (prior to, lasting 5 minutes), a visual N-Back task (subsequent to, lasting 10 minutes), and a visual pavlovian conditioning working memory task (subsequent to, lasting 10 minutes).

The visual N-Back task working memory task data and the visual pavlovian conditioning task are not included or referred to in this thesis.

5.2.4. Functional magnetic resonance imaging acquisition

As with experiment 1 (chapter 4), data was acquired on a 3T Trio MR scanner (Siemens, Erlangen, Germany) using a transmit body coil and a 12-channel receive-only head coil. A T1-weighted sagittal MPRAGE structural image was obtained prior to the acquisition of functional images (176 slices). 336 functional images were acquired using a BOLD contrast sensitive gradient echo echo-planar sequence (TE = 30ms; TR = 2500ms; FOV = 240mm; matrix size = 64x64).

5.2.5. Functional magnetic resonance imaging preprocessing

See method section *4.2.7* in chapter 4 for a description.

5.2.6. Selection of ROIs

DMN seed regions were the same as those used in experiment 1: LLP, MPFC, PCC and RLP. As previously stated, these regions were functionally defined as 10mm spheres centered at locations reported in Fox et al. (2005).

5.2.7. ROI seed based functional connectivity analysis using CONN toolbox

As with experiment 1, outlined in chapter 4, functional connectivity was assessed using the Matlab toolbox, *CONN*. However, in this analysis, a more recent version of the toolbox was used (version 13i (v.13i); http;//www.nitrc.org/projects/conn). V.13i differed from version 12i

that was used in experiment 1, in that, in addition to BA defined regions, v.13i also generated *rsREL* regions. rsREL regions represented seeds in close proximity to DMN seed regions defined by Fox et al. (2005; LLP, MPFC, PCC, RLP). The authors of the CONN toolbox suggested that they were strongly and robustly functionally connected to one another and were representative portions of the DMN (Whitfield-Gabrieli & Nieto-Castanon, 2012). Analysis steps conducted in CONN, including task related information for both analyses in this experiment are available in appendices C and D.

5.3. Results

5.3.1 Analysis 1: Is DMN activity observed in an active auditory attention task designed to induce activity in the goal- and stimulus-driven attention networks?

5.3.1.1. Single-subject first-level DMN contrast maps

First-level connectivity measures for each participant for each DMN ROI (LLP, MPFC, PCC, RLP, and total) are displayed in figure 5.1. The threshold *.05* was selected, meaning that correlation coefficients above this value are illustrated on the maps. Subsequent to this, the appropriate bivariate correlations were run for all participants, constructing ROI-to-ROI connectivity matrices for each DMN region.

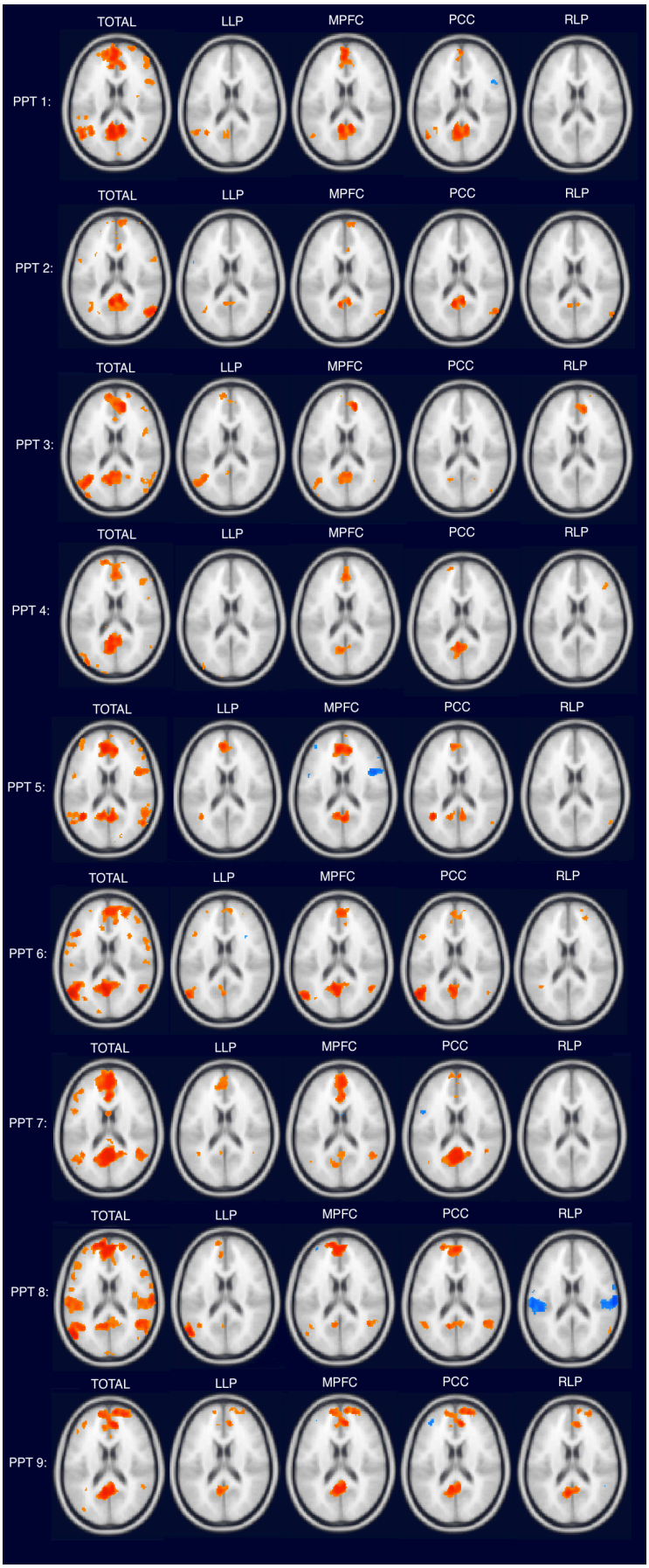

Figure 5.1. DMN contrast maps across 9 participants. Images from left to right: TOTAL contrast map (showing connectivity for all DMN sources), thereafter on a single source basis: LLP, MPFC, PCC, RLP (threshold: 0.5)

Figure 5.1 shows when DMN seed regions are individually inspected (on a participant-by-participant basis) MPFC, PCC and LLP are functionally connected to a number of other DMN regions, this is particularly prominent for midline components (MPFC, PCC). In comparison, RLP connectivity is reduced, with participant 8 suggesting that there is negative relationship between RLP and the auditory cortices/surrounding temporal regions. On inspection of *TOTAL* contrast maps (images on left), participants 1, 3, 5, 6, 7, 8 appear to exhibit strong functional connectivity between all DMN-associated areas and surrounding structures; however, this is somewhat less apparent in participants 2, 4 and 9 with only MPFC and PCC connectivity remaining prominent.

5.3.1.2. ROI-to-ROI functional connectivity results

Connectivity between DMN ROIs (LLP, MPFC, PCC and RLP; Fox et al., 2005) and the whole of the cerebral cortex are shown in figure 5.2. Tables 5.1.1-5.1.4 illustrate the Brodmann's Area (BA)/ROI/rsREL, label, strength of connectivity (*B* value) and significance (*p* value). Within the tables DMN ROIs are displayed in *italics* and highlighted grey and rsREL regions are displayed in *italics*. In both the figures and the tables, positive correlations are shown in red text and negative correlations are shown in blue, and significant ($p<.05$) correlations only are reported. It should also be noted that the CONN toolbox implemented a built-in correction method (FWE/FDR) for multiple ROI-to-ROI calculations in order to alleviate any potential multiple comparison issues (essential for ROI-to-ROI predicted calculations, but not essential for seed-to-voxel exploratory analyses).

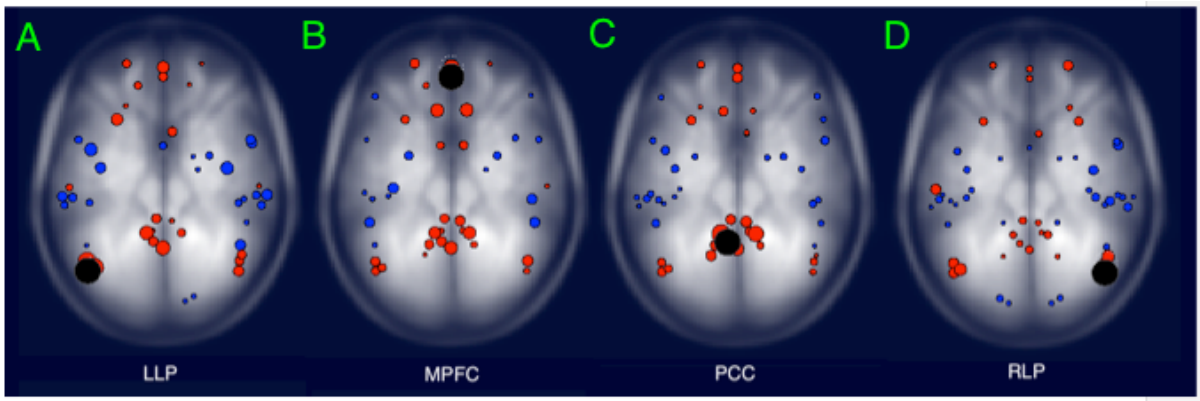

Figure 5.2. Relationship between DMN ROIs and regions covering the whole of the cerebral cortex in an 840s active auditory attention task.

Table 5.1.1. Left lateral parietal (LLP) connectivity to all cerebral regions in 840s of active auditory attention data and their significance.

Brodmann area	Brain region	*B*	*p*	Correlation
rsREL	*Left Inferior Parietal Lobe*	*1.65*	*<0.001*	+
rsREL	*Left Superior Frontal Gyrus*	*0.54*	*<0.001*	+
rsREL	*Left Anterior Sup Temp Gyrus*	*-0.34*	*<0.001*	-
rsREL	*Left Posterior Sup Temp Gyrus*	*-0.23*	*0.004*	-
Seed ROI	*Medial Prefrontal Cortex*	*0.47*	*0.001*	+
rsREL	*Medial Prefrontal Cortex*	*0.48*	*<0.001*	+
Seed ROI	*Posterior Cingulate Cortex*	*0.60*	*0.001*	+
rsREL	*Precuneus (PCC)*	*0.67*	*<0.001*	+
rsREL	*Cingulate Gyrus*	*-0.31*	*0.004*	-
Seed ROI	*Right Lateral Parietal*	*0.61*	*<0.001*	+
rsREL	*Right Anterior Sup Temp Gyrus*	*-0.29*	*0.001*	-
rsREL	*Right Posterior Sup Temp Gyrus*	*-0.30*	*0.002*	-
BA 2 (R)	Primary Somatosensory Cortex	-0.21	0.015	-
BA 6 (R)	Premotor Cortex	-0.24	0.004	-
BA 8 (L)	Dorsal Frontal Cortex	0.44	0.033	+
BA 10 (L)	Anterior Prefrontal Cortex	0.37	0.002	+
BA 10 (R)	Anterior Prefrontal Cortex	0.17	0.046	+
BA 11 (L)	Orbitofrontal Cortex	0.20	0.004	+
BA 11 (R)	Orbitofrontal Cortex	0.12	0.041	+
BA 13 (L)	Insular Cortex	-0.33	<0.001	-
BA 13 (R)	Insular Cortex	-0.33	<0.001	-
BA 17 (R)	Primary Visual Cortex	-0.15	0.033	-
BA 18 (R)	Secondary VisualCortex	-0.13	0.030	-
BA 21 (L)	Middle Temporal Gyrus	0.34	0.006	+
BA 21 (R)	Middle Temporal Gyrus	0.14	0.032	+
BA 22 (L)	Superior Temporal Gyrus	-0.20	0.001	-
BA 22 (R)	Superior Temporal Gyrus	-0.21	0.002	-
BA 23 (L)	Ventral Posterior Cingulate Cortex	0.31	0.001	+
BA 23 (R)	Ventral Posterior Cingulate Cortex	0.17	0.023	+
BA 28 (R)	Posterior Entorhinal Cortex	-0.09	0.026	-
BA 29 (L)	Retrosplenial Cingulate Cortex	0.17	0.018	+

BA 31 (L)	Dorsal Posterior Cingulate Cortex	0.63	<0.001	+
BA 31 (R)	Dorsal Posterior Cingulate Cortex	0.34	0.002	+
BA 33 (R)	Anterior Cingulate Cortex	0.15	0.001	+
BA 34 (R)	Anterior Entorhinal Cortex	-0.12	0.037	-
BA 37 (L)	Fusiform gyrus	-0.10	0.042	-
BA 37 (R)	Fusiform gyrus	-0.23	<0.001	-
BA 39 (L)	Angular gyrus	1.25	<0.001	+
BA 39 (R)	Angular gyrus	0.58	0.001	+
BA 40 (R)	Supramarginal Gyrus	-0.22	0.023	-
BA 41 (L)	Primary Auditory Cortex	-0.14	0.005	-
BA 41 (R)	Primary Auditory Cortex	-0.16	0.004	-
BA 42 (L)	Primary Auditory Cortex	-0.19	0.001	-
BA 42 (R)	Primary Auditory Cortex	-0.17	<0.001	-
BA 44 (L)	IFC pars opercularis	-0.19	0.003	-
BA 44 (R)	IFC pars opercularis	-0.35	0.001	-

As shown in figure 5.2A and table 5.1.1, LLP was positively correlated to areas in close proximity to the MPFC, including the left dorsal frontal cortex (BA8) and the left/right anterior prefrontal (BA10) and orbital frontal (BA11) cortices. LLP was also positively correlated with a cluster of regions surrounding the PCC, including the precuneus (rsREL), left/right ventral/dorsal posterior cingulate cortex (BA23, BA31) and left retrosplenial cingulate cortex (BA29. Significant positive correlations were also found with the right inferior parietal lobe (rsREL) and angular gyrus (BA39). Significant negative correlations were apparent between LLP and the left/right fusiform gyri (BA37) and right primary/secondary visual cortices (BA17, BA18). There were also significant negative correlations with the left/right pars operculari (BA44), anterior superior temporal gyri (rsREL), insular (BA13), and primary auditory cortices (BA41, BA42). Interestingly, within this group of areas the left/right middle temporal gyrus (BA21) was positively correlated with LLP. All other positive and negative correlations are displayed in table 5.1.1.

Table 5.1.2. Medial prefrontal cortex (MPFC) connectivity to all cerebral regions in 840s of active auditory attention data and their significance.

Brodmann	Brain region	*B*	*p*	Correlation

area

Seed ROI	*Left Lateral Parietal*	*0.47*	*0.001*	+
rsREL	*Left Inferior Parietal Lobe*	*0.38*	*0.003*	+
rsREL	*Left Superior Frontal Gyrus*	*0.29*	*0.002*	+
rsREL	*Medial Prefrontal Cortex*	*1.16*	*<0.001*	+
Seed ROI	*Posterior Cingulate Cortex*	*0.65*	*0.001*	+
rsREL	*Precuneus (PCC)*	*0.88*	*<0.001*	+
Seed ROI	*Right Lateral Parietal*	*0.36*	*0.009*	+
BA 1 (L)	Primary Somatosensory Cortex	-0.16	0.030	-
BA 2 (L)	Primary Somatosensory Cortex	-0.20	0.024	-
BA 2 (R)	Primary Somatosensory Cortex	-0.23	0.001	-
BA 3 (L)	Primary Somatosensory Cortex	-0.17	0.030	-
BA 4 (L)	Primary Motor Cortex	-0.18	0.001	-
BA 6 (L)	Premotor Cortex	-0.21	0.002	-
BA 6 (R)	Premotor Cortex	-0.35	0.003	-
BA 7 (L)	Somatosensory Association Cortex	0.12	0.042	+
BA 10 (L)	Anterior Prefrontal Cortex	0.31	0.001	+
BA 10 (R)	Anterior Prefrontal Cortex	0.15	0.045	+
BA 11 (L)	Orbitofrontal Cortex	0.15	0.011	+
BA 21 (R)	Middle Temporal Gyrus	0.13	0.039	+
BA 23 (L)	Ventral Posterior Cingulate Cortex	0.49	0.001	+
BA 23 (R)	Ventral Posterior Cingulate Cortex	0.42	0.001	+
BA 24 (L)	Ventral Anterior Cingulate Cortex	0.28	0.003	+
BA 24 (R)	Ventral Anterior Cingulate Cortex	0.23	0.002	+
BA 28 (R)	Posterior Entorhinal Cortex	-0.12	0.035	-
BA 29 (L)	Retrosplenial Cingulate Cortex	0.36	0.007	+
BA 29 (R)	Retrosplenial Cingulate Cortex	0.35	0.007	+
BA 30 (L)	Cingulate Cortex	0.48	0.001	+
BA 30 (R)	Cingulate Cortex	0.25	0.008	+
BA 31 (L)	Dorsal Posterior Cingulate Cortex	0.76	<0.001	+
BA 31 (R)	Dorsal Posterior Cingulate Cortex	0.58	<0.001	+
BA 32 (L)	Dorsal Anterior Cingulate Cortex	0.66	<0.001	+
BA 32 (R)	Dorsal Anterior Cingulate Cortex	0.53	<0.001	+
BA 37 (L)	Fusiform gyrus	-0.15	0.025	-
BA 38 (R)	Temporopolar Area	-0.12	0.008	-
BA 39 (L)	Angular gyrus	0.42	0.001	+
BA 39 (R)	Angular gyrus	0.37	0.001	+
BA 40 (L)	Supramarginal Gyrus	-0.42	0.001	-
BA 40 (R)	Supramarginal Gyrus	-0.45	0.001	-
BA 44 (L)	IFC pars opercularis	-0.22	0.045	-
BA 44 (R)	IFC pars opercularis	-0.35	0.010	-
BA 46 (L)	Dorsolateral Prefrontal Cortex	-0.26	0.009	-
BA 46 (R)	Dorsolateral Prefrontal Cortex	-0.22	0.043	-

MPFC (see figure 5.2B, table 5.1.2) was positively correlated with the left/right anterior prefrontal (BA10), dorsal anterior cingulate (BA32) and ventral anterior cingulate (BA24) cortices, and the left/right angular gyri (BA39). MPFC was also positively correlated with the left superior frontal gyrus (rsREL), precuneus (rsREL), left somatosensory association cortex

(BA7), along with the left/right ventral posterior cingulate (BA23), retrosplenial cingulate (BA29), cingulate (BA30) and dorsal posterior cingulate (BA31) cortices. MPFC was negatively correlated with the left/right dorsolateral prefrontal cortices (BA46), extending to the IFC pars operculari (BA44), premotor cortices (BA6), primary somatosensory areas (BA2) and supramarginal gyri (BA40). Additional negative correlations were apparent between MPFC and the left primary motor cortex (BA4) and fusiform gyrus (BA37). All other positive and negative correlations are displayed in table 5.1.2.

Table 5.1.3. Posterior cingulate cortex (PCC) connectivity to all cerebral regions in 840s of active auditory attention data and their significance.

Brodmann area	Brain region	*B*	*p*	Correlation
Seed ROI	*Left Lateral Parietal*	*0.60*	*0.001*	+
rsREL	*Left Inferior Parietal Lobe*	*0.56*	*0.003*	+
rsREL	*Left Superior Frontal Gyrus*	*0.38*	*0.002*	+
rsREL	*Left Anterior Sup Temp Gyrus*	*-0.23*	*0.002*	-
rsREL	*Left Posterior Sup Temp Gyrus*	*-0.13*	*0.038*	-
Seed ROI	*Medial Prefrontal Cortex*	*0.65*	*0.001*	+
rsREL	*Medial Prefrontal Cortex*	*0.59*	*0.001*	+
rsREL	*Precuneus (PCC)*	*1.12*	*<0.001*	+
Seed ROI	*Right Lateral Parietal*	*0.36*	*0.009*	+
rsREL	*Right Inferior Parietal lobe*	*0.29*	*0.046*	+
BA 1 (L)	Primary Somatosensory Cortex	-0.23	0.010	-
BA 2 (L)	Primary Somatosensory Cortex	-0.20	0.010	-
BA 2 (R)	Primary Somatosensory Cortex	-0.25	0.012	-
BA 3 (L)	Primary Somatosensory Cortex	-0.18	0.038	-
BA 4 (L)	Primary Motor Cortex	-0.18	0.047	-
BA 6 (L)	Premotor Cortex	-0.17	0.013	-
BA 6 (R)	Premotor Cortex	-0.37	0.006	-
BA 7 (L)	Somatosensory Association Cortex	0.49	0.001	+
BA 8 (L)	Dorsal Frontal Cortex	0.22	0.043	+
BA 10 (L)	Anterior Prefrontal Cortex	0.31	0.005	+
BA 13 (L)	Insular Cortex	-0.29	0.003	-
BA 13 (R)	Insular Cortex	-0.28	0.011	-
BA 22 (L)	Superior Temporal Gyrus	-0.16	0.005	-
BA 23 (L)	Ventral Posterior Cingulate Cortex	0.59	0.001	+
BA 23 (R)	Ventral Posterior Cingulate Cortex	0.52	0.001	+
BA 25 (R)	Subgenual cortex	0.15	0.019	+
BA 29 (L)	Retrosplenial Cingulate Cortex	0.47	0.004	+
BA 29 (R)	Retrosplenial Cingulate Cortex	0.46	0.002	+
BA 30 (L)	Cingulate Cortex	0.48	0.001	+
BA 30 (R)	Cingulate Cortex	0.27	0.004	+
BA 31 (L)	Dorsal Posterior Cingulate Cortex	1.13	<0.001	+

BA 31 (R)	Dorsal Posterior Cingulate Cortex	0.79	<0.001	+
BA 32 (L)	Dorsal Anterior Cingulate Cortex	0.33	0.001	+
BA 32 (R)	Dorsal Anterior Cingulate Cortex	0.22	0.016	+
BA 33 (R)	Anterior Cingulate Cortex	0.11	0.016	+
BA 34 (R)	Anterior Entorhinal Cortex	-0.08	0.013	-
BA 37 (R)	Fusiform gyrus	-0.17	0.044	-
BA 39 (L)	Angular gyrus	0.62	0.003	+
BA 39 (R)	Angular gyrus	0.43	0.004	+
BA 40 (L)	Supramarginal Gyrus	-0.35	0.003	-
BA 40 (R)	Supramarginal Gyrus	-0.31	0.012	-
BA 41 (L)	Primary Auditory Cortex	-0.11	0.040	-
BA 41 (R)	Primary Auditory Cortex	-0.16	0.005	-
BA 42 (L)	Primary Auditory Cortex	-0.15	0.016	-
BA 44 (L)	IFC pars opercularis	-0.23	0.010	-
BA 44 (R)	IFC pars opercularis	-0.34	0.002	-
BA 45 (R)	IFC pars triangularis	-0.16	0.015	-
BA 46 (L)	Dorsolateral Prefrontal Cortex	-0.22	0.019	-
BA 46 (R)	Dorsolateral Prefrontal Cortex	-0.23	0.010	-

Figure 5.2C and table 5.1.3 reveal that PCC was positively correlated with the left/right dorsal anterior cingulate cortices (BA32), left superior frontal gyrus (rsREL) and the right anterior cingulate cortex (BA33). PCC was also positively correlated with the left somatosensory association cortex (BA7), precuneus (rsREL), and the left/right ventral posterior cingulate (BA23), retrosplenial cingulate (BA29), cingulate (BA30) and the dorsal posterior cingulate (BA31) cortices. Significant positive correlations between the PCC and the left/right angular gyri (BA39) and inferior parietal lobes (rsREL) were also found. Several significant negative correlations were apparent between PCC and the left/right dorsolateral prefrontal cortices (BA46), IFC pars operculari (BA44), premotor (BA6), insular (BA13) and primary auditory (BA41) cortices, primary somatosensory areas (BA2), and the supramarginal gyri (BA40). PCC was also negative correlated to the left posterior superior temporal gyrus (rsREL), primary somatosensory (BA1, BA3) primary motor (BA4) and primary auditory (BA42) cortices and the superior temporal area (BA22). All other positive and negative correlations are displayed in table 5.1.3.

Table 5.1.4. Right lateral parietal (RLP) connectivity to all cerebral regions in 840s of active auditory attention data and their significance.

Brodmann area	Brain region	*B*	*p*	Correlation
Seed ROI	*Left Lateral Parietal*	*0.61*	*0.001*	+
rsREL	*Left Inferior Parietal Lobe*	*0.58*	*<0.001*	+
rsREL	*Left Superior Frontal Gyrus*	*0.25*	*0.004*	+
rsREL	*Left Anterior Sup Temp Gyrus*	*-0.22*	*0.007*	-
rsREL	*Left Posterior Sup Temp Gyrus*	*-0.20*	*0.039*	-
Seed ROI	*Medial Prefrontal Cortex*	*0.36*	*0.010*	+
rsREL	*Medial Prefrontal Cortex*	*0.30*	*0.010*	+
Seed ROI	*Posterior Cingulate Cortex*	*0.36*	*0.009*	+
rsREL	*Precuneus (PCC)*	*0.46*	*0.004*	+
rsREL	*Cingulate Gyrus*	*-0.22*	*0.031*	-
rsREL	*Right Inferior Parietal lobe*	*0.85*	*<0.001*	+
rsREL	*Right Superior Frontal Gyrus*	*0.42*	*0.002*	+
rsREL	*Right Anterior Sup Temp Gyrus*	*-0.29*	*0.001*	-
rsREL	*Right Posterior Sup Temp Gyrus*	*-0.31*	*0.004*	-
BA 1 (L)	Primary Somatosensory Cortex	-0.18	0.044	-
BA 1 (R)	Primary Somatosensory Cortex	-0.22	0.012	-
BA 2 (L)	Primary Somatosensory Cortex	-0.22	0.039	-
BA 2 (R)	Primary Somatosensory Cortex	-0.30	0.002	-
BA 3 (L)	Primary Somatosensory Cortex	-0.24	0.010	-
BA 3 (R)	Primary Somatosensory Cortex	-0.23	0.004	-
BA 4 (L)	Primary Motor Cortex	-0.19	0.018	-
BA 4 (R)	Primary Motor Cortex	-0.22	0.016	-
BA 5 (L)	Somatosensory Association Cortex	-0.16	0.044	-
BA 5 (R)	Somatosensory Association Cortex	-0.21	0.025	-
BA 6 (R)	Premotor Cortex	-0.16	0.039	-
BA 7 (L)	Somatosensory Association Cortex	0.13	0.039	+
BA 7 (R)	Somatosensory Association Cortex	0.21	0.023	+
BA 8 (R)	Dorsal Frontal Cortex	0.31	0.016	+
BA 10 (L)	Anterior Prefrontal Cortex	0.20	0.009	+
BA 10 (R)	Anterior Prefrontal Cortex	0.26	0.001	+
BA 13 (L)	Insular Cortex	-0.27	0.008	-
BA 13 (R)	Insular Cortex	-0.33	0.002	-
BA 17 (L)	Primary Visual Cortex	-0.15	0.030	-
BA 17 (R)	Primary Visual Cortex	-0.20	0.024	-
BA 18 (L)	Secondary Visual Cortex	-0.19	0.007	-
BA 18 (R)	Secondary Visual Cortex	-0.23	0.012	-
BA 21 (L)	Middle Temporal Gyrus	0.15	0.001	+
BA 22 (L)	Superior Temporal Gyrus	-0.20	0.007	-
BA 22 (R)	Superior Temporal Gyrus	-0.24	0.010	-
BA 23 (L)	Ventral Posterior Cingulate Cortex	0.24	0.005	+
BA 23 (R)	Ventral Posterior Cingulate Cortex	0.22	0.010	+
BA 29 (R)	Retrosplenial Cingulate Cortex	0.17	0.027	+
BA 31 (L)	Dorsal Posterior Cingulate Cortex	0.38	0.007	+
BA 31 (R)	Dorsal Posterior Cingulate Cortex	0.38	0.005	+
BA 33 (R)	Anterior Cingulate Cortex	0.16	0.007	+
BA 34 (L)	Anterior Entorhinal Cortex	-0.12	0.030	-
BA 34 (R)	Anterior Entorhinal Cortex	-0.14	0.031	-
BA 37 (R)	Fusiform gyrus	-0.21	0.011	-
BA 39 (L)	Angular gyrus	0.47	0.001	+
BA 39 (R)	Angular gyrus	1.02	<0.001	+

BA 40 (L)	Supramarginal Gyrus	-0.24	0.016	-
BA 41 (L)	Primary Auditory Cortex	-0.16	0.048	-
BA 41 (R)	Primary Auditory Cortex	-0.16	0.017	-
BA 42 (R)	Primary Auditory Cortex	-0.23	0.039	-
BA 44 (R)	IFC pars opercularis	-0.30	0.007	-

RLP (see figure 5.2D, table 5.1.4) was positively correlated with the left/right anterior prefrontal cortices (BA10), superior frontal gyri (rsRELs), angular gyri (BA39), and inferior parietal lobes (rsREL). RLP was also positively correlated with the PCC, precuneus (rsREL), right retrosplenial cingulate cortex (BA29) and the left/right somatosensory association (BA7), ventral posterior cingulate (BA23) and dorsal posterior cingulate (BA31) cortices. Negative correlations were apparent between RLP and the left anterior/posterior superior temporal gyri (rsRELs), right IFC pars opercularis (BA44) and right fusiform gyrus (BA37). In both hemispheres RLP was negatively correlated with the somatosensory association (BA5), primary somatosensory (BA1, BA2, BA3), primary motor (BA4), insular (BA13) and primary auditory (BA41) cortices along with superior temporal areas (BA22). All other positive and negative correlations are displayed in table 5.1.4.

5.3.1.3. Summary of analysis 1

The above results confirm that activation of the DMN was apparent during an active auditory attention task. ROIs LLP, MPFC, PCC and RLP were significantly positively correlated with one another, along with a number of rsREL regions in close proximity, thus supporting the first hypothesis of this experiment. On exploration of the way in which the DMN interacts with regions covering the rest of the cortex, each ROI was negatively correlated with areas in the temporal lobes, including primary auditory, motor and somatosensory areas. In addition to this, LLP and RLP also exhibited negative relationships to primary and secondary visual regions,

raising questions about the relationship between the DMN and regions implicated in the processing of sensory information from the external world. Results also revealed that activity in some nodes of the DMN was coupled with down-regulation of activity in regions implicated in other large-scale control networks, i.e. parietal regions involved in the dorsal attention (goal-driven network) and dorsolateral prefrontal regions implicated in the executive control network, raising questions about interactions between large-scale brain networks.

5.3.1.4 Whole brain contrasts of the relationship between DMN regions as identified by Fox et al. (2005) and regions covering the whole of the cerebral cortex

As with experiment 1, due to the above analysis (comparing DMN ROIs to regions across the whole of the cortex) possibly being constrained by the use of BA definitions, whole brain positive/negative/two-sided maximum intensity projection maps were generated. As previously stated, this removed the BA restriction and allowed for a further exploration of the extent of correlated regions in the current population. Positive, negative and two-sided contrasts maps for each seed region are shown in figure 5.3 on the next page.

As shown in figure 5.3, whole brain positive contrast maps (top row of images) confirm the pattern of connectivity observed between DMN ROIs and the rest of the cerebral cortex,

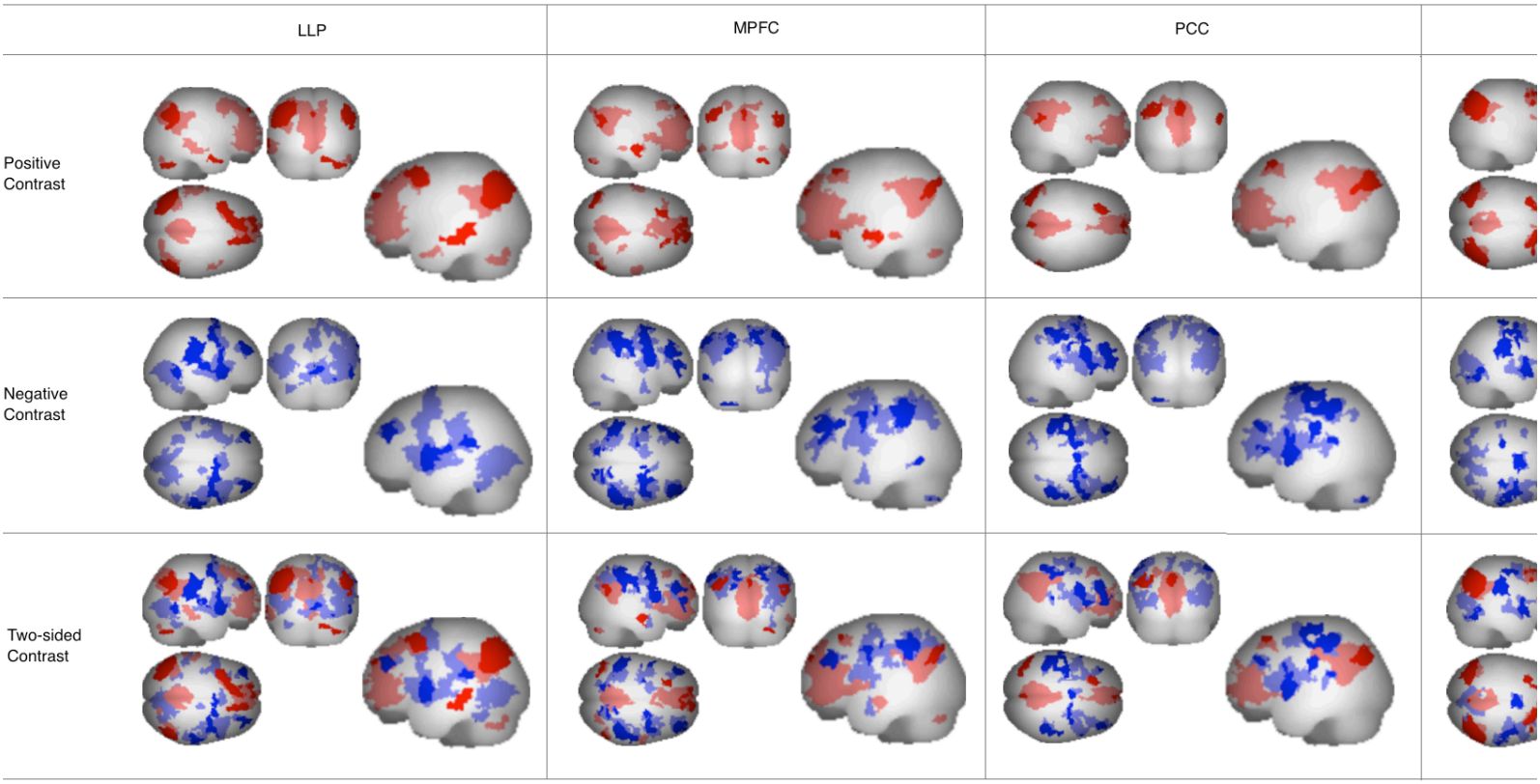

Figure 5.3. Whole brain positive, negative and two-sided maximum intensity projection maps for DMN seed regions in an 840s active auditory at parietal: LLP; medial prefrontal cortex: MPFC; posterior cingulate cortex: PCC and right lateral parietal: RLP (height (voxel-level) threshold: p=. threshold: p=.05) Top images represent positive contrasts; middle images are negative contrasts; and lower images are two-sided (positive/neg the same map.

revealing activations across frontal, posterior and parietal regions commonly implicated in the DMN. The negative contrasts (middle row of images) are interesting, as they appear to map out quite differently for each ROI. For example, down-regulation of occipital regions appears to be associated with LLP and RLP (with MPFC and PCC showing little or no association to these regions); conversely, down-regulation of parietal regions appears to be strongly linked with MPFC and PCC (with LLP and RLP showing little or no association to these regions). This infers that midline and lateral DMN components interact with the rest of the cortex in different ways. In turn, this suggests while the DMN may be considered as a coherent system in relation to resting-state/sentinel functions/stream of thought, each DMN region may differentially influence/be being influenced by other brain structures/network regions; this is considered in

more detail in the discussion of this experiment. Whilst the two-sided contrast maps (lower images; showing positive/negative contrasts on single maps) illustrate interactions between the DMN (frontal/posterior/parietal regions shown in red) and other brain regions, clusters of negatively correlated activity in regions in the vicinity of/overlapping with other neuronal networks (i.e. parietal and frontal regions implicated in the goal-driven network which would be expected to be active based on the task demands) raise questions about the interaction between the DMN and neural networks predominantly involved in the processing of the *external* world.

5.3.2. Analysis 2: Does DMN activity vary over the task duration?

5.3.2.1. Analysis 2a: Analysing reaction times as a behavioural index of DMN activity: If DMN activity changes over time, reaction times will show participants were slower to respond to task-relevant stimuli in condition 2 than condition 1, and slower in condition 3 than conditions 2 and 1.

Participants' average reaction times towards task-relevant goal-driven stimuli are shown in figure 5.4 across each condition (shown on a single-participant basis).

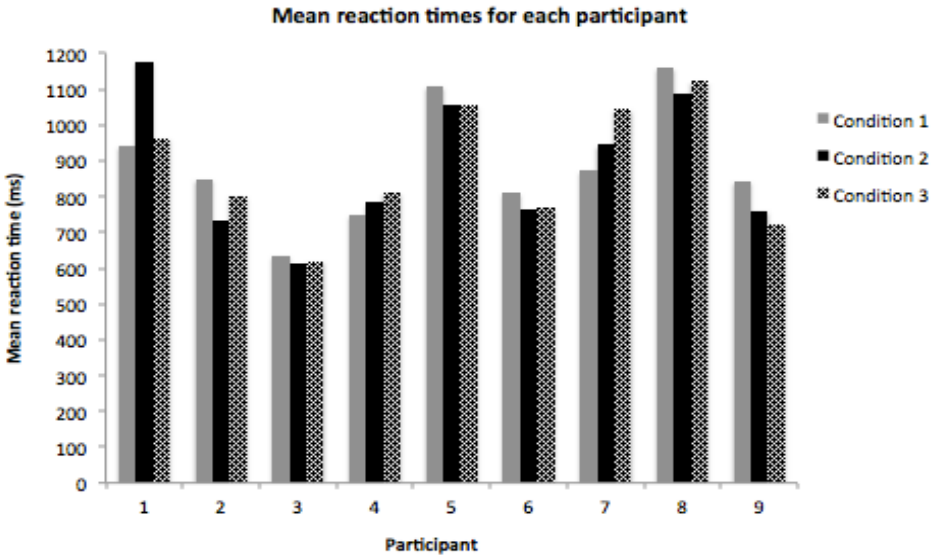

Figure 5.4. Participants' average reaction times across conditions 1, 2 and 3 (single-participant basis).

On visual inspection of figure 5.4, there appears to be variation in the average time taken to respond to goal-driven stimuli. For example, participant 1 elicits increased reaction times in condition 2 compared to conditions 1 and 3; participant 4 illustrates an increase in reaction time across conditions 1-3, whilst participant 9 shows a reduction in reaction times across conditions. Average reaction times for each condition at a group level are displayed in figure 5.5.

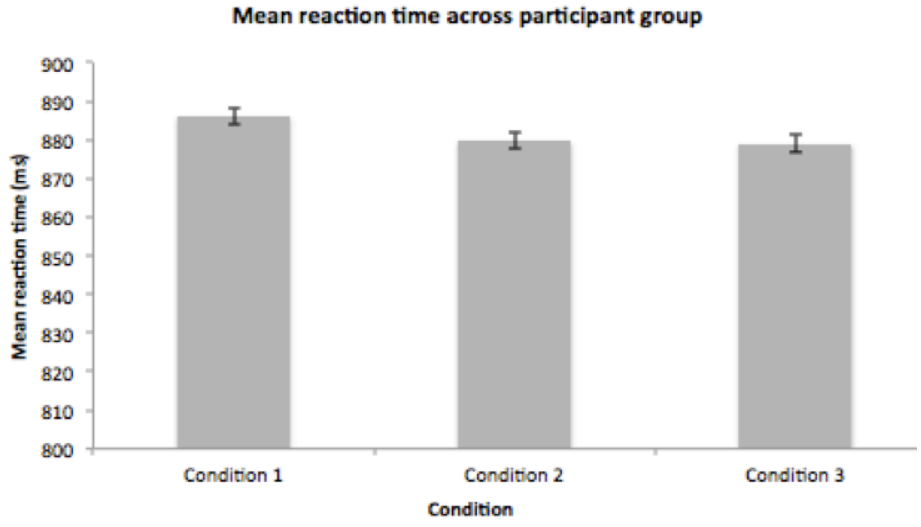

Figure 5.5. Average reaction times across participants for conditions 1, 2 and 3.

On visual inspection of figure 5.5, differences in reaction times towards goal-driven stimuli at a group level appear marginal. In order to assess changes in reaction time across conditions, a one-way ANOVA was conducted, with results revealing no significant main effect of condition on reaction time ($F(2,26)=0.004$; $p=.996$). This result suggests that participants exhibited no change in their response time towards task-relevant goal-driven stimuli across conditions, despite their individual reports of increased difficulty in maintaining concentration in the latter part of the task. This suggests that DMN activity may not increase in the latter part of the task (following the logic that reaction times are a behavioural index of DMN activity).

Based on outcome of this analysis, for the subsequent exploration of the strength and number of functionally correlated DMN regions, it was predicted that there would be no significant change in functional connectivity of the DMN across conditions.

5.3.2.2. Analysis 2b: Given that reaction times suggest that there is no change in DMN activity over time, there will be no significant change in functional connectivity of the DMN across conditions

As previously stated, in order to determine whether DMN connectivity varied over task duration three conditions were created within the auditory data. Condition 1 assessed DMN connectivity between 0-280s of the task duration, condition 2 assessed connectivity between 280-560s, and condition 3 assessed connectivity between 560-840s (note that the set up of this analysis in CONN is available in appendix D). As an initial single-participant exploration of the data, figure 5.6 illustrates the *total* first-level connectivity maps for participants 1-9 across conditions.

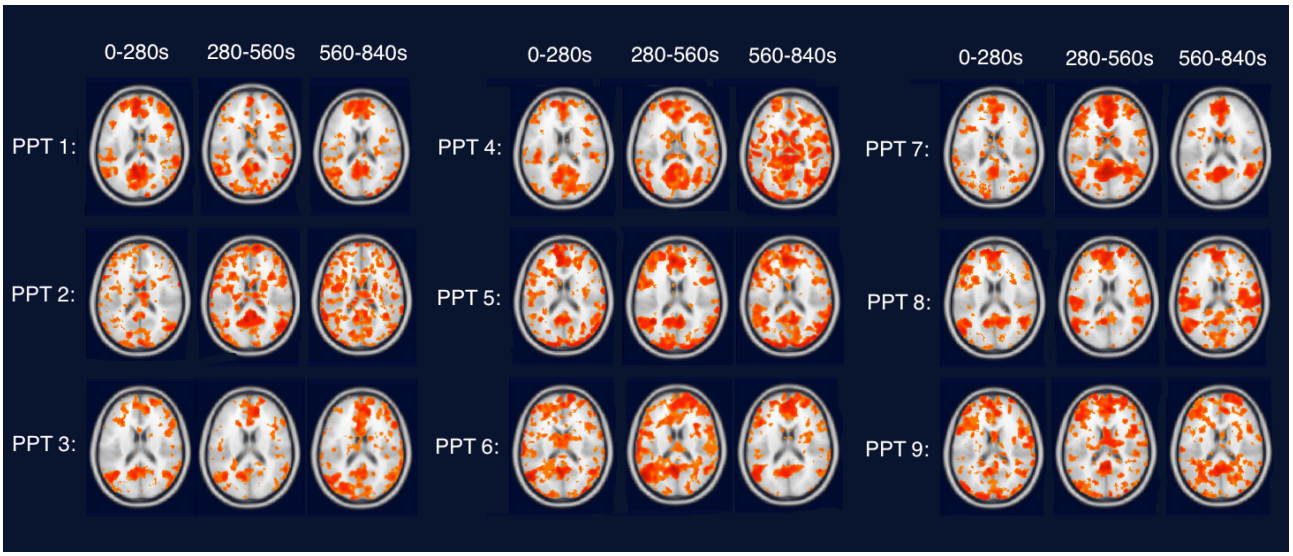

Figure 5.6. First-level analyses maps for participants 1-9 for conditions 1 (0-280s), 2 (280-560s) and 3 (560-840s) respectively. Note that these maps represent total connectivity for each DMN source: LLP, MPFC, PCC and RLP (threshold 0.5).

On visual inspection of figure 5.6, functional connectivity for each participant appears to be variable across conditions. In participants 2, 3, 4, 5 and 8 greater connectivity is apparent in condition 3 versus condition 2 and in condition 2 versus condition 1 respectively. However this pattern is not observed in participants 6, 7 and 9, who in general show greater connectivity in condition 2 compared to condition 1; and greater connectivity in condition 1 versus condition 3. In participant 1 fluctuations of connectivity appear across conditions, with greater overall connectivity in condition 1. It should be noted: on the whole, these individual fluctuations do not map on well with fluctuations in reaction time as shown in figure 5.4, with the exception of one or two participants (i.e. participant 4; this is discussed in more detail in section *5.4.3*).

5.3.2.3. ROI-to-ROI functional connectivity results

Connectivity between DMN ROIs: LLP, MPFC, PCC and RLP and the whole of the cerebral cortex are shown in figures 5.7-5.10. Tables 5.2.1-5.2.3 illustrate the BA/ROI/rsREL, label,

strength of connectivity (*B* value) and significance (*p* value). Within the tables DMN seed regions are displayed in *italics* and highlighted grey and rsREL regions are displayed in *italics*. In both the figures and the tables, positive correlations are shown in red text and negative correlations are shown in blue. Note also that significant (p<.05) correlations only are reported.

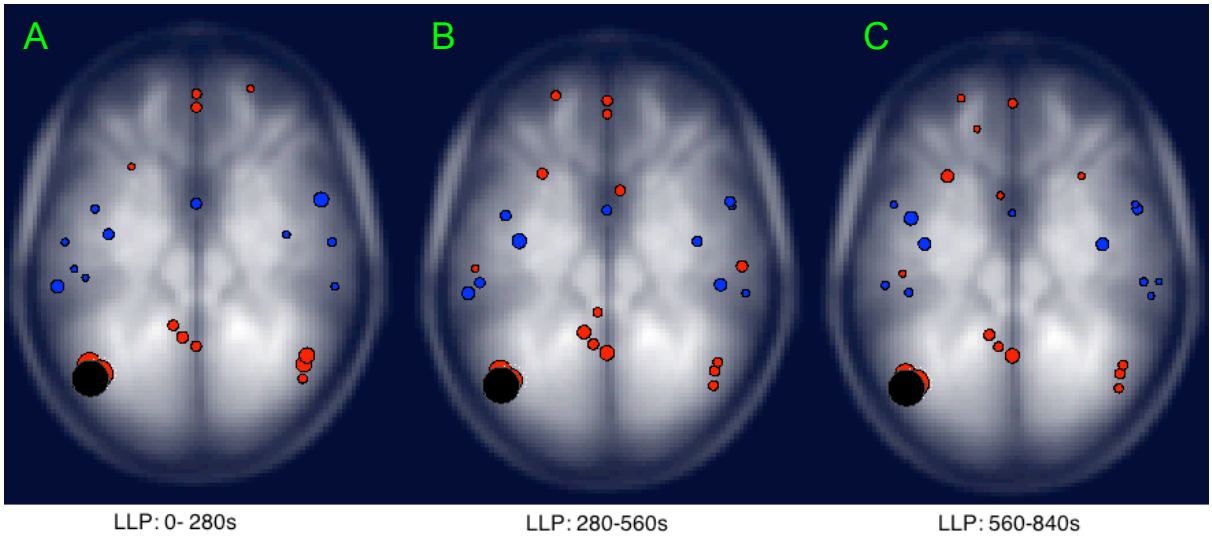

Figure 5.7. Relationship between DMN seed region LLP and areas covering the whole of the cerebral cortex for: (A) condition 1 (0-280s); (B) condition 2 (280-560s); and (C) condition 3 (560-840s).

Table 5.2.1. Left lateral parietal (LLP) connectivity to all cerebral regions for condition 1 (0-280s) and their significance.

Brodmann area	Brain region	*B*	*p*	Correlation
rsREL	*Left Posterior Sup Temp Gyrus*	*-0.28*	*0.003*	-
rsREL	*Left Anterior Sup Temp Gyrus*	*-0.30*	*0.025*	-
rsREL	*Left Superior Frontal Gyrus*	*0.38*	*0.048*	+
Seed ROI	*Medial prefrontal cortex*	*0.42*	*0.010*	+
rsREL	*Medial Prefrontal Cortex*	*0.41*	*0.013*	+
Seed ROI	*Posterior cingulate cortex*	*0.48*	*0.005*	+
rsREL	*Cingulate Gyrus*	*-0.36*	*0.009*	-
rsREL	*Precuneus (PCC)*	*0.49*	*0.010*	+
Seed ROI	*Right lateral parietal*	*0.47*	*0.017*	+
rsREL	*Right Inferior Parietal Lobe*	*0.67*	*0.001*	+
rsREL	*Right Anterior Sup Temp Gyrus*	*-0.22*	*0.001*	+
rsREL	*Right Posterior Sup Temp Gyrus*	*-0.22*	*0.041*	-
1 (L)	Primary Somatosensory Cortex	-0.21	0.047	-

2 (L)	Primary Somatosensory	-0.23	0.047	-
10 (R)	Anterior Prefrontal Cortex	0.31	0.041	+
13 (L)	Insular Cortex	-0.35	0.009	-
13 (R)	Insular Cortex	-0.30	0.040	-
31 (L)	Dorsal Posterior Cingulate Cortex	0.47	0.01	+
39 (L)	Angular gyrus	1.18	<0.001	+
39 (R)	Angular gyrus	0.55	<0.001	+
43 (L)	Subcentral Area	-0.18	0.041	-
43 (R)	Subcentral Area	-0.26	0.019	-

As shown in table 5.2.1 and figure 5.7A, significant positive correlations were found between LLP and frontal areas including the MPFC (seed ROI, rsREL), left superior frontal gyrus (rsREL) and right anterior prefrontal cortex (BA10R). Positive correlations with posterior regions, including the PCC (seed ROI) and precuneus (rsREL); and parietal areas, including the RLP (seed ROI), right inferior parietal (rsREL), and left/right angular gyri (BA39) were also apparent. Significant negative correlations were observed with the left posterior/anterior superior temporal gyrus (rsREL), cingulate gyrus (rsREL), primary somatosensory cortices (BA1, BA2), along with the right anterior superior temporal gyrus (rsREL) and posterior superior temporal gyrus (rsREL). Negative correlations between LLP and left/right insular (BA13) and subcentral (BA43) area were also apparent.

Table 5.2.2. Left lateral parietal (LLP) connectivity to all cerebral regions for condition 2 (280-560s) and their significance.

Brodmann area	Brain region	*B*	*p*	Correlation
rsREL	*Left Inferior Parietal Lobe*	*1.73*	*<0.001*	+
rsREL	*Left Posterior Sup Temp Gyrus*	*-0.30*	*0.004*	-
rsREL	*Left Anterior Sup Temp Gyrus*	*-0.41*	*0.007*	-
rsREL	*Left Superior Frontal Gyrus*	*0.52*	*0.007*	+
Seed ROI	*Medial prefrontal cortex*	*0.41*	*0.009*	+
rsREL	*Medial Prefrontal Cortex*	*0.48*	*0.007*	+
Seed ROI	*Posterior cingulate cortex*	*0.67*	*0.007*	+
rsREL	*Precuneus (PCC)*	*0.70*	*0.002*	+
rsREL	*Cingulate Gyrus*	*-0.35*	*0.008*	-
Seed ROI	*Right lateral parietal*	*0.59*	*0.009*	+
rsREL	*Right Inferior Parietal lobe*	*0.68*	*0.009*	+

rsREL	*Right Anterior Sup Temp Gyrus*	*-0.24*	*0.044*	-
rsREL	*Right Posterior Sup Temp Gyrus*	*-0.32*	*0.030*	-
2 (R)	Primary Somatosensory Cortex	-0.28	0.004	-
10 (L)	Anterior Prefrontal Cortex	0.49	0.008	+
13 (L)	Insular Cortex	-0.45	0.002	-
13 (R)	Insular Cortex	-0.36	0.008	-
21 (L)	Middle Temporal Gyrus	0.43	0.026	+
21 (R)	Middle Temporal Gyrus	0.29	0.007	+
22 (L)	Superior Temporal Gyrus	-0.22	0.007	-
23 (L)	Ventral Posterior Cingulate Cortex	0.35	0.01	+
31 (L)	Dorsal Posterior Cingulate Cortex	0.66	0.003	+
33 (R)	Anterior Cingulate Cortex	0.17	0.007	+
39 (L)	Angular gyrus	1.31	<0.001	+
39 (R)	Angular gyrus	0.62	0.007	+
44 (R)	IFC pars opercularis	-0.43	0.007	-

Table 5.2.2 and figure 5.7B show LLP was positively correlated with frontal areas including the MPFC (seed ROI, rsREL), left superior frontal gyrus (rsREL) and right anterior prefrontal cortex (BA10R). Positive correlations with the PCC (seed ROI), precuneus (rsREL) and parietal areas, including RLP (seed ROI), right inferior parietal (rsREL), and left/right angular gyri (BA39) were also apparent. This seed was also positively correlated with the left ventral/dorsal posterior cingulate cortices (BA23/BA31), right anterior cingulate cortex (BA33) and the left/right middle temporal gyrus (BA21). LLP was significantly negatively correlated with the left/right anterior/posterior superior temporal (rsREL) and cingulate (rsREL) gyri. Negative correlations were also found between LLP and the right primary somatosensory cortex (BA2), IFC pars opercularis (BA44), left superior temporal gyrus (BA22) and the left/right insular cortices (BA13).

Table 5.2.3. Left lateral parietal (LLP) connectivity to all cerebral regions for condition 3 (560-840s) and their significance.

Brodmann area	Brain region	*B*	*p*	Correlation
rsREL	*Left Inferior Parietal Lobe*	*1.66*	*<0.001*	+

rsREL	*Left Anterior Sup Temp Gyrus*	*-0.42*	*0.003*	-
rsREL	*Left Superior Frontal Gyrus*	*0.49*	*0.004*	+
Seed ROI	*Medial prefrontal cortex*	*0.41*	*0.009*	+
rsREL	*Medial Prefrontal Cortex*	*0.48*	*0.014*	+
Seed ROI	*Posterior cingulate cortex*	*0.59*	*0.002*	+
rsREL	*Precuneus (PCC)*	*0.64*	*0.002*	+
rsREL	*Cingulate Gyrus*	*-0.28*	*0.042*	-
Seed ROI	*Right lateral parietal*	*0.54*	*0.018*	+
rsREL	*Right Anterior Sup Temp Gyrus*	*-0.27*	*0.011*	-
rsREL	*Right Posterior Sup Temp Gyrus*	*-0.28*	*0.042*	-
rsREL	*Right Inferior Parietal lobe*	*0.60*	*0.014*	+
rsREL	*Right Superior Frontal Gyrus*	*0.30*	*0.042*	+
10 (L)	Anterior Prefrontal Cortex	0.36	0.032	+
11 (L)	Orbitofrontal Cortex	0.28	0.047	+
13 (L)	Insular Cortex	-0.36	0.004	-
13 (R)	Insular Cortex	-0.36	0.004	-
20 (L)	Inferior Temporal Gyrus	0.21	0.042	+
22 (L)	Superior Temporal Gyrus	-0.23	0.033	-
22 (R)	Superior Temporal Gyrus	-0.23	0.026	-
25 (L)	Subgenual cortex	0.20	0.042	+
31 (L)	Dorsal Posterior Cingulate Cortex	0.60	0.01	+
39 (L)	Angular gyrus	1.19	<0.001	+
39 (R)	Angular gyrus	0.52	0.011	+
41 (L)	Primary Auditory Cortex	-0.14	0.025	-
42 (R)	Primary Auditory Cortex	-0.16	0.047	-
44 (L)	IFC pars opercularis	-0.22	0.042	-
44 (R)	IFC pars opercularis	-0.29	0.042	-

Similar to the results above, table 5.2.3 and figure 5.7C show significant positive correlations between LLP and MPFC (seed ROI, rsREL), left superior frontal gyrus (rsREL) and right anterior prefrontal cortex (BA10R). Positive correlations were also apparent between LLP and posterior regions, including the PCC (seed ROI), precuneus (rsREL); and parietal areas, including the RLP (seed ROI), right inferior parietal (rsREL), and left/right angular gyri (BA39). LLP was also positively correlated with the left anterior prefrontal cortex (BA10), orbitofrontal cortex (BA11), inferior temporal gyrus (BA20), subgenual cortex (BA25) and the left dorsal posterior cingulate cortex (BA31). Negative correlations were found between LLP and the left/right insular cortices (BA13), superior temporal gyrus (BA22) and IFC pars opercularis (BA44), along with the left (BA41) and right (BA42) primary auditory cortices.

5.3.2.3.1. Summary of LLP connectivity across conditions 1, 2 and 3

The above results reveal that functional connectivity between LLP and all other DMN ROIs remained prominent in each condition. On visual inspection, results also suggest that there was no extensive change in the functional connectivity between LLP and other cortical regions over time, with between-subjects contrasts in CONN confirming this. For this portion of the DMN, results support the outcome of analysis 2a: showing reaction times as a behavioural index of DMN activity suggest that there is no change in DMN activity across task duration.

Connectivity between MPFC and the whole of the cerebral cortex are shown in figure 5.8 and tables 5.2.4-5.2.6.

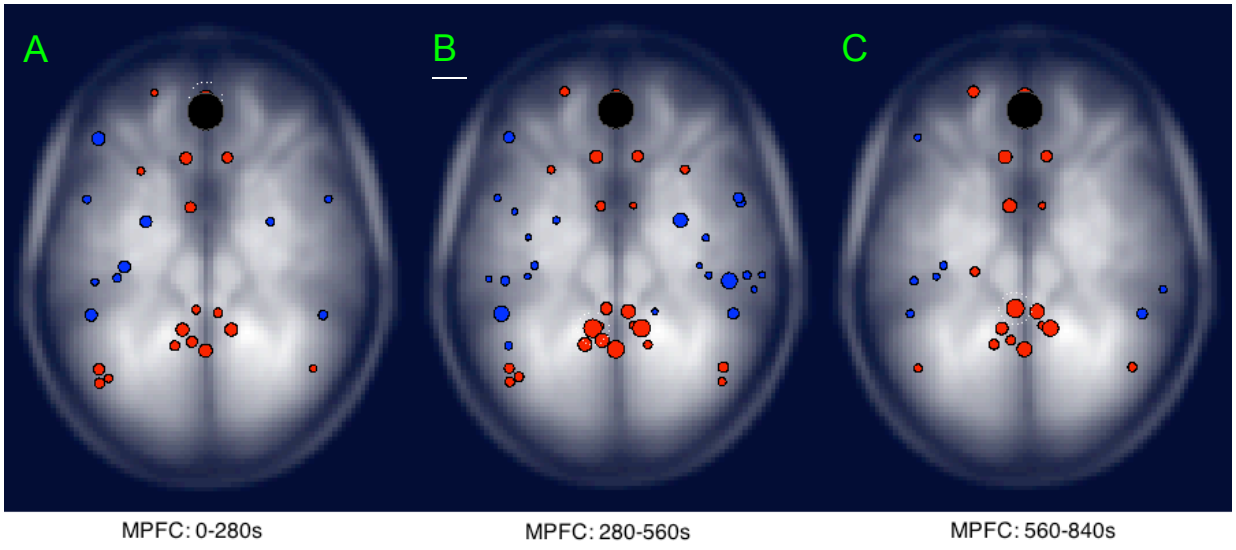

Figure 5.8. Relationship between DMN seed region MPFC and areas covering the whole of the cerebral cortex for: (A) condition 1 (0-280s); (B) condition 2 (280-560s); and (C) condition 3 (560-840s).

Table 5.2.4. Medial prefrontal cortex (MPFC) connectivity to all cerebral regions for condition 1 (0-280s) and their significance.

Brodmann	Brain region	*B*	*p*	Correlation	area
Seed ROI	*Left lateral parietal*	*0.42*	*0.008*	+	
rsREL	*Left Inferior Parietal Lobe*	*0.38*	*0.019*	+	

rsREL	*Left Superior Frontal Gyrus*	*0.31*	*0.024*	+
rsREL	*Medial Prefrontal Cortex*	*1.18*	*0.004*	+
Seed ROI	*Posterior cingulate cortex*	*0.61*	*0.006*	+
rsREL	*Precuneus (PCC)*	*0.80*	*0.004*	+
Seed ROI	*Right lateral parietal*	*0.54*	*0.018*	+
2 (L)	Primary Somatosensory Cortex	-0.19	0.033	-
3 (L)	Primary Somatosensory Cortex	-0.18	0.018	-
4 (L)	Primary Motor Cortex	-0.22	0.005	-
6 (L)	Premotor Cortex	-0.29	0.005	-
6 (R)	Premotor Cortex	-0.33	0.019	-
10 (L)	Anterior Prefrontal Cortex	0.32	0.049	+
23 (L)	Ventral Posterior Cingulate Cortex	0.45	0.018	+
23 (R)	Ventral Posterior Cingulate Cortex	0.36	0.013	+
24 (L)	Ventral Anterior Cingulate Cortex	0.31	0.006	+
30 (L)	Cingulate Cortex	0.41	0.010	+
31 (L)	Dorsal Posterior Cingulate Cortex	0.76	0.004	+
31 (R)	Dorsal Posterior Cingulate Cortex	0.49	0.004	+
32 (L)	Dorsal Anterior Cingulate Cortex	0.65	0.005	+
32 (R)	Dorsal Anterior Cingulate Cortex	0.39	0.007	+
39 (L)	Angular gyrus	0.45	0.006	+
39 (R)	Angular gyrus	0.21	0.032	+
40 (L)	Supramarginal Gyrus	-0.38	0.005	-
40 (R)	Supramarginal Gyrus	-0.42	0.013	-
44 (L)	IFC pars opercularis	-0.30	0.019	-
44 (R)	IFC pars opercularis	-0.32	0.031	-
46 (L)	Dorsolateral Prefrontal Cortex	-0.30	0.004	-

Table 5.2.4 and figure 5.8A reveal MPFC was significantly positively correlated with other frontal areas including MPFC (rsREL), left superior frontal gyrus (rsREL) and anterior prefrontal cortex (BA10). Positive correlations with posterior regions, including PCC (seed ROI), precuneus (rsREL), and parietal areas, including LLP (seed ROI), left inferior parietal lobe (reREL) and RLP (seed ROI, rsREL) were also apparent. MPFC was also positively correlated with the left ventral anterior cingulate (BA24) and cingulate (BA30) cortices, along with the left/right angular gyri (BA39), ventral/dorsal posterior (BA23, BA31) and dorsal anterior cingulate (BA32) cortices. Significant negative correlations were observed between MPFC and the left primary somatosensory (BA2 BA3), primary motor (BA4) and dorsolateral prefrontal

(BA46) cortices and the left/right premotor cortices (BA6), supramarginal gyri (BA40) and IFC operculari (BA44).

Table 5.2.5. Medial prefrontal cortex (MPFC) connectivity to all cerebral regions for condition 2 (280-560s) and their significance.

Brodmann area	Brain region	*B*	*p*	Correlation
Seed ROI	*Left Lateral Parietal*	*0.41*	*0.009*	+
resREL	*Left Inferior Parietal Lobe*	*0.34*	*0.009*	+
rsREL	*Left Superior Frontal Gyrus*	*0.24*	*0.018*	+
rsREL	*Left Anterior Superior Temp Gyrus*	*-0.25*	*0.035*	-
rsREL	*Medial Prefrontal Cortex*	*1.13*	*0.001*	+
Seed ROI	*Posterior Cingulate Cortex*	*0.65*	*0.001*	+
rsREL	*Precuneus (PCC)*	*0.93*	*<0.001*	+
Seed ROI	*Right Lateral Parietal*	*0.33*	*0.016*	+
rsREL	*Right Anterior Sup Temp Gyrus*	*-0.27*	*0.009*	-
rsREL	*Right Superior Frontal Gyrus*	*0.21*	*0.011*	+
rsREL	*Right Posterior Sup Temp Gyrus*	*-0.25*	*0.033*	-
2 (L)	Primary Somatosensory Cortex	-0.26	0.009	-
2 (R)	Primary Somatosensory Cortex	-0.36	0.001	-
3 (L)	Primary Somatosensory Cortex	-0.20	0.038	-
3 (R)	Primary Somatosensory Cortex	-0.21	0.029	-
4 (L)	Primary Motor Cortex	-0.18	0.020	-
4 (R)	Primary Motor Cortex	-0.15	0.047	-
5 (R)	Somatosensory Association Cortex	-0.16	0.041	-
6 (L)	Premotor Cortex	-0.29	0.027	-
6 (R)	Premotor Cortex	-0.37	0.001	-
10 (L)	Anterior Prefrontal Cortex	0.34	0.009	+
13 (L)	Insular Cortex	-0.27	0.041	-
13 (R)	Insular Cortex	-0.25	0.027	-
22 (L)	Superior Temporal Gyrus	-0.23	0.038	-
22 (R)	Superior Temporal Gyrus	-0.18	0.016	-
23 (L)	Ventral Posterior Cingulate Cortex	0.57	0.003	+
23 (R)	Ventral Posterior Cingulate Cortex	0.49	0.001	+
24 (L)	Ventral Anterior Cingulate Cortex	0.36	0.008	+
24 (R)	Ventral Anterior Cingulate Cortex	0.25	0.033	+
29 (L)	Retrosplenial Cingulate Cortex	0.37	0.045	+
29 (R)	Retrosplenial Cingulate Cortex	0.38	0.031	+
30 (L)	Cingulate Cortex	0.49	0.001	+
30 (R)	Cingulate Cortex	0.31	0.013	+
31 (L)	Dorsal Posterior Cingulate Cortex	0.83	<0.001	+
31 (R)	Dorsal Posterior Cingulate Cortex	0.64	<0.001	+
32 (L)	Dorsal Anterior Cingulate Cortex	0.67	0.001	+
32 (R)	Dorsal Anterior Cingulate Cortex	0.56	0.004	+
37 (L)	Fusiform gyrus	-0.28	0.017	-
39 (L)	Angular gyrus	0.39	0.008	+
39 (R)	Angular gyrus	0.34	0.006	+

40 (L)	Supramarginal Gyrus	-0.57	0.001	-
40 (R)	Supramarginal Gyrus	-0.51	0.005	-
42 (R)	Primary Auditory Cortex	-0.15	0.032	-
44 (L)	IFC pars opercularis	-0.35	0.028	-
44 (R)	IFC pars opercularis	-0.44	0.006	-
46 (L)	Dorsolateral Prefrontal Cortex	-0.35	0.005	-

As shown in table 5.2.5 and figure 5.8B MPFC was significantly positively correlated with MPFC (rsREL) left/right superior frontal gyri (rsREL), posterior regions, including the PCC (seed ROI), precuneus (rsREL), and parietal areas, including the left inferior parietal lobe (reREL) and LLP/RLP (seed ROIs). MPFC was also positively correlated with the left anterior prefrontal (BA10), left/right ventral/dorsal posterior/anterior cingulate (BA23, BA24, BA31, BA32), retrosplenial cingulate (BA29) and cingulate (BA30) cortices, along with the angular gyri (BA39). Significant negative correlations were found between MPFC and the left/right anterior superior temporal gyri (rsRELs), primary somatosensory (BA2, BA3), primary motor (BA4) premotor (BA6) and insular (BA13) cortices, IFC pars operculari (BA44), superior temporal (BA22) and supramarginal (BA40) gyri. Negative correlations were also apparent between MPFC and the fusiform gyrus (BA37) and dorsolateral prefrontal cortex (BA46) in the left hemisphere and the posterior superior temporal gyrus (rsREL), somatosensory association (BA5) and primary auditory (BA46) cortices in the right hemisphere.

Table 5.2.6. Medial prefrontal cortex (MPFC) connectivity to all cerebral regions for condition 3 (560-840s) and their significance.

Brodmann	Brain region	*B*	*p*	Correlation	area
Seed ROI	*Posterior Cingulate Cortex*	*0.56*	*0.014*	+	
rsREL	*Precuneus (PCC)*	*0.80*	*0.001*	+	
rsREL	*Right Posterior Sup Temp Gyrus*	*-0.12*	*0.037*	-	
2 (L)	Primary Somatosensory Cortex	-0.28	0.031	-	
3 (L)	Primary Somatosensory Cortex	-0.24	0.042	-	
4 (L)	Primary Motor Cortex	-0.28	0.031	-	

10 (L)	Anterior Prefrontal Cortex	0.39	0.006	+
23 (L)	Ventral Posterior Cingulate Cortex	0.41	0.001	+
23 (R)	Ventral Posterior Cingulate Cortex	0.42	0.001	+
24 (L)	Ventral Anterior Cingulate Cortex	0.35	0.002	+
24 (R)	Ventral Anterior Cingulate Cortex	0.24	0.037	+
29 (R)	Retrosplenial Cingulate Cortex	0.40	0.037	+
30 (L)	Cingulate Cortex	0.42	0.01	+
31 (L)	Dorsal Posterior Cingulate Cortex	0.66	0.003	+
31 (R)	Dorsal Posterior Cingulate Cortex	0.54	0.001	+
32 (L)	Dorsal Anterior Cingulate Cortex	0.65	0.002	+
32 (R)	Dorsal Anterior Cingulate Cortex	0.52	0.006	+
35 (L)	Perirhinal cortex	0.20	0.015	+
39 (L)	Angular gyrus	0.36	0.027	+
39 (R)	Angular gyrus	0.24	0.018	+
40 (L)	Supramarginal Gyrus	-0.37	0.030	-
40 (R)	Supramarginal Gyrus	-0.38	0.008	-
46 (L)	Dorsolateral Prefrontal Cortex	-0.27	0.04	-

Table 5.2.6 and figure 5.8C show that MPFC was positively correlated with the precuneus (rsREL), PCC (seed ROI), left anterior prefrontal (BA10), cingulate (BA30) and perirhinal (BA35) cortices; and the right retrosplenial cingulate cortex (BA39). Positive correlations were also apparent with MPFC and the left/right ventral/dorsal anterior/posterior cingulate cortices (BA23, BA24, BA31, BA32) and the angular gyri (BA39). Significant negative correlations were found between MPFC and the right posterior superior temporal gyrus (rsREL), and the left primary somatosensory (BA2, BA3), primary motor (BA4) and dorsolateral prefrontal (BA46) cortices. MPFC was also negatively correlated with the left/right supramarginal gyri (BA40).

5.3.2.3.2. Summary of MPFC connectivity across conditions 1, 2 and 3

As shown in figure 5.8 and tables 5.2.4-5.2.6, MPFC was positively correlated to a number of DMN and rsREL regions in conditions 1 and 2. However, in condition 3, MPFC was positively correlated to posterior DMN regions only. On visual inspection of figure 5.8 there appears to be more robust and widespread connectivity in condition 2 compared to conditions 1 and 3. Between-subjects contrasts in CONN, however, revealed no significant change in connectivity

between MPFC and any other brain region over time. For this portion of the DMN results support the outcome of analysis 2a: showing reaction times as a behavioural index of DMN activity suggest there is no change across task duration.

Connectivity between PCC and the whole of the cerebral cortex are shown in figure 5.9 and tables 5.2.7-5.2.9.

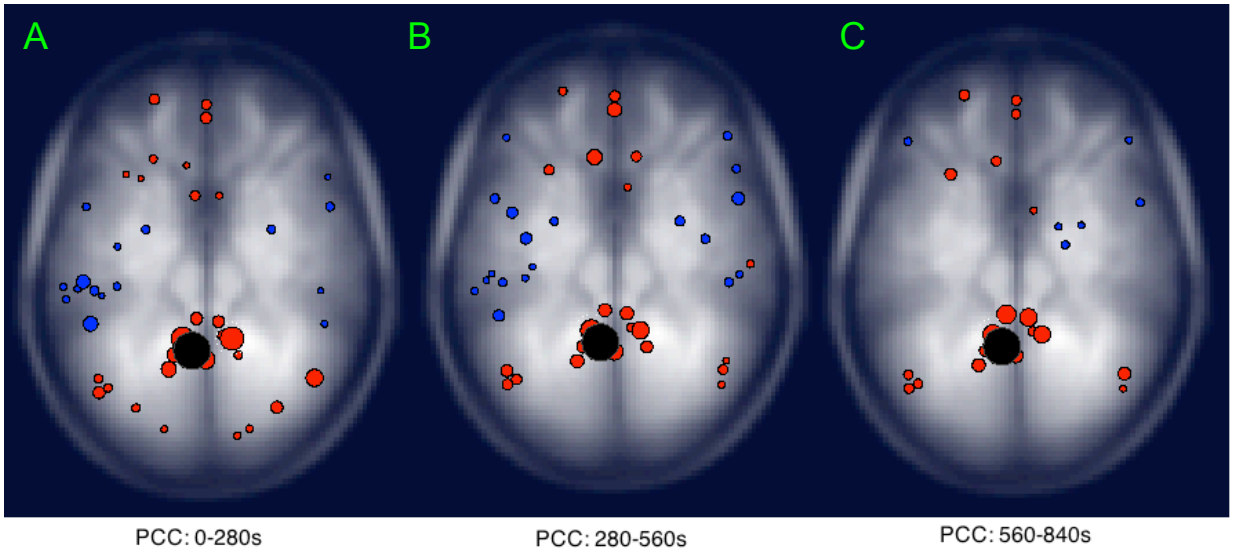

Figure 5.9. Relationship between DMN seed region PCC and areas covering the whole of the cerebral cortex for: (A) condition 1 (0-280s); (B) condition 2 (280-560s); and (C) condition 3 (560-840s).

Table 5.2.7. Posterior cingulate cortex (PCC) connectivity to all cerebral regions for condition 1 (0-280s) and their significance.

Brodmann area	Brain region	*B*	*p*	Correlation
Seed ROI	*Left Lateral Parietal*	*0.48*	*0.004*	+
rsREL	*Left Inferior Parietal Lobe*	*0.46*	*0.016*	+
rsREL	*Left Posterior Sup Temp Gyrus*	*-0.19*	*0.027*	-
rsREL	*Left Superior Frontal Gyrus*	*0.32*	*0.048*	+
Seed ROI	*Medial Prefrontal Cortex*	*0.61*	*0.005*	+
rsREL	*Medial Prefrontal Cortex*	*0.52*	*0.009*	+
2 (L)	Primary Somatosensory Cortex	-0.29	0.012	-

2 (R)	Primary Somatosensory Cortex	-0.22	0.046	-
3 (L)	Primary Somatosensory Cortex	-0.24	0.022	-
6 (L)	Premotor Cortex	-0.28	0.016	-
6 (R)	Premotor Cortex	-0.33	0.016	-
8 (L)	Dorsal Frontal Cortex	0.24	0.020	+
10 (L)	Anterior Prefrontal Cortex	0.37	0.008	+
13 (L)	Insular Cortex	-0.28	0.033	-
17 (R)	Primary Visual Cortex	0.23	0.022	+
18 (L)	Secondary Visual Cortex	0.20	0.033	+
18 (R)	Secondary Visual Cortex	0.24	0.022	+
19 (L)	Associative Visual Cortex	0.27	0.017	+
22 (L)	Superior Temporal Gyrus	-0.24	0.022	-
23 (R)	Ventral Posterior Cingulate Cortex	0.50	0.004	+
29 (L)	Retrosplenial Cingulate Cortex	0.41	0.009	+
29 (R)	Retrosplenial Cingulate Cortex	0.41	0.008	+
30 (R)	Cingulate Cortex	0.31	0.017	+
32 (L)	Dorsal Anterior Cingulate Cortex	0.30	0.044	+
33 (L)	Anterior Cingulate Cortex	0.16	0.009	+
33 (R)	Anterior Cingulate Cortex	0.10	0.033	+
39 (L)	Angular gyrus	0.51	0.014	+
40 (R)	Supramarginal Gyrus	-0.26	0.033	-
41 (L)	Primary Auditory Cortex	-0.19	0.046	-
42 (L)	Primary Auditory Cortex	-0.22	0.033	-
44 (L)	IFC pars opercularis	-0.26	0.022	-
44 (R)	IFC pars opercularis	-0.30	0.014	-
45 (R)	IFC pars triangularis	-0.20	0.05	-
47 (L)	Inferior Prefrontal Gyrus	0.17	0.040	+

Table 5.2.7 and figure 5.9A show that PCC was positively correlated with the LLP (seed ROI) left inferior parietal (rsREL), superior frontal gyrus (rsREL) and MPFC (seed ROI, rsREL). This seed was also positively correlated with the left dorsal frontal (BA8) anterior prefrontal (BA10), associative visual (BA19) and dorsal anterior cingulate (BA32) cortices. PCC was also positively correlated with the angular (BA39) and inferior prefrontal (BA47) gyri, along with the right primary visual (BA17), ventral posterior cingulate (BA23) and cingulate (BA30) cortices. PCC was positively correlated to the secondary visual (BA18), retrosplenial cingulate (BA29) and anterior cingulate (BA33) cortices in both hemispheres. Negative correlations were apparent between PCC and the left posterior superior temporal gyrus (rsREL), superior temporal gyrus (BA22), primary somatosensory (BA3), insular (BA13) and primary auditory (BA41, BA42)

cortices, along with the right supramarginal gyrus (BA40) and IFC pars triangularis (BA45). PCC was also negatively correlated with the left/right primary somatosensory (BA2) and premotor (BA6) cortices, and the IFC pars operculari (BA44).

Table 5.2.8. Posterior cingulate cortex (PCC) connectivity to all cerebral regions for condition 2 (280-560s) and their significance.

Brodmann	Brain region	*B*	*p*	Correlation	area
Seed ROI	*Left Lateral Parietal*	*0.67*	*0.005*	+	
rsREL	*Left Anterior Sup Temp Gyrus*	*-0.28*	*0.004*	-	
rsREL	*Left Inferior Parietal Lobe*	*0.61*	*0.006*	+	
rsREL	*Left Superior Frontal Gyrus*	*0.31*	*0.006*	+	
rsREL	*Left Posterior Sup Temp Gyrus*	*-0.17*	*0.021*	-	
Seed ROI	*Medial Prefrontal Cortex*	*0.65*	*0.002*	+	
rsREL	*Medial Prefrontal Cortex*	*0.56*	*0.005*	+	
Seed ROI	*Right Lateral Parietal*	*0.38*	*0.022*	+	
rsREL	*Right Inferior Parietal lobe*	*0.34*	*0.033*	+	
1 (L)	Primary Somatosensory Cortex	-0.25	0.033	-	
1 (R)	Primary Somatosensory Cortex	-0.20	0.025	-	
2 (L)	Primary Somatosensory Cortex	-0.25	0.014	-	
2 (R)	Primary Somatosensory Cortex	-0.33	0.011	-	
3 (L)	Primary Somatosensory Cortex	-0.18	0.025	-	
4 (L)	Primary Motor Cortex	-0.17	0.029	-	
6 (L)	Premotor Cortex	-0.24	0.014	-	
6 (R)	Premotor Cortex	-0.38	0.008	-	
10 (L)	Anterior Prefrontal Cortex	0.38	0.014	+	
13 (L)	Insular Cortex	-0.37	0.004	-	
13 (R)	Insular Cortex	-0.32	0.010	-	
21 (R)	Middle Temporal Gyrus	0.22	0.022	+	
22 (L)	Superior Temporal Gyrus	-0.18	0.033	-	
29 (L)	Retrosplenial Cingulate Cortex	0.51	0.016	+	
29 (R)	Retrosplenial Cingulate Cortex	0.47	0.010	+	
30 (R)	Cingulate Cortex	0.36	0.003	+	
32 (R)	Dorsal Anterior Cingulate Cortex	0.28	0.006	+	
33 (R)	Anterior Cingulate Cortex	0.12	0.021	+	
39 (L)	Angular gyrus	0.68	0.003	+	
39 (R)	Angular gyrus	0.47	0.008	+	
40 (L)	Supramarginal Gyrus	-0.39	0.004	-	
44 (L)	IFC pars opercularis	-0.25	0.010	-	
44 (R)	IFC pars opercularis	-0.46	0.003	-	
45 (R)	IFC pars triangularis	-0.22	0.016	-	
46 (L)	Dorsolateral Prefrontal Cortex	-0.23	0.025	-	
46 (R)	Dorsolateral Prefrontal Cortex	-0.30	0.014	-	

As shown in table 5.2.8 and figure 5.9B, PCC was significantly positively correlated with the MPFC (rsREL), left/right inferior parietal lobe (rsREL), left superior frontal gyrus (rsREL) and LLP/RLP (seed ROIs). PCC was also positively correlated with the left anterior prefrontal cortex (BA10), right middle temporal gyrus (BA21), and right cingulate (BA30), dorsal anterior cingulate (BA32) and anterior cingulate (BA33) cortices. In both hemispheres, PCC was positively correlated with the retrosplenial cingulate cortices (BA29) and the angular gyri (BA39). Significant negative correlations were found between PCC and the left posterior superior temporal gyrus (rsREL), primary somatosensory (BA3), primary motor (BA4) cortices, superior temporal gyrus (BA22) supramarginal gyrus (BA40) and the right IFC pars triangularis (BA45). PCC was also negatively correlated with the left/right insular (BA13), primary somatosensory (BA1, BA2) and premotor (BA6) cortices, IFC pars operculari (BA44) and dorsolateral prefrontal cortices (BA46).

Table 5.2.9. Posterior cingulate cortex (PCC) connectivity to all cerebral regions for condition 3 (560-840s) and their significance.

Brodmann area	Brain region	*B*	*p*	Correlation
Seed ROI	*Left Lateral Parietal*	*0.59*	*0.011*	+
rsREL	*Left Superior Frontal Gyrus*	*0.35*	*0.006*	+
rsREL	*Left Inferior Parietal Lobe*	*0.57*	*0.014*	+
Seed ROI	*Medial Prefrontal Cortex*	*0.56*	*0.011*	+
rsREL	*Medial Prefrontal Cortex*	*0.51*	*0.011*	+
rsREL	*Precuneus (PCC)*	*1.07*	*0.002*	+
Seed ROI	*Right Lateral Parietal*	*0.36*	*0.047*	+
6 (R)	Premotor Cortex	-0.25	0.046	-
7 (L)	Somatosensory Association Cortex	0.53	0.003	+
10 (L)	Anterior Prefrontal Cortex	0.26	0.008	+
23 (L)	Ventral Posterior Cingulate Cortex	0.53	<0.001	+
23 (R)	Ventral Posterior Cingulate Cortex	0.49	<0.001	+
24 (R)	Ventral Anterior Cingulate Cortex	0.15	0.045	+
28 (R)	Posterior Entorhinal Cortex	-0.12	0.026	-
29 (L)	Retrosplenial Cingulate Cortex	0.43	0.011	+
29 (R)	Retrosplenial Cingulate Cortex	0.44	0.011	+
30 (L)	Cingulate Cortex	0.40	0.008	+

31 (L)	Dorsal Posterior Cingulate Cortex	1.09	<0.001	+
31 (R)	Dorsal Posterior Cingulate Cortex	0.76	<0.001	+
32 (L)	Dorsal Anterior Cingulate Cortex	0.32	0.011	+
34 (R)	Anterior Entorhinal Cortex	-0.15	0.046	-
39 (L)	Angular gyrus	0.64	0.011	+
39 (R)	Angular gyrus	0.45	0.004	+
44 (R)	IFC pars opercularis	-0.24	0.024	-
46 (L)	Dorsolateral Prefrontal Cortex	-0.26	0.026	-
46 (R)	Dorsolateral Prefrontal Cortex	-0.20	0.043	-

Table 5.2.9 figure 5.9C reveal significant positive correlations between PCC and the left superior frontal gyrus (rsREL), inferior parietal lobe (rsREL), LLP/RLP (seed ROIs), MPFC (seed ROI, rsREL) and precuneus (rsREL). Significant positive correlations were also found with the left somatosensory association (BA7), anterior prefrontal (BA10), cingulate (BA30) and dorsal anterior cingulate (BA32) cortices, and the right ventral anterior cingulate cortex (BA24). In both hemispheres PCC was positively correlated with the ventral/dorsal posterior cingulate (BA23, BA31), retrosplenial cingulate (BA29) cortices and the angular gyri (BA39). Negative correlations were found between PCC and the right premotor cortex (BA6), posterior/anterior entorhinal cortices (BA28, BA34) and IFC pars opecularis (BA44), along with the left/right dorsolateral prefrontal cortices (BA46).

5.3.2.3.3. Summary of PCC connectivity across conditions 1, 2 and 3

On visual inspection of figure 5.9 and tables 5.2.7-5.2.9 PCC was positively correlated with a number of visual regions in condition 1, which became attenuated in conditions 2 and 3. A left lateralised spread of negative correlated activity, particularly in temporal regions (e.g. somatosensory and premotor regions) was prominent in conditions 1 and 2 compared to condition 3, and in terms of other DMN regions, PCC was positively correlated LLP, MPFC and RLP across each condition. Between-conditions contrasts in CONN revealed that there were

significant changes in functional connectivity between conditions 3 and 1 only. However, these changes were apparent in visual regions only, including the left/right primary visual cortices (BA17: left: *B*=-0.26; *p*=0.01; right: *B*=-0.29; *p*=0.01) and the right secondary visual cortex (BA18: *B*=-0.26; *p*=0.01). For this portion of the DMN results support the outcome of analysis 2a: showing reaction times as a behavioural index of DMN activity infer there is no change in activity across task duration. However, results do raise questions regarding the relationship between PCC and visual regions, which is considered in the discussion of this experiment.

Connectivity between DMN seed region RLP and the whole of the cerebral cortex are shown in figure 5.10 and table 5.2.10-5.2.12.

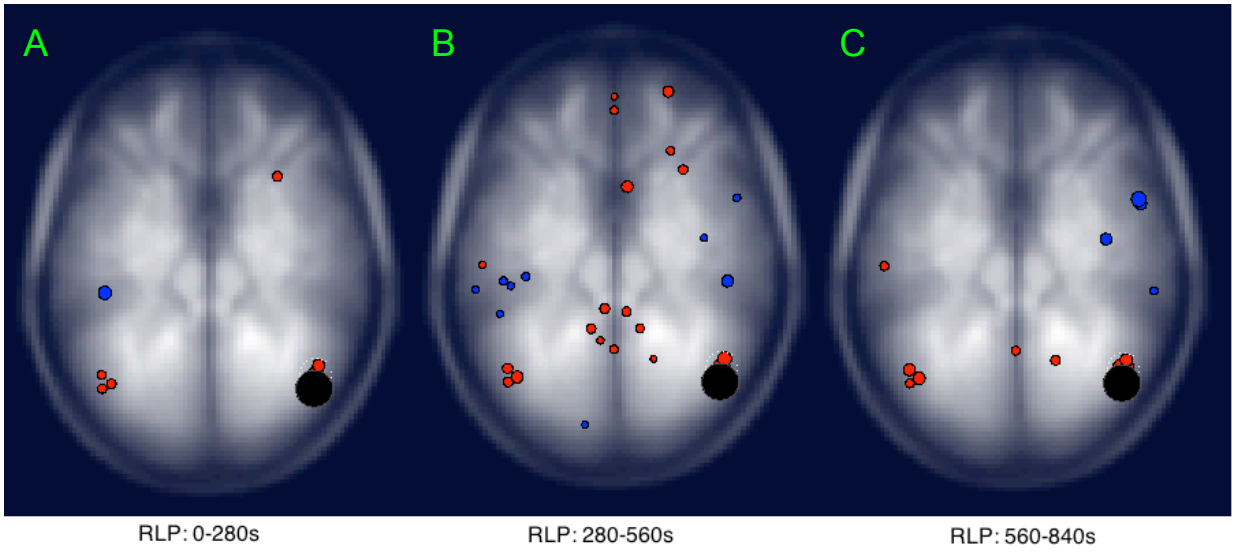

Figure 5.10. Relationship between DMN seed region RLP and areas covering the whole of the cerebral cortex for: (A) condition 1 (0-280s); (B) condition 2 (280-560s); and (C) condition 3 (560-840s).

Table 5.2.10. Right lateral parietal (RLP) connectivity to all cerebral regions for condition 1 (0-280s) and their significance.

Brodmann area	Brain region	*B*	*p*	Correlation

Seed ROI	*Left Lateral Parietal*	*0.47*	*0.040*	+
rsREL	*Left Inferior Parietal Lobe*	*0.44*	*0.034*	+
rsREL	*Right Inferior Parietal lobe*	*0.79*	*0.012*	+
rsREL	*Right Superior Frontal Gyrus*	*0.28*	*0.034*	+
39 (L)	Angular gyrus	0.34	0.043	+
39 (R)	Angular gyrus	0.98	0.006	+
41 (L)	Primary Auditory Cortex	-0.20	0.008	-

Table 5.2.10 and figure 5.10A reveal that RLP was positively correlated with the left/right inferior parietal lobe (rsREL), along with the right superior frontal gyrus (rsRELs) and the left/right angular gyri (BA39). RLP was negatively correlated with the left primary auditory cortex (BA41). Interestingly, compared to other DMN ROIs, RLP revealed a reduced spread of connectivity to other cerebral regions; and in terms of its connectivity to other DMN ROIs was only positively correlated to LLP.

Table 5.2.11. Right lateral parietal (RLP) connectivity to all cerebral regions for condition 2 (280-560s) and their significance.

Brodmann area	Brain region	*B*	*p*	Correlation
Seed ROI	*Left Lateral Parietal*	*0.59*	*0.018*	+
rsREL	*Left Posterior Sup Temp Gyrus*	*-0.35*	*0.037*	-
rsREL	*Left Inferior Parietal Lobe*	*0.57*	*0.009*	+
Seed ROI	*Medial Prefrontal Cortex*	*0.33*	*0.025*	+
rsREL	*Medial Prefrontal Cortex*	*0.29*	*0.048*	+
Seed ROI	*Posterior Cingulate Cortex*	*0.38*	*0.036*	+
rsREL	*Precuneus (PCC)*	*0.50*	*0.025*	+
rsREL	Right Inferior Parietal lobe	0.93	0.006	+
rsREL	*Right Superior Frontal Gyrus*	*0.45*	*0.018*	+
2 (L)	Primary Somatosensory Cortex	-0.30	0.032	-
2 (R)	Primary Somatosensory Cortex	-0.25	0.009	-
3 (L)	Primary Somatosensory Cortex	-0.26	0.025	-
7 (R)	Somatosensory Association Cortex	0.35	0.047	+
8 (R)	Dorsal Frontal Cortex	0.37	0.025	+
10 (R)	Anterior Prefrontal Cortex	0.40	0.012	+
13 (R)	Insular Cortex	-0.39	0.037	-
17 (L)	Primary Visual Cortex	-0.26	0.05	-
21 (L)	Middle Temporal Gyrus	0.30	0.037	+
23 (L)	Ventral Posterior Cingulate Cortex	0.30	0.018	+
23 (R)	Ventral Posterior Cingulate Cortex	0.24	0.020	+

31 (L)	Dorsal Posterior Cingulate Cortex	0.45	0.018	+
31 (R)	Dorsal Posterior Cingulate Cortex	0.45	0.025	+
33 (R)	Anterior Cingulate Cortex	0.20	0.009	+
39 (L)	Angular gyrus	0.47	0.017	+
39 (R)	Angular gyrus	1.14	0.001	+
40 (L)	Supramarginal Gyrus	-0.26	0.038	-
41 (L)	Primary Auditory Cortex	-0.23	0.036	-
44 (R)	IFC pars opercularis	-0.44	0.036	-

Table 5.2.11 and figure 5.10B shows that RLP was positively correlated to LLP (seed ROI), left inferior parietal lobe (rsREL), MPFC (seed ROI; rsREL), PCC (seed ROI), precuneus (PCC; rsREL), and the right inferior parietal lobe (rsREL) and superior frontal gyrus (rsREL). RLP was also positively correlated with the left middle temporal gyrus (BA21) and the right somatosensory association (BA7), dorsal frontal (BA8), anterior prefrontal (BA10) and anterior cingulate (BA33) cortices. In both hemispheres RLP was positively correlated with the ventral/dorsal posterior cingulate cortices (BA23, BA31) and the angular gyri (BA39). Significant negative correlations were found between RLP and the left posterior superior temporal gyrus (rsREL), left primary somatosensory (BA3), primary visual (BA17) and primary auditory (BA41) cortices and the supramarginal gyrus (BA40). RLP was also negatively correlated with the right insular cortex (BA13), IFC pars opercularis (BA44) and the left/right primary somatosensory cortices (BA2).

Table 5.2.12. Right lateral parietal (RLP) connectivity to all cerebral regions for condition 3 (560-840s) and their significance.

Brodmann area	Brain region	*B*	*p*	Correlation
Seed ROI	*Left Lateral Parietal*	*0.54*	*0.028*	+
rsREL	*Left Inferior Parietal Lobe*	*0.58*	*0.006*	+
rsREL	*Precuneus (PCC)*	*0.43*	*0.028*	+
rsREL	*Right Inferior Parietal lobe*	*0.75*	*0.006*	+
rsREL	*Right Anterior Sup Temp Gyrus*	*-0.38*	*0.006*	-
rsREL	*Right Posterior Sup Temp Gyrus*	*-0.26*	*0.047*	-
7 (R)	Somatosensory Association Cortex	0.26	0.023	+

13 (R)	Insular Cortex	-0.38	0.007	-
21 (L)	Middle Temporal Gyrus	0.30	0.028	+
39 (L)	Angular gyrus	0.48	0.006	+
39 (R)	Angular gyrus	1.08	<0.001	+
44 (R)	IFC pars opercularis	-0.30	0.0028	-

Table 5.2.12 and figure 5.10C reveal that RLP was significantly positively correlated with LLP (seed ROI), left/right inferior parietal lobe (rsREL), precuneus (PCC; rsREL), and the right somatosensory association cortex (BA7). Positive correlations were also found between RLP and the left middle temporal gyrus (BA21) and the left/right angular gyri (BA39). RLP was negatively correlated with the right anterior/posterior superior temporal gyrus (rsRELs) and the right insular cortex (BA13) and IFC pars opercularis (BA44).

5.3.2.3.4. Summary of RLP connectivity across conditions 1, 2 and 3

On visual inspection of figure 5.10 and tables 5.2.10-5.2.11, RLP appears to be associated with widespread connectivity in condition 2 compared to condition 1; however this connectivity is then attenuated in condition 3. In comparison to other ROIs, RLP revealed reduced functional connectivity to other brain regions over time, showing positive correlations to all other ROIs in condition 2, and positive correlations to LLP only in conditions 1 and 3. Between-conditions contrasts in CONN revealed that there was a significant change in connectivity in the left secondary visual cortex (BA18: B=-0.26; p=0.038) only between conditions 2 and 1. For this portion of the DMN results support the outcome of analysis 2a: showing reaction times as a behavioural index of DMN activity infer there is no change in activity across the task. However, results do raise questions regarding the relationship between RLP and the left secondary visual cortex (considered further in the discussion of this experiment).

5.4. Discussion

This experiment had two main aims: (1) to determine whether DMN activity was observed in an active auditory attention task designed to induce activity in the goal- and stimulus-driven attention networks; and (2) to investigate whether DMN activity increased over task duration (explored in terms of increasing reaction times towards goal-driven stimuli and changes in functional connectivity of the DMN over time). Discussion of results pertaining to each aim is outlined below.

5.4.1. Confirmation of DMN activity during an active auditory attention task

DMN ROIs (LLP, MPFC, PCC, RLP; Fox et al., 2005) were significantly positively correlated with one another in the analysis 1 of this experiment. In line with Raichle et al. (2001) this supports the notion that the DMN is a continuous running system whose activity is not abolished when individuals engage in goal-directed behaviours, but is instead *modulated*. Whilst the strength of functional connectivity between DMN ROIs in the current data set was not actively compared to the 5-minute resting-state data obtained from the same participant group (previously reported in experiment 1), it is assumed that overall DMN activity would have been attenuated in the current experiment. This theory is in line with previous studies showing attenuation of the DMN in active conditions relative to rest (e.g. Fransson, 2006; Greicius & Menon, 2004; Hahn et al., 2007) and because the task employed in the current experiment was designed to induce activity in several other large-scale brain networks (i.e. dorsal/ventral attention networks).

5.4.2. Interaction between the DMN and other brain regions in an active task

An interesting finding of analysis 1 was that each ROI was negatively correlated with areas in the temporal lobes, including primary auditory, motor and somatosensory areas. Activations of lateral parietal DMN regions (LLP/RLP) were also associated with down-regulation/suppression (hence reduced functional activation) of activity in primary and secondary visual regions. Together these findings raise questions about the relationship between the DMN and regions implicated in the processing of sensory information from the external world; note that similar findings from the eyes-closed rest condition reported in experiment 1 were interpreted as the DMN suppressing activity in sensory-associated brain regions as a method of preventing external sensory information interfering with internal thought processes. In the current experiment, however, based on the fact that an oddball task was employed (in which distractor items were randomly presented), and that frontal and parietal regions (in close proximity to the DMN's MPFC, LLP and RLP) are also implicated in attention function, it is possible that findings reflect top-down modulation of sensory cortical activity: thus decreases in activity in auditory/motor/visual regions in response to task-irrelevant (distracting) stimuli. This is considered further in the general discussion of this thesis (chapter 7).

As discussed in section *5.3.1.4* maximum intensity projection maps were informative in showing the variation in interaction between midline and lateral components of the DMN and the rest of the brain. For example, midline DMN components (MPFC/PCC) were associated with down-regulation of parietal regions, whereas lateral parietal regions (LLP/RLP) were associated with down-regulation of occipital regions. These results are interesting because as previously stated they suggest that whilst the DMN may be considered as a coherent system in relation to resting-state/sentinel functions/stream of thought, each DMN region may differentially influence or be

being differentially influenced by, other brain structures/regions implicated in other large-scale brain networks. This in turn raises questions as to whether individual components of the DMN adopt different roles in the generation of DMN functions, i.e. are midline components associated with stream of thought whilst parietal areas (also implicated in attention function) are implicated in sentinel functions? The similar response of brain regions towards MPFC and PCC components, for example, could suggest these midline DMN components are communicating with one another in relation to receiving information from the external world (through PCC) in order to modulate internal stream of thought; a theory that supports one of the functions of PCC in monitoring and directing the focus of attention (Gusnard & Raichle, 2001; Hahn et al., 2007). The down-regulation of other brain regions and clusters of negatively correlated activity in regions in the vicinity of/overlapping with other neuronal networks raise questions about the interaction between the DMN and networks predominantly involved in the processing of the *external* world. Thus, an obvious next step would be to explore the nature of these interactions further in the current data set; this experiment is reported in chapter 6.

5.4.3. DMN activity does not vary over task duration

Results of analysis 2 in the current experiment aimed to determine whether DMN activity increased as a function of increasing task duration. Exploration based on reaction times (as a behavioural index of DMN activity) revealed no significant difference in the average time taken to respond to task-relevant goal-driven stimuli across conditions/blocks. Between-condition contrasts in CONN also failed to show any significant change in the functional connectivity of the DMN over time. Results did, however, reveal significant changes in visual regions associated with the PCC and RLP components of the DMN, suggesting sensory regions become

increasingly negatively correlated with PCC and RLP DMN ROIs across task duration. Whilst this is somewhat difficult to interpret, perhaps PCC simply exercises more 'control' over visual sensory regions in comparison to frontal DMN regions. Similarly, given the potential overlap between putative regions of the goal-driven network (GDN) and DMN in the parietal lobes (e.g. the angular gyri: close to the GDN's intraparietal sulci), perhaps these regions communicate with one another in the control and maintenance of one of the task instructions: to keep eyes-closed.

Interestingly, on visual inspection of first-level contrast maps (showing total projections of correlated activity; see figure 5.6) and reaction times on a single-participant basis (see figure 5.4), a trend between these DMN measures is may exist for some participants (i.e. participant 4). This highlights that researchers should be somewhat cautious when averaging across participants; and also suggests that if between-subjects contrasts in CONN had been performed on a single participant basis, results may have yielded a different outcome. Future research should consider this and could perhaps aim to regress reaction times against brain activity as a method of determining whether increases/decreases in reaction time truly are associated with increases/decreases in DMN activity.

It could be argued that no significant increase in DMN activity over task duration would have been expected. Behaviourally relevant stimuli presented throughout the task were designed to engage the goal-driven network (GDN), whilst task-irrelevant stimuli were designed to provoke responses in the stimulus-driven network (see chapter 3 sections *3.3.1-3.3.3* for reviews of the functions of these networks). Therefore, one could argue task demands and distracting stimuli prevented participants engaging in internal modes of cognition to such an extent that significant

fluctuations in DMN activity would not have been observed. On the other hand, it is also interesting that a decrease in DMN activity over time was not apparent, given participants were directing their resources and paying attention to the external world (GDN engaged), and also that distractors were randomly presented (SDN engaged). This could perhaps offer support to the sentinel hypothesis of the function of the DMN, suggesting it was involved in the monitoring of the external environment throughout the task.

5.4.4. Conclusions

To conclude, through the use of a ROI/seed-based functional connectivity approach, the current experiment was successful in determining DMN activity was apparent during an active auditory attention task. As discussed, findings have raised questions about the interaction between DMN regions and other brain regions (i.e. frontal/parietal regions implicated in the dorsal attention network). No variation in DMN activity over time also raises questions about the functions of the DMN, for example, suggesting it could be involved in the monitoring of the external environment (in support of the sentinel hypothesis). Confident in the fact that DMN activity is observed in the current data set, and in order to better understand the function of the DMN, an obvious next step is to further explore interaction between this network and several other brain systems thought to be implicated in the current task. This experiment is reported in chapter 6.

CHAPTER 6

Experiment 3: Functional connectivity of the attention-orienting, executive/frontoparietal control and salience networks, and their relationship to the default mode network

6.1. Aim of experiment

The overall aim of this experiment was to explore the functional connectivity of several large-scale brain networks and their relationship to the default mode network (DMN). An interesting outcome of the two previous experiments has been that DMN regions-of-interest (ROIs) appear to interact with components of several other large-scale brain networks (e.g. frontal/parietal regions implicated in the dorsal (goal-driven) attention network). The current experiment sought to explore these interactions further by conducting four separate analyses on the active auditory attention data (previously utilised for analysis in experiment 2) in order to investigate connectivity within the goal-driven, stimulus-driven, executive/frontoparietal control and salience networks respectively, along with their relationship to the DMN.

6.1.1. Rationale and hypotheses

The rationale and hypotheses relating to the exploration of functional connectivity in each network are outlined below.

6.1.1.1. Goal-driven network

As discussed in chapter 3, the goal-driven network (GDN) is implicated in the selection of sensory information from the external world based on internal goals, intentions and expectations

(see section *3.3.1*, chapter 3 for a review). The functions and brain regions associated with this network are commonly investigated whilst participants respond to behaviourally relevant stimuli. For example, in target-detection tasks, which require detecting and responding to goal-directed stimuli, activity within frontal and parietal nodes of the GDN is prominent (Corbetta & Shulman, 2002). These tasks, in particular 'oddball' paradigms, also provide insight into the functional relationship between the GDN and stimulus-driven network (SDN). This is because during task completion participants are typically required to ignore task-relevant/irrelevant oddball stimuli/distractors that provoke response within the SDN (reviewed in chapter 3, section *3.3.3*). The current experiment employed an auditory odd/even number decision task, in which task-relevant and irrelevant/distractor stimuli were presented at random time intervals (see chapter 5, method section *5.2.2* for a description). Based on: (1) the nature of this task, requiring participants to respond to target 'goal' stimuli/inhibit response to task-irrelevant 'oddballs'/distractors; and (2) the task duration, provoking fluctuations in the GDN's response over time, it was hypothesised that strong functional connectivity in the GDN would be observed (analysis 1, prediction 1). Predictions relating to the SDN are outlined in section *6.1.1.2*.

Further to this, as discussed in the introductory chapters, a number of researchers have shown deactivation of the DMN is common during goal-directed tasks in which the GDN is engaged (i.e. Shulman et al., 1997; Mazoyer et al., 2001; see chapter 1). Studies (e.g. Fransson, 2006) have also shown that relative to resting-state, DMN activity is not completely abolished, but *attenuated*, during attention-demanding tasks designed to induce activity in the GDN. Given the task in this experiment was designed to activate the GDN, and in line with previous research, a

secondary hypothesis was that increases in activity in the GDN would be associated with down-regulation of the DMN (analysis 1, prediction 2).

6.1.1.2. Stimulus-driven network

As reviewed in chapter 3, the SDN is implicated in the detection and response to unanticipated events outwith the current focus of attention. This network typically responds together with the GDN towards behaviourally relevant stimuli (Corbetta & Shulman, 2000), with enhanced activation apparent (particularly in the SDN) if stimuli are behaviourally irrelevant, if they appear in unanticipated locations, or if they appear at infrequent time intervals (Arrington, Carr, Mayer & Rao, 2000; Bledowski, Pryulovic, Goebel, Zanella & Linden, 2004; Corbetta et al., 2000; Kincade, Abrams, Astafiev, Shulman & Corbetta, 2005; see sections *3.3.2* and *3.3.3*, chapter 3 for a review). In the context of the current experiment, based on the fact that distractors were randomly presented throughout the task, it was hypothesised that strong functional connectivity within the SDN would be observed (analysis 2, prediction 1).

As addressed in chapter 3, the relationship between the SDN and the DMN is unclear. It has been argued that, based on the reorienting function of the SDN, and its anatomical segregation from the GDN and DMN, the SDN adopts a modulatory/switching role between external (GDN) and internal (DMN) modes of cognition (Corbetta et al., 2008). Alternatively, results from target-detection tasks suggest the SDN and DMN may assume similar roles in the monitoring of the external environment: a view based on the similarity in response of SDN and DMN regions that are in close proximity to one another when stimuli are presented in unpredictable locations (i.e. Hahn et al., 2007; see section *3.3.4*, chapter 3; see section *1.7.1*, chapter 1 for a review of the

sentinel hypothesis of DMN function). Whilst similarity in the sentinel function of the SDN and DMN is supported by suppression/down-regulation of each network by the GDN during goal-directed tasks (i.e. Shulman et al., 2007), it should be noted that reductions in activity within nodes of SDN and DMN could in fact be related to different task components (i.e. attention components: GDN engaged/SDN suppressed; versus sensory components: GDN engaged/DMN deactivated; Corbetta et al., 2008). Furthermore, studies have also shown that the temporoparietal junction (a putative region of the SDN, also linked with the DMN; Hahn et al., 2007) is positively correlated to the DMN during working memory encoding, but decouples from the DMN during working memory maintenance, in which distractor stimuli are presented (Anticevik et al., 2010). This suggests that although there is functional interaction between the SDN and DMN, the networks respond differently to unpredictable events, thus disentangling the sentinel function of each network. In the current experiment, based on (1) that the task employed was designed to selectively activate the GDN in the case of goal relevant stimuli and activate the SDN in the case of distractors, (2) the internal mentation hypothesis of DMN function (the view that the DMN supports internal mentation alone, and is largely detached from the external world; Buckner et al. 2008; see section *1.7.2*, chapter 1 for a review), and (3) that distractor items were presented randomly and throughout the whole of the task, it was hypothesised that activity in this network would be associated with down-regulation of the DMN.

6.1.1.3. Executive/frontoparietal control network

The executive control network (ECN) is implicated in the monitoring and control of thoughts, feelings and responses (Posner & Rothbart, 2007). As discussed in chapter 3, it has been proposed that in some circumstances, the ECN modulates activity in the orienting networks by

acting directly on the GDN in order to maintain and adjust goal-driven attention for current task demands (Corbetta, Patel & Shulman, 2008; see sections *3.2.3* and *3.4* in chapter 3 for further discussion). Activation of this network during auditory oddball paradigms has been confirmed in previous studies, with impaired task performance and network disruption apparent in populations who experience difficulty in the processing of novel/salient stimuli (i.e. patients with schizophrenia; Kim et al., 2009; Wolf et al., 2008). In the current experiment, based on the ECN's role in the maintenance of the task goals, it was predicted strong functional connectivity of the ECN would be observed (analysis 3, prediction 1).

As previously discussed (see section *3.4.1*, chapter 3) findings suggest goal-driven tasks that require some form of executive control, i.e. working memory tasks, have been shown to suppress activity/reduce functional connectivity within the DMN (e.g. McKiernan et al., 2003; Fransson, 2006). Although the task in this experiment did not actively engage working memory components, based on the fact the ECN is implicated in target detection tasks (e.g. Kim et al., 2009), it was hypothesised that functional connectivity in the ECN would be coupled with down-regulation of the DMN (analysis 3, prediction 2) in this particular task: note that this prediction is based on the ECN being engaged in an *externally-directed* attention-demanding task, in which one of its roles is monitoring/maintaining the response of the GDN. Therefore, this hypothesis does not take into account the role of the ECN in the monitoring of the 'internal' world (DMN engaged), in which a functional relationship between the ECN and DMN has been proposed (e.g. Christoff et al., 2009; Gerlach et al., 2011; see section *3.4.1*, chapter 3).

It should be pointed out, as discussed in chapter 3 a related concept of frontal control has been suggested. This is built around patterns of activation observed in a set of regions known as the Frontoparietal Control Network (FCN). Based on its anatomical interposition between the GDN and DMN (Vincent et al., 2008) the FCN is assumed to facilitate the functional interplay and integration of information between networks (see chapter 3, section *3.6* for a review). While the FCN may not perform all of the functions typically ascribed to the ECN it certainly seems to have a significant role in cognitive control. Based on: (1) the FCN has been shown to couple with the GDN/DMN depending on task requirements (e.g. Spreng et al., 2010); (2) the task in the current experiment was designed to activate the GDN; and (3) DMN activity was previously observed in this task (experiment 2, chapter 5); it was predicted that functional connectivity within the FCN would be apparent. It was also predicted that the bias of the task would likely result in a negative relationship between the FCN and DMN (as the FCN would couple with the GDN). Given the overlap in the some of the anatomical areas identified as parts of the ECN and FCN (along with an overlap in *control* functions) these networks are collectively referred to as the *ECN* in this analysis.

6.1.1.4. Salience network

The salience network (SN), whose cortical regions overlap with the ECN and orienting networks (Seeley et al., 2007), is involved in the monitoring of internal processes and the detection of external salient events. Researchers suggest the SN is involved in the switching between brain networks when an externally salient event is detected, and guiding the appropriate behavioural response(s) towards the event (Menon & Uddin, 2010; see section *3.5*, chapter 3). Given that the task employed in the current experiment was designed to induce activity in the GDN, SDN and

ECN, and novel (salient) oddball/distractor stimuli were presented, it was hypothesised that strong functional connectivity within the SN would be observed (analysis 4, prediction 1).

As discussed in chapter 3, the association between the SN and DMN has been investigated in terms of the their functional relationship to one another (i.e. SN active/DMN down-regulated; Seeley et al., 2007), and also in terms of the SN being considered as a modulatory/switcher network (Sridharan et al., 2008). In investigating the role of the SN in switching between the ECN and DMN, Sridharan et al. (2008) found that during an active auditory task, in which salient events were presented, activations in the ECN and SN were coupled with deactivation of the DMN. Findings also suggested a crucial role for the fronto-insular component of the SN in activating the ECN and deactivating the DMN, thus supporting the notion that this network encompasses 'switching' properties (see section *3.5.1*, chapter 3). In line with the predictions made regarding the ECN's response in the current experiment (ECN engaged/DMN down-regulated), and given distractors were randomly presented throughout the task (engaging activity in the SN as well as the SDN), it was hypothesised that activity in the SN would be associated with down-regulation of the DMN (analysis 4, prediction 2).

6.2. Method

The method pertaining to this experiment was the same as experiment 2 (see chapter 5, section *5.2*). Conn setup varied in relation to the ROIs used in each analysis, and is outlined in appendix E. ROIs relating to each large-scale network are detailed in the relevant analyses sections below.

6.3. Results

Functional connectivity results of each analysis are outlined in the following five sections (*6.3.1*: GDN, *6.3.2*: SDN, *6.3.3*: ECN/FCN, *6.3.4*: SN).

6.3.1. Results of analysis 1:

Functional connectivity within the attention-orienting dorsal frontoparietal network (goal-driven network) in an 840s active auditory attention task, and its relationship to the default mode network

As previously stated in section *6.1.1.1,* based on (1) the nature of this task, requiring participants to respond to target 'goal' stimuli/inhibit response to task-irrelevant oddballs/ distractors; and (2) the task duration, provoking fluctuations in the GDN's response over time, it was hypothesised that strong functional connectivity in the GDN would be observed (prediction 1).

It was also hypothesised that functional connectivity in the GDN would be associated with down-regulation of the DMN (prediction 2).

6.3.1.1. Goal-driven network ROIs

GDN ROIs were based on those identified by Corbetta et al. (2008), which included the dorsal parietal cortex, particularly the intraparietal sulcus and the superior parietal lobule; and the dorsal frontal cortex, particularly the precentral sulcus near the frontal eye field. There was some disparity between the identification of GDN regions proposed by Corbetta and colleagues and those available using the *conn* software in the current experiment. Therefore, ROIs were chosen based on their close proximity to typical GDN regions and included the left and right somatosensory association cortex (BA5, BA7: closest match to superior parietal lobule); premotor cortex (BA6: closest match to precentral sulcus); dorsal frontal cortex (BA8: GDN

match); angular gyrus (BA39: closest match to intraparietal sulcus) and the supramarginal gyrus (BA40: closest match to intraparietal sulcus).

6.3.1.2. Goal-driven network functional connectivity analysis

Connectivity between GDN seed regions (BA5, BA6, BA7, BA8, BA39, BA40) and the whole of the cerebral cortex are shown in figure 6.1. Tables 6.1.1-6.1.12, illustrate the conn region, BA label, strength of connectivity (*Beta (B)* value) and significance (*p* value) across all participants. In each figure and table, positive correlations are displayed in red text and negative correlations are displayed in blue. GDN ROIs are displayed in *italics* and highlighted grey, and DMN seed (Fox et al., 2005)/rsREL regions are displayed in **bold** text. Note that significant ($p<.05$) correlations only are presented, and also as addressed in chapter 5 (see section *5.3.1.2*) the CONN toolbox implemented a built-in correction method (FWE/FDR) for multiple ROI-to-ROI calculations in order to alleviate any potential multiple comparison issues.

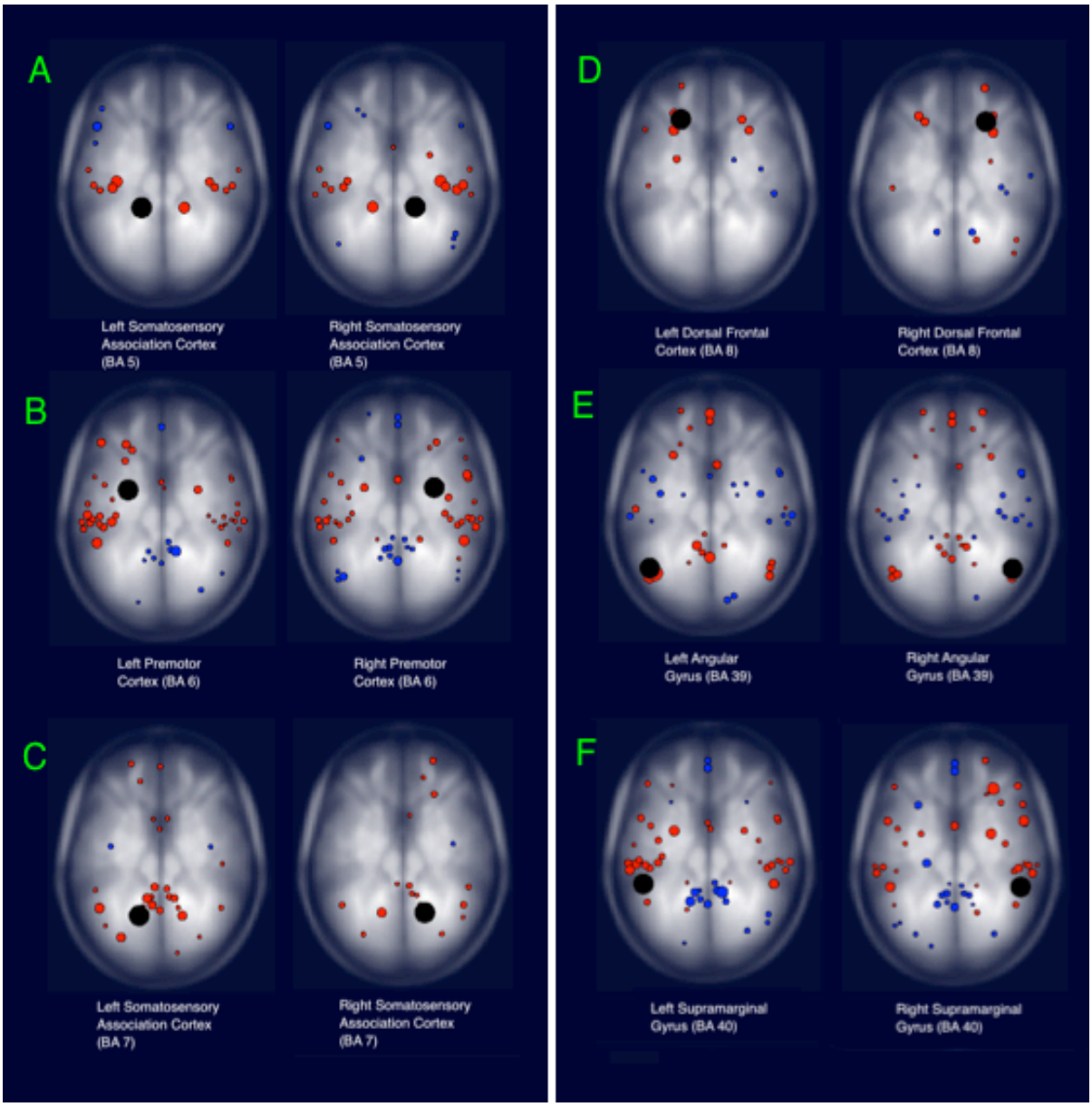

Figure 6.1. Relationship between GDN seed regions and areas covering the whole of the cerebral cortex in an 840s auditory attention task. (A) BA5, (B) BA6, (C) BA7, (D) BA8, (E) BA39, (F) BA40.

BA5: Somatosensory association cortex (closest match to superior parietal lobule)

Table 6.1.1. Left somatosensory association cortex (BA5L) connectivity to all cerebral regions in 840s of active auditory attention data and their significance.

Brodmann area	Brain region	*B*	*p*	Correlation
1 (L)	Primary Somatosensory Cortex	0.38	0.005	+
1 (R)	Primary Somatosensory Cortex	0.29	0.004	+
2 (L)	Primary Somatosensory Cortex	0.49	0.006	+
2 (R)	Primary Somatosensory Cortex	0.35	0.008	+
3 (L)	Primary Somatosensory Cortex	0.54	<0.001	+
3 (R)	Primary Somatosensory Cortex	0.46	0.002	+
4 (L)	Primary Motor Cortex	0.60	<0.001	+
4 (R)	Primary Motor Cortex	0.50	0.001	+
5 (R)	*Somatosensory Association Cortex*	*0.90*	*<0.001*	+
43 (L)	Subcentral Area	0.22	0.028	+
43 (R)	Subcentral Area	0.26	0.04	+
44 (L)	IFC pars opercularis	-0.20	0.038	-
45 (L)	IFC pars triangularis	-0.36	0.001	-
45 (R)	IFC pars triangularis	-0.23	0.005	-
46 (L)	*Dorsolateral Prefrontal Cortex*	*-0.19*	*0.023*	-

Figure 6.1A and table 6.1.1 show that left BA5 (BA5L) was positively correlated with the left/right primary somatosensory (BA1, BA2, BA3) and primary motor (BA4) cortices, along with subcentral areas (BA43). BA5L was also positively correlated with the right somatosensory association cortex (BA5). Negative correlations were apparent between BA5L and the left IFC pars opercularis (BA44), dorsolateral prefrontal cortex (BA46) and left/right IFC pars triangularis (BA45). This ROI was not correlated with any DMN region.

Table 6.1.2. Right somatosensory association cortex (BA5R) connectivity to all cerebral regions in 840s of active auditory attention data and their significance.

Brodmann area	Brain region	B	p	Correlation
DMN region	**Right Lateral Parietal**	**-0.21**	**0.046**	**-**
rsREL	**Cingulate Gyrus**	**0.34**	**0.038**	**+**
rsREL	**Left Inferior Parietal Lobe**	**-0.20**	**0.039**	**-**
rsREL	**Left Posterior Sup Temp Gyrus**	**0.24**	**0.026**	**+**
rsREL	**Right Posterior Sup Temp Gyrus**	**0.36**	**0.027**	**+**

rsREL	**Right Inferior Parietal Lobe**	**-0.29**	**0.013**	**-**
1 (L)	Primary Somatosensory Cortex	0.33	0.018	+
1 (R)	Primary Somatosensory Cortex	0.41	<0.001	+
2 (L)	Primary Somatosensory Cortex	0.45	0.008	+
2 (R)	Primary Somatosensory Cortex	0.54	<0.001	+
3 (L)	Primary Somatosensory Cortex	0.47	0.001	+
3 (R)	Primary Somatosensory Cortex	0.57	<0.001	+
4 (L)	Primary Motor Cortex	0.52	0.002	+
4 (R)	Primary Motor Cortex	0.59	<0.001	+
5 (L)	*Somatosensory Association Cortex*	*0.90*	*<0.001*	+
6 (R)	*Premotor Cortex*	*0.31*	*0.009*	+
8 (L)	*Dorsal Frontal Cortex*	*-0.22*	*0.041*	-
9 (L)	*Dorsolateral Prefrontal Cortex*	*-0.20*	*0.039*	-
39 (R)	*Angular gyrus*	*-0.22*	*0.029*	-
43 (L)	Subcentral Area	0.23	0.015	+
43 (R)	Subcentral Area	0.33	0.021	+
45 (L)	IFC pars triangularis	-0.34	0.003	-
45 (R)	IFC pars triangularis	-0.22	0.027	-

Figure 6.1A and table 6.1.2 show that right BA5 (BA5R) was positively correlated to the cingulate gyrus (rsREL), and left/right posterior superior temporal gyri (rsRELs). BA5R was also positively correlated with the left/right primary somatosensory (BA1, BA2, BA3), primary motor (BA4) and subcentral (BA43) areas, along with the left somatosensory association (BA5; GDN region) and right premotor (BA6; GDN region) cortices. Negative correlations were found between BA5R and RLP (DMN region), left/right inferior parietal lobe (rsRELs), left dorsal frontal (BA8; GDN region) and dorsolateral prefrontal (BA9) cortices. Negative correlations were also found between BA5R and the right angular gyrus (BA39; GDN region) and the left/right IFC pars triangularis (BA45).

6.3.1.2.1. Overall summary of GDN region BA5 (closest match to superior parietal lobule)

Overall, left/right BA5 were positively correlated to temporal regions including somatosensory and motor regions. The activation of these regions and correlated activity is perhaps expected given that participants were required to make a physical response to stimuli, and that these regions are implicated in touch and control of movement. It is somewhat surprising however that

no positive relationships to auditory regions were found given that participants were completing an auditory attention-demanding task. There was also a difference in the number of putative GDN and DMN regions that left/right BA5 were correlated with. Whilst correlated with one another, BA5L was not correlated with any other GDN/DMN region; however, BA5R was negatively correlated to RLP (DMN region), and positively correlated a region chosen to represent to GDN's precentral sulcus (BA6). Unpredicted was that BA5R was negatively correlated with the left dorsal frontal cortex (BA8) and one of the BAs selected to represent the GDN's right intraparietal sulcus (BA39). Overall these unpredicted results suggest that this region was not a reliable selection as a representative of the GDN's superior parietal lobule.

BA6: Premotor cortex (closest match to the precentral sulcus)

Table 6.1.3. Left premotor cortex (BA6L) connectivity to all cerebral regions in 840s of active auditory attention data and their significance.

Brodmann area	Brain region	*B*	*p*	Correlation
DMN region	**MPFC**	**-0.21**	**0.002**	**-**
rsREL.	**Left Superior Frontal Gyrus**	**0.23**	**0.003**	**+**
rsREL.	**Left Posterior Sup Temp Gyrus**	**0.22**	**0.004**	**+**
rsREL.	**Left Anterior Sup Temp Gyrus**	**0.15**	**0.010**	**+**
rsREL.	**Cingulate Gyrus**	**0.29**	**0.007**	**+**
DMN region	**PCC**	**-0.17**	**0.015**	**-**
rsREL.	**Precuneus (PCC)**	**-0.21**	**0.013**	**-**
rsREL.	**Right Anterior Sup Temp Gyrus**	**0.20**	**0.015**	**+**
rsREL.	**Right Posterior Sup Temp Gyrus**	**0.18**	**0.028**	**+**
1 (L)	Primary Somatosensory Cortex	0.35	0.004	+
1 (R)	Primary Somatosensory Cortex	0.20	0.048	+
2 (L)	Primary Somatosensory Cortex	0.39	0.004	+
2 (R)	Primary Somatosensory Cortex	0.23	0.048	+
3 (L)	Primary Somatosensory Cortex	0.44	0.001	+
3 (R)	Primary Somatosensory Cortex	0.21	0.034	+
4 (L)	Primary Motor Cortex	0.42	0.003	+
4 (R)	Primary Motor Cortex	0.21	0.034	+
6 (R)	*Premotor Cortex*	*0.57*	*0.001*	+
8 (L)	*Dorsal Frontal Cortex*	*0.47*	*0.002*	+
9 (L)	*Dorsolateral Prefrontal Cortex*	*0.40*	*0.001*	+
13 (L)	Insular Cortex	0.26	0.020	+

18 (L)	Secondary Visual Cortex	-0.16	0.048	-
19 (R)	Associative Visual Cortex	-0.19	0.009	-
20 (L)	Inferior Temporal Gyrus	0.19	0.002	+
20 (R)	Inferior Temporal Gyrus	0.16	0.018	+
21 (L)	Middle Temporal Gyrus	0.21	0.001	+
21 (R)	Middle Temporal Gyrus	0.12	0.010	+
22 (L)	Superior Temporal Gyrus	0.35	0.002	+
22 (R)	Superior Temporal Gyrus	0.21	0.022	+
23 (R)	Ventral Posterior Cingulate Cortex	-0.24	0.007	-
29 (R)	Retrosplenial Cingulate Cortex	-0.23	0.002	-
30 (L)	Cingulate Cortex -	0.15	0.027	-
31 (L)	Dorsal Posterior Cingulate Cortex	-0.20	0.011	-
31 (R)	Dorsal Posterior Cingulate Cortex	-0.38	<0.001	-
39 (R)	*Angular gyrus*	*-0.15*	*0.031*	*-*
40 (L)	*Supramarginal Gyrus*	*0.63*	*<0.001*	*+*
40 (R)	*Supramarginal Gyrus*	*0.26*	*0.005*	*+*
41 (L)	Primary Auditory Cortex	0.31	0.001	+
41 (R)	Primary Auditory Cortex	0.21	0.009	+
42 (L)	Primary Auditory Cortex	0.23	0.004	+
42 (R)	Primary Auditory Cortex	0.25	0.004	+
43 (L)	Subcentral Area	0.22	0.008	+
43 (R)	Subcentral Area	0.21	0.021	+
44 (L)	IFC pars opercularis	0.34	0.020	+
44 (R)	IFC pars opercularis	0.18	0.026	+
46 (L)	*Dorsolateral Prefrontal Cortex*	*0.27*	*0.001*	+

As shown in figure 6.1B and table 6.1.3, left BA6 (BA6L) was positively correlated to the cingulate gyrus (rsREL) and the left/right anterior/posterior superior temporal gyri (rsRELs) primary somatosensory (BA1, BA2, BA3) motor (BA4) and auditory (BA41, BA42) cortices. BA6L was also positively correlated to the left/right inferior temporal gyrus (BA20), middle temporal (BA21), superior temporal (BA22) gyri, subcentral areas (BA43), IFC pars operculari (BA44) and the GDN's supramarginal (BA40) gyri. BA6L was positively correlated to the left superior frontal gyrus (rsREL), insular cortex (BA13), dorsal frontal (BA8; GDN region), and dorsolateral prefrontal (BA9, BA46) cortices; and to the right premotor cortex (BA6; GDN region). Negative correlations were found between BA6L and the MPFC, PCC (DMN regions), precuneus (PCC; rsREL) and left/right dorsal posterior cingulate cortices (BA31). BA6L was also negatively correlated to the left secondary visual (BA18) and cingulate (BA30) cortices; and

the right associative visual (BA19), ventral posterior cingulate (BA23), retrosplenial cingulate (BA29) cortices, and the angular gyrus (BA39).

Table 6.1.4. Right premotor cortex (BA6R) connectivity to all cerebral regions in 840s of active auditory attention data and their significance.

Brodmann area	Brain region	*B*	*p*	Correlation
DMN region	**Left Lateral Parietal**	**-0.24**	**0.005**	**-**
DMN region	**Medial Prefrontal Cortex**	**-0.35**	**0.003**	**-**
DMN region	**Posterior Cingulate Cortex**	**-0.37**	**0.006**	**-**
DMN region	**Right Lateral Parietal**	**-0.16**	**0.038**	**-**
rsREL	**Cingulate Gyrus**	**0.42**	**0.002**	**+**
rsREL	**Left Anterior Sup Temp Gyrus**	**0.22**	**0.006**	**+**
rsREL	**Left Inferior Parietal Lobe**	**-0.25**	**0.001**	**-**
rsREL	**Left Posterior Sup Temp Gyrus**	**0.30**	**0.003**	**+**
rsREL	**Left Superior Frontal Gyrus**	**-0.15**	**0.007**	**-**
rsREL	**Medial Prefrontal Cortex**	**-0.36**	**0.003**	**-**
rsREL	**Precuneus (PCC)**	**-0.42**	**0.001**	**-**
rsREL	**Right Anterior Sup Temp Gyrus**	**0.30**	**0.001**	**+**
rsREL	**Right Posterior Sup Temp Gyrus**	**0.40**	**0.002**	**+**
1 (L)	Primary Somatosensory Cortex	0.24	0.038	+
1 (R)	Primary Somatosensory Cortex	0.30	0.006	+
2 (L)	Primary Somatosensory Cortex	0.30	0.016	+
2 (R)	Primary Somatosensory Cortex	0.37	0.004	+
3 (L)	Primary Somatosensory Cortex	0.35	0.007	+
3 (R)	Primary Somatosensory Cortex	0.40	0.004	+
4 (L)	Primary Motor Cortex	0.37	0.010	+
4 (R)	Primary Motor Cortex	0.45	0.002	+
5 (L)	*Somatosensory Association Cortex*	*0.21*	*0.030*	+
5 (R)	*Somatosensory Association Cortex*	*0.31*	*0.004*	+
6 (L)	*Premotor Cortex*	*0.57*	*0.001*	+
8 (R)	*Dorsal Frontal Cortex*	*0.33*	*0.016*	+
9 (R)	*Dorsolateral Prefrontal Cortex*	*0.38*	*0.003*	+
10 (L)	Anterior Prefrontal Cortex	-0.16	0.040	-
13 (L)	Insular Cortex	0.30	0.014	+
13 (R)	Insular Cortex	0.35	0.002	+
22 (L)	Superior Temporal Gyrus	0.38	0.002	+
22 (R)	Superior Temporal Gyrus	0.31	0.002	+
23 (L)	Ventral Posterior Cingulate Cortex	-0.27	0.015	-
23 (R)	Ventral Posterior Cingulate Cortex	-0.26	0.007	-
29 (L)	Retrosplenial Cingulate Cortex	-0.28	0.003	-
29 (R)	Retrosplenial Cingulate Cortex	-0.23	0.015	-
30 (L)	Cingulate Cortex	-0.31	0.010	-
31 (L)	Dorsal Posterior Cingulate Cortex	-0.38	0.003	-
31 (R)	Dorsal Posterior Cingulate Cortex	-0.30	0.008	-
37 (R)	Fusiform gyrus	0.19	0.030	+
39 (L)	*Angular gyrus*	*-0.23*	*0.014*	-
39 (R)	*Angular gyrus*	*-0.16*	*0.049*	-
40 (L)	*Supramarginal Gyrus*	*0.41*	*0.003*	+
40 (R)	*Supramarginal Gyrus*	*0.56*	*0.001*	+

41 (L)	Primary Auditory Cortex	0.31	0.007	+
41 (R)	Primary Auditory Cortex	0.24	0.004	+
42 (L)	Primary Auditory Cortex	0.34	0.003	+
42 (R)	Primary Auditory Cortex	0.27	0.006	+
43 (L)	Subcentral Area	0.29	0.007	+
43 (R)	Subcentral Area	0.29	0.011	+
44 (L)	IFC pars opercularis	0.22	0.008	+
44 (R)	IFC pars opercularis	0.38	0.001	+
45 (R)	IFC pars triangularis	0.12	0.025	+
46 (L)	*Dorsolateral Prefrontal Cortex*	*0.14*	*0.038*	+
46 (R)	*Dorsolateral Prefrontal Cortex*	*0.19*	*0.037*	+

Figure 6.1B and table 6.1.4 shows that right BA6 (BA6R) was positively correlated with the cingulate gyrus (rsREL), and the left/right anterior/posterior superior temporal gyri (rsRELs), primary somatosensory (BA1, BA2, BA3), primary motor (BA4), somatosensory association (BA5; GDN regions) and insular (BA13) cortices. BA6R was also positively correlated with the left/right supramarginal gyri (BA40; GDN regions), primary auditory cortices (BA41, BA42), subcentral areas (BA43), IFC pars operculari (BA44) and dorsolateral prefrontal cortices (BA46). In the left hemisphere BA6R was positively correlated with the premotor cortex (BA6; GDN region) and in the right hemisphere BA6R was positively correlated with the dorsal frontal (BA8; GDN region) and dorsolateral prefrontal (BA9) cortices, fusiform gyrus (BA37), and the IFC pars triangularis (BA45). Interestingly, BA6R was negatively correlated with DMN regions including, LLP, MPFC, PCC and RLP, and with the left inferior parietal lobe (rsREL), superior frontal (rsREL), medial prefrontal cortex (rsREL) and the precuneus (PCC; rsREL). Negative correlations were also apparent with the left anterior prefrontal (BA10) and cingulate (BA30) cortices, and the left/right ventral/dorsal posterior cingulate cortex (BA23, BA31), retrosplenial cingulate (BA29) cortices and angular gyri (BA39; GDN region).

6.3.1.2.2. Overall summary of GDN region BA6 (closest match to precentral sulcus)

Overall BA6 appears to be a reliable representative portion of the GDN, particularly in the right hemisphere. Left BA6 shows left lateralised positive correlations to frontal regions including the dorsal frontal cortex (BA8; GDN region), as well as positive correlations to the left/right representatives of the GDN intraparietal sulcus region. Interestingly, this ROI was negatively correlated to portions of the DMN including the MPFC and PCC, supporting the hypothesised relationship between networks (GDN engaged/DMN down-regulated). Right BA6 was positively correlated to a number of regions selected to represent the GDN's superior parietal lobule (BA5), precentral sulcus (BA6), dorsal frontal cortex (BA8) and intraparietal sulcus (BA40); suggesting that there was strong functional connectivity within the GDN during this task and supporting the role of the right hemisphere in attention. Interestingly, this ROI was also negative correlated to all DMN regions defined by Fox et al. (2005), including LLP, MPFC, PCC and RLP, as well as rsREL regions in close proximity (i.e. precuneus) to these regions. These negative correlations can be interpreted as this portion of the GDN down-regulating activity within the DMN, and thus supporting the second hypothesis of this analysis.

BA7: Somatosensory association cortex (closest match to superior parietal lobule)

Table 6.1.5. Left somatosensory association cortex (BA7L) connectivity to all cerebral regions in 840s of active auditory attention data and their significance.

Brodmann area	Brain region	*B*	*p*	Correlation
DMN region	**Posterior Cingulate Cortex**	**0.49**	**0.001**	**+**
rsREL	**Cingulate Gyrus**	**0.17**	**0.026**	**+**
rsREL	**Left Inferior Parietal Lobe**	**0.24**	**0.040**	**+**
rsREL	**Medial Prefrontal Cortex**	**0.21**	**0.014**	**+**
rsREL	**Precuneus (PCC)**	**0.25**	**0.003**	**+**
7 (R)	*Somatosensory Association Cortex*	*0.77*	*0.001*	*+*
10 (L)	Anterior Prefrontal Cortex	0.32	0.011	+
11 (L)	Orbitofrontal Cortex	0.20	0.018	+
13 (L)	Insular Cortex	-0.20	0.014	-

13 (R)	Insular Cortex	-0.17	0.026	-
17 (R)	Primary Visual Cortex	0.25	0.040	+
19 (L)	Associative Visual Cortex	0.41	0.001	+
19 (R)	Associative Visual Cortex	0.22	0.040	+
20 (R)	Inferior Temporal Gyrus	0.09	0.029	+
23 (L)	Ventral Posterior Cingulate Cortex	0.36	0.002	+
23 (R)	Ventral Posterior Cingulate Cortex	0.26	0.007	+
25 (L)	Subgenual cortex	0.18	0.034	+
25 (R)	Subgenual cortex	0.22	0.018	+
29 (L)	Retrosplenial Cingulate Cortex	0.37	0.014	+
29 (R)	Retrosplenial Cingulate Cortex	0.35	0.007	+
30 (L)	Cingulate Cortex	0.31	0.007	+
30 (R)	Cingulate Cortex	0.25	0.022	+
31 (L)	Dorsal Posterior Cingulate Cortex	0.38	0.001	+
31 (R)	Dorsal Posterior Cingulate Cortex	0.29	0.003	+
37 (L)	Fusiform gyrus	0.29	0.001	+
37 (R)	Fusiform gyrus	0.19	0.016	+
40 (L)	*Supramarginal Gyrus*	*0.24*	*0.031*	+

As shown in figure 6.1C and table 6.1.5, left BA7 (BA7L) was positively correlated to PCC (DMN region) along with rsRELs including the cingulate gyrus, left inferior parietal lobe, medial prefrontal cortex and precuneus (PCC). BA7L was also positively correlated with the left anterior prefrontal (BA10) and orbitofrontal (BA11) cortices, along with the supramarginal gyrus (BA40; GDN region). BA7L was positively correlated with the right somatosensory association (BA7; GDN region) and primary visual (BA17) cortices, and the inferior temporal gyrus (BA20). Positive correlations were also found between BA7L and the left/right associative visual (BA19), ventral posterior cingulate (BA23), subgenual (BA25), retrosplenial (BA29), cingulate (BA30), dorsal posterior cingulate (BA31) cortices and the fusiform gyri (BA37). BA7L was negatively correlated with the left/right insular cortices (BA13).

Table 6.1.6. Right somatosensory association cortex (BA7R) connectivity to all cerebral regions in 840s of active auditory attention data and their significance.

Brodmann area	Brain region	*B*	*p*	Correlation
7 (L)	*Somatosensory Association Cortex*	*0.77*	*0.002*	+

8 (R)	*Dorsal Frontal Cortex*	*0.23*	*0.015*	+
10 (R)	Anterior Prefrontal Cortex	0.35	0.015	+
11 (R)	Orbitofrontal Cortex	0.22	0.046	+
13 (R)	Insular Cortex	-0.14	0.046	-
19 (L)	Associative Visual Cortex	0.23	0.029	+
19 (R)	Associative Visual Cortex	0.29	0.029	+
23 (L)	Ventral Posterior Cingulate Cortex	0.22	0.049	+
23 (R)	Ventral Posterior Cingulate Cortex	0.27	0.015	+
25 (R)	Subgenual cortex	0.18	0.049	+
29 (R)	Retrosplenial Cingulate Cortex	0.30	0.029	+
30 (R)	Cingulate Cortex	0.16	0.029	+
31 (R)	Dorsal Posterior Cingulate Cortex	0.27	0.049	+
37 (L)	Fusiform gyrus	0.21	0.015	+
37 (R)	Fusiform gyrus	0.30	0.015	+
39 (R)	*Angular gyrus*	*0.21*	*0.049*	+
40 (R)	*Supramarginal Gyrus*	*0.31*	*0.027*	+

Figure 6.1C and table 6.1.6 reveals that right BA7 (BA7R) was positively correlated with the left somatosensory association cortex (BA7; GDN region) and the right dorsal frontal (BA8; GDN region), anterior prefrontal (BA10), orbitofrontal (BA11), subgenual (BA25), retrosplenial cingulate (BA29), cingulate (BA30) and dorsal posterior cingulate (BA31) cortices, and the angular (BA39; GDN region) and supramarginal (BA40) gyri. In the left and right hemispheres, BA7R was positively correlated with the associative visual (BA19) and ventral posterior cingulate (BA23) cortices, along with the fusiform gyri (BA37). BA7R was negatively correlated with the right insular cortex (BA13).

6.3.1.2.3. Overall summary of GDN region BA7 (closest match to superior parietal lobule)

Overall, the pattern of correlated activity associated with BA7 revealed BA7L was positively correlated with the left supramarginal gyrus (BA40; a region representing the GDN's intraparietal sulcus); BA7R was positively correlated with regions representing the GDN's superior parietal lobule (BA7), dorsal frontal cortex (BA8) and intraparietal sulcus (BA39). The widespread correlated activity between this ROI and other putative regions of the GDN suggest

that there was strong functional connectivity within the GDN during this task. In terms of the predicted relationship between the GDN and DMN (GDN active/DMN down-regulated), this ROI is somewhat difficult to interpret. This is because a positive correlation between BA7L and PCC, along with cluster of regions surrounding this DMN region was found, whereas BA7R did not show this or any other form of relationship to the DMN.

BA8L Dorsal frontal cortex (GDN match)

Table 6.1.7. Left dorsal frontal cortex (BA8L) connectivity to all cerebral regions in 840s of active auditory attention data and their significance.

Brodmann area	Brain region	*B*	*p*	Correlation
rsREL	**Left Superior Frontal Gyrus**	**0.73**	**0.001**	+
rsREL	**Right Superior Frontal Gyrus**	**0.41**	**0.002**	+
2 (R)	Primary Somatosensory Cortex	-0.21	0.012	-
6 (L)	*Premotor Cortex*	*0.47*	*0.004*	+
8 (R)	*Dorsal Frontal Cortex*	*0.47*	*0.002*	+
9 (L)	*Dorsolateral Prefrontal Cortex*	*0.78*	*0.001*	+
10 (L)	Anterior Prefrontal Cortex	0.46	0.017	+
13 (R)	Insular Cortex	-0.23	0.049	-
20 (L)	Inferior Temporal Gyrus	0.22	0.049	+
34 (R)	Anterior Entorhinal Cortex	-0.13	0.049	-
45 (L)	IFC pars triangularis	0.30	0.049	+

Figure 6.1D and table 6.1.7 reveals that left BA8 (BA8L) was positively correlated to the left/right superior frontal gyri (rsREL). Positive correlations were also apparent with the left premotor (BA6; GDN region), dorsolateral prefrontal (BA9; GDN region) and anterior prefrontal (BA10) cortices, and the inferior temporal gyrus (BA20) and IFC pars triangularis (BA45). In the right hemisphere BA8L was positively correlated with the dorsal frontal cortex (BA8). Negative correlations were apparent between BA8L and the right primary somatosensory (BA2), insular (BA13) and anterior entorhinal (BA34) cortices.

Table 6.1.8. Right dorsal frontal cortex (BA8R) connectivity to all cerebral regions in 840s of active auditory attention data and their significance.

Brodmann area	Brain region	*B*	*p*	Correlation
DMN region	**Right Lateral Parietal**	**0.31**	**0.043**	+
rsREL	**Right Superior Frontal Gyrus**	**0.82**	**0.001**	+
rsREL	**Right Inferior Parietal Lobe**	**0.44**	**0.029**	+
3 (R)	Primary Somatosensory Cortex	-0.20	0.046	-
4 (R)	Primary Motor Cortex	-0.24	0.018	-
6 (R)	*Premotor Cortex*	*0.33*	*0.046*	+
7 (R)	*Somatosensory Association Cortex*	*0.23*	*0.008*	+
8 (L)	*Dorsal Frontal Cortex*	*0.47*	*0.002*	+
9 (L)	*Dorsolateral Prefrontal Cortex*	*0.33*	*0.001*	+
9 (R)	*Dorsolateral Prefrontal Cortex*	*0.72*	*0.001*	+
10 (R)	Anterior Prefrontal Cortex	0.50	0.002	+
20 (L)	Inferior Temporal Gyrus	0.18	0.027	+
30 (L)	Cingulate Cortex	-0.20	0.008	-
30 (R)	Cingulate Cortex	-0.12	0.004	-
43 (R)	Subcentral Area	-0.18	0.033	-

Figure 6.1D and table 6.1.8 shows that right BA8 (BA8R) was positively correlated with the RLP (DMN region), right superior frontal gyrus and inferior parietal lobe (rsRELs). Positive correlations were also found with the left dorsal frontal cortex (BA8; GDN region), inferior temporal gyrus (BA20) and with the right premotor (BA6; GDN region), somatosensory association (BA7; GDN region) and anterior prefrontal (BA10) cortices. BA8R was positively correlated with the left/right dorsolateral prefrontal cortices (BA9). Significant negative correlations were found between BA8R and the right primary somatosensory (BA3) and primary motor (BA6) cortices, subcentral area (BA43), and with the left/right cingulate cortices (BA30)

6.3.1.2.4. Overall summary of GDN region BA8 (GDN match)

Overall these results show that BA8L and BA8R were positively correlated with each other and with the regions chosen to represent the GDN's precentral sulcus (BA6), superior parietal lobule (BA7) and dorsal frontal cortex (BA8). No correlations were found between this ROI and those

chosen to represent the intraparietal sulcus portion of the GDN. This is surprising given that frontal and parietal portions of the GDN are typically co-activated during attention demanding tasks (Corbetta & Shulman, 2002). However, it should be noted BA8R did reveal a positive correlation with the RLP component of the DMN, perhaps suggesting that the parietal node of the GDN overlaps with the RLP region of the DMN. Detachment from other DMN components might also suggest that this GDN region plays a key role in the allocation of attention given the goal-driven nature of the task.

BA39: Angular gyrus (closest match to intraparietal sulcus)

Table 6.1.9. Left angular gyrus (BA39L) connectivity to all cerebral regions in 840s of active auditory attention data and their significance.

Brodmann area	Brain region	*B*	*p*	Correlation
DMN region	**Left Lateral Parietal**	**1.25**	**<0.001**	+
DMN region	**Medial Prefrontal Cortex**	**0.42**	**0.002**	+
DMN region	**Posterior Cingulate Cortex**	**0.62**	**0.003**	+
DMN region	**Right Lateral Parietal**	**0.47**	**0.001**	+
rsREL	**Cingulate Gyrus**	**-0.35**	**0.010**	-
rsREL	**Left Anterior Sup Temp Gyrus**	**-0.31**	**0.002**	-
rsREL	**Left Inferior Parietal Lobe**	**1.21**	**<0.001**	+
rsREL	**Left Superior Frontal Gyrus**	**0.57**	**0.001**	+
rsREL	**Medial Prefrontal Cortex**	**0.48**	**<0.001**	+
rsREL	**Precuneus (PCC)**	**0.65**	**<0.001**	+
rsREL	**Right Anterior Sup Temp Gyrus**	**-0.30**	**0.004**	-
rsREL	**Right Inferior Parietal Lobe**	**0.51**	**0.002**	+
rsREL	**Right Posterior Sup Temp Gyrus**	**-0.30**	**0.010**	-
6 (R)	*Premotor Cortex*	*-0.23*	*0.018*	-
7 (L)	*Somatosensory Association Cortex*	*0.25*	*0.040*	+
8 (L)	*Dorsal Frontal Cortex*	*0.50*	*0.025*	+
10 (L)	Anterior Prefrontal Cortex	0.41	0.007	+
11 (L)	Orbitofrontal Cortex	0.24	0.008	+
13 (L)	Insular Cortex	-0.32	0.002	-
13 (R)	Insular Cortex	-0.32	0.002	-
17 (R)	Primary Visual Cortex	-0.13	0.002	-
18 (R)	Secondary Visual Cortex	-0.12	0.003	-
21 (L)	Middle Temporal Gyrus	0.42	0.002	+
21 (R)	Middle Temporal Gyrus	0.17	0.047	+
22 (R)	Superior Temporal Gyrus	-0.18	0.018	-
23 (L)	Ventral Posterior Cingulate Cortex	0.27	0.018	+
28 (L)	Posterior Entorhinal Cortex	-0.08	0.032	-

28 (R)	Posterior Entorhinal Cortex	-0.11	0.045	-
31 (L)	Dorsal Posterior Cingulate Cortex	0.61	<0.001	+
31 (R)	Dorsal Posterior Cingulate Cortex	0.30	0.010	+
33 (R)	Anterior Cingulate	0.12	0.001	+
34 (R)	Anterior Entorhinal Cortex	-0.13	0.018	-
39 (R)	*Angular gyrus*	*0.57*	*0.002*	+
41 (L)	Primary Auditory Cortex	-0.13	0.047	-
41 (R)	Primary Auditory Cortex	-0.16	0.010	-
42 (L)	Primary Auditory Cortex	-0.20	0.003	-
42 (R)	Primary Auditory Cortex	-0.22	0.002	-
44 (L)	IFC pars opercularis	-0.12	0.030	-
44 (R)	IFC pars opercularis	-0.36	0.008	-

Figure 6.1E and table 6.1.9 reveal left BA39 (BA39L) was positively correlated to the LLP, MPFC, PCC, RLP (DMN regions), left superior frontal gyrus, medial prefrontal cortex, precuneus (PCC) and the right inferior parietal lobe (rsRELs). Significant positive correlations were also found between BA39L and the left somatosensory association (BA7; GDN region), dorsal frontal (BA8; GDN region), anterior prefrontal (BA10) and orbitofrontal (BA11) cortices. BA39L was also positively correlated to the right anterior cingulate cortex (BA33), right angular gyrus (BA39; GDN region) and the left/right middle temporal gyri (BA21) and dorsal posterior cingulate cortex (BA31). Negative correlations were found between BA39L and the cingulate gyrus, right anterior superior temporal gyrus and the left/right anterior superior temporal gyri (rsRELs). Negative correlations were also found between BA39L and the right premotor (BA6; GDN region) and right primary/secondary visual (BA17, BA18) cortices, along with the right anterior entorhinal cortex (BA34). In the left/right hemispheres BA39L was negatively correlated with the insular (BA13), posterior entorhinal (BA28), primary auditory (BA41, BA42) cortices and the IFC pars operculari (BA44).

Table 6.1.10. Right angular gyrus (BA39R) connectivity to all cerebral regions in 840s of active auditory attention data and their significance.

Brodmann	Brain region	*B*	*p*	Correlation

area

DMN region	**Left Lateral Parietal**	**0.58**	**0.002**	**+**
DMN region	**Medial Prefrontal Cortex**	**0.37**	**0.001**	**+**
DMN region	**Posterior Cingulate Cortex**	**0.43**	**0.007**	**+**
DMN region	**Right Lateral Parietal**	**1.02**	**<0.001**	**+**
rsREL	**Left Anterior Sup Temp Gyrus**	**-0.20**	**0.033**	**-**
rsREL	**Left Inferior Parietal Lobe**	**0.57**	**0.001**	**+**
rsREL	**Left Superior Frontal Gyrus**	**0.25**	**0.032**	**+**
rsREL	**Medial Prefrontal Cortex**	**0.34**	**0.002**	**+**
rsREL	**Precuneus (PCC)**	**0.51**	**0.002**	**+**
rsREL	**Right Anterior Sup Temp Gyrus**	**-0.26**	**0.008**	**-**
rsREL	**Right Inferior Parietal Lobe**	**0.87**	**<0.001**	**+**
rsREL	**Right Posterior Sup Temp Gyrus**	**-0.27**	**0.018**	**-**
rsREL	**Right Superior Frontal Gyrus**	**0.47**	**0.004**	**+**
1 (L)	Primary Somatosensory Cortex	-0.23	0.017	-
1 (R)	Primary Somatosensory Cortex	-0.18	0.032	-
2 (L)	Primary Somatosensory Cortex	-0.28	0.029	-
2 (R)	Primary Somatosensory Cortex	-0.28	0.007	-
3 (L)	Primary Somatosensory Cortex	-0.27	0.008	-
3 (R)	Primary Somatosensory Cortex	-0.22	0.011	-
4 (L)	Primary Motor Cortex	-0.26	0.012	-
4 (R)	Primary Motor Cortex	-0.24	0.007	-
5 (L)	Somatosensory Association Cortex	-0.19	0.035	-
5 (R)	Somatosensory Association Cortex	-0.22	0.018	-
6 (L)	*Premotor Cortex*	*-0.15*	*0.032*	-
7 (R)	*Somatosensory Association Cortex*	*0.21*	*0.025*	+
8 (R)	*Dorsal Frontal Cortex*	*0.33*	*0.035*	+
10 (L)	Anterior Prefrontal Cortex	0.23	0.007	+
10 (R)	Anterior Prefrontal Cortex	0.27	0.002	+
11 (L)	Orbitofrontal Cortex	0.14	0.034	+
11 (R)	Orbitofrontal Cortex	0.18	0.018	+
13 (L)	Insular Cortex	-0.27	0.032	-
13 (R)	Insular Cortex	-0.29	0.008	-
18 (R)	Secondary Visual Cortex	-0.14	0.016	-
21 (L)	Middle Temporal Gyrus	0.21	0.028	+
23 (L)	Ventral Posterior Cingulate Cortex	0.24	0.017	+
23 (R)	Ventral Posterior Cingulate Cortex	0.24	0.008	+
29 (R)	Retrosplenial Cingulate Cortex	0.18	0.025	+
31 (L)	Dorsal Posterior Cingulate Cortex	0.42	0.007	+
31 (R)	Dorsal Posterior Cingulate Cortex	0.45	0.002	+
33 (R)	Anterior Cingulate	0.12	0.007	+
39 (L)	*Angular gyrus*	*0.57*	*0.002*	+
40 (L)	*Supramarginal Gyrus*	*-0.30*	*0.008*	-
43 (R)	Subcentral Area	-0.23	0.020	-
44 (R)	IFC pars opercularis	-0.26	0.002	-

Figure 6.1E and table 6.1.10 show that right BA39 (BA39R) was positively correlated to LLP, MPFC, PCC, RLP (DMN regions), and the left/right inferior parietal lobes, left/right superior frontal gyri, medial prefrontal cortex and precuneus (PCC; rsRELs). BA39R was positively

correlated with the left middle temporal (BA21) and angular (BA39; GDN region) gyri and the right somatosensory association (BA7; GDN region), dorsal frontal (BA8; GDN region), retrosplenial cingulate (BA29) and anterior cingulate (BA33) cortices. BA39R was also positively correlated with the left/right anterior prefrontal (BA10) orbitofrontal (BA11) and ventral/dorsal posterior cingulate (BA23, BA31) cortices. Negative correlations were found between BA39R and the right posterior superior temporal gyrus and the left/right anterior superior temporal gyri (rsRELs). Negative correlations were also apparent with the left premotor cortex (BA6), supramarginal gyrus (BA40; GDN region), and the right secondary visual cortex (BA18), subcentral area (BA43) and IFC opercularis (BA44). In both hemispheres BA39R was negatively correlated with the primary somatosensory (BA1, BA2, BA3), primary motor (BA4), somatosensory association (BA5) and insular (BA13) cortices.

6.3.1.2.5. Overall summary of GDN region BA39 (closest match to intraparietal sulcus)

The position of BA39 in the left and right hemispheres (see figure 6.1E) and associated patterns of connectivity suggests that perhaps this ROI is not a reliable representation of the intraparietal sulcus component of the GDN. Instead, this seed appears to map on well with the DMN's left/right lateral parietal regions and also mimics connectivity patterns associated with this network: particularly increases in frontal, midline and parietal activity (MPFC, PCC, LLP, RLP); and reductions auditory, visual and somatosensory areas.

BA40: Supramarginal gyrus (closest match to intraparietal sulcus)

Table 6.1.11. Left supramarginal gyrus (BA40L) connectivity to all cerebral regions in 840s of active auditory attention data and their significance.

Brodmann area	Brain region	*B*	*p*	Correlation
DMN region	**Medial Prefrontal Cortex**	**-0.42**	**0.001**	**-**
DMN region	**Posterior Cingulate Cortex**	**-0.35**	**0.002**	**-**
DMN region	**Right Lateral Parietal**	**-0.24**	**0.014**	**-**
rsREL	**Cingulate Gyrus**	**0.36**	**0.005**	**+**
rsREL	**Left Anterior Sup Temp Gyrus**	**0.26**	**0.003**	**+**
rsREL	**Left Posterior Sup Temp Gyrus**	**0.50**	**<0.001**	**+**
rsREL	**Left Superior Frontal Gyrus**	**-0.16**	**0.048**	**-**
rsREL	**Medial Prefrontal Cortex**	**-0.32**	**0.003**	**-**
rsREL	**Precuneus (PCC)**	**-0.47**	**0.001**	**-**
rsREL	**Right Anterior Sup Temp Gyrus**	**0.33**	**0.003**	**+**
rsREL	**Right Posterior Sup Temp Gyrus**	**0.40**	**0.003**	**+**
rsREL	**Right Superior Frontal Gyrus**	**-0.20**	**0.047**	**-**
1 (L)	Primary Somatosensory Cortex	0.49	0.002	+
1 (R)	Primary Somatosensory Cortex	0.30	0.011	+
2 (L)	Primary Somatosensory Cortex	0.63	0.001	+
2 (R)	Primary Somatosensory Cortex	0.50	0.002	+
3 (L)	Primary Somatosensory Cortex	0.45	0.001	+
3 (R)	Primary Somatosensory Cortex	0.23	0.047	+
4 (L)	Primary Motor Cortex	0.36	0.002	+
5 (L)	*Somatosensory Association Cortex*	*0.30*	*0.039*	+
5 (R)	*Somatosensory Association Cortex*	*0.23*	*0.047*	+
6 (L)	*Premotor Cortex*	*0.63*	*<0.001*	+
6 (R)	*Premotor Cortex*	*0.41*	*0.002*	+
7 (L)	*Somatosensory Association Cortex*	*0.24*	*0.017*	+
9 (L)	*Dorsolateral Prefrontal Cortex*	*0.16*	*0.047*	+
13 (L)	Insular Cortex	0.31	0.002	+
13 (R)	Insular Cortex	0.22	0.011	+
18 (L)	Secondary Visual Cortex	-0.13	0.035	-
19 (R)	Associative Visual Cortex	-0.21	0.005	-
22 (L)	Superior Temporal Gyrus	0.37	<0.001	+
22 (R)	Superior Temporal Gyrus	0.28	0.007	+
23 (R)	Ventral Posterior Cingulate Cortex	-0.30	0.004	-
29 (L)	Retrosplenial Cingulate Cortex	-0.22	0.010	-
29 (R)	Retrosplenial Cingulate Cortex	-0.25	0.001	-
30 (L)	Cingulate Cortex	-0.29	<0.001	-
30 (R)	Cingulate Cortex	-0.23	0.002	-
31 (L)	Dorsal Posterior Cingulate Cortex	-0.37	0.001	-
31 (R)	Dorsal Posterior Cingulate Cortex	-0.44	<0.001	-
37 (L)	Fusiform gyrus	0.27	0.003	+
39 (R)	*Angular gyrus*	*-0.30*	*0.005*	-
40 (R)	*Supramarginal Gyrus*	*0.69*	*<0.001*	+
41 (L)	Primary Auditory Cortex	0.28	0.001	+
41 (R)	Primary Auditory Cortex	0.21	0.002	+
42 (L)	Primary Auditory Cortex	0.36	0.001	+
42 (R)	Primary Auditory Cortex	0.29	0.002	+
43 (L)	Subcentral Area	0.21	0.021	+
44 (L)	IFC pars opercularis	0.36	0.002	+
44 (R)	IFC pars opercularis	0.37	0.003	+
46 (L)	*Dorsolateral Prefrontal Cortex*	*0.34*	*0.005*	+
46 (R)	*Dorsolateral Prefrontal Cortex*	*0.20*	*0.049*	+

Figure 6.1F and table 6.1.11 show that left BA40 (BA40L) was positively correlated with cingulate gyrus and left/right anterior/posterior superior temporal gyri (rsRELs). BA40L was also positively correlated with the left primary motor (BA4), somatosensory association (BA7; GDN region) and dorsolateral prefrontal (BA9; GDN region) cortices, as well as the left fusiform gyrus (BA37) and subcentral area (BA43). BA40L was positively correlated with right supramarginal gyrus (BA40; GDN region), and the left/right primary somatosensory (BA1, BA2, BA3), somatosensory association (BA5; GDN region), premotor (BA6; GDN region) and insular (BA13) cortices. BA40L was also positively correlated with the left/right superior temporal gyrus (BA22), primary auditory cortices (BA41, BA42) and the IFC pars operculari (BA44). Negative correlations were found between BA40L and the MPFC, PCC, RLP (DMN regions), left/right superior frontal gyri, medial prefrontal cortex and precuneus (PCC: rsRELs). BA40L was also negatively correlated with the left secondary visual cortex (BA18) and the right associative visual (BA19) ventral posterior cingulate (BA23) cortices and angular gyrus (BA39; now assumed an unreliable representation of the GDN region). In both the left and right hemispheres negative correlations were apparent between BA40L and the retrosplenial cingulate (BA29), cingulate (BA30) and dorsal posterior cingulate (BA31) cortices.

Table 6.1.12. Right supramarginal gyrus (BA40R) connectivity to all cerebral regions in 840s of active auditory attention data and their significance.

Brodmann area	Brain region	*B*	*p*	Correlation
DMN region	**Left Lateral Parietal**	**-0.22**	**0.021**	**-**
DMN region	**Medial Prefrontal Cortex**	**-0.45**	**0.001**	**-**
DMN region	**Posterior Cingulate Cortex**	**-0.31**	**0.011**	**-**
rsREL	**Cingulate Gyrus**	**0.34**	**0.001**	**+**
rsREL	**Left Anterior Sup Temp Gyrus**	**0.27**	**0.006**	**+**
rsREL	**Left Inferior Parietal Lobe**	**-0.18**	**0.033**	**-**
rsREL	**Left Posterior Sup Temp Gyrus**	**0.37**	**0.001**	**+**
rsREL	**Left Superior Frontal Gyrus**	**-0.21**	**0.001**	**-**
rsREL	**Medial Prefrontal Cortex**	**-0.42**	**0.001**	**-**

rsREL	**Precuneus (PCC)**	**-0.49**	**0.001**	**-**
rsREL	**Right Anterior Sup Temp Gyrus**	**0.36**	**0.004**	**+**
rsREL	**Right Posterior Sup Temp Gyrus**	**0.53**	**0.001**	**+**
1 (R)	Primary Somatosensory Cortex	0.23	0.019	+
2 (R)	Primary Somatosensory Cortex	0.46	0.001	+
5 (R)	*Somatosensory Association Cortex*	*0.20*	*0.036*	+
6 (L)	*Premotor Cortex*	*0.26*	*0.004*	+
6 (R)	*Premotor Cortex*	*0.56*	*<0.001*	+
7 (R)	*Somatosensory Association Cortex*	*0.31*	*0.006*	+
8 (R)	*Dorsal Frontal Cortex*	*0.24*	*0.036*	+
9 (R)	*Dorsolateral Prefrontal Cortex*	*0.41*	*<0.001*	+
10 (R)	Anterior Prefrontal Cortex	0.23	0.003	+
13 (L)	Insular Cortex	0.27	0.012	+
13 (R)	Insular Cortex	0.32	0.004	+
18 (L)	Secondary Visual Cortex	-0.15	0.020	-
19 (L)	Associative Visual Cortex	-0.19	0.010	-
19 (R)	Associative Visual Cortex	-0.12	0.004	-
22 (L)	Superior Temporal Gyrus	0.33	0.003	+
22 (R)	Superior Temporal Gyrus	0.31	0.001	+
23 (L)	Ventral Posterior Cingulate Cortex	-0.23	0.049	-
23 (R)	Ventral Posterior Cingulate Cortex	-0.21	0.016	-
29 (L)	Retrosplenial Cingulate Cortex	-0.25	0.001	-
29 (R)	Retrosplenial Cingulate Cortex	-0.20	0.004	-
30 (L)	Cingulate Cortex	-0.33	0.002	-
30 (R)	Cingulate Cortex	-0.19	0.040	-
31 (L)	Dorsal Posterior Cingulate Cortex	-0.40	0.004	-
31 (R)	Dorsal Posterior Cingulate Cortex	-0.30	0.004	-
35 (L)	Perirhinal cortex	-0.17	0.001	-
37 (L)	Fusiform gyrus	0.17	0.039	+
37 (R)	Fusiform gyrus	0.26	0.004	+
40 (L)	*Supramarginal Gyrus*	*0.69*	*<0.001*	+
41 (L)	Primary Auditory Cortex	0.20	0.025	+
41 (R)	Primary Auditory Cortex	0.23	0.005	+
42 (L)	Primary Auditory Cortex	0.25	0.009	+
42 (R)	Primary Auditory Cortex	0.24	0.026	+
44 (L)	IFC pars opercularis	0.40	0.001	+
44 (R)	IFC pars opercularis	0.57	0.000	+
45 (R)	IFC pars triangularis	0.29	0.003	+
46 (L)	*Dorsolateral Prefrontal Cortex*	*0.34*	*0.005*	+
46 (R)	*Dorsolateral Prefrontal Cortex*	*0.43*	*0.002*	+
47 (R)	Inferior Prefrontal Gyrus	0.30	0.004	+

Figure 6.1F and table 6.1.12 show that right BA40 (BA40R) was positively correlated with the cingulate gyrus and left/right anterior/posterior superior temporal gyri (rsRELs). In the left hemisphere BA40R was positively correlated with supramarginal gyrus (BA40; GDN region). In the right hemisphere BA40R was positively correlated with the primary somatosensory (BA1, BA2), somatosensory association (BA5, BA7; GDN regions), dorsal frontal (BA8; GDN region),

dorsolateral prefrontal (BA9) and anterior prefrontal (BA10) cortices, as well as the IFC pars triangularis (BA45) and inferior prefrontal cortex (BA47). BA40R was also positively correlated with the left/right premotor (BA6; GDN region), insular (BA13), primary auditory (BA41, BA42) and dorsolateral prefrontal (BA46) cortices, along with the IFC pars operculari (BA45). Negative correlations were apparent between BA40R and the LLP, MPFC, PCC (DMN regions), left inferior parietal lobe, superior frontal gyrus, medial prefrontal cortex and the precuneus (PCC; rsRELs). Negative correlations were also found between BA40R and the left secondary visual (BA18) and perirhinal (BA35) cortices, and the left/right associative visual (BA19), ventral/dorsal posterior cingulate (BA23, BA31), retrosplenial (BA29) and cingulate (BA30) cortices.

6.3.1.2.6. Overall summary of GDN region BA40 (closest match to intraparietal sulcus)

Overall, BA40 shows strong connectivity to frontal and parietal regions associated with the GDN. This area was also positively correlated to somatosensory, auditory and other temporal areas assumed to be active given the nature of the task. This supports the first hypothesis that there would be strong connectivity within the GDN. BA40L was negatively correlated to MPFC, PCC and RLP; and BA40R was negatively related to MPFC, PCC and LLP. These patterns of correlated activity offer support to the prediction that activity in the GDN would be associated with down-regulation of the DMN. These results also suggest that BA40 is a more reliable representation of the GDN's intraparietal sulcus in comparison to BA39.

6.3.2. Results of analysis 2:

Connectivity within the attention-orienting ventral frontoparietal network (stimulus-driven network) in an 840s active auditory attention task, and its relationship to the DMN

This analysis explored functional connectivity of the SDN. As outlined in section *6.1.1.2*, based on the fact that distractors were randomly presented throughout the task, it was hypothesised that strong functional connectivity within the SDN would be observed (prediction 1).

A secondary hypothesis was that activity in the SDN would be associated with down-regulation of the DMN (prediction 2).

6.3.2.1. Stimulus-driven network ROIs

According to Corbetta et al. (2008) SDN regions include the temporoparietal junction cortex (defined as the posterior region of the superior temporal sulcus/gyrus and ventral part of the supramarginal gyrus), along with the frontal operculum, ventral frontal cortex, regions of the middle frontal gyrus, inferior frontal gyrus, and anterior insula. As with the GDN there were some differences in the identification of SDN regions identified by Corbetta and colleagues and those available using the *conn* software. SDN ROIs were therefore chosen based on their close proximity to typical SDN regions and included the left and right anterior prefrontal cortex (BA10: ventral frontal cortex), insular cortex (BA13: anterior insula), superior temporal gyrus (BA22: SDN match), supramarginal gyrus (BA40: SDN match), IFC pars opercularis (BA44: frontal operculum), IFC pars triangularis (BA45: frontal operculum) and the inferior prefrontal gyrus (BA47: inferior frontal gyrus). Note that BA40 corresponding to the SDN's supramarginal

gyrus, overlapped with the use of this BA in the previous analysis, where it was considered as a representative of the GDN's intraparietal sulcus.

6.3.2.2. Stimulus-driven network functional connectivity analysis

Connectivity between SDN seed regions (BA10, BA13, BA22, BA40, BA44, BA45, BA47) and the whole of the cerebral cortex are shown in figure 6.2. Tables 6.2.1-6.2.14, illustrate the conn region, BA label, strength of connectivity (*Beta (B)* value) and significance (*p* value) across all participants. In each figure and table, positive correlations are displayed in red text and negative correlations are displayed in blue. SDN ROIs are displayed in *italics* and highlighted grey, and DMN seed (Fox et al., 2005)/rsREL regions are displayed in **bold** text. Note that significant ($p<.05$) correlations only are presented.

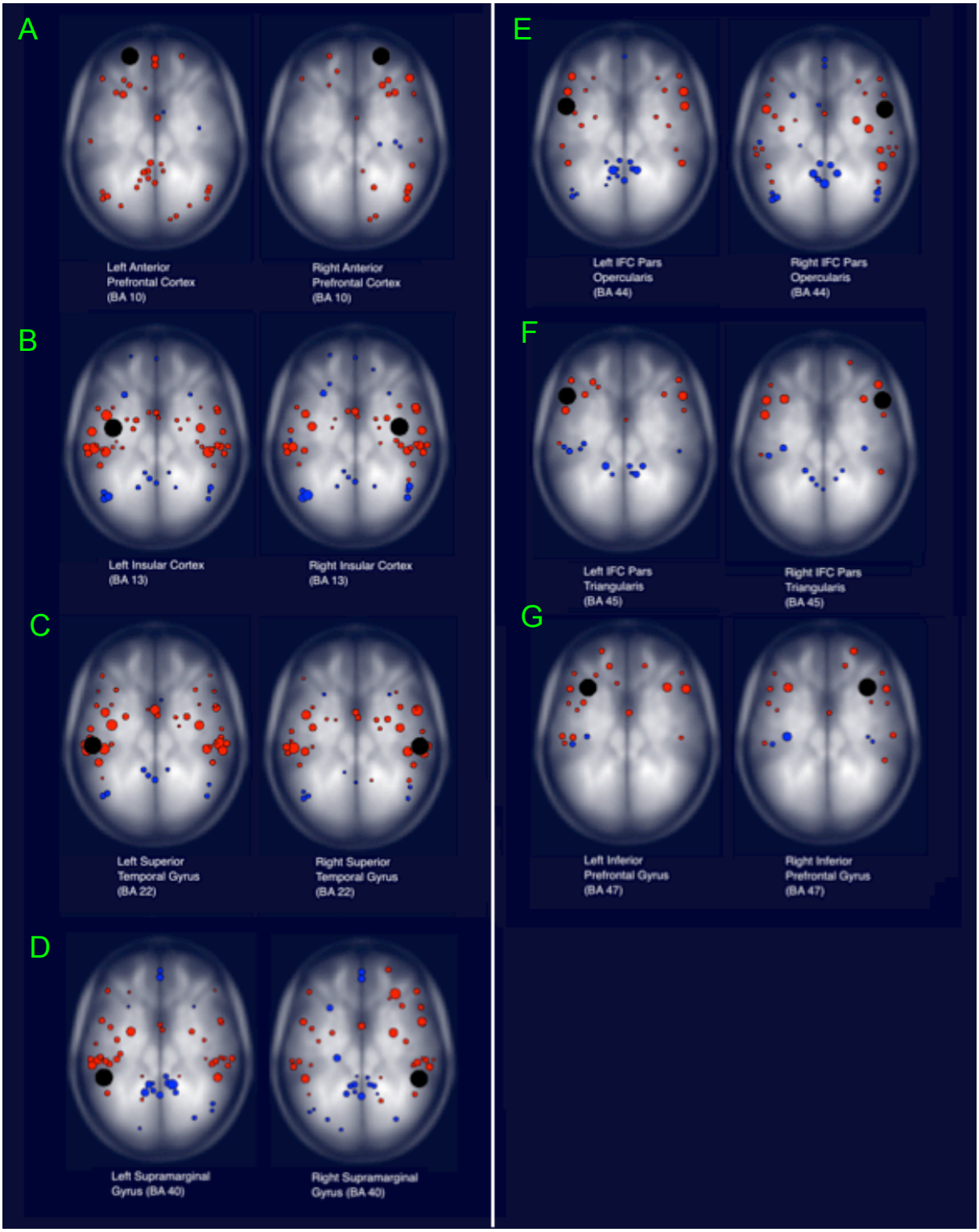

Figure 6.2. Relationship between SDN seed regions and areas covering the whole of the cerebral cortex in an 840s auditory attention task. (A) BA10, (B) BA13, (C) BA22, (D) BA40, (E) BA44, (F) BA45, (G) BA47.

BA10: Left anterior prefrontal cortex (closest match to ventral frontal cortex)

Table 6.2.1. Left anterior prefrontal cortex (BA10L) connectivity to all cerebral regions in 840s of active auditory attention data and their significance.

Brodmann area	Brain region	*B*	*p*	Correlation
DMN region	**Left Lateral Parietal**	**0.37**	**0.005**	+
DMN region	**Medial Prefrontal Cortex**	**0.31**	**0.003**	+
DMN region	**Posterior Cingulate Cortex**	**0.31**	**0.007**	+
DMN region	**Right Lateral Parietal**	**0.20**	**0.010**	+
rsREL	**Left Inferior Parietal Lobe**	**0.41**	**0.004**	+
rsREL	**Left Superior Frontal Gyrus**	**0.32**	**0.003**	+
rsREL	**Medial Prefrontal Cortex**	**0.42**	**0.003**	+
rsREL	**Precuneus (PCC)**	**0.30**	**0.007**	+
rsREL	**Right Inferior Parietal Lobe**	**0.20**	**0.007**	+
7 (L)	Somatosensory Association Cortex	0.32	0.007	+
8 (L)	Dorsal Frontal Cortex	0.46	0.007	+
9 (L)	Dorsolateral Prefrontal Cortex	0.44	0.008	+
10 (R)	*Anterior Prefrontal Cortex*	*0.54*	*0.007*	+
13 (R)	*Insular Cortex*	*-0.17*	*0.031*	-
17 (R)	Primary Visual Cortex	0.20	0.022	+
18 (R)	Secondary Visual Cortex	0.24	0.008	+
19 (L)	Associative Visual Cortex	0.18	0.010	+
19 (R)	Associative Visual Cortex	0.15	0.018	+
21 (L)	Middle Temporal Gyrus	0.21	0.016	+
23 (L)	Ventral Posterior Cingulate Cortex	0.28	0.003	+
23 (R)	Ventral Posterior Cingulate Cortex	0.15	0.011	+
24 (R)	Ventral Anterior Cingulate Cortex	-0.16	0.044	-
29 (L)	Retrosplenial Cingulate Cortex	0.27	0.004	+
29 (R)	Retrosplenial Cingulate Cortex	0.21	0.016	+
30 (L)	Cingulate Cortex	0.22	0.014	+
31 (L)	Dorsal Posterior Cingulate Cortex	0.30	0.004	+
32 (L)	Dorsal Anterior Cingulate Cortex	0.17	0.049	+
39 (L)	Angular gyrus	0.41	0.008	+
39 (R)	Angular gyrus	0.23	0.007	+
46 (L)	Dorsolateral Prefrontal Cortex	0.25	0.007	+
47 (L)	*Inferior Prefrontal Gyrus*	*0.33*	*0.007*	+

Table 6.2.1 and figure 6.2A reveal that left BA10 (BA10L) was positively correlated with LLP, MPFC (DMN region, rsREL), PCC, RLP (DMN regions), left/right inferior parietal lobe, left superior frontal gyrus and precuneus (PCC; rsREL). BA10L was also positively correlated with the left somatosensory (BA7), dorsal frontal (BA8) and dorsolateral prefrontal (BA9) cortices, middle temporal gyrus (BA21) cingulate (BA30), dorsolateral prefrontal (BA46) and inferior prefrontal (BA47; SDN region) cortices; and the right anterior prefrontal (BA10; SDN region),

and primary/secondary visual (BA17, BA18) cortices. Positive correlations were also found between BA10L and the left/right associative visual (BA19), ventral posterior cingulate (BA23) and retrosplenial cingulate (BA29) cortices and the angular gyri (BA39). BA10L was negatively correlated with the right insular cortex (BA13; SDN region) and the right ventral anterior cingulate cortex (BA24).

Table 6.2.2. Right anterior prefrontal cortex (BA10R) connectivity to all cerebral regions in 840s of active auditory attention data and their significance.

Brodmann area	Brain region	*B*	*p*	Correlation
DMN region	**Right Lateral Parietal**	**0.26**	**0.002**	+
rsREL	**Right Inferior Parietal Lobe**	**0.44**	**0.002**	+
rsREL	**Right Superior Frontal Gyrus**	**0.31**	**0.008**	+
3 (R)	Primary Somatosensory Cortex	-0.18	0.030	-
4 (R)	Primary Motor Cortex	-0.17	0.017	-
7 (R)	Somatosensory Association Cortex	0.35	0.006	+
8 (L)	Dorsal Frontal Cortex	0.15	0.039	+
8 (R)	Dorsal Frontal Cortex	0.50	0.002	+
9 (R)	Dorsolateral Prefrontal Cortex	0.39	0.005	+
10 (L)	*Anterior Prefrontal Cortex*	*0.54*	*0.011*	+
11 (L)	Orbitofrontal Cortex	0.23	0.017	+
17 (R)	Primary Visual Cortex	0.21	0.017	+
18 (R)	Secondary Visual Cortex	0.24	0.013	+
21 (R)	Middle Temporal Gyrus	0.22	0.029	+
29 (R)	Retrosplenial Cingulate Cortex	0.15	0.039	+
35 (R)	Perirhinal cortex	-0.13	0.022	-
39 (R)	Angular gyrus	0.27	0.003	+
40 (R)	*Supramarginal Gyrus*	*0.23*	*0.008*	+
45 (R)	*IFC pars triangularis*	*0.20*	*0.019*	+
46 (L)	Dorsolateral Prefrontal Cortex	0.22	0.029	+
46 (R)	Dorsolateral Prefrontal Cortex	0.40	0.002	+
47 (R)	*Inferior Prefrontal Gyrus*	*0.34*	*0.002*	+

Right BA10 (BA10R; see figure 6.2A and table 6.2.2) was positively correlated to the RLP (DMN region), right inferior parietal lobe and the right superior frontal gyrus (rsRELs). BA10R was also positively correlated with the left anterior prefrontal (BA10; SDN region) and oribitofrontal (BA11) cortices; along with the right somatosensory association (BA7),

dorsolateral prefrontal (BA9), primary/secondary visual (BA17, BA18) cortices, middle temporal gyrus (BA21), retrosplenial cingulate cortex (BA29), angular gyrus (BA39), supramarginal gyrus (BA40; SDN region), IFC pars triangularis (BA45; SDN region) and the inferior prefrontal cortex (BA47; SDN region). BA10R was also positively correlated with the left/right dorsal frontal (BA8) and dorsolateral prefrontal (BA46) cortices. Negative correlations were apparent between BA10R and the right primary somatosensory (BA3), primary motor (BA4) and perirhinal (BA35) cortices.

6.3.2.2.1. Overall summary of SDN region BA10 (closest match to ventral frontal cortex)

Overall the patterns of connectivity of BA10 show that this area responds differently in each hemisphere. BA10L shows widespread positive correlations across the cortex, including to DMN regions LLP, MPFC, PCC, RLP and surrounding rsREL regions. Conversely, BA10R shows a somewhat right lateralised spread of correlated activity and is only positively correlated with the RLP component of the DMN. Although difficult to interpret, this difference in connectivity across hemispheres could suggest right BA10 is more involved in the detection of unpredictable events than its homologous region in the left hemisphere. Alternatively, the positive correlations observed between left BA10 and DMN regions may support the sentinel hypothesis of DMN function, in that this portion of the SDN may selectively recruit portions of the DMN in order to adopt a similar role in the detection of unpredictable events.

BA13: Left insular cortex (closest match to anterior insula)

Table 6.2.3. Left insular cortex (BA13L) connectivity to all cerebral regions in 840s of active auditory attention data and their significance.

Brodmann	Brain region	*B*	*p*	Correlation

area

DMN region	**Left Lateral Parietal**	**-0.33**	**0.001**	**-**
DMN region	**Posterior Cingulate Cortex**	**-0.29**	**0.002**	**-**
DMN region	**Right Lateral Parietal**	**-0.27**	**0.007**	**-**
rsREL	**Cingulate Gyrus**	**0.47**	**0.002**	**+**
rsREL	**Left Anterior Sup Temp Gyrus**	**0.93**	**<0.001**	**+**
rsREL	**Left Inferior Parietal Lobe**	**-0.34**	**<0.001**	**-**
rsREL	**Left Posterior Sup Temp Gyrus**	**0.57**	**0.001**	**+**
rsREL	**Left Superior Frontal Gyrus**	**-0.19**	**0.002**	**-**
rsREL	**Medial Prefrontal Cortex**	**-0.17**	**0.022**	**-**
rsREL	**Precuneus (PCC)**	**-0.27**	**0.005**	**-**
rsREL	**Right Anterior Sup Temp Gyrus**	**0.48**	**0.001**	**+**
rsREL	**Right Inferior Parietal Lobe**	**-0.33**	**0.002**	**-**
rsREL	**Right Posterior Sup Temp Gyrus**	**0.57**	**0.002**	**+**
rsREL	**Right Superior Frontal Gyrus**	**-0.23**	**0.013**	**-**
1 (L)	Primary Somatosensory Cortex	0.29	0.025	+
1 (R)	Primary Somatosensory Cortex	0.35	0.002	+
2 (L)	Primary Somatosensory Cortex	0.29	0.016	+
2 (R)	Primary Somatosensory Cortex	0.37	0.003	+
3 (L)	Primary Somatosensory Cortex	0.34	0.016	+
3 (R)	Primary Somatosensory Cortex	0.29	0.013	+
4 (L)	Primary Motor Cortex	0.23	0.049	+
4 (R)	Primary Motor Cortex	0.29	0.024	+
6 (L)	Premotor Cortex	0.26	0.017	+
6 (R)	Premotor Cortex	0.30	0.015	+
7 (L)	Somatosensory Association Cortex	-0.20	0.007	-
7 (R)	Somatosensory Association Cortex	-0.21	0.022	-
10 (L)	*Anterior Prefrontal Cortex*	*-0.14*	*0.038*	*-*
13 (R)	*Insular Cortex*	*0.91*	*<0.001*	*+*
22 (L)	*Superior Temporal Gyrus*	*0.61*	*<0.001*	*+*
22 (R)	*Superior Temporal Gyrus*	*0.49*	*0.001*	*+*
24 (L)	Ventral Anterior Cingulate Cortex	0.26	0.010	+
28 (L)	Posterior Entorhinal Cortex	0.24	0.004	+
28 (R)	Posterior Entorhinal Cortex	0.17	0.026	+
31 (L)	Dorsal Posterior Cingulate Cortex	-0.23	0.010	-
31 (R)	Dorsal Posterior Cingulate Cortex	-0.19	0.023	-
34 (L)	Anterior Entorhinal Cortex	0.22	0.002	+
34 (R)	Anterior Entorhinal Cortex	0.22	0.012	+
36 (L)	Parahippocampal Cortex	0.17	0.018	+
38 (L)	Temporopolar Area	0.25	0.022	+
38 (R)	Temporopolar Area	0.14	0.040	+
39 (L)	Angular gyrus	-0.32	0.002	-
39 (R)	Angular gyrus	-0.27	0.026	-
40 (L)	*Supramarginal Gyrus*	*0.31*	*0.002*	*+*
40 (R)	*Supramarginal Gyrus*	*0.27*	*0.013*	*+*
41 (L)	Primary Auditory Cortex	0.71	<0.001	+
41 (R)	Primary Auditory Cortex	0.47	<0.001	+
42 (L)	Primary Auditory Cortex	0.54	0.001	+
42 (R)	Primary Auditory Cortex	0.41	0.003	+
43 (L)	Subcentral Area	0.60	<0.001	+
43 (R)	Subcentral Area	0.47	0.002	+
44 (L)	*IFC pars opercularis*	*0.46*	*0.006*	*+*
44 (R)	*IFC pars opercularis*	*0.41*	*0.002*	*+*

Figure 6.2B and table 6.2.3 show that left BA13 (BA13L) was positively correlated with the cingulate gyrus and left/right anterior/posterior superior temporal gyri (rsRELs). This seed was also positively correlated with the left ventral anterior cingulate (BA24) and parahippocampal (BA36) cortices and the right insular cortex (BA13; SDN region). BA13L was positively correlated with the left/right primary somatosensory (BA1, BA2, BA3), primary motor (BA4) and premotor (BA6) cortices, superior temporal gyrus (BA22; SDN region), posterior/anterior entorhinal cortices (BA28, BA34), temporopolar areas (BA38), supramarginal gyri (BA40; SDN region), primary auditory cortices (BA41, BA42), subcentral areas (BA43) and IFC operculari (BA44; SDN region). Significant negative correlations were apparent between BA13L and LLP, PCC, RLP (DMN regions), left/right inferior parietal lobe, left superior frontal gyrus, medial prefrontal cortex (rsREL), precuneus (PCC) and right superior frontal gyrus (rsRELs). BA13L was also negatively correlated with the left anterior prefrontal cortex (BA10; SDN region), and the left/right somatosensory association cortices (BA7), dorsal posterior cingulate cortex BA31) and the angular gyri (BA39).

Table 6.2.4. Right insular cortex (BA13R) connectivity to all cerebral regions in 840s of active auditory attention data and their significance.

Brodmann area	Brain region	*B*	*p*	Correlation
DMN region	**Left Lateral Parietal**	**-0.33**	**<0.001**	**-**
DMN region	**Posterior Cingulate Cortex**	**-0.28**	**0.011**	**-**
DMN region	**Right Lateral Parietal**	**-0.33**	**0.001**	**-**
rsREL	**Cingulate Gyrus**	**0.51**	**<0.001**	**+**
rsREL	**Left Anterior Sup Temp Gyrus**	**0.64**	**<0.001**	**+**
rsREL	**Left Inferior Parietal Lobe**	**-0.35**	**<0.001**	**-**
rsREL	**Left Posterior Sup Temp Gyrus**	**0.50**	**0.001**	**+**
rsREL	**Left Superior Frontal Gyrus**	**-0.25**	**0.001**	**-**
rsREL	**Medial Prefrontal Cortex**	**-0.17**	**0.014**	**-**
rsREL	**Precuneus (PCC)**	**-0.27**	**0.003**	**-**
rsREL	**Right Anterior Sup Temp Gyrus**	**0.66**	**<0.00§**	**+**
rsREL	**Right Inferior Parietal Lobe**	**-0.36**	**0.001**	**-**
rsREL	**Right Posterior Sup Temp Gyrus**	**0.71**	**0.001**	**+**
rsREL	**Right Superior Frontal Gyrus**	**-0.25**	**0.018**	**-**

1 (R)	Primary Somatosensory Cortex	0.37	0.003	+
2 (R)	Primary Somatosensory Cortex	0.39	0.004	+
3 (R)	Primary Somatosensory Cortex	0.37	0.002	+
4 (R)	Primary Motor Cortex	0.42	0.004	+
6 (R)	Premotor Cortex	0.35	0.001	+
7 (L)	Somatosensory Association Cortex	-0.17	0.013	-
7 (R)	Somatosensory Association Cortex	-0.14	0.014	-
8 (L)	Dorsal Frontal Cortex	-0.23	0.012	-
10 (L)	*Anterior Prefrontal Cortex*	*-0.17*	*0.020*	-
11 (R)	Orbitofrontal Cortex	-0.21	0.026	-
13 (L)	*Insular Cortex*	*0.91*	*<0.001*	+
21 (L)	Middle Temporal Gyrus	-0.13	0.020	-
22 (L)	*Superior Temporal Gyrus*	*0.54*	*<0.001*	+
22 (R)	*Superior Temporal Gyrus*	*0.70*	*<0.001*	+
24 (L)	Ventral Anterior Cingulate Cortex	0.23	0.004	+
28 (L)	Posterior Entorhinal Cortex	0.17	0.037	+
28 (R)	Posterior Entorhinal Cortex	0.21	0.018	+
31 (L)	Dorsal Posterior Cingulate Cortex	-0.23	0.014	-
34 (L)	Anterior Entorhinal Cortex	0.14	0.037	+
34 (R)	Anterior Entorhinal Cortex	0.27	0.012	+
35 (R)	Perirhinal cortex	0.16	0.026	+
37 (R)	Fusiform gyrus	0.19	0.013	+
38 (R)	Temporopolar Area	0.21	0.006	+
39 (L)	Angular gyrus	-0.32	0.002	-
39 (R)	Angular gyrus	-0.29	0.005	-
40 (L)	*Supramarginal Gyrus*	*0.22*	*0.012*	+
40 (R)	*Supramarginal Gyrus*	*0.32*	*0.003*	+
41 (L)	Primary Auditory Cortex	0.54	0.001	+
41 (R)	Primary Auditory Cortex	0.63	<0.001	+
42 (L)	Primary Auditory Cortex	0.51	0.001	+
42 (R)	Primary Auditory Cortex	0.55	0.002	+
43 (L)	Subcentral Area	0.46	0.004	+
43 (R)	Subcentral Area	0.60	<0.001	+
44 (L)	*IFC pars opercularis*	*0.30*	*0.01*	+
44 (R)	*IFC pars opercularis*	*0.58*	*<0.001*	+

As shown in figure 6.2B and table 6.2.4, right BA13 (BA13R) was positively correlated with the cingulate gyrus and the left/right anterior/posterior superior temporal gyri (rsRELs). BA13R was also positively correlated with the left insular cortex (BA13; SDN region), ventral anterior cingulate cortex (BA24); and right primary somatosensory (BA1, BA2, BA3), primary motor (BA4) premotor (BA6), perirhinal (BA35) cortices, fusiform gyrus (BA37) and temporopolar area (BA38). In the left/right hemispheres BA13R was positively correlated with the superior temporal gyri (BA22; SDN region), posterior/anterior entorhinal cortices (BA28, BA34),

supramarginal gyri (BA40; SDN region), primary auditory cortices (BA41, BA42), subcentral areas (BA43) and IFC pars operculari (BA44; SDN region). BA13R was negatively correlated with the LLP, PCC, RLP (DMN regions), left/right inferior parietal lobe, left/right superior frontal gyri, MPFC and the precuneus (PCC; rsREL). BA13R was also negatively correlated with the left dorsal frontal (BA8), anterior prefrontal (BA10; SDN region) and dorsal posterior cingulate (BA31) cortices, right orbitofrontal cortex and the left/right somatosensory association cortices (BA7) and angular gyri (BA39).

6.3.2.2.2. Overall summary of SDN region BA13 (closest match to anterior insula)

These results show that the left/right BA13 seeds are positively correlated with each other and produce an almost symmetrical pattern of correlated activity. This symmetry is apparent in terms of their relationship to other putative regions of the SDN and also in relation to their association with DMN regions, with each ROI correlated to the exact same number of DMN regions and showing the same directional relationship with each DMN region. This region of the SDN is also coupled with activations in somatosensory and auditory areas in the left/right hemispheres, along with GDN regions (i.e. BA40; a representative of the GDN's intraparietal sulcus). These results could suggest that this portion of the SDN (left/right BA13) interacts with other task-related brain regions in order to maintain optimal performance in the detection of unpredictable events. This may also explain why this region is associated with down-regulation of the DMN, in that, down-regulation of a network that is typically implicated in internal thought processes, would prevent interference with vigilance functions of the SDN.

BA22: Left superior temporal gyrus (SDN match)

Table 6.2.5. Left superior temporal gyrus (BA22L) connectivity to all cerebral regions in 840s of active auditory attention data and their significance.

Brodmann area	Brain region	*B*	*p*	Correlation
DMN region	**Left Lateral Parietal**	**-0.20**	**0.002**	**-**
DMN region	**Posterior Cingulate Cortex**	**-0.16**	**0.005**	**-**
DMN region	**Right Lateral Parietal**	**-0.20**	**0.006**	**-**
rsREL	**Cingulate Gyrus**	**0.44**	**<0.001**	**+**
rsREL	**Left Anterior Sup Temp Gyrus**	**0.67**	**<0.001**	**+**
rsREL	**Left Inferior Parietal Lobe**	**-0.22**	**0.002**	**-**
rsREL	**Left Posterior Sup Temp Gyrus**	**0.63**	**<0.001**	**+**
rsREL	**Precuneus (PCC)**	**-0.20**	**0.001**	**-**
rsREL	**Right Anterior Sup Temp Gyrus**	**0.62**	**<0.001**	**+**
rsREL	**Right Inferior Parietal Lobe**	**-0.15**	**0.013**	**-**
rsREL	**Right Posterior Sup Temp Gyrus**	**0.50**	**<0.001**	**+**
1 (R)	Primary Somatosensory Cortex	0.20	0.015	+
2 (L)	Primary Somatosensory Cortex	0.18	0.031	+
2 (R)	Primary Somatosensory Cortex	0.19	0.016	+
3 (L)	Primary Somatosensory Cortex	0.20	0.007	+
6 (L)	Premotor Cortex	0.35	0.001	+
6 (R)	Premotor Cortex	0.38	0.001	+
13 (L)	*Insular Cortex*	*0.61*	*<0.001*	+
13 (R)	*Insular Cortex*	*0.54*	*<0.001*	+
21 (L)	Middle Temporal Gyrus	0.35	<0.001	+
21 (R)	Middle Temporal Gyrus	0.30	0.003	+
22 (R)	*Superior Temporal Gyrus*	*0.85*	*<0.001*	+
24 (L)	Ventral Anterior Cingulate Cortex	0.16	0.039	+
28 (R)	Posterior Entorhinal Cortex	0.09	0.044	+
31 (L)	Dorsal Posterior Cingulate Cortex	-0.21	0.003	-
31 (R)	Dorsal Posterior Cingulate Cortex	-0.16	0.016	-
33 (R)	Anterior Cingulate Cortex	-0.15	0.046	-
34 (R)	Anterior Entorhinal Cortex	0.19	0.010	+
37 (L)	Fusiform gyrus	0.21	0.045	+
38 (L)	Temporopolar Area	0.22	0.024	+
38 (R)	Temporopolar Area	0.14	0.040	+
40 (L)	*Supramarginal Gyrus*	*0.37*	*<0.001*	+
40 (R)	*Supramarginal Gyrus*	*0.33*	*0.003*	+
41 (L)	Primary Auditory Cortex	0.77	<0.001	+
41 (R)	Primary Auditory Cortex	0.58	<0.001	+
42 (L)	Primary Auditory Cortex	0.85	<0.001	+
42 (R)	Primary Auditory Cortex	0.60	0.001	+
43 (L)	Subcentral Area	0.41	0.001	+
43 (R)	Subcentral Area	0.35	0.011	+
44 (L)	*IFC pars opercularis*	*0.32*	*0.007*	+
44 (R)	*IFC pars opercularis*	*0.34*	*0.011*	+
45 (L)	*IFC pars triangularis*	*0.12*	*0.046*	+
45 (R)	*IFC pars triangularis*	*0.24*	*0.021*	+
46 (L)	Dorsolateral Prefrontal Cortex	0.18	0.011	+
46 (R)	Dorsolateral Prefrontal Cortex	0.17	0.037	+
47 (L)	*Inferior Prefrontal Gyrus*	*0.22*	*0.007*	+
47 (R)	*Inferior Prefrontal Gyrus*	*0.30*	*0.008*	+

Left BA22 (BA22L; see figure 6.2C and table 6.2.5) was positively correlated with the cingulate gyrus and the left/right anterior/posterior superior temporal gyri (rsRELs). BA22L was also positively correlated with the left primary somatosensory (BA3), ventral anterior cingulate (BA24) cortices and fusiform gyrus (BA37). BA22L was also positively correlated with the right primary somatosensory cortex (BA1), superior temporal gyrus (BA22; SDN region), and posterior/anterior entorhinal cortices (BA28, BA34). Positive correlations were also found between BA22L and the left/right primary somatosensory (BA2), premotor (BA6) and insular (BA13; SDN region) cortices, middle temporal gyri (BA21), temporopolar areas (BA38), supramarginal gyri (BA40; SDN region), primary auditory cortices (BA41, BA42), subcentral areas (BA43), IFC pars operculari/triangulari (BA44, BA45; SDN regions), dorsolateral prefrontal (BA46) and inferior prefrontal (BA47; SDN region) cortices. Negative correlations were found between BA22L and the LLP, PCC, RLP (DMN regions), left/right inferior parietal lobe and the precuneus (PCC; rsRELs). BA22L was also negatively correlated with the left/right dorsal posterior cingulate (BA31) and right anterior cingulate (BA33) cortices.

Table 6.2.6. Right superior temporal gyrus (BA22R) connectivity to all cerebral regions in 840s of active auditory attention data and their significance.

Brodmann area	Brain region	*B*	*p*	Correlation
DMN region	**Left Lateral Parietal**	**-0.21**	**0.003**	**-**
DMN region	**Right Lateral Parietal**	**-0.24**	**0.011**	**-**
rsREL	**Cingulate Gyrus**	**0.45**	**0.001**	**+**
rsREL	**Left Anterior Sup Temp Gyrus**	**0.52**	**<0.001**	**+**
rsREL	**Left Inferior Parietal Lobe**	**-0.22**	**0.006**	**-**
rsREL	**Left Posterior Sup Temp Gyrus**	**0.52**	**0.004**	**+**
rsREL	**Left Superior Frontal Gyrus**	**-0.19**	**0.023**	**-**
rsREL	**Precuneus (PCC)**	**-0.15**	**0.034**	**-**
rsREL	**Right Anterior Sup Temp Gyrus**	**1.02**	**<0.001**	**+**
rsREL	**Right Inferior Parietal Lobe**	**-0.21**	**0.017**	**-**
rsREL	**Right Posterior Sup Temp Gyrus**	**0.61**	**<0.001**	**+**
rsREL	**Right Superior Frontal Gyrus**	**-0.20**	**0.030**	**-**
1 (R)	Primary Somatosensory Cortex	0.23	0.011	+
2 (R)	Primary Somatosensory Cortex	0.22	0.037	+

3 (L)	Primary Somatosensory Cortex	0.22	0.032	+
6 (L)	Premotor Cortex	0.21	0.025	+
6 (R)	Premotor Cortex	0.31	0.002	+
13 (L)	*Insular Cortex*	*0.49*	*0.001*	+
13 (R)	*Insular Cortex*	*0.70*	*<0.001*	+
21 (L)	Middle Temporal Gyrus	0.18	0.030	+
21 (R)	Middle Temporal Gyrus	0.45	0.003	+
22 (L)	*Superior Temporal Gyrus*	*0.85*	*<0.001*	+
28 (R)	Posterior Entorhinal Cortex	0.21	0.018	+
30 (R)	Cingulate Cortex	0.16	0.037	+
31 (L)	Dorsal Posterior Cingulate Cortex	-0.15	0.037	-
34 (L)	Anterior Entorhinal Cortex	0.17	0.037	+
34 (R)	Anterior Entorhinal Cortex	0.34	0.005	+
37 (R)	Fusiform gyrus	0.30	0.011	+
38 (L)	Temporopolar Area	0.19	0.019	+
38 (R)	Temporopolar Area	0.29	0.003	+
39 (L)	Angular gyrus	-0.18	0.019	-
40 (L)	*Supramarginal Gyrus*	*0.28*	*0.011*	+
40 (R)	*Supramarginal Gyrus*	*0.31*	*0.003*	+
41 (L)	Primary Auditory Cortex	0.65	<0.001	+
41 (R)	Primary Auditory Cortex	0.69	<0.001	+
42 (L)	Primary Auditory Cortex	0.69	0.001	+
42 (R)	Primary Auditory Cortex	0.85	<0.001	+
43 (L)	Subcentral Area	0.39	0.009	+
43 (R)	Subcentral Area	0.41	0.011	+
44 (R)	*IFC pars opercularis*	*0.34*	*0.023*	+
46 (L)	Dorsolateral Prefrontal Cortex	0.17	0.037	+
47 (R)	*Inferior Prefrontal Gyrus*	*0.32*	*0.037*	+

Right BA22 (BA22R; see figure 6.2C and table 6.2.6) was positively correlated with the cingulate gyrus and the left/right anterior/posterior superior temporal gyri (rsRELs). BA22R was also positively correlated with the left primary somatosensory cortex (BA3), superior temporal gyrus (BA22; SDN region) and dorsolateral prefrontal cortex (BA46). Positive correlations were also found between BA22R and the right primary somatosensory (BA1/BA2) and cingulate (BA30) cortices, fusiform gyrus (BA37), IFC pars opercularis (BA44; SDN region) and the inferior prefrontal cortex (BA37; SDN region). In the left/right hemispheres this seed was positively correlated with the premotor (BA6) and insular (BA13; SDN region) cortices, middle temporal gyrus (BA21), anterior entorhinal cortices (BA34), temporopolar areas (BA38), supramarginal gyri (BA40; SDN region), primary auditory cortices (BA41, BA42) and

subcentral areas (BA43). Negative correlations were found between BA22R and the LLP, RLP (DMN regions), left/right inferior parietal lobe, left/right superior frontal gyri, precuneus (PCC; rsRELs), the left dorsal posterior cingulate cortex (BA31) and the left angular gyrus (BA39).

6.3.2.2.3. Overall summary of SDN region BA22 (SDN match)

The patterns of connectivity associated with BA22 mimics that of left/right BA13 (representative of the anterior insula of the SDN). It is therefore assumed that these portions of the SDN adopt similar roles during task completion and in terms of their down-regulation of the DMN.

BA40: Supramarginal gyrus (SDN match)

Table 6.2.7. Left supramarginal gyrus (BA40L) connectivity to all cerebral regions in 840s of active auditory attention data and their significance.

Brodmann area	Brain region	*B*	*p*	Correlation
DMN region	**Medial Prefrontal Cortex**	**-0.42**	**0.001**	**-**
DMN region	**Posterior Cingulate Cortex**	**-0.35**	**0.002**	**-**
DMN region	**Right Lateral Parietal**	**-0.24**	**0.014**	**-**
rsREL	**Cingulate Gyrus**	**0.36**	**0.005**	**+**
rsREL	**Left Anterior Sup Temp Gyrus**	**0.26**	**0.003**	**+**
rsREL	**Left Posterior Sup Temp Gyrus**	**0.50**	**<0.001**	**+**
rsREL	**Left Superior Frontal Gyrus**	**-0.16**	**0.048**	**-**
rsREL	**Medial Prefrontal Cortex**	**-0.32**	**0.003**	**-**
rsREL	**Precuneus (PCC)**	**-0.47**	**0.001**	**-**
rsREL	**Right Anterior Sup Temp Gyrus**	**0.33**	**0.003**	**+**
rsREL	**Right Posterior Sup Temp Gyrus**	**0.40**	**0.003**	**+**
rsREL	**Right Superior Frontal Gyrus**	**-0.20**	**0.047**	**-**
1 (L)	Primary Somatosensory Cortex	0.49	0.002	+
1 (R)	Primary Somatosensory Cortex	0.30	0.011	+
2 (L)	Primary Somatosensory Cortex	0.63	0.001	+
2 (R)	Primary Somatosensory Cortex	0.50	0.002	+
3 (L)	Primary Somatosensory Cortex	0.45	0.001	+
3 (R)	Primary Somatosensory Cortex	0.23	0.047	+
4 (L)	Primary Motor Cortex	0.36	0.002	+
5 (L)	Somatosensory Association Cortex	0.30	0.039	+
5 (R)	Somatosensory Association Cortex	0.23	0.047	+
6 (L)	Premotor Cortex	0.63	<0.001	+
6 (R)	Premotor Cortex	0.41	0.002	+

7 (L)	Somatosensory Association Cortex	0.24	0.017	+
9 (L)	Dorsolateral Prefrontal Cortex	0.16	0.047	+
13 (L)	*Insular Cortex*	*0.31*	*0.002*	+
13 (R)	*Insular Cortex*	*0.22*	*0.011*	+
18 (L)	Secondary Visual Cortex	-0.13	0.035	-
19 (R)	Associative Visual Cortex	-0.21	0.005	-
22 (L)	*Superior Temporal Gyrus*	*0.37*	*<0.001*	+
22 (R)	*Superior Temporal Gyrus*	*0.28*	*0.007*	+
23 (R)	Ventral Posterior Cingulate Cortex	-0.30	0.004	-
29 (L)	Retrosplenial Cingulate Cortex	-0.22	0.010	-
29 (R)	Retrosplenial Cingulate Cortex	-0.25	0.001	-
30 (L)	Cingulate Cortex	-0.29	<0.001	-
30 (R)	Cingulate Cortex	-0.23	0.002	-
31 (L)	Dorsal Posterior Cingulate Cortex	-0.37	0.001	-
31 (R)	Dorsal Posterior Cingulate Cortex	-0.44	<0.001	-
37 (L)	Fusiform gyrus	0.27	0.003	+
39 (R)	Angular gyrus	-0.30	0.005	-
40 (R)	*Supramarginal Gyrus*	*0.69*	*<0.001*	+
41 (L)	Primary Auditory Cortex	0.28	0.001	+
41 (R)	Primary Auditory Cortex	0.21	0.002	+
42 (L)	Primary Auditory Cortex	0.36	0.001	+
42 (R)	Primary Auditory Cortex	0.29	0.002	+
43 (L)	Subcentral Area	0.21	0.021	+
44 (L)	*IFC pars opercularis*	*0.36*	*0.002*	+
44 (R)	*IFC pars opercularis*	*0.37*	*0.003*	+
46 (L)	Dorsolateral Prefrontal Cortex	0.34	0.005	+
46 (R)	Dorsolateral Prefrontal Cortex	0.20	0.049	+

As shown in figure 6.2D and table 6.2.7, positive correlations were found between left BA40 (BA40L) and the cingulate gyrus and left/right anterior/posterior superior temporal gyri (rsRELs). This seed was also positively correlated with the left primary motor (BA4), somatosensory association (BA7) and dorsolateral prefrontal (BA9) cortices, as well as the left fusiform gyrus (BA37) and subcentral area (BA43). In the right hemisphere BA40L was positively correlated with supramarginal gyrus (BA40; SDN region), and in both hemispheres BA40L was positively correlated with the primary somatosensory (BA1, BA2, BA3), somatosensory association (BA5), premotor (BA6) and insular (BA13; SDN regions) cortices. BA40L was also positively correlated with the left and right Superior Temporal Gyrus (BA22; SDN regions), primary auditory cortices (BA41, BA42) and the IFC pars operculari (BA44; SDN regions). Negative correlations were apparent between BA40L and the MPFC, PCC, RLP

(DMN regions), left/Right Superior Frontal Gyrus, medial prefrontal cortex and the precuneus (PCC: rsRELs). BA40L was also negatively correlated with the secondary visual cortex (BA18) in the left hemisphere, and the associative visual cortex (BA19) ventral posterior cingulate cortex (BA23) and angular gyrus (BA39) in the right hemisphere. In both the left and right hemispheres negative correlations were apparent between BA40L and the retrosplenial cingulate (BA29), cingulate (BA30) and dorsal posterior cingulate (BA31) cortices.

Table 6.2.8. Right supramarginal gyrus (BA40R) connectivity to all cerebral regions in 840s of active auditory attention data and their significance.

Brodmann area	Brain region	*B*	*p*	Correlation
DMN region	**Left Lateral Parietal**	**-0.22**	**0.021**	**-**
DMN region	**Medial Prefrontal Cortex**	**-0.45**	**0.001**	**-**
DMN region	**Posterior Cingulate Cortex**	**-0.31**	**0.011**	**-**
rsREL	**Cingulate Gyrus**	**0.34**	**0.001**	**+**
rsREL	**Left Anterior Sup Temp Gyrus**	**0.27**	**0.006**	**+**
rsREL	**Left Inferior Parietal Lobe**	**-0.18**	**0.033**	**-**
rsREL	**Left Posterior Sup Temp Gyrus**	**0.37**	**0.001**	**+**
rsREL	**Left Superior Frontal Gyrus**	**-0.21**	**0.001**	**-**
rsREL	**Medial Prefrontal Cortex**	**-0.42**	**0.001**	**-**
rsREL	**Precuneus (PCC)**	**-0.49**	**0.001**	**-**
rsREL	**Right Anterior Sup Temp Gyrus**	**0.36**	**0.004**	**+**
rsREL	**Right Posterior Sup Temp Gyrus**	**0.53**	**0.001**	**+**
1 (R)	Primary Somatosensory Cortex	0.23	0.019	+
2 (R)	Primary Somatosensory Cortex	0.46	0.001	+
5 (R)	Somatosensory Association Cortex	0.20	0.036	+
6 (L)	Premotor Cortex	0.26	0.004	+
6 (R)	Premotor Cortex	0.56	<0.001	+
7 (R)	Somatosensory Association Cortex	0.31	0.006	+
8 (R)	Dorsal Frontal Cortex	0.24	0.036	+
9 (R)	Dorsolateral Prefrontal Cortex	0.41	<0.001	+
10 (R)	*Anterior Prefrontal Cortex*	*0.23*	*0.003*	+
13 (L)	*Insular Cortex*	*0.27*	*0.012*	+
13 (R)	*Insular Cortex*	*0.32*	*0.004*	+
18 (L)	Secondary Visual Cortex	-0.15	0.020	-
19 (L)	Associative Visual Cortex	-0.19	0.010	-
19 (R)	Associative Visual Cortex	-0.12	0.004	-
22 (L)	*Superior Temporal Gyrus*	*0.33*	*0.003*	+
22 (R)	*Superior Temporal Gyrus*	*0.31*	*0.001*	+
23 (L)	Ventral Posterior Cingulate Cortex	-0.23	0.049	-
23 (R)	Ventral Posterior Cingulate Cortex	-0.21	0.016	-
29 (L)	Retrosplenial Cingulate Cortex	-0.25	0.001	-
29 (R)	Retrosplenial Cingulate Cortex	-0.20	0.004	-
30 (L)	Cingulate Cortex	-0.33	0.002	-

30 (R)	Cingulate Cortex	-0.19	0.040	-
31 (L)	Dorsal Posterior Cingulate Cortex	-0.40	0.004	-
31 (R)	Dorsal Posterior Cingulate Cortex	-0.30	0.004	-
35 (L)	Perirhinal cortex	-0.17	0.001	-
37 (L)	Fusiform gyrus	0.17	0.039	+
37 (R)	Fusiform gyrus	0.26	0.004	+
40 (L)	*Supramarginal Gyrus*	*0.69*	*<0.001*	+
41 (L)	Primary Auditory Cortex	0.20	0.025	+
41 (R)	Primary Auditory Cortex	0.23	0.005	+
42 (L)	Primary Auditory Cortex	0.25	0.009	+
42 (R)	Primary Auditory Cortex	0.24	0.026	+
44 (L)	*IFC pars opercularis*	*0.40*	*0.001*	+
44 (R)	*IFC pars opercularis*	*0.57*	*0.000*	+
45 (R)	*IFC pars triangularis*	*0.29*	*0.003*	+
46 (L)	Dorsolateral Prefrontal Cortex	0.34	0.005	+
46 (R)	Dorsolateral Prefrontal Cortex	0.43	0.002	+
47 (R)	*Inferior Prefrontal Gyrus*	*0.30*	*0.004*	+

Right BA40 (BA40R; see figure 6.2D and table 6.2.8) was positively correlated with the cingulate gyrus and left/right anterior/posterior superior temporal gyri (rsRELs). In the left hemisphere BA40R was positively correlated with supramarginal gyrus (BA40; SDN region). In the right hemisphere BA40R was positively correlated with the primary somatosensory (BA1, BA2), somatosensory association (BA5, BA7), dorsal frontal (BA8), dorsolateral prefrontal (BA9) and anterior prefrontal (BA10; SDN region) cortices, as well as the IFC pars triangularis (BA45; SDN region) and inferior prefrontal gyrus (BA47; SDN region). In both hemispheres BA40R was positively correlated with the premotor (BA6), insular (BA13; SDN regions), primary auditory (BA41, BA42) and dorsolateral prefrontal (BA46) cortices, along with the superior temporal gyri (BA22; SDN region) and IFC pars operculari (BA44; SDN region). Negative correlations were apparent between BA40R and the LLP, MPFC, PCC (DMN regions), left inferior parietal lobe, Left Superior Frontal Gyrus, medial prefrontal cortex and the precuneus (PCC; rsRELs). Negative correlations were also found between this seed and the left Secondary Visual Cortex (BA18) and left perirhinal (BA35) cortices, and the left/right

associative visual (BA19), ventral/dorsal posterior cingulate (BA23, BA31), retrosplenial (BA29) and cingulate (BA30) cortices.

6.3.2.2.4. Overall summary of SDN region BA40 (SDN match)

As previously stated, BA40 was included as a putative region of the GDN as a ROI closely matching the intraparietal sulcus. In terms of this region's involvement in the SDN, overall, BA40L was strongly positively correlated to its homologous region in the right hemisphere and to a number of other SDN regions, including: left/right BA13 (representative of the SDN's anterior insula); BA22 (match for the SDN's superior temporal gyri); and BA44 (representative of the SDN's frontal operculum). BA40R was strongly positively correlated to: right BA10 (representing the SDN's ventral frontal cortex); BA45 (representing the SDN's frontal operculum); BA47 (closes match to the SDN's inferior prefrontal gyrus); along with the left/right BA13, BA22 and BA44. Overall these results support the hypothesis that there would be strong functional connectivity in the SDN based on the task employed. Interestingly, left/right BA40 also showed negative correlations to several DMN regions (as well as rsREL regions in close proximity), BA40L was negatively correlated to MPFC, PCC, RLP; and BA40R was negatively correlated to MPFC, PCC and RLP. These results support the hypothesis that activity in the SDN would be coupled with down-regulation of the DMN.

BA44: IFC pars opercularis (closest match to frontal operculum)

Table 6.2.9. Left IFC pars opercularis (BA44L) connectivity to all cerebral regions in 840s of active auditory attention data and their significance.

Brodmann area	Brain region	*B*	*p*	Correlation

DMN region	**Left Lateral Parietal**	**-0.19**	**0.007**	**-**
DMN region	**Posterior Cingulate Cortex**	**-0.23**	**0.014**	**-**
rsREL	**Left Anterior Sup Temp Gyrus**	**0.35**	**0.014**	**+**
rsREL	**Left Inferior Parietal Lobe**	**-0.17**	**0.025**	**-**
rsREL	**Medial Prefrontal Cortex**	**-0.25**	**0.017**	**-**
rsREL	**Precuneus (PCC)**	**-0.35**	**0.003**	**-**
5 (L)	Somatosensory Association Cortex	-0.20	0.020	-
6 (L)	Premotor Cortex	0.34	0.025	+
6 (R)	Premotor Cortex	0.22	0.014	+
7 (L)	Somatosensory Association Cortex	-0.11	0.048	-
9 (L)	Dorsolateral Prefrontal Cortex	0.26	0.040	+
9 (R)	Dorsolateral Prefrontal Cortex	0.22	0.020	+
13 (L)	Insular Cortex	0.46	0.011	+
13 (R)	Insular Cortex	0.30	0.016	+
22 (L)	Superior Temporal Gyrus	0.32	0.012	+
23 (L)	Ventral Posterior Cingulate Cortex	-0.19	0.009	-
23 (R)	Ventral Posterior Cingulate Cortex	-0.24	0.008	-
29 (L)	Retrosplenial Cingulate Cortex	-0.19	0.017	-
29 (R)	Retrosplenial Cingulate Cortex	-0.23	0.005	-
30 (L)	Cingulate Cortex	-0.17	0.014	-
31 (L)	Dorsal Posterior Cingulate Cortex	-0.33	<0.001	-
31 (R)	Dorsal Posterior Cingulate Cortex	-0.36	0.001	-
39 (L)	Angular gyrus	-0.12	0.032	-
40 (L)	Supramarginal Gyrus	0.36	0.004	+
40 (R)	Supramarginal Gyrus	0.40	0.002	+
41 (R)	Primary Auditory Cortex	0.18	0.020	+
44 (R)	IFC pars opercularis	0.46	<0.001	+
45 (L)	IFC pars triangularis	0.78	0.001	+
45 (R)	IFC pars triangularis	0.49	<0.001	+
46 (L)	Dorsolateral Prefrontal Cortex	0.41	0.001	+
46 (R)	Dorsolateral Prefrontal Cortex	0.30	0.007	+
47 (L)	Inferior Prefrontal Gyrus	0.41	0.020	+
47 (R)	Inferior Prefrontal Gyrus	0.30	0.011	+

Figure 6.2E and table 6.2.9 shows that this left BA44 (BA44L) was positively correlated with the left anterior and superior temporal gyri (rsREL, BA22; SDN region). BA44L was also positively correlated with the right primary auditory cortex (BA41) and right IFC pars opercularis (BA 44; SDN region). In the left and right hemispheres this seed was positively correlated with the premotor (BA6), dorsolateral prefrontal (BA9), insular (BA13; SDN regions) cortices, supramarginal gyri (BA40; SDN regions), IFC triangularis (BA45; SDN regions), dorsolateral prefrontal (BA46) and inferior prefrontal (BA47; SDN regions) cortices. Negative correlations were found between BA44L and LLP, PCC (DMN regions), left inferior parietal, medial

prefrontal cortex and precuneus (PCC; rsRELs). Negative correlations were also found with the left somatosensory association cortices (BA5, BA7), left cingulate cortex (BA30) angular gyrus (BA39) and the left/right ventral/Dorsal Posterior Cingulate Cortex (BA23, BA 31) and retrosplenial cingulate cortices (BA29).

Table 6.2.10. Right IFC pars opercularis (BA44R) connectivity to all cerebral regions in 840s of active auditory attention data and their significance.

Brodmann area	Brain region	*B*	*p*	Correlation
DMN region	**Left Lateral Parietal**	**-0.35**	**0.002**	**-**
DMN region	**Medial Prefrontal Cortex**	**-0.35**	**0.009**	**-**
DMN region	**Posterior Cingulate Cortex**	**-0.34**	**0.003**	**-**
DMN region	**Right Lateral Parietal**	**-0.30**	**0.006**	**-**
rsREL	**Cingulate Gyrus**	**0.39**	**0.007**	**+**
rsREL	**Left Anterior Sup Temp Gyrus**	**0.40**	**0.007**	**+**
rsREL	**Left Inferior Parietal Lobe**	**-0.34**	**0.002**	**-**
rsREL	**Left Posterior Sup Temp Gyrus**	**0.38**	**0.007**	**+**
rsREL	**Left Superior Frontal Gyrus**	**-0.23**	**0.004**	**-**
rsREL	**Medial Prefrontal Cortex**	**-0.33**	**0.007**	**-**
rsREL	**Precuneus (PCC)**	**-0.46**	**<0.001**	**-**
rsREL	**Right Anterior Sup Temp Gyrus**	**0.55**	**0.007**	**+**
rsREL	**Right Inferior Parietal Lobe**	**-0.22**	**0.024**	**-**
rsREL	**Right Posterior Sup Temp Gyrus**	**0.54**	**0.006**	**+**
2 (R)	Primary Somatosensory Cortex	0.27	0.002	+
6 (L)	Premotor Cortex	0.18	0.024	+
6 (R)	Premotor Cortex	0.38	0.001	+
9 (R)	Dorsolateral Prefrontal Cortex	0.27	0.009	+
13 (L)	*Insular Cortex*	*0.41*	*0.004*	+
13 (R)	*Insular Cortex*	*0.58*	*<0.001*	+
21 (L)	Middle Temporal Gyrus	-0.15	0.009	-
22 (L)	*Superior Temporal Gyrus*	*0.34*	*0.012*	+
22 (R)	*Superior Temporal Gyrus*	*0.34*	*0.020*	+
23 (L)	Ventral Posterior Cingulate Cortex	-0.27	0.002	-
23 (R)	Ventral Posterior Cingulate Cortex	-0.25	0.002	-
25 (L)	Subgenual cortex	-0.09	0.012	-
31 (L)	Dorsal Posterior Cingulate Cortex	-0.41	0.001	-
31 (R)	Dorsal Posterior Cingulate Cortex	-0.38	0.001	-
35 (L)	Perirhinal cortex	-0.17	0.023	-
37 (L)	Fusiform gyrus	0.18	0.013	+
37 (R)	Fusiform gyrus	0.27	0.012	+
39 (L)	Angular gyrus	-0.36	0.007	-
39 (R)	Angular gyrus	-0.26	0.002	-
40 (L)	*Supramarginal Gyrus*	*0.37*	*0.004*	+
40 (R)	*Supramarginal Gyrus*	*0.57*	*<0.001*	+
42 (L)	Primary Auditory Cortex	0.27	0.019	+
42 (R)	Primary Auditory Cortex	0.28	0.042	+
43 (R)	Subcentral Area	0.31	0.047	+

44 (L)	*IFC pars opercularis*	*0.46*	*<0.001*	+
45 (L)	*IFC pars triangularis*	*0.16*	*0.012*	+
45 (R)	*IFC pars triangularis*	*0.53*	*0.007*	+
46 (L)	Dorsolateral Prefrontal Cortex	0.22	0.023	+
46 (R)	Dorsolateral Prefrontal Cortex	0.40	0.007	+
47 (R)	*Inferior Prefrontal Gyrus*	*0.38*	*0.017*	+

Right BA44 (BA44R; see figure 6.2E and table 6.2.10) was positively correlated with the cingulate gyrus and the left/right anterior/posterior cingulate cortices (rsRELs). Positive correlations were also found between BA44R and the left IFC pars opercularis (BA44; SDN region), and the right dorsolateral prefrontal (BA9), primary somatosensory (BA2) cortices, subcentral area (BA43; SDN region) and the inferior prefrontal cortex (BA47; SDN region). In the left and right hemispheres, BA44R was positively correlated with the premotor (BA6) and insular (BA13; SDN regions) cortices, Superior Temporal Gyrus (BA22; SDN regions), fusiform gyri (BA37), supramarginal gyri (BA40; SDN regions), primary auditory cortices (BA42), IFC pars triangularis (BA45; SDN regions), and dorsolateral prefrontal cortices (BA46). Negative correlations were found between this seed and LLP, MPFC, PCC, RLP)DMN regions), left/right inferior parietal lobe, left superior frontal gyrus, medial prefrontal cortex and the precuneus (PCC; rsRELs). BA44R was also negatively correlated with the left middle temporal gyrus (BA21), subgenual (BA25) and perirhinal (BA35) cortices, and with the left/right ventral/Dorsal Posterior Cingulate Cortex (BA23, BA31) and the angular gyri (BA39; SDN region).

6.3.2.2.5. Overall summary of SDN region BA44 (closest match to frontal operculum)

Overall, the pattern of correlated activity associated with BA44 suggests that these seeds are reliable representatives of the SDN's frontal operculum. Left/right BA44 showed widespread positive correlations to a number of other putative SDN regions as shown in figure 6.2E and tables 6.2.9-6.2.10, suggestive of strong functional connectivity in this network. Negative

correlations between left/right BA44 and DMN/rsREL regions including LLP, MPFC, PCC and RLP, also supports the hypothesis that activity of the SDN is associated with down-regulation of the DMN.

BA45: IFC pars triangularis (closest match to frontal operculum)

Table 6.2.11. Left IFC pars triangularis (BA45L) connectivity to all cerebral regions in 840s of active auditory attention data and their significance.

Brodmann area	Brain region	*B*	*p*	Correlation
1 (L)	Primary Somatosensory Cortex	-0.23	0.014	-
2 (L)	Primary Somatosensory Cortex	-0.24	0.004	-
2 (R)	Primary Somatosensory Cortex	-0.13	0.036	-
3 (L)	Primary Somatosensory Cortex	-0.24	0.025	-
4 (L)	Primary Motor Cortex	-0.27	0.009	-
5 (L)	Somatosensory Association Cortex	-0.36	0.001	-
5 (R)	Somatosensory Association Cortex	-0.34	0.004	-
8 (L)	Dorsal Frontal Cortex	0.30	0.025	+
9 (L)	Dorsolateral Prefrontal Cortex	0.37	0.003	+
21 (L)	Middle Temporal Gyrus	0.16	0.029	+
23 (R)	Ventral Posterior Cingulate Cortex	-0.15	0.009	-
29 (R)	Retrosplenial Cingulate Cortex	-0.17	0.027	-
31 (L)	Dorsal Posterior Cingulate Cortex	-0.12	0.017	-
31 (R)	Dorsal Posterior Cingulate Cortex	-0.24	0.003	-
44 (L)	*IFC pars opercularis*	*0.78*	*0.001*	+
44 (R)	*IFC pars opercularis*	*0.16*	*0.025*	+
45 (R)	*IFC pars triangularis*	*0.57*	*0.001*	+
46 (L)	Dorsolateral Prefrontal Cortex	0.58	0.004	+
46 (R)	Dorsolateral Prefrontal Cortex	0.33	0.005	+
47 (L)	*Inferior Prefrontal Gyrus*	*0.58*	*0.003*	+
47 (R)	*Inferior Prefrontal Gyrus*	*0.27*	*0.009*	+

Left BA45 (BA45L; see figure 6.2F and table 6.2.11) was positively correlated with the dorsal frontal (BA8) and dorsolateral prefrontal (BA9) cortices, left Middle Temporal Gyrus (BA21) and the right IFC pars triangularis (BA45; SDN region). This seed was also positively correlated with the left/right IFC pars operculari (BA44; SDN regions), dorsolateral prefrontal (BA46) and inferior prefrontal (BA47; SDN regions) cortices. Negative correlations were found between

BA45L and the left primary somatosensory (BA1, BA3) and primary motor (BA4) cortices, and the right ventral posterior cingulate (BA23) and retrosplenial cingulate (BA29) cortices. BA45L was also negatively correlated with the left/right primary somatosensory (BA2), somatosensory association (BA5) and dorsal posterior cingulate (BA31) cortices.

Table 6.2.12. Right IFC pars triangularis (BA45R) connectivity to all cerebral regions in 840s of active auditory attention data and their significance.

Brodmann area	Brain region	*B*	*p*	Correlation
DMN region	**Posterior Cingulate Cortex**	**-0.16**	**0.032**	**-**
rsREL	**Precuneus (PCC)**	**-0.18**	**0.036**	**-**
2 (L)	Primary Somatosensory Cortex	-0.16	0.006	-
4 (L)	Primary Motor Cortex	-0.25	0.002	-
4 (R)	Primary Motor Cortex	-0.18	0.010	-
5 (L)	Somatosensory Association Cortex	-0.23	0.006	-
5 (R)	Somatosensory Association Cortex	-0.22	0.029	-
10 (R)	*Anterior Prefrontal Cortex*	*0.20*	*0.023*	+
22 (L)	*Superior Temporal Gyrus*	*0.24*	*0.042*	+
31 (L)	Dorsal Posterior Cingulate Cortex	-0.22	0.010	-
31 (R)	Dorsal Posterior Cingulate Cortex	-0.17	0.029	-
40 (R)	*Supramarginal Gyrus*	*0.29*	*0.006*	+
44 (L)	*IFC pars opercularis*	*0.49*	*<0.001*	+
44 (R)	*IFC pars opercularis*	*0.53*	*0.012*	+
45 (L)	*IFC pars triangularis*	*0.57*	*<0.001*	+
46 (L)	Dorsolateral Prefrontal Cortex	0.25	0.029	+
46 (R)	Dorsolateral Prefrontal Cortex	0.49	0.001	+
47 (L)	*Inferior Prefrontal Gyrus*	*0.39*	*<0.001*	+
47 (R)	*Inferior Prefrontal Gyrus*	*0.64*	*0.001*	+

As shown in figure 6.2F and table 6.2.12, this right BA45 (BA45R) was positively correlated with the left Superior Temporal Gyrus (BA22; SDN region), IFC pars triangularis (BA45; SDN region), and the right anterior prefrontal cortex (BA10; SDN region) and right supramarginal gyrus (BA40; SDN region). BA45R was also positively correlated with the IFC pars operculari (BA44; SDN regions), dorsolateral prefrontal (BA46) and inferior prefrontal (BA47; SDN regions) cortices in the left and right hemispheres. Negative correlations were found between BA45R and the PCC (DMN region) and precuneus (PCC; rsREL), along with the left primary

somatosensory (BA2) and the left/right primary motor (BA4), somatosensory association (BA5) and dorsal posterior cingulate (BA31) cortices.

6.3.2.2.6. Overall summary of SDN region BA45 (closest match to frontal operculum)

These results show that left/right BA45 areas of the SDN were positively correlated with each other and other putative parts of the SDN, including the supramarginal gyrus (BA40) and the IFC pars opercularis (BA44; a representative of the SDN's frontal operculum). This portion of the SDN was also associated with down-regulation of the posterior part of the DMN and surrounding regions only, which suggests this was not a reliable representative of the SDN's frontal operculum and that its neighbouring region BA44 (pars opercularis), summarised in section *6.3.2.2.5,* in fact was.

BA47: Inferior prefrontal gyrus (closest match to inferior frontal gyrus)

Table 6.2.13. Left inferior prefrontal gyrus (BA47L) connectivity to all cerebral regions in 840s of active auditory attention data and their significance.

Brodmann area	Brain region	*B*	*p*	Correlation
rsREL	**Left Anterior Sup Temp Gyrus**	**0.32**	**0.029**	+
2 (L)	Primary Somatosensory Cortex	-0.24	0.007	-
4 (L)	Primary Motor Cortex	-0.28	0.007	-
9 (L)	Dorsolateral Prefrontal Cortex	0.35	0.019	+
10 (L)	*Anterior Prefrontal Cortex*	*0.33*	*0.007*	+
11 (L)	Orbitofrontal Cortex	0.36	0.004	+
11 (R)	Orbitofrontal Cortex	0.22	0.013	+
20 (L)	Inferior Temporal Gyrus	0.27	0.004	+
20 (R)	Inferior Temporal Gyrus	0.20	0.019	+
21 (L)	Middle Temporal Gyrus	0.30	0.006	+
22 (L)	*Superior Temporal Gyrus*	*0.22*	*0.017*	+
32 (L)	Dorsal Anterior Cingulate Cortex	0.15	0.022	+
38 (L)	Temporopolar Area	0.32	0.006	+
44 (L)	*IFC pars opercularis*	*0.41*	*0.029*	+
45 (L)	*IFC pars triangularis*	*0.58*	*0.004*	+
45 (R)	*IFC pars triangularis*	*0.39*	*<0.001*	+
46 (L)	Dorsolateral Prefrontal Cortex	0.25	0.019	+
46 (R)	Dorsolateral Prefrontal Cortex	0.26	0.030	+
47 (R)	*Inferior Prefrontal Gyrus*	*0.50*	*<0.001*	+

Left BA47 (BA47L; see figure 6.2G and table 6.2.13) was positively correlated to the left anterior superior temporal gyrus (rsREL), left dorsolateral prefrontal (BA9) and anterior prefrontal (BA10; SDN region) cortices. BA47 was also positively correlated with the left middle temporal (BA21) and superior temporal (BA22; SDN region) gyri, dorsal anterior cingulate cortex (BA32), temporopolar area (BA38), IFC pars opercularis (BA44; SDN region) and the right inferior prefrontal cortex (BA47; SDN region). Positive correlations were also apparent between this seed and the left/right orbitofrontal cortices (BA11), inferior temporal gyrus (BA20), IFC triangularis (BA45; SDN regions) and dorsolateral prefrontal cortices (BA46) in the left and right hemispheres. Negative correlations were found between BA47L and the left primary somatosensory (BA2) and primary motor (BA4) cortices.

Table 6.2.14. Right inferior prefrontal gyrus (BA47R) connectivity to all cerebral regions in 840s of active auditory attention data and their significance.

Brodmann area	Brain region	*B*	*p*	Correlation
rsREL	**Left Anterior Sup Temp Gyrus**	**0.24**	**0.048**	+
2 (L)	Primary Somatosensory Cortex	-0.21	0.014	-
3 (R)	Primary Somatosensory Cortex	-0.19	0.038	-
4 (L)	Primary Motor Cortex	-0.30	<0.001	-
4 (R)	Primary Motor Cortex	-0.18	0.046	-
10 (R)	*Anterior Prefrontal Cortex*	*0.34*	*0.002*	+
11 (R)	Orbitofrontal Cortex	0.27	0.014	+
21 (R)	Middle Temporal Gyrus	0.28	0.007	+
22 (L)	*Superior Temporal Gyrus*	*0.30*	*0.019*	+
38 (R)	Temporopolar Area	0.20	0.046	+
40 (R)	*Supramarginal Gyrus*	*0.30*	*0.014*	+
44 (L)	*IFC pars opercularis*	*0.30*	*0.016*	+
44 (R)	*IFC pars opercularis*	*0.38*	*0.042*	+
45 (L)	*IFC pars triangularis*	*0.27*	*0.014*	+
45 (R)	*IFC pars triangularis*	*0.64*	*0.002*	+
46 (L)	Dorsolateral Prefrontal Cortex	0.20	0.046	+
46 (R)	Dorsolateral Prefrontal Cortex	0.37	0.018	+
47 (L)	*Inferior Prefrontal Gyrus*	*0.50*	*<0.001*	+

Figure 6.2G and table 6.2.14 shows that right BA47 (BA47R) was positively correlated with the Left Anterior Sup Temp Gyrus (rsREL), left Superior Temporal Gyrus (BA22; SDN region) and inferior prefrontal cortex (BA47; SDN region). In the right hemisphere BA47R was positively correlated with the anterior prefrontal (BA10; SDN region) and orbitofrontal (BA11) cortices, Middle Temporal Gyrus (BA21), temporopolar area (BA38) and supramarginal gyrus (BA40; SDN region). Positive correlations were also found between this seed and the left/right IFC pars operculari/triangulari (BA44, BA45; SDN regions) and the dorsolateral prefrontal cortices (BA46). Negative correlations were found between BA46R and the left primary somatosensory (BA2), right primary somatosensory (BA3) and the left/right primary motor (BA4) cortices.

6.3.2.2.7. Overall summary of SDN region BA47 (closest match to inferior frontal gyrus)

Overall these results show that left/right BA47 areas of the SDN were positively correlated with each other and a number of other putative parts of the SDN, i.e. the superior temporal gyri (BA22), IFC pars operculari/triangulari (BA44, BA45 representing the SDN's frontal operculum) suggesting strong connectivity within the SDN during this task. Left/right BA47 showed no correlation to DMN regions. Given that one of the functions of this region is inhibitory control, it suggests that perhaps this is the route for signals from the SDN associated with inhibiting response(s) to distractor stimuli, and thus remains largely detached from the DMN.

6.3.3. Results of analysis 3:

Connectivity of the executive / frontoparietal control network in an 840s active auditory attention task and its relationship to the reorienting networks, salience network and the DMN

This analysis explored functional connectivity in the executive/frontoparietal control network which will be labelled ECN in this analysis. As stated in section *6.1.1.3*, based on the ECN's role in the maintenance of the task goals, and the FCN's bias towards the GDN, it was predicted that strong functional connectivity of the ECN would be observed (prediction 1).

A secondary hypothesis was that activity in the ECN would be coupled with down-regulation of the DMN (prediction 2).

6.3.3.1. Executive Control and default mode ROIs

ECN regions were based on those identified in the literature as being representative portions of the executive control network (Seeley et al., 2007; Sridharan et al., 2008; Menon & Uddin, 2010, Vincent et al., 2008) and included the left/right dorsolateral prefrontal cortex (BA9, BA46), anterior prefrontal cortex (BA10), anterior cingulate cortex (BA33) and portions of the posterior parietal cortex. The left/right somatosensory association cortices (BA5, BA7) were chosen as representative regions of the ECN within the posterior parietal cortex. DMN connectivity seed regions remained constant (LLP, MPFC, PCC, RLP; Fox et al., 2005). Note that BA5 and BA7, chosen as representative regions of the ECN in the posterior parietal cortex, overlapped with the use of these BAs in the GDN analysis, where they were considered as a closest matches to the GDN's superior parietal lobule. Similarly, BA10, characterising the ECN's anterior prefrontal

cortex, was previously used in the GDN analysis in which it was considered as a close match to the GDN's ventral frontal cortex.

6.3.3.2. Executive control network functional connectivity analysis

Connectivity between left/right ECN seed regions (BA5, BA7, BA9, BA10, BA33, BA46) and the whole of the cerebral cortex are shown in figure 6.3, positive correlations are shown in red text and negative correlations are shown in blue. Tables 6.3.1-6.3.6, illustrate the conn region, BA label, strength of connectivity (*Beta (B)* value) and significance (*p* value) across all participants. In each figure and table, positive correlations are displayed in red text and negative correlations are displayed in blue. ECN ROIs are displayed in *italics* and highlighted grey, and DMN seed (Fox et al., 2005)/rsREL regions are displayed in **bold** text. Note that significant ($p<.05$) correlations only are presented.

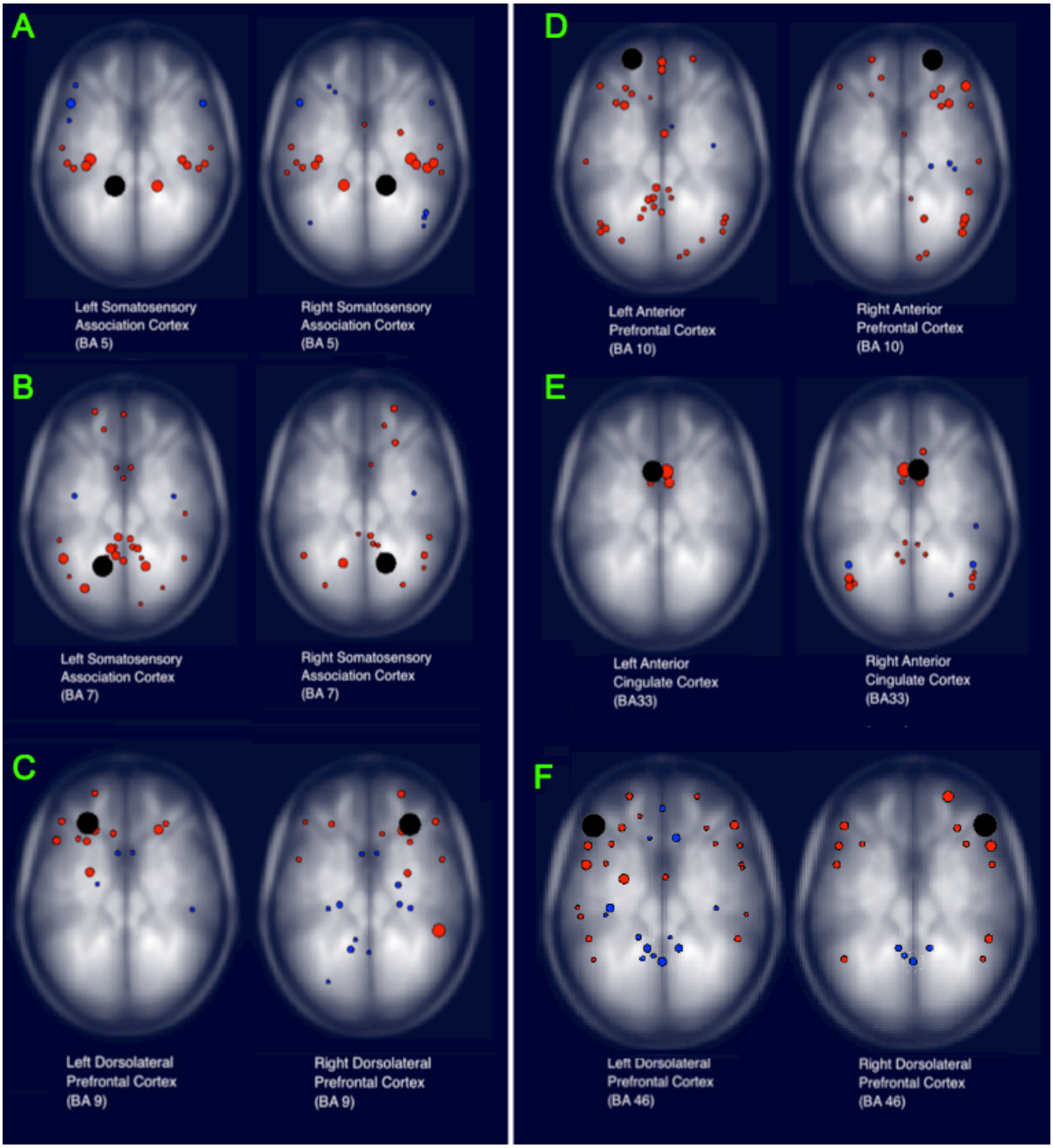

Figure 6.3. Relationship between ECN seed regions and areas covering the whole of the cerebral cortex in an 840s auditory attention task. (A) BA5), (B) BA7, (C) BA9, (D) BA10, (E) BA33, (F) BA46.

6.3.3.2.1. Overall summary of ECN region BA5 (representative of the ECN in the posterior parietal cortex)

Functional connectivity of the somatosensory association cortex (BA5) was considered in section *6.3.1.2.1* where it was considered as a representative of the GDN's superior parietal lobule. In terms of the ECN (see figure 6.3A), where BA5 was chosen as a representative of the ECN in the posterior parietal cortex, left/right BA5 were positively correlated to each other; unexpectedly negatively correlated to the left dorsolateral prefrontal cortex (BA9, BA46); and showed no relationship to any other putative regions of the ECN. BA5L showed no relationship to any DMN region, whilst BA5R was negatively correlated to the RLP and the left/right inferior parietal lobe (rsRELs). Overall, these results suggest that this ROI was perhaps not a reliable representative of the ECN in the posterior parietal cortex.

6.3.3.2.2. Overall summary of ECN region BA7 (representative of the ECN in the posterior parietal cortex)

The functional connectivity of the somatosensory association cortex (BA7) was explored in section *6.3.1.2.3* where it was selected as a representative of the GDN's superior parietal lobule. In terms of the ECN (see figure 6.3B), where BA7 was chosen as a representative of the ECN in the posterior parietal cortex, left/right BA7 were positively correlated to each other and to the anterior prefrontal cortices (BA10). In comparison to BA5, BA7 may be a more reliable representative of the ECN in the posterior parietal cortex, with its positive correlation to the anterior prefrontal cortex perhaps representative of communication with frontal regions implicated in changing task demands. Left BA7 showed positive correlations to the PCC (DMN

region) and a number of rsREL regions including the MPFC, PCC and left inferior parietal lobule, whilst right BA5 showed no correlation to any DMN region. Although this does not support the hypothesis suggesting that activity in the ECN would be coupled with down-regulation of the DMN, it perhaps lends support to the notion that the ECN is also involved in internal modes of cognition.

BA9: Dorsolateral prefrontal cortex (ECN match)

Table 6.3.1. Left dorsolateral prefrontal cortex (BA9L) connectivity to all cerebral regions in 840s of active auditory attention data and their significance.

Brodmann area	Brain region	*B*	*p*	Correlation
rsREL	**Left Superior Frontal Gyrus**	**0.33**	**0.008**	+
2 (R)	Primary Somatosensory Cortex	-0.16	0.047	-
6 (L)	*Premotor Cortex*	*0.40*	*0.002*	+
8 (L)	*Dorsal Frontal Cortex*	*0.78*	*0.001*	+
8 (R)	*Dorsal Frontal Cortex*	*0.33*	*0.002*	+
9 (R)	*Dorsolateral Prefrontal Cortex*	*0.46*	*0.019*	+
10 (L)	Anterior Prefrontal Cortex	0.44	0.019	+
25 (L)	Subgenual cortex	-0.18	0.035	-
25 (R)	Subgenual cortex	-0.17	0.048	-
28 (L)	Posterior Entorhinal Cortex	-0.10	0.047	-
32 (L)	Dorsal Anterior Cingulate Cortex	0.28	0.015	+
45 (L)	IFC pars triangularis	0.37	0.005	+
46 (L)	*Dorsolateral Prefrontal Cortex*	*0.24*	*0.011*	+
47 (L)	Inferior Prefrontal Gyrus	0.35	0.027	+

Figure 6.3C and table 6.3.1. show that left BA9 (BA9L) was positively correlated with the left superior frontal gyrus (rsREL), premotor (BA6), anterior prefrontal (BA10; ECN region), dorsal anterior cingulate (BA32), dorsolateral prefrontal (BA46; ECN region) and inferior prefrontal (BA47) cortices and the IFC pars triangularis (BA45). BA9L was also positively correlated with the right dorsolateral prefrontal cortex (BA9; ECN region) and with the left/right dorsal frontal cortex (BA8). Negative correlations were found between BA9R and the left posterior entorhinal

cortex (BA28), right primary somatosensory cortex (BA2), and with the left/right subgenual cortices (BA25).

Table 6.3.2. Right dorsolateral prefrontal cortex (BA9R) connectivity to all cerebral regions in 840s of active auditory attention data and their significance.

Brodmann area	Brain region	*B*	*p*	Correlation
rsREL	**Precuneus (PCC)**	**-0.26**	**0.049**	**-**
rsREL	**Right Superior Frontal Gyrus**	**0.33**	**0.025**	**+**
6 (R)	*Premotor Cortex*	*0.38*	*0.009*	+
8 (R)	*Dorsal Frontal Cortex*	*0.72*	*0.001*	+
9 (L)	*Dorsolateral Prefrontal Cortex*	*0.46*	*0.017*	+
10 (R)	Anterior Prefrontal Cortex	0.39	0.009	+
19 (L)	Associative Visual Cortex	-0.17	0.049	-
25 (L)	Subgenual cortex	-0.25	0.033	-
25 (R)	Subgenual cortex	-0.20	0.040	-
28 (R)	Posterior Entorhinal Cortex	-0.22	0.013	-
30 (L)	Cingulate Cortex	-0.25	0.010	-
31 (L)	Dorsal Posterior Cingulate Cortex	-0.24	0.049	-
32 (R)	Dorsal Anterior Cingulate Cortex	0.26	0.034	+
35 (L)	Perirhinal cortex	-0.19	0.011	-
35 (R)	Perirhinal cortex	-0.21	0.018	-
36 (L)	Parahippocampal Cortex	-0.16	0.040	-
36 (R)	Parahippocampal Cortex	-0.18	0.018	-
40 (R)	*Supramarginal Gyrus*	*0.41*	*<0.001*	+
44 (L)	IFC pars opercularis	0.22	0.034	+
44 (R)	IFC pars opercularis	0.27	0.023	+
46 (L)	*Dorsolateral Prefrontal Cortex*	*0.20*	*0.044*	+
46 (R)	*Dorsolateral Prefrontal Cortex*	*0.40*	*0.011*	+

Figure 6.3C and table 6.3.2 show that right BA9 (BA9R) was positively correlated with the right superior frontal gyrus (rsREL), premotor (BA6), dorsal frontal (BA8), anterior prefrontal (BA10; ECN region) and dorsal anterior cingulate (BA32) cortices and right supramarginal gyrus (BA40). BA9R was also positively correlated with the left dorsolateral prefrontal cortex (BA9; ECN region); along with the left/right IFC pars opercularis (BA44) and dorsolateral prefrontal cortex (BA46; ECN regions). Negative correlations were found BA9R and the precuneus (PCC; rsREL), left associative visual (BA19) and right Posterior Entorhinal Cortex (BA28). BA9R was

also negatively correlated with the left/right subgenual (BA25) perirhinal (BA35) and parahippocampal (BA36) cortices.

6.3.3.2.3. Overall summary of ECN region BA9 (ECN match)

The patterns of connectivity associated with BA9L show this seed was positively correlated to frontal regions and that overall connectivity was largely lateralised to the left hemisphere. BA9R was positively correlated to frontal regions, particularly in the right hemisphere, and showed widespread negative correlations to regions across the cortex, including the PCC region of the DMN. Given the extent of connectivity to frontal regions, and that executive functions are largely reliant on these regions, results suggests the ECN was strongly implicated in this task.

6.3.3.2.4. Overall summary of ECN region BA10 (ECN match)

The correlated activity associated with left/right BA10 was discussed in section *6.3.2.2.1* when it was considered as a representative of the anterior insular component of the SDN. In terns of the ECN (see figure 6.3D), where BA10 is a match to the ECN's anterior prefrontal cortex, this region was positively correlated to BA7 (representative of the ECN in the posterior parietal cortex) and to BA9 and BA46 (ECN's dorsolateral prefrontal cortex). This is suggestive of strong functional connectivity in the ECN during task completion. Unexpectedly, left BA10 was positively correlated to DMN regions including LLP, MPFC, PCC and RLP; and right BA10 was positively correlated to RLP. As with BA7, whilst this does not support the hypothesis of the current experiment, which suggested that activity in the ECN would be coupled with down-regulation of the DMN, it perhaps lends support to the notion that the ECN is also involved in internal modes of cognition and is functionally related to the DMN.

BA33: Anterior Cingulate Cortex (ECN match)

Table 6.3.3. Left anterior cingulate cortex (BA33L) connectivity to all cerebral regions in 840s of active auditory attention data and their significance.

Brodmann area	Brain region	*B*	*p*	Correlation
24 (L)	Ventral Anterior Cingulate Cortex	0.35	0.036	+
24 (R)	Ventral Anterior Cingulate Cortex	0.32	0.001	+
33 (R)	*Anterior Cingulate Cortex*	*0.61*	*<0.001*	+

Left BA33 (BA33L; see figure 6.3E) was positively correlated to the left/right ventral anterior cingulate cortices (BA24) and the right anterior cingulate cortex (BA33; ECN region).

Table 6.3.4. Right anterior cingulate cortex (BA33R) connectivity to all cerebral regions in 840s of active auditory attention data and their significance.

Brodmann area	Brain region	*B*	*p*	Correlation
DMN region	**LLP**	**0.15**	**0.004**	+
DMN region	**PCC**	**0.11**	**0.042**	+
DMN region	**RLP**	**0.16**	**0.016**	+
rsREL	**Left Inferior Parietal Lobe**	**0.13**	**0.016**	+
rsREL	**Right Inferior Parietal Lobe**	**0.13**	**0.048**	+
2 (R)	Primary Somatosensory Cortex	-0.08	0.042	-
19 (R)	Associative Visual Cortex	-0.16	0.049	-
23 (L)	Ventral Posterior Cingulate Cortex	0.12	0.042	+
23 (R)	Ventral Posterior Cingulate Cortex	0.14	0.048	+
24 (L)	Ventral Anterior Cingulate Cortex	0.21	0.024	+
24 (R)	Ventral Anterior Cingulate Cortex	0.40	0.002	+
31 (L)	Dorsal Posterior Cingulate Cortex	0.14	0.048	+
31 (R)	Dorsal Posterior Cingulate Cortex	0.15	0.042	+
32 (R)	Dorsal Anterior Cingulate Cortex	0.20	0.009	+
33 (L)	*Anterior Cingulate Cortex*	*0.61*	*<0.001*	+
37 (L)	Fusiform gyrus	-0.18	0.009	-
37 (R)	Fusiform gyrus	-0.20	0.013	-
39 (L)	Angular gyrus	0.12	0.002	+
39 (R)	Angular gyrus	0.12	0.014	+

Right BA33 (BA33R; see figure 6.3E) was positively correlated to LLP, PCC, RLP (DMN regions), and the left/right inferior parietal lobe (rsRELs). Positive correlations were also found between BA33R and the left anterior cingulate cortex (BA33; ECN region), right dorsal anterior cingulate cortex (BA32), and the left/right ventral/dorsal posterior cingulate (BA23, BA31), ventral anterior cingulate (BA24) cortices and the angular gyri (BA39).

6.3.3.2.5. Overall summary of ECN region BA33 (ECN match)

Overall the pattern of activity associated with left/right BA33 show that these ROIs were positively correlated with surrounding cingulate cortices, remaining relatively detached from other cortical regions. BA33R showed a positive relationship to LLP, PCC and RLP regions of the DMN. Similar to the correlated activity between BA7 (representative of the ECN in the posterior parietal cortex) and BA10 (anterior prefrontal cortex) with DMN regions, this perhaps lends support to the notion that the ECN is also involved in internal modes of cognition.

BA46: Dorsolateral prefrontal cortex (ECN match)

Table 6.3.5. Left dorsolateral prefrontal cortex (BA46L) connectivity to all cerebral regions in 840s of active auditory attention data and their significance.

Brodmann area	Brain region	*B*	*p*	Correlation
DMN region	**Medial Prefrontal Cortex**	**-0.26**	**0.016**	**-**
DMN region	**Posterior Cingulate Cortex**	**-0.22**	**0.033**	**-**
rsREL	**Precuneus (PCC)**	**-0.34**	**0.004**	**-**
rsREL	**Right Anterior Sup Temp Gyrus**	**0.18**	**0.043**	**+**
3 (L)	Primary Somatosensory Cortex	-0.11	0.049	-
4 (L)	Primary Motor Cortex	-0.16	0.004	-
4 (R)	Primary Motor Cortex	-0.10	0.037	-
5 (L)	*Somatosensory Association Cortex*	*-0.19*	*0.016*	*-*
6 (L)	*Premotor Cortex*	*0.27*	*0.002*	*+*
9 (L)	*Dorsolateral Prefrontal Cortex*	*0.24*	*0.007*	*+*
9 (R)	*Dorsolateral Prefrontal Cortex*	*0.20*	*0.033*	*+*

10 (L)	Anterior Prefrontal Cortex	0.25	0.011	+
10 (R)	Anterior Prefrontal Cortex	0.22	0.026	+
11 (L)	Orbitofrontal Cortex	0.17	0.034	+
21 (L)	Middle Temporal Gyrus	0.14	0.037	+
22 (L)	Superior Temporal Gyrus	0.18	0.021	+
22 (R)	Superior Temporal Gyrus	0.17	0.047	+
23 (R)	Ventral Posterior Cingulate Cortex	-0.16	0.045	-
30 (L)	Cingulate Cortex	-0.12	0.022	-
31 (L)	Dorsal Posterior Cingulate Cortex	-0.25	0.004	-
31 (R)	Dorsal Posterior Cingulate Cortex	-0.25	0.004	-
32 (L)	Dorsal Anterior Cingulate Cortex	-0.19	0.043	-
32 (R)	Dorsal Anterior Cingulate Cortex	-0.27	0.004	-
37 (L)	Fusiform gyrus	0.32	0.033	+
38 (L)	Temporopolar Area	0.13	0.030	+
40 (L)	*Supramarginal Gyrus*	*0.34*	*0.012*	+
40 (R)	*Supramarginal Gyrus*	*0.34*	*0.012*	+
44 (L)	IFC pars opercularis	0.41	0.002	+
44 (R)	IFC pars opercularis	0.22	0.034	+
45 (L)	IFC pars triangularis	0.58	0.004	+
45 (R)	IFC pars triangularis	0.25	0.023	+
46 (R)	*Dorsolateral Prefrontal Cortex*	*0.55*	*0.004*	+
47 (L)	Inferior Prefrontal Gyrus	0.25	0.016	+
47 (R)	Inferior Prefrontal Gyrus	0.20	0.033	+

Figure 6.3F and table 6.3.5 show that left BA46 (BA46L) was positively correlated to the right anterior superior temporal gyrus (rsREL), left premotor (BA6) and orbitofrontal (BA11) cortices, middle temporal (BA21) and fusiform (BA37) gyri and temporopolar area (BA38). BA46L was also positively correlated to the right dorsolateral prefrontal cortex (BA46; ECN region) and the left/right dorsolateral prefrontal (BA9; ECN regions) and anterior prefrontal (BA10; ECN regions) cortices, superior temporal gyrus (BA22), supramarginal gyri (BA40), IFC pars opercularis/triangularis (BA44, BA45) and the inferior prefrontal cortices (BA47). Negative correlations were found between BA46L and the MPFC, PCC (DMN regions), precuneus (PCC; rsREL), left primary somatosensory (BA3) and somatosensory association (BA5; ECN region) cortices and the cingulate cortex (BA30). BA46L was also negatively correlated to the right ventral posterior cingulate cortex (BA23), and to the left/right primary motor cortices (BA4) and the left/right dorsal posterior/anterior cingulate cortices (BA31, BA32).

Table 6.3.6. Right dorsolateral prefrontal cortex (BA46R) connectivity to all cerebral regions in 840s of active auditory attention data and their significance.

Brodmann area	Brain region	*B*	*p*	Correlation
DMN region	**Posterior Cingulate Cortex**	**-0.23**	**0.021**	**-**
rsREL	**Precuneus (PCC)**	**-0.32**	**0.008**	**-**
9 (R)	*Dorsolateral Prefrontal Cortex*	*0.40*	*0.010*	+
10 (R)	Anterior Prefrontal Cortex	0.40	0.001	+
31 (L)	Dorsal Posterior Cingulate Cortex	-0.27	0.011	-
31 (R)	Dorsal Posterior Cingulate Cortex	-0.21	0.013	-
37 (L)	Fusiform gyrus	0.22	0.011	+
37 (R)	Fusiform gyrus	0.25	0.021	+
40 (R)	*Supramarginal Gyrus*	*0.43*	*0.007*	+
44 (L)	IFC pars opercularis	0.30	0.010	+
44 (R)	IFC pars opercularis	0.40	0.014	+
45 (L)	IFC pars triangularis	0.33	0.008	+
45 (R)	IFC pars triangularis	0.49	0.001	+
46 (L)	*Dorsolateral Prefrontal Cortex*	*0.55*	*0.006*	+
47 (L)	Inferior Prefrontal Gyrus	0.26	0.037	+
47 (R)	Inferior Prefrontal Gyrus	0.37	0.017	+

Figure 6.3F and table 6.3.6 show that right BA46 (BA46R) was positively correlated to the left/right dorsolateral prefrontal (BA9, BA46; ECN regions) and anterior prefrontal (BA10; ECN region) cortices, and supramarginal gyrus (BA40). BA46R was also positively correlated with the left/right fusiform gyri (BA37), IFC pars operculari/triangulari (BA44, BA45) and the inferior prefrontal cortices (BA47). Negative correlations were found between BA46R and the PCC (DMN region), precuneus (PCC; rsREL) and the left/right dorsal posterior cingulate cortices (BA31).

6.3.3.2.6. Overall summary of ECN region BA46 (ECN match)

Overall, these patterns of correlated activity show that BA46 was positively correlated with frontal ECN regions, but not with posterior parietal regions (e.g. BA7). They also hint at the notion of down-regulation of DMN regions when the ECN is active, this is because negative

correlations were observed with regions surrounding the PCC and MPFC (although it should be noted that only left BA46 showed a negative correlation to MPFC).

6.3.4. Results of analysis 4:

Connectivity of the salience network in an 840s active auditory attention task, and its relationship to the DMN

This analysis explored functional connectivity within the SN. As stated in section *6.1.1.4*, given that the task employed in the current experiment was designed to induce activity in the GDN, SDN and ECN, and that novel (salient) oddball/distractor stimuli were presented, it was hypothesised that strong functional connectivity within the SN would be observed (prediction 1).

It was also hypothesised that activity in the SN would be associated with down-regulation of the DMN.

6.3.4.1. Salience and default mode ROIs

SN regions were based on those identified by Sridharan et al. (2008), which included the ventrolateral prefrontal cortex, anterior cingulate cortex and the fronto-insular cortex (also referred to as the anterior insula). Additional regions implicated in this network include the dorsal and ventral anterior cingulate cortices (Seeley et al., 2007). As with previous analyses, there was some disparity between previously identified SN regions and those available using the conn toolbox. Therefore, ROIs were chosen based on their close proximity to typical SN regions and included the anterior prefrontal cortex (BA10; closest match to the ventrolateral prefrontal cortex), insular cortex (BA13; closest representative of the fronto-insular/anterior insular) and the ventral/dorsal/anterior cingulate cortices (BA24, BA32, BA33; SN matches). Two out of the five Brodmann areas identified as portions of the SD overlapped with putative regions of the

SDN. These included, BA10 (where it was previously considered as a the closest match to the SDN's ventrolateral prefrontal cortex) and BA13 (previously considered as a representative of the SDN's anterior insula). BA33 (anterior cingulate cortex) was previously included as part of the executive control network in analysis 3.

6.3.4.2. Salience Network functional connectivity analysis

Connectivity between SN seed regions (left/right BA10, BA13, BA24, BA32, BA33) and the whole of the cerebral cortex are shown in figure 6.4. Tables 6.4.1-6.4.4 illustrate the conn region, BA label, strength of connectivity (*Beta (B)* value) and significance (*p* value) across all participants. In both the figures and the tables, positive correlations are shown in red text and negative correlations are shown in blue. SN ROIs are displayed in *italics* and highlighted grey, and DMN seed (Fox et al., 2005)/rsREL regions are displayed in **bold** text. Note that significant ($p<.05$) correlations only are presented.

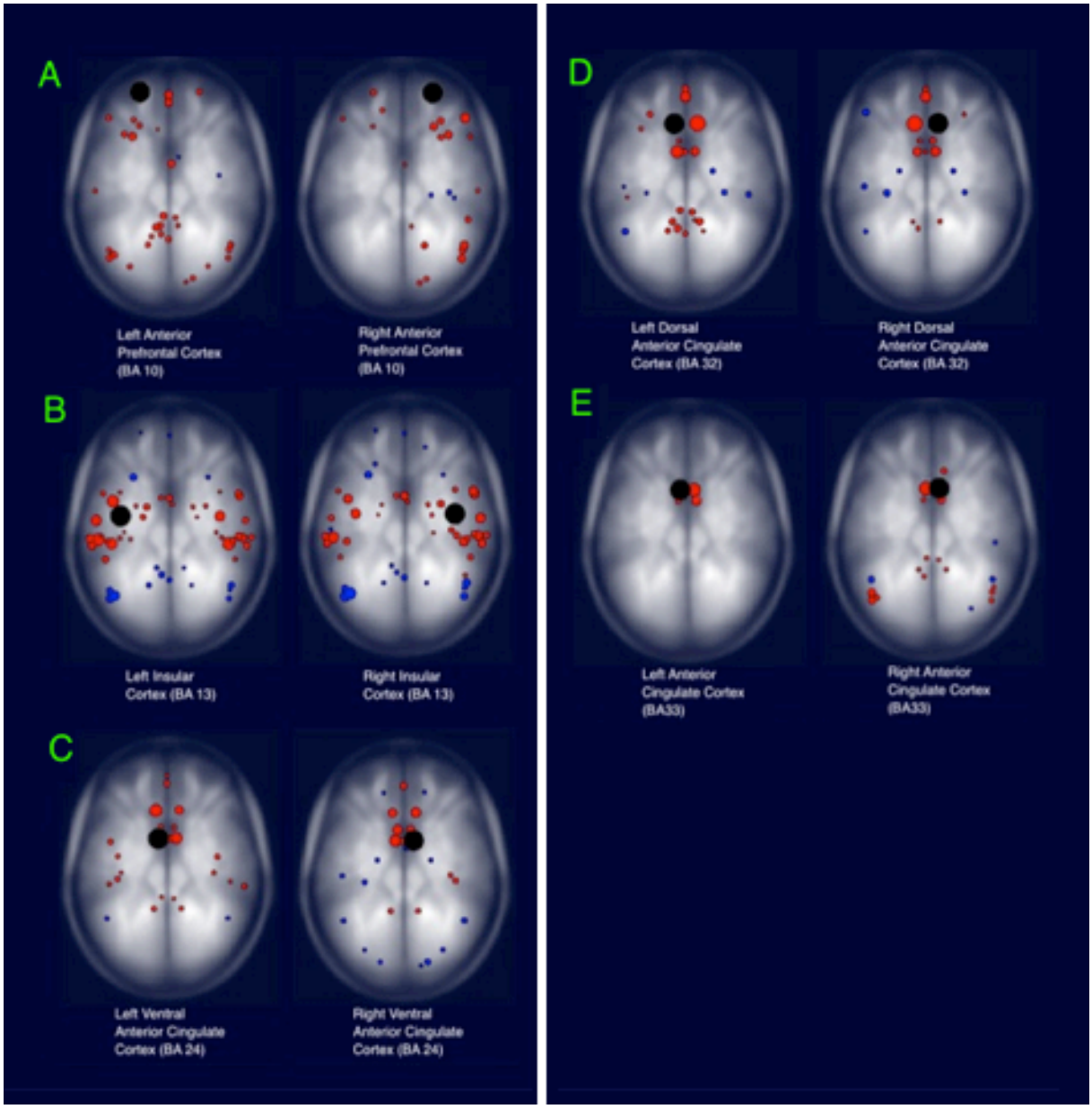

Figure 6.4. Relationship between SN seed regions and areas covering the whole of the cerebral cortex in an 840s auditory attention task. (A) BA10, (B) BA13, (C) BA24, (D) BA32, (E) BA33.

6.3.3.2.1. Overall summary of SN region BA10 (closest match to ventrolateral prefrontal cortex)

The correlated activity associated with left/right BA10 was discussed in section *6.3.2.2.1*, where it was considered as a putative region of the SDN. In terms of the SN (see figure 6.4A), BA10L was positively correlated to its homologous region in the right hemisphere and to the SN's dorsal anterior cingulate cortex (BA32). Unexpectedly, BA10L was negatively correlated to BA13 (closest representative to the fronto-insular cortex) and to the ventral anterior cingulate cortex (BA24). Contrary to the prediction that activity in the SN would be associated with down-regulation of the DMN, BA10L was positively correlated with LLP, MPFC, PCC and RLP and to a number of rsREL regions in close proximity. In the right hemisphere BA10 (BA10R) was only positively correlated to the DMN's RLP. It is difficult to interpret these results. More widespread connectivity between BA10L and other cortical regions might imply that this ROI is implicated in the brain's SN to a greater extent that right BA10. In terms of the relationship between the SN and DMN, whereby down-regulation of the DMN was predicted as a function of SN activation, the fact that positive correlations were observed could be indicative of a role of the SN in monitoring and responding to internally-directed events.

6.3.3.2.2. Overall summary of SN region BA13 (closest match to fronto-insular cortex)

The correlated activity associated with left/right BA13 was discussed in section *6.3.2.2.2*, where it was considered as a putative region of the brain's SDN. In terms of the SN (see figure 6.4B), left/right BA13 produce a symmetrical pattern of correlated activity across the brain, showing negative correlations to BA10 (closest match to the SN's ventrolateral prefrontal cortex) and

BA24 (SN's ventral anterior cingulate cortex). BA13L was also negatively correlated with the DMN's LLP, PCC and RLP regions. Whilst negative correlations were not anticipated between SN regions, given that this region has been implicated in the switching between networks (Sridharan et al., 2008) it is feasible to assume that this was the predominant function of this region in comparison to other SN regions. This could also account for the negative correlations with DMN regions, in that it was modulating activity in this network.

BA24: Ventral anterior cingulate cortex (SN match)

Table 6.4.1. Left ventral anterior cingulate cortex (BA24L) connectivity to all cerebral regions in 840s of active auditory attention data and their significance.

Brodmann area	Brain region	*B*	*p*	Correlation
DMN region	**Medial Prefrontal Cortex**	**0.28**	**0.015**	+
rsREL	**Left Anterior Sup Temp Gyrus**	**0.23**	**0.015**	+
rsREL	**Medial Prefrontal Cortex**	**0.19**	**0.037**	+
rsREL	**Right Posterior Sup Temp Gyrus**	**0.25**	**0.015**	+
rsREL	**Cingulate Gyrus**	**0.77**	**<0.001**	+
2 (R)	Primary Somatosensory Cortex	0.11	0.044	+
3 (L)	Primary Somatosensory Cortex	0.16	0.015	+
4 (L)	Primary Motor Cortex	0.17	0.046	+
4 (R)	Primary Motor Cortex	0.19	0.025	+
13 (L)	*Insular Cortex*	*0.26*	*0.023*	+
13 (R)	*Insular Cortex*	*0.23*	*0.015*	+
23 (L)	Ventral Posterior Cingulate Cortex	0.25	0.033	+
23 (R)	Ventral Posterior Cingulate Cortex	0.22	0.046	+
24 (R)	*Ventral Anterior Cingulate Cortex*	*0.90*	*<0.001*	+
31 (L)	Dorsal Posterior Cingulate Cortex	0.23	0.015	+
31 (R)	Dorsal Posterior Cingulate Cortex	0.26	0.023	+
32 (L)	*Dorsal Anterior Cingulate Cortex*	*0.73*	*<0.001*	+
32 (R)	*Dorsal Anterior Cingulate Cortex*	*0.56*	*0.001*	+
33 (L)	*Anterior Cingulate Cortex*	*0.35*	*0.015*	+
33 (R)	*Anterior Cingulate Cortex*	*0.21*	*0.022*	+
37 (L)	Fusiform gyrus	-0.14	0.032	-
37 (R)	Fusiform gyrus	-0.11	0.042	-
41 (L)	Primary Auditory Cortex	0.24	0.025	+

Figure 6.4C and table 6.4.1 show that this left BA24 (BA24L) was positively correlated with the MPFC (DMN region/rsREL), left anterior superior temporal gyrus, right posterior superior temporal gyrus and cingulate gyrus (rsRELs). This seed was also positively correlated with the left primary somatosensory (BA3) and primary auditory (BA41) cortices, along with the right primary somatosensory (BA2) and ventral anterior cingulate (BA24; SN region) cortices. Positive correlations were also apparent with the left/right primary motor (BA4), insular (BA13; SN regions), ventral/dorsal posterior cingulate (BA23, BA31), dorsal anterior cingulate (BA32; SN regions) and anterior cingulate (BA33; SN regions) cortices. This seed was negatively correlated with the left/right fusiform gyri (BA37).

Table 6.4.2. Right ventral anterior cingulate cortex (BA24R) connectivity to all cerebral regions in 840s of active auditory attention data and their significance.

Brodmann area	Brain region	*B*	*p*	Correlation
DMN region	**Medial Prefrontal Cortex**	**0.23**	**0.005**	+
rsREL	**Cingulate Gyrus**	**0.48**	**0.003**	+
3 (R)	Primary Somatosensory Cortex	0.19	0.009	+
4 (R)	Primary Motor Cortex	0.16	0.016	+
11 (L)	Orbitofrontal Cortex	-0.16	0.048	-
11 (R)	Orbitofrontal Cortex	-0.18	0.047	-
17 (R)	Primary Visual Cortex	-0.19	0.049	-
18 (L)	Secondary Visual Cortex	-0.21	0.024	-
18 (R)	Secondary Visual Cortex	-0.26	0.008	-
19 (L)	Associative Visual Cortex	-0.17	0.037	-
19 (R)	Associative Visual Cortex	-0.17	0.021	-
20 (L)	Inferior Temporal Gyrus	-0.24	0.021	-
24 (L)	*Ventral Anterior Cingulate Cortex*	*0.90*	*<0.001*	+
28 (L)	Posterior Entorhinal Cortex	-0.13	0.016	-
28 (R)	Posterior Entorhinal Cortex	-0.11	0.021	-
31 (L)	Dorsal Posterior Cingulate Cortex	0.21	0.016	+
31 (R)	Dorsal Posterior Cingulate Cortex	0.25	0.016	+
32 (L)	*Dorsal Anterior Cingulate Cortex*	*0.50*	*0.001*	+
32 (R)	*Dorsal Anterior Cingulate Cortex*	*0.64*	*<0.001*	+
33 (L)	*Anterior Cingulate Cortex*	*0.32*	*<0.001*	+
33 (R)	*Anterior Cingulate Cortex*	*0.40*	*0.001*	+
36 (L)	Parahippocampal Cortex	-0.18	0.015	-
37 (L)	Fusiform gyrus	-0.18	0.016	-
37 (R)	Fusiform gyrus	-0.21	0.009	-

Right BA24 (BA24R; see figure 6.4C and table 6.4.2) was positively correlated with the MPFC (DMN region), cingulate gyrus (rsREL), left ventral anterior cingulate cortex (BA24; SN region) and right primary somatosensory (BA3) and primary motor (BA4) cortices. BA24R was also positively correlated with the left/right dorsal posterior/anterior cingulate cortices (BA31, BA32 (BA32: SN regions)) and the anterior cingulate cortices (BA33; SN regions). Negative correlations were found between this seed and the left inferior temporal gyrus (BA20), parahippocampal cortex (BA36), and also the right primary visual cortex (BA17). In the left and right hemispheres this seed was negatively correlated with the oribitofrontal (BA11), secondary visual (BA18) and associative visual (BA19) cortices, Posterior Entorhinal Cortex (BA28) and the fusiform gyri (BA37).

6.3.3.2.3. Overall summary of SN region BA24 (SN match)

These results show that left/right BA24 were positively correlated with each other, along with a number of other regions of the SN, including BA13 (representative of the SN's fronto-insular cortex), BA32 (dorsal anterior cingulate cortex) and BA33 (anterior cingulate cortex). This suggests strong functional connectivity in the SN during this task, supporting the first prediction of this analysis. Unexpectedly, both left/right BA24 were positively correlated with the MPFC component of the DMN and revealed no relationship to any other DMN region.

BA32: Dorsal anterior cingulate cortex (SN match)

Table 6.4.3. Left dorsal anterior cingulate cortex (BA32L) connectivity to all cerebral regions in 840s of active auditory attention data and their significance.

Brodmann area	Brain region	*B*	*p*	Correlation
DMN region	**Medial Prefrontal Cortex**	**0.66**	**<0.001**	**+**

DMN region	**Posterior Cingulate Cortex**	**0.33**	**0.003**	**+**
rsREL	**Cingulate Gyrus**	**0.41**	**0.009**	**+**
rsREL	**Medial Prefrontal Cortex**	**0.36**	**0.003**	**+**
rsREL	**Precuneus (PCC)**	**0.34**	**0.010**	**+**
2 (R)	Primary Somatosensory Cortex	-0.14	0.007	-
9 (L)	Dorsolateral Prefrontal Cortex	0.28	0.007	+
20 (L)	Inferior Temporal Gyrus	-0.22	0.045	-
23 (L)	Ventral Posterior Cingulate Cortex	0.33	0.005	+
23 (R)	Ventral Posterior Cingulate Cortex	0.30	0.005	+
24 (L)	*Ventral Anterior Cingulate Cortex*	*0.73*	*<0.001*	+
24 (R)	*Ventral Anterior Cingulate Cortex*	*0.50*	*0.001*	+
28 (R)	Posterior Entorhinal Cortex	-0.17	0.009	-
29 (R)	Retrosplenial Cingulate Cortex	0.17	0.039	+
30 (L)	Cingulate Cortex	0.26	0.009	+
30 (R)	Cingulate Cortex	0.15	0.042	+
31 (L)	Dorsal Posterior Cingulate Cortex	0.38	0.005	+
31 (R)	Dorsal Posterior Cingulate Cortex	0.33	0.003	+
33 (L)	*Anterior Cingulate Cortex*	*0.24*	*0.029*	+
36 (L)	Parahippocampal Cortex	-0.15	0.035	-
36 (R)	Parahippocampal Cortex	-0.11	0.007	-
37 (L)	Fusiform gyrus	-0.21	0.005	-
41 (L)	Primary Auditory Cortex	0.14	0.047	+
47 (L)	Inferior Prefrontal Gyrus	0.15	0.020	+

Left BA32 (BA32L; see figure 6.4D and table 6.4.3) was positively correlated with the MPFC, PCC (DMN regions), cingulate gyrus, medial prefrontal cortex and precuneus (PCC; rsRELs). This seed was also positively correlated with the left dorsolateral prefrontal (BA9), anterior cingulate (BA33; SN region), primary auditory (BA41) and inferior prefrontal (BA47) cortices and with the right retrosplenial cingulate cortex (BA29). In the left and right hemispheres BA32L was positively correlated with the ventral posterior/anterior cingulate (BA23, BA24 (BA24; SN regions)), cingulate (BA30) and dorsal posterior cingulate (BA31) cortices. Negative correlations were found between BA32L and the left inferior temporal gyrus (BA20), fusiform gyrus (BA37), right primary somatosensory cortex (BA2), posterior entorhinal cortex (BA28) and the left/right parahippocampal cortex (BA36).

Table 6.4.4. Right dorsal anterior cingulate cortex (BA32R) connectivity to all cerebral regions in 840s of active auditory attention data and their significance.

Brodmann area	Brain region	*B*	*p*	Correlation
DMN region	**Medial Prefrontal Cortex**	**0.53**	**<0.001**	+
DMN region	**Posterior Cingulate Cortex**	**0.22**	**0.036**	+
rsREL	**Cingulate Gyrus**	**0.33**	**0.044**	+
rsREL	**Medial Prefrontal Cortex**	**0.22**	**0.015**	+
9 (R)	Dorsolateral Prefrontal Cortex	0.26	0.033	+
20 (L)	Inferior Temporal Gyrus	-0.23	0.013	-
24 (L)	*Ventral Anterior Cingulate Cortex*	*0.56*	*0.001*	+
24 (R)	*Ventral Anterior Cingulate Cortex*	*0.64*	*<0.001*	+
28 (L)	Posterior Entorhinal Cortex	-0.21	0.020	-
28 (R)	Posterior Entorhinal Cortex	-0.21	0.015	-
31 (L)	Dorsal Posterior Cingulate Cortex	0.25	0.049	+
31 (R)	Dorsal Posterior Cingulate Cortex	0.29	0.023	+
32 (L)	*Dorsal Anterior Cingulate Cortex*	*0.99*	*<0.001*	+
33 (L)	*Anterior Cingulate Cortex*	*0.21*	*0.023*	+
33 (R)	*Anterior Cingulate Cortex*	*0.20*	*0.008*	+
36 (L)	Parahippocampal Cortex	-0.25	0.004	-
36 (R)	Parahippocampal Cortex	-0.17	0.015	-
37 (L)	Fusiform gyrus	-0.23	0.023	-
46 (L)	Dorsolateral Prefrontal Cortex	-0.27	0.004	-

Figure 6.4D and table 6.4.4 shows that right BA32 (BA32R) was positively correlated with MPFC (DMN region/rsREL), PCC (DMN region), and cingulate gyrus (rsREL).This seed was also positively correlated with the left dorsal anterior cingulate (BA32; SN region) and the right dorsolateral prefrontal (BA9) cortices. In the left and right hemispheres BA32R was positively correlated with the ventral anterior cingulate (BA24; SN regions), dorsal posterior cingulate (BA31) and the anterior cingulate (BA33; SN regions) cortices. Negative correlations were apparent between this seed and the left Inferior Temporal Gyrus (BA20), fusiform gyrus (BA37) and dorsolateral prefrontal cortex (BA46), and with the left/right posterior entorhinal (BA28) and parahippocampal (BA36) cortices.

6.3.3.2.4. Overall summary of SN region BA32 (SN match)

Overall, this portion of the SN was largely positively associated with other cingulate regions of the SN, along with posterior cingulate and medial prefrontal regions of the DMN. Whilst these

results support the hypothesis that there would be strong connectivity in the SN, they do not support the prediction that activity in the SN would be associated with down-regulation of the DMN. The pattern of connectivity associated with this SN ROI, along with BA24 (SN region: ventral anterior cingulate cortex), suggests the SN and frontal portions of the DMN in particular may communicate with one another. This raises questions regarding the relationship between the SN and DMN; considered further in the discussion of this experiment.

6.3.3.2.5. Overall summary of SN region BA33 (SN match)

The correlated activity associated with left/right BA33 was discussed in section *6.3.3.2.5*, where it was considered as a putative region of the ECN. In terms of the SN (see figure 6.4E), the pattern of connectivity associated with BA33L/R shows that these ROIs were positively related to surrounding cingulate regions implicated in the SN. BA33R also showed a positive relationship to the LLP, PCC and RLP regions of the DMN, which may be due to the role of the anterior cingulate cortex in conflict monitoring between thoughts and feelings. Nonetheless, this unpredicted positive relationship does raise questions regarding the association between the SN and the DMN, which will be considered further in the discussion of this experiment.

6.4. Discussion

The overall aim of the current experiment was to explore the functional connectivity of several large-scale brain networks and their relationship to the DMN. As shown, four analyses were conducted on active auditory attention data in order to investigate connectivity within the goal-driven, stimulus-driven, executive/frontoparietal control and salience networks respectively, along with their relationship to the DMN. The results of each analysis are discussed below.

6.4.1. Functional connectivity within the GDN and its relationship to the DMN

As previously stated, based on (1) the nature of the task, requiring participants to respond to target 'goal' stimuli/inhibit response to task-relevant/irrelevant distractors, and (2) the task duration, provoking fluctuations in the GDN's response over time, it was hypothesised that strong functional connectivity in the GDN would be observed in the current experiment. A secondary hypothesis was that functional connectivity in the GDN would be associated with down-regulation of the DMN.

Overall, results revealed that for some portions of the GDN, i.e. the precentral and intraparietal sulci, the predictions on this analysis were met. In particular, the right precentral sulcus (frontal portion of the GDN) revealed strong functional connectivity to a number of other putative GDN regions, supporting the notion that the right hemisphere is implicated in attention function to a greater extent than the left hemisphere. This GDN ROI also revealed strong negative correlations to all DMN regions, as well as a number of rsREL regions. A similar pattern was observed for the right intraparietal sulcus (parietal portion of the GDN), which illustrated strong positive correlations to a number of right frontal regions and suppression of medial prefrontal,

posterior and lateral DMN regions. Together, these results support activation of frontal and parietal GDN regions during target detection tasks (i.e. Corbetta & Shulman, 2002) and also offer support to the widely reported anti-correlated relationship between the GDN and DMN, and deactivation of the DMN during goal-driven tasks (Shulman et al., 1997; Mazoyer et al., 2001; see chapter 1 for a review).

Other selected GDN ROIs, i.e. the right dorsal frontal cortex (BA8; match in CONN with Corbetta et al. defined region), appeared to interact with regions representing the GDN's precentral sulcus and superior parietal lobule in the right hemisphere (further supporting the role of this hemisphere in attention function) but remained largely detached from the DMN and was in fact positively correlated with RLP. Whilst unpredicted, it is likely this relationship reflects communication between frontal and attentive right parietal regions, again as previously stated, supporting activation of frontal and parietal regions during target detection tasks (e.g. Corbetta & Shulman, 2002) and suggesting there is an overlap in putative GDN and DMN regions. This finding also supports studies showing that one of the functions of the dorsal frontal cortex is awareness and allocation of attention (e.g. Asplund, Todd, Snyder & Marois, 2010): therefore, perhaps this BA8 focuses attention resources on the external world to such an extent that interaction with other brain regions (i.e. DMN regions) is reduced in order to prevent interference of internal streams of thought with achieving task goals.

As previously addressed in the discussion of experiment 1, whilst the CONN toolbox was reliable in measuring the strength of correlated activity between network components, a fundamental issue that could have influenced some of the results of the current experiment was

disparity between the identification of GDN regions by Corbetta et al. (2008) and the definition and position of these BAs produced in CONN. Therefore a number of GDN regions selected as ROIs in the current experiment were based on being the closest match/representative to GDN regions defined by Corbetta and colleagues and for some GDN components this appeared to be problematic. For example, whilst functional connectivity associated with BA5 (somatosensory association cortex in CONN: chosen as a representative of the GDN's superior parietal lobule) could be linked to the GDN from a motor control perspective (showing positive correlations to somatosensory and motor regions), its negative relationship to other putative GDN and DMN regions suggest that BA5 was not a reliable candidate as part of the GDN. Similarly, BA39 in CONN (angular gyrus), originally chosen to represent the GDN's intraparietal sulcus, was significantly positively correlated to each DMN component: an unpredicted finding previously interpreted due its the anatomical overlap with LLP and RLP regions of the DMN. However, when the supramarginal gyrus (BA40 in CONN) was then considered as a representative of the intraparietal sulcus, predicted effects were found: strong connectivity with other GDN components coupled with down-regulation of the DMN.

6.4.2. Functional connectivity within the SDN and its relationship to the DMN

Based on the fact that distractors were randomly presented throughout the task in the current experiment it was predicted that strong functional connectivity within the SDN would be observed. As predicted, findings revealed a number of positive correlations between SDN ROIs and other putative regions of this network: supporting previous research implicating the SDN in the detection and monitoring of the external environment for behaviourally-irrelevant/distracting

stimuli (i.e. Arrington et al., 2000; Bledowski et al., 2004; Corbetta et al., 2000; Kincade et al., 2005; see section *3.3.2* in chapter 3 for a review of SDN functions).

A secondary hypothesis of this analysis was that activity in the SDN network would be associated with down-regulation of the DMN. As previously stated, this hypothesis was based on: (1) that the task employed was designed to selectively activate the GDN in the case of goal relevant stimuli and activate the SDN in the case of distractors; (2) the internal mentation hypothesis of DMN function (the view that the DMN supports internal mentation alone, and is largely detached from the external world; Buckner et al. 2008; see section *1.7.2*, chapter 1 for a review); and (3) that distractor items (engaging the SDN) were presented randomly across the whole task duration. Results revealed multiple SDN ROIs were associated with down-regulation of all or a number of DMN regions; this was particularly evident for BAs selected in CONN as representative portions of the SDN's anterior insula, supramarginal gyri and frontal operculari regions.

Interestingly, patterns of connectivity associated with left/right BA10 (closest match to the SDN's ventral frontal cortex) revealed a different response in each hemisphere. Whilst left BA10 was positively correlated to all DMN regions, right BA10 was positively correlated with RLP only. As previously addressed, this might suggest that right BA10 is focussed on the detection of distractors to a greater extent than left BA10. Alternatively, it is possible left BA10 may selectively recruit the DMN to aid the detection of unpredictable events: thus supporting the sentinel hypothesis of DMN function. It should be noted, however, that no other SDN ROI revealed this pattern of positively correlated activity to DMN regions: it is therefore unclear as to

whether the observed results are due to the sentinel role of the DMN or that the selection of BA10 in conn as the ventral frontal cortex was an unreliable candidate as part of the SDN. Another interesting finding was that BA47 (inferior prefrontal gyrus in CONN) selected as the closest match to the SDN's inferior frontal gyrus was correlated with SDN components only and remained largely detached from not only the DMN but also from regions implicated in the GDN. As previously stated, given one of the functions of this region is inhibitory control, it suggests that perhaps this region is the route for signals from the SDN associated with inhibiting response(s) to distractor stimuli. Hence, its detachment/non-interaction with other brain regions implicated in stream of thought (DMN regions), achieving goals (GDN regions), reward/punishment (other frontal regions) could be prevention of interference with function.

In comparison to the GDN, the SDN could be considered as being more informative about some of the functions associated with the DMN. Down-regulation of DMN regions in response to activation of SDN regions appears to support the internal mentation hypothesis of this network. It is feasible to assume suppression of activity of the DMN by the SDN occurs in order to prevent interference of internal modes of cognition (i.e. stream of thought/self-referential mental activity) in the detection of events from the external world, which in turn distinguishes between the internal and sentinel hypotheses of DMN function.

6.4.3. Functional connectivity within the ECN and its relationship to the DMN

Note that as previously stated given the overlap in anatomical regions/associated functions, the ECN and FCN were collectively referred to as the *ECN* in this experiment. Based on the ECN's role in the maintenance of the task goals and the bias of the task, it was predicted that strong

functional connectivity of the ECN would be observed. Overall, results revealed for some components of the ECN, i.e. the anterior prefrontal cortex, this prediction was met. This region in particular showed strong functional connectivity to the ECN's dorsolateral prefrontal cortex and to several other frontal and parietal regions overlapping with ECN, GDN and DMN structures. In terms of the relationship between overlapping ECN and GDN regions, this result supports previous studies reporting interaction between these networks associated with the maintenance and adjustment of goal-driven attention (Corbetta, Patel & Shulman, 2008). However, in relation to the DMN, this finding fails to support the second prediction of this analysis, suggesting functional connectivity in the ECN would be coupled with down-regulation of the DMN.

As previously stated in section *6.1.1.3*, the hypothesis pertaining to the relationship between the ECN and DMN (predicting that activation of the ECN would be associated with down-regulation of the DMN) was based on the fact participants were completing an *externally-directed* attention-demanding task. Thus, it was assumed that preoccupation with the goal set and interaction with the GDN in monitoring and maintaining its response towards task-relevant stimuli would result in the ECN being predominantly involved in the allocation of resources to external world processing. This prediction, however, did not take into account the role of the ECN in the monitoring and control of internally-associated functions in which the DMN is implicated. And, interestingly the current results revealed that a number of ECN components (i.e. right anterior cingulate cortex and parietal representatives of the ECN including the somatosensory association cortex) were positively correlated to multiple/all DMN components. Whilst this finding fails to support the current hypothesis, it does lend support to previous studies

in which a positive functional relationship between these typically external- (ECN/FCN) and internal- (DMN) associated networks has been reported (e.g. Christoff et al., 2009; Gerlach et al., 2011).

The functional implications of the current results suggest that the ECN could be implicated in the monitoring and control of the external *and* internal processes simultaneously. Some ECN components i.e. the dorsolateral prefrontal cortex were negatively correlated with posterior regions of the DMN: suggesting that frontal ECN regions down-regulate internal-associated brain regions in order to prevent interference with the monitoring/interaction with the GDN in the allocation of its resources to the external world. Alternatively, the right anterior cingulate node of the ECN remained relatively detached from all other ECN regions but showed positive correlations with the DMN's PCC, LLP and RLP. This perhaps suggests that this putative ECN region monitors and controls the internal world; a theory in line with Botvinick et al. (2005) who proposed one of the functions of the anterior cingulate cortex is to monitor internal mental states as a means of signalling the need for modulation/redirection of attention and control.

Overall, these results could suggest the ECN distributes its resources to the monitoring and control of external and internal processes respectively, so that activation in one network (i.e. the DMN) does not over-rule/abolish activity in another network (i.e. GDN), which would ultimately interfere with the goal of the task. Thus, perhaps in low-level attention demanding tasks or when participants become habituated to task demands, the ECN works in conjunction with the DMN to a greater extent than the GDN in order to control and restrict stream of thought: a proposal which would account for the fact that during active tasks DMN activity is observed at attenuated levels

in comparison to rest. In a similar fashion perhaps the ECN as a coherent system might be implicated in the control of the GDN's response in the initial stages of a task, but in the latter stages decouples from this network as executive resources become less required and couples with the DMN in order to control internal modes of cognition. A future experiment might aim to explore this by investigating changes in the ECN over task duration in a similar way to which the DMN was explored in analysis 2 of experiment 2.

6.4.4. Functional connectivity within the SN and its relationship to the DMN

Given the task employed in the current experiment was designed to induce activity in the GDN, SDN and ECN, and that novel (salient) stimuli were presented, it was hypothesised that strong functional connectivity within the SN would be observed. In line with the predictions made regarding the ECN's response in the current experiment (ECN engaged/DMN down-regulated), and given that distractors were randomly presented throughout the task (engaging activity in the SN as well as the SDN), it was hypothesised that activity in the SN would be associated with down-regulation of the DMN.

Overall, the results of the current analysis revealed ventral, dorsal and anterior cingulate regions of the SN were strongly functionally connected to one another: thus supporting the first prediction of the current analysis. Interestingly, the ventrolateral prefrontal cortex remained largely detached from other SN regions and revealed widespread positive correlations with DMN regions. Whilst this was previously interpreted as this region monitoring the *internal* environment for salient events (i.e. task-unrelated thoughts), it should also be noted that there was disparity in the identification of this region in CONN, with the anterior prefrontal cortex

selected as its closest match. Thus, as previously addressed disparity in the selection of regions with the BAs available in CONN could account for the observed reductions in functional connectivity between this SN ROI and other SN regions and for the unpredicted positive correlation with DMN regions.

The fronto-insular component of the SN (BA13 in CONN) revealed unpredicted negative correlations with frontal and anterior cingulate nodes of the SN, and was also negatively correlated with posterior and lateral regions of the DMN. Whilst this result supports the second prediction of this analysis (SN active/DMN down-regulated) it is unclear as to why this region was not positively correlated with other putative SN regions. One possibility is given this region has been previously implicated in the switching between large-scale brain networks (i.e. the ECN and DMN; Sridharan et al., 2008) and also that an interaction between the ECN and DMN was observed in the previous analysis, the SN may remain largely detached from other SN components and instead focus its resources on not only switching between the ECN and DMN; but also down-regulating the DMN in order to prevent distracting (salient) internal thoughts having a detrimental effect on the ECN's role in task completion.

Interestingly, the anterior cingulate and dorsal/ventral anterior cingulate regions were positively correlated with a number of DMN regions. Interaction between dorsal/ventral anterior cingulate regions and frontal DMN regions might suggest that these cingulate areas were monitoring stream of thought produced by the MPFC (i.e. self-reflective thoughts) for particularly salient thoughts that would cause distraction from the task at hand. Alternatively, these correlations may be explained in terms of these regions selectively recruiting DMN regions to aid with the

monitoring of the external environment of particularly salient events (oddball stimuli; supporting the sentinel hypothesis of DMN function). Unpredicted was that the right anterior cingulate cortex was positively correlated with the DMN's PCC, LLP and RLP components. Given this region has been previously implicated in conflict monitoring (Botvinick et al., 2004) and that it is also known to be involved in self-control and emotion (e.g. Allman, Hakeem, Erwin, Nimchinsky & Hof, 2001), perhaps this region interacts with posterior and lateral DMN regions in the detection and control of emotional salient thoughts which could potentially interfere with the task at hand.

6.4.5. Conclusions

Results of the current experiment reveal there is functional interplay between several large-scale brain networks when participants engage their attention on an externally-directed task. Interestingly, an overarching finding from each analysis was that specific network components interacted with putative regions of the brain's DMN in different ways. This suggests in order to disentangle some of the functions associated with large-scale brain networks; investigation on a component-by-component basis may be more insightful. Furthermore, exploring the response of network components over time might also provide greater insight into the toggling that occurs between internal and external modes of cognition. For example, given the ECN is implicated in both forms of cognition, investigating the interaction between ROIs of this network and GDN and DMN regions might help better understand the function of the DMN; this will be considered further in the general discussion of this thesis.

CHAPTER 7

GENERAL DISCUSSION

7.1. A brief reminder of the aims of this thesis and overview of chapter

As outlined in section *3.8* in chapter 3 the main aim of this research thesis was to attempt to gain a better understanding of the function of the Default Mode Network (DMN) by exploring the relationship between the DMN and other cognitive control networks. An initial focus was the investigation of the relationship between electroencephalographic (EEG) and functional magnetic resonance imaging (fMRI) markers of the DMN. However, as shown in experiment 1, frequency content in the Beta range (13-30 Hz) did not significantly predict spontaneous low frequency (SLF) fluctuations in the fMRI BOLD signal in DMN regions identified using functional connectivity analysis. Based on this null result, a shift in the focus of this thesis resulted in investigation of the DMN (within the same participant group) in an active auditory attention task, along with its response over task duration in fMRI data only. Having demonstrated that DMN activity was prominent in this task and with results hinting at potential relationships with other large-scale control networks, experiment 3 utilised technical development data further and explored functional connectivity within several control networks along with their interaction with the DMN.

In this chapter key experimental findings are summarised along with the way in which they fit in/add to existing DMN literature. Following on from this, the implications of the current results in better understanding the function of the DMN are addressed, along with ideas about how we

might gain better insight into the DMN. Finally, suggestions for further research aimed at better elucidation of the function of the DMN are outlined.

7.2. Key experimental findings and how they fit in/add to existing DMN literature

7.2.1. Experiment 1: Resting-state functional connectivity and electrophysiological investigation of the DMN

In experiment 1, functional connectivity analysis (a new technique to the School of Psychology, University of Dundee) revealed several frontal, posterior and parietal nodes of the DMN were significantly positively correlated with one another. These results supported existing research showing activation of the DMN is prominent during task-free rest (e.g. Fox et al., 2005; Greicius et al., 2003; Raichle et al., 2001; reviewed in chapters 1 and 2).

Exploration of the relationship between the DMN and a task-positive network identified by Fox et al. (2005) revealed only individual components of each network were anti-correlated with one another. This provides a possible insight into the functions of the links between networks. Whilst most regions identified in the literature corresponded well to the predefined ROIs in CONN some unexpected correlations suggested problems in the delineation of Brodmann Areas (BAs) using the CONN toolbox. Nevertheless, results hinted at the notion that relationships between DMN regions and other networks should be considered on an individual component-to-component basis (discussed further in sections *7.2.3* and *7.3.1*). ROI-ROI results also raised questions regarding the function of the posterior cingulate cortex (PCC) in particular. PCC activity appeared to be largely unrelated to task-positive regions apart from an area representing

the intraparietal sulcus (commonly implicated in the goal-driven network: GDN) to which it was unexpectedly positively correlated. In turn, this finding brought into question whether parietal regions of the GDN could be the facilitator/route of signal for generating DMN associated thoughts. Note that activation of the medial prefrontal cortex (MPFC) was also associated with down-regulation of parietal supramarginal GDN regions in analysis 1b. Thus, given portions of the GDN and DMN are located in parietal areas, perhaps goal-driven parietal regions (intraparietal sulcus) interact with PCC in the facilitation or suppression of thought. In turn, signals generated in MPFC (an area implicated in reward/punishment) as a result of particular thoughts may feedback to PCC and on to parietal areas to influence activity in the GDN parietal region. This model is merely speculation, but given that DMN components are yet to be disentangled in relation to factors such as the generation, influence and continuation of *stream of thought* it is plausible.

Experiment 1 also revealed activation of the DMN was coupled with down-regulation of a number of regions implicated in the processing of sensory information. In terms of existing literature, reductions in activity in auditory areas have been reported as a function of scanner background noise (e.g. Gaab, Gabrieli, & Glover, 2007) and habituation to repeated auditory stimulation (e.g. Mutschler et al., 2010), with reductions in visual areas reported in terms of exhibiting a deactivation response during eyes-closed rest (e.g. Raichle et al., 2001). Reductions in groups of sensory regions have also been interpreted as signifying additional low-frequency resting state networks during task-free undirected rest (e.g. Mantini et al., 2007). In terms of the *functional relationship* between these areas and the DMN, as previously suggested in the results and discussion of experiment 1, the DMN may exercise some form of *control* over these regions:

down-regulating them in order to prevent information from the external world interfering with the current stream of thought. This notion supports the *perceptual decoupling* theory proposed by Smallwood and colleagues (Smallwood, Baracaia, Lowe & Obonsawinb, 2003; see Smallwood, Brown, Baird, Schooler, 2012 for a recent review) that suggests engagement in stream of thought (DMN active) down-regulates sensory-associated regions in order to reduce focus on the external world. To test this theory analysing changes in resting-state functional connectivity over time might be beneficial (note that changes in functional connectivity over time in the current study were investigated in an *active* task). One would anticipate that as *resting-state* duration increases and participants become increasingly engaged in internal modes of cognition, sensory regions would become increasingly negatively correlated with DMN regions signalling increased suppression of input as participants become increasingly engaged in internal thought). Alternatively, this finding can be interpreted in relation to the anti-correlation between the DMN and task-positive network in the resting brain (Fox et al., 2005). Hence, sensory-associated regions implicated in visual/auditory external goals/tasks and typically influenced by the GDN are not so much down-regulated by the DMN as possibly not being up-regulated by the GDN.

7.2.2. Experiment 2: Exploration of the DMN in an active auditory attention task and investigation of its activity over time

Experiment 2 revealed DMN regions were positively correlated with one another in an active auditory attention task (designed to engaged the GDN and stimulus-driven network: SDN). These results supported existing research showing that fluctuations in DMN activity is not only

observed during task-free rest, but also when attention resources are focussed on the external world (e.g. Fransson, 2006; Greicius & Menon, 2004; Hahn et al., 2007; see chapters 1-3).

In addition, experiment 2 also highlighted the reliability of using reaction time measures as a behavioural index of DMN activity (in line with studies discussed in chapter 1, e.g. Weissman et al., 2006). No significant change in response time towards task-relevant goal-driven stimuli across task duration (suggestive of no change in DMN activity) was confirmed by an analysis in CONN, revealing no change in functional connectivity of the DMN over time. However, as previously discussed (see section *5.4.3* in chapter 5), some participants exhibited increases/decreases in reaction times across conditions that appeared to correlate with increases/decreases in DMN activity respectively (on visual inspection only); this is one of the caveats associated with averaging across participants. Given some of the cognitive processes implicated with DMN activity (i.e. self-referential thought, episodic recall etc.), it is unclear as to whether some participants who took part in technical development work were more likely to engage in daydreaming, or alternatively be more 'distracted' by their internal world, compared to others who were more task-focussed and/or able to 'control' their internal world. Whilst Mason et al. (2007; see section *1.6.1.1* in chapter 1 for a review) reported a positive correlation between daydreaming tendencies and the magnitude of activity in DMN regions, the authors did not determine *why* participants exhibited differences in daydreaming tendencies. A recent publication by Kynazev, Bocharov and Pylkova (2012) reported attenuated DMN activity in participants who scored high on the personality trait *extraversion* in comparison to those who scored high on the trait *introversion*. Therefore, it is a possibility that overlooking factors such

as individual differences in personality and/or self-control/focus is limiting current research on the DMN in neurologically healthy individuals.

Another interesting finding of experiment 2 was that, similar to experiment 1, activity of the DMN was associated with down-regulation of regions involved in the processing of sensory information. Given task-demands in experiment 2 required participants to listen for task-relevant/irrelevant stimuli, make a physical response etc. (engaging auditory, premotor, somatosensory regions), it is feasible to assume the goal-driven nature of engaging these sensory regions is a possible explanation for DMN signals being anti-correlated with them. Recent research suggests that, during the processing of task-relevant visual information, visual cortical regions couple with the Frontoparietal Control Network (FCN); however, when task-irrelevant information is presented visual regions show a coupling with the DMN (Chadick & Gazzaley, 2011). In line with these results, one might question why some nodes of the DMN did not show a positive correlation with auditory regions, given the attention task presented task-relevant and irrelevant stimuli. However, it should be noted that no dissociation was made between responses towards task-relevant/irrelevant stimuli in the analyses.

7.2.3. Experiment 3: Functional connectivity of the attention reorienting, executive/frontoparietal control and salience networks, and their relationship to the DMN

In line with predictions, experiment 3 revealed strong functional connectivity within several large-scale brain networks (GDN, SDN, ECN/FCN, Salience Network (SN)), which were anticipated to be involved in the task for different reasons. Results also revealed individual nodes of each network interacted with portions of the DMN in different ways (see sections *6.4.1*-

6.4.4 in chapter 6 for a detailed overview of results). As previously alluded to in section *7.2.1*, this suggests interaction between the DMN and other large-scale brain networks should be considered on a component-by-component basis and that current DMN literature perhaps over-generalises results when reporting network interactions. This is because they may fail to take into account: (1) specific network components may drive/control the response of individual regions belonging to other networks; and (2) network components may vary in their response and interaction with one another over time/as task-processing demands change.

An interesting outcome of analysis 1 in experiment 3 was that an area representing the superior parietal lobe of the GDN was positively correlated to a cluster of areas surrounding and including the DMN's PCC. As previously discussed, it is feasible to assume communication between GDN/DMN regions located in the parietal lobes and the PCC is what brings to the forefront and/or drives/changes the current stream of thought. Note that the GDN's intraparietal sulcus was also positively correlated with PCC, whilst all frontal GDN regions were negatively correlated with DMN region: further supporting this notion, and suggesting that parietal GDN regions may send control signals to DMN regions. It should be pointed out that parietal portions of the ECN were also positively correlated with PCC, suggesting if GDN parietal regions interact with the PCC in the proposed way (generation/changing the stream of thought), parietal ECN regions may also exert some form of control over this process.

It is suggested the current results add to the existing literature by providing a better understanding of the role of the PCC in DMN function. Buckner et al. (2008; see section *2.3.4* chapter 2) proposed the PCC is best described as an anatomical 'hub' to which all other DMN

regions are correlated to (in the resting brain). Furthermore, similar to the current results, Fransson and Marrelec (2008) reported that during a working memory task the PCC portion of the DMN was strongly positively correlated with the inferior parietal lobule (GDN region). Based on the response of other DMN regions the authors also suggested that the PCC is a *convergence* region whose key role is the integration of information between DMN subsystems. More recently, Hayden, Smith and Platt (2010) found suppression of PCC activity in rhesus monkeys facilitated cognitive control during task switching; inferring that suppression of DMN PCC function enhances task performance. Together, these studies and the current set of results highlight the fundamental role of the PCC in the generation/facilitation of stream of thought: suggesting that this DMN component warrants further research. Certainly some of the most up-to-date research (e.g. Leech, Braga & Sharp, 2012) has suggested that by fractionating the PCC into dorsal and ventral regions reveals the dorsal PCC is implicated in the balance of internal and external modes of cognition coupling activity in FCN regions, whilst the ventral PCC is highly correlated with activity in other putative DMN regions, suggesting it is implicated in internal modes of cognition only.

7.3. Working towards a better understanding of the function of the DMN: implications of the current results

7.3.1. Considering network interaction on a component-by-component basis to control what enters stream of thought

As previously addressed perhaps consideration of the DMN on a component-by-component basis is the best way forward in better understanding the DMN, particularly in terms of its

involvement/interaction with regions of other large-scale networks concerning what enters and is maintained in stream of thought. As shown by the current results and previous research (e.g. Greicius et al., 2003; Fransson, 2006; Raichle et al. 2001; see studies discussed in chapters 1 and 2), a consistent set of DMN regions (LLP, MPFC, PCC, RLP; Fox et al., 2005), are strongly functionally connected during both rest and active task conditions. These results are consistent with participant experience of a continuous flow of thought occurring in the mind; with the extent to which engagement occurs being influenced by external world demands. What remains unclear at present is which DMN component(s) influences fluctuations in stream of thought. When completing an externally-directed novel or mundane task if something spontaneous pops into mind, internal processes must evaluate the behavioural and motivational significance of the thought in order to determine whether it is relevant enough to interrupt the externally-directed process. Failure to pay attention to these 'pop in' thoughts and failure to filter/suppress them would undoubtedly have a detrimental effect on completion of the most simple everyday tasks. Whilst the evaluation of the *significance* of a 'pop in' thought might suggest involvement of the MPFC (based on its role in reward/punishment), the results from the current series of experiments suggest a bias in the interaction between parietal regions of the GDN and DMN. Given their anatomical closeness and the fact they are supplied by the same vascular territory, this questions whether it is the interaction between GDN and DMN parietal regions that drives the seed of thought.

Although previously addressed in section *7.2.3*, the involvement of PCC at a component level is worth emphasising further. As previously suggested, given PCC's interaction with parietal GDN and DMN regions along with frontal DMN regions, it is possible this DMN component is

involved in the evaluation of what enters stream of thought. In experiment 2, when DMN connectivity was compared across the duration of the task, PCC was significantly positively correlated to all other DMN regions across each of the task conditions, with other DMN regions showing variability in their connectivity to other DMN regions across task duration. This emphasises that at a component level, PCC is perhaps one of the most crucial nodes of DMN function. In healthy neurological ageing, attenuated task-related deactivation (indicative of more DMN activity) of PCC in particular has been reported in a number of studies (e.g. Miller et al., 2008; Sambarto et al., 2010; see Mevel, Chetelat, Eustache & Desgranges, 2011 for a review). Given some of the compromises that arise with ageing in relation to task-related performance, it suggests greater PCC activity/weakened deactivation results in reduced ability in the switching between internal and external modes of cognition and the suppression of DMN activity (Grady, Springer, Hongwanishkul, McIntosh & Winocur, 2006), thus highlighting the role of the PCC in the influence and maintenance of stream of thought (although note that other DMN components have also been investigated in analysing the relationship between this network's function and role and ageing; see Mevel et al., 2011 for a review).

7.3.2. Extending the current results to enhance understanding of the role of the DMN in Neurological and Psychiatric populations

A number of studies have been conducted in order to investigate DMN abnormalities in neurological (e.g. alzheimer's disease, mild cognitive impairment) and psychiatric disorders (e.g. schizophrenia, depression; see Broyd et al., 2008 for a review). Whilst the experiments outlined in this thesis concentrated on neurologically healthy individuals only, consideration of how of the current results may apply to improved understanding of atypical functional

connectivity/reduced deactivation of the DMN are considered below. The example used is that of *schizophrenia*.

Research suggests when patients with schizophrenia are engaged in externally-directed tasks, an over-enthusiastic orientation to internally-directed modes of cognition/lack of DMN suppression contributes to some of the cognitive deficits (i.e. impaired working memory performance) and positive symptoms (i.e. delusions/hallucinations) associated with the disorder (Anticevik et al., 2012). The results from experiment 3 in this thesis are key in showing that in neurological healthy individuals there is flexible interaction between the DMN and ECN. This suggests each network exerts some form of 'control' over the other: the DMN controls the ECN's involvement in internal stream of thought, and the ECN controls the DMN in order to prevent task interference. Applying this notion to patients with schizophrenia, it is therefore unclear as to whether working memory cognitive impairments and symptoms are related to deficits in the ECN (thus failure to control the DMN) or deficits in the DMN (thus over-activity impairing ECN function). Analysis of the relationship between the ECN and DMN in experiment 3 revealed the anterior cingulate portion of the ECN was positively correlated with posterior and parietal DMN regions. Given: (1) the role of the anterior cingulate cortex in conflict monitoring (Botvinick et al., 1999; 2004); and (2) the proposed model that communication between posterior and parietal DMN regions is what drives the stream of thought; perhaps the current focus of research should be at a component-based level in order to disentangle control functions of the ECN/DMN in schizophrenia.

7.3.3. The misconception surrounding the 'task-negative' and 'task-positive' networks

The results of each experiment in this thesis challenge the *task-negative* and *task-positive* terminology frequently used in the literature (in reference to the DMN and GDN/ECN). Initially coined by Fox et al. (2005), these terms are somewhat ambiguous for two reasons: (1) 'task-negative' infers DMN activity is abolished/shut-down during external goal-driven tasks; however, as shown in experiments 2 and 3 along with previous studies (e.g. Fransson, 2006; Greicius & Menon, 2004; Hahn et al., 2007), DMN activity remains prominent when resources are focussed on the external world; and (2) the 'task-positive' network in reference to the GDN/ECN infers that these networks are implicated in external goal-driven tasks only. That being said, the results of experiment 3 in fact revealed components of the ECN and DMN interacted with one another, suggestive of a role for the ECN in monitoring and controlling internal modes of cognition (see also Christoff et al., 2009; Gerlach et al., 2011 discussed in chapter 3). Furthermore, based on the model presented in this chapter, that parietal GDN regions interact with parietal and posterior portions of the DMN in the generation/influence/maintenance of stream of thought: this infers the GDN is not best described as a task-positive network. The restrictive nature of categorising this large-scale network using the task-positive/negative terminology ultimately fails to take into account the interaction and involvement of each network in both internal and external modes of cognition (note that Spreng, 2012 has also recently challenged the task-positive versus task-negative distinction).

7.3.4. Does the DMN as a whole really exhibit 'sentinel' functions?

As discussed in section *1.7.1* in chapter 1, the *sentinel hypothesis* of DMN function suggests the DMN maintains low-level attention processes and monitors the external world for unpredictable/significant events (Buckner et al., 2008). In support of this hypothesis, experiment

3 revealed individual components of the SDN (in particular the ventral frontal cortex) were positively correlated with DMN regions. However, results also revealed a significant number of SDN components down-regulated regions of the DMN, thus providing support for the *internal mentation* hypothesis (the proposal that the DMN is implicated in internalised functions only). As with the fallacy surrounding task-positive/task-negative terminology, there is clear disparity and over-generalisation in the function of the DMN associated with these two hypotheses. This therefore provides further support for the suggestion that the DMN should be considered on a component-by-component basis (to map internal/sentinel functions on to specific DMN components): supporting previous research doubting the exclusiveness of each hypothesis (internal mentation versus sentinel), e.g. Stawarczyk et al. (2011).

7.4. What can we do to better understand the function of the DMN?

7.4.1. Will future research involve fractionating the DMN into more than one Default Mode Network?

As discussed in chapters 1 and 2, the DMN has been proposed to represent a network of interacting *subsystems* that congregate around *hubs*, i.e. the PCC/MPFC. Buckner et al. (2008) suggested a *medial temporal lobe subsystem* utilises existing memories and associations in order to stimulate mental reproductions/thoughts, and that a *medial prefrontal subsystem* then utilises this information in the creation and integration of self-relevant thoughts. More recently, Kim (2012) proposed a *cortical midline subsystem* is implicated in the mediation of self-referential processing, and a *parieto-temporal subsystem* is involved in the support of memory retrieval. The results of the current series of experiments and the model outlined in section *7.2.1*,

suggesting communication between posterior/parietal nodes of the DMN and forwarding of information on to MPFC is what drives stream of thought, offers support to these dual-subsystem accounts of the DMN and in particular Kim's proposed *parieto-temporal subsystem* (although note: as previously stated, no direct measure of participants thought processes were obtained throughout this research; therefore, whilst it is likely they would have been engaged in typical DMN thought processes, i.e. self-referential thought/episodic memory retrieval etc., it is unclear as to when, to what extent, and what type of thought they were engaged/focused on).

As outlined in the introductory chapters, Posner and Petersen (1990) were among the first to propose that attention is not a function of the brain as a whole and is instead attributable to three distinct systems: alerting, orienting and executive control (see section *3.2* in chapter 3 for a review). Focussing on the *orienting* of attention in particular, Corbetta & Shulman (2002) fractionated this aspect of attention further, suggesting that two control networks, the GDN and SDN, are major contributors to orienting. Subsequent to this, over the years numerous researchers have investigated the GDN and SDN using different methods to explore their independent and/or simultaneous functioning (see Corbetta et al., 2008 for a review). Applying the same principle to the current DMN literature, it is somewhat surprising that even some of the most up-to-date DMN research continues to investigate this network as a whole; especially given the vast array of functions implicated. One would argue fractioning this network into DMN's' or concentrating on DMN *subsystems* to a greater extent (thus allowing for the development of measures that could tap into specific DMN components) would provide better insight into the overall function of this network.

7.4.2. What insight have we and can we gain from alternative neuroimaging and analysis techniques?

As addressed in the introductory chapters, Positron Emission Tomography (PET) and fMRI have proven reliable techniques in assessing the anatomy and functional response of the DMN in the resting and active brain. Given one of the recurring themes in this chapter (based on findings of the current series of experiments) has been the role of the PCC and parietal GDN/DMN regions in driving the stream of thought, it is possible that techniques such as transcranial magnetic stimulation (TMS) would be beneficial in assessing these hypothesised functions and interactions further. This in turn could allow for inference to be made about whether a specific DMN component(s) influences over-activity/reduced deactivation of the DMN in clinical and ageing populations. In terms of insight gained from EEG, as previously stated and as shown by the results of experiment 1, there is currently an inconsistency in correlating specific EEG frequencies with the DMN. Recent literature has, however, highlighted the promising role of EEG microstate analysis in establishing electrophysiological signatures of the DMN and several other resting-state networks, including attention, visual, sensorimotor and auditory networks (e.g. Yuan, Zotev, Phillips, Drevets & Bodurka, 2011). Furthermore, this analysis technique has proven to be a promising tool in monitoring changes in brain state from wakefulness to sleep (Brodbeck et al., 2012), highlighting its future potential in determining when participants are likely to shift from one mode of brain function to the another during rest of active task completion (thus, switching between the external and internal worlds).

7.4.3. Is the key to building a better model of DMN function the study of relationships with other networks?

As discussed in section *7.3.2* it is unclear as to whether some of the symptoms and cognitive deficits in schizophrenia are resultant of: (1) lack of suppression of the DMN by the ECN; or (2) lack of control by the DMN in relation to the extent to which the ECN becomes involved in the control and monitoring of the internal world. This suggests further exploration of network interactions at a component level is required. In neurologically healthy individuals, the current results show that when engaged in an externally-directed task, there is a flexible interaction between components of several large-scale control networks. Given there was no significant change in reaction time across task duration, this also suggests each network exerts control over one another in order to maintain optimal cognitive performance (although one recognises that analysis of task performance in detection of task-relevant stimuli would be a better indicator of this). It is only recently that the role of the ECN, more specifically the FCN, has started to receive considerable interest in relation to its control over the DMN and involvement in the generation of the stream of thought (see Smallwood et al. 2012 for a review). Thus, perhaps investigation of the ECN in particular and the role of the anterior cingulate cortex in the monitoring of posterior/parietal DMN component interaction is what research should concentrate on. This would also allow for exploration into how likely individuals are to switch from being focussed on the external world to becoming caught up and distracted by their internal world.

7.5. How can the limitations of the current experiments be addressed?

There are four main limitations of the current experiments. Firstly, no self-report measure of participants' thought processes were obtained in experiment 1, and as such, interpretation about what they were likely to be thinking about was based on previous literature. Employing a simple questionnaire or asking participants to detail their thought processes would alleviate this problem

in future studies. Secondly, as discussed at several points throughout there was some disparity between the selection of ROIs and those available in the CONN toolbox, an issue that could be eliminated in future experiments by loading functional images detailing pre-defined ROIs (a feature available in the CONN software). Thirdly, on visual inspection only and on a single-participant basis, increases/decreases in DMN were apparent as a function of increasing task duration. Given that the likelihood to engage in internal modes of cognition is very much an individual-based process, with studies linking personality traits extraversion/introversion to likelihood in daydreaming tendencies and DMN activity (Kynazev et al., 2010), perhaps categorising participants on the basis of personality would have yielded different results. The categorisation into high/low extraversion tendencies could have provided further insight into the posterior/parietal interaction and involvement in stream of thought, with perhaps introverts showing greater connectivity in these regions than extroverts. Finally, on reflection, failing to subdivide the beta frequency range (similar to Laufs et al., 2003) and/or restricting of the EEG analysis to a single frequency band could have affected the results obtained; thus, although existing literature remains somewhat mixed, adopting a similar data-driven independent component analysis approach similar to Mantini et al. (2007) could have in fact yielded different results.

7.6. Suggested future research strategy to better understand and explore the function of the DMN

Utilising the technical development data further I would aim to analyse whether there is a point in time at which the executive control network appears to decouple from the GDN and couple with the DMN, perhaps by using Dynamic Causal Modelling. Or, whether it is the case that

from the start of the task, components of the ECN are involved in the monitoring of the internal world, whilst others are involved in the external world. I would also aim to gain better understanding of the posterior/parietal interaction in the involvement in stream of thought. A recent study by Kim and Lee (2011) revealed greater variability in posterior DMN regions compared to anterior DMN regions when the same group of participants were scanned under the same resting-state conditions at three different time points. This variability in the posterior regions emphasises the need to consider the DMN at a component/subsystem level and develop methods and studies better designed to tap into posterior DMN regions only. I would also plan on developing expertise in EEG microstate analysis because at present this technique appears to be more consistent in identifying electrophysiological correlates of resting-state networks. Thus, given DMN activity is altered in individuals with certain neurological disease/clinical disorders as shown by fMRI, defining EEG correlates of DMN activity could in the future be used as diagnostic tool for these individuals or high-risk individuals: reducing research and national health service costs substantially. One of main benefits of microstate analysis is that it offers a potential alternative view of discrete network activity in the form of brief periods (~100-300ms) of stability in the distribution of the EEG signal which may be correlated with fluctuations in the fMRI BOLD signal over ~1000s of ms. As shown by the current set of results, there is interaction at a component level between several large-scale control networks; however, the temporal resolution limitations associated with fMRI means it is almost impossible to determine at which point in time specific networks/components of networks appear dominant in their activation. For example, in the current task it is likely that portions of the GDN and SDN (due to the bias of the task) were more active in the initial stages of task completion; however, in latter stages perhaps the activity in the ECN may have become pronounced in order to maintain the

response of the GDN. A benefit of using microstate analysis in order to investigate this is that it allows for stable patterns of EEG in the ~100-300ms range to be analysed: thus, when correlated with the fMRI BOLD signal could provide better insight into network interactions over time.

7.7. Concluding comments

In summary, this research thesis was intended to investigate the function of the DMN in term of its fluctuations in activity and interaction with other large-scale control networks in the brain. As summarised in this chapter, results support existing resting-state research revealing that during task-free rest several frontal, posterior and parietal DMN regions are strongly functionally connected to one another. Results also suggest a putative interactive role of the posterior and parietal DMN regions in driving the stream of thought. Overall, however, perhaps the most significant finding is that there is flexible interaction between the DMN and other large-scale control networks in the brain; and more specifically this interaction is at a component-based level, suggesting future research should focus more on fractionating the DMN in order to better understand its function.

REFERENCES

Addis, D.R., Wong, A.T., & Schacter, D.L. (2007). Remembering the past and imagining the future: common and distinct neural substrates during event construction and elaboration. *Neuropsychologia, 45*(7), 1363-1377.

Allman, J.M., Hakeem, A., Erwin, J.M., Nimchinsky, E., & Hof, P. (2001). The anterior cingulate cortex. The evolution of an interface between emotion and cognition. *Annals of the New York Academy of Sciences, 935*, 107-117.

Amedi, A., Malach, R., & Pascual-Leone, A. (2005). Negative BOLD differentiates visual imagery and perception. *Neuron, 48*, 859-872.

Amodio, D. & Frith, C. (2006). Meeting of minds: the medial frontal cortex and social cognition. *Nature Reviews Neuroscience 7*, 268-277.

Andreasen, N.C., O'Leary, D.S., Cizadlo, T., Arndt, S., Rezai, K., Watkins, L., Ponto, L.L., & Hichwa, D. (1995). Remembering the past: two facets of episodic memory explored with positron emission tomography. *American Journal of Psychiatry, 152,* 1576-1585.

Andrews-Hanna, J.R. (2012). The Brain's Default Network and Its Adaptive Role in Internal Mentation. *Neuroscientist, 18*, 251-270.

Andrews-Hanna, J.R., Reidler, J.S., Huang, C., & Buckner, R. (2010b). Evidence for the default network's role in spontaneous cognition. *Journal of Neurophysiology, 104*, 322-335.

Andrews-Hanna, J.R., Reidler, J.S., Sepulcre, J., Poulin, R., & Buckner, R. (2010a). Functional-anatomic fractionation of the brain's default network. *Neuron 65*(4), 550-562.

Anticevic, A., Cole, M.W., Murray, J.D., Corlett, P.R., Wang, X.J., & Krystal, J.H. (2012). The role of default network deactivation in cognition and disease. *Trends in Cognitive*

Sciences, 16(12), 583-592.

Anticevic, A., Repovs, G., Shulman, G.L., & Barch, D.M. (2010). When less is more: TPJ and default network deactivation during encoding predicts working memory performance. *NeuroImage, 49*, 2638-2648.

Antrobus, J.S. (1968). Information theory and stimulus-independent thought. *British Journal of Psychology, 59,* 423-430.

Antrobus, J. S., Singer, J.L., Goldstein, S., & Fortgang, M. (1970). Mindwandering and cognitive structure. *Transactions of the New York Academy of Sciences, 32,* 242-252.

Antrobus, J. S.,Singer, J.L., & Greenberg, S. (1966). Studies in the stream of consciousness: experimental enhancement and suppression of spontaneous cognitive processes. *Perceptual and Motor Skills, 23,* 399-417.

Arrington, C.M., Carr, T.H., Mayer, A.R., & Rao, S.M. (2000). Neural mechanisms of visual attention: object-based selection of a region in space. *Journal of Cognitive Neuroscience, 12,* 106-117.

Asplund, C.L., Todd, J.J., Snyder, A.P., & Marois, R. (2010). A central role for the lateral prefrontal cortex in goal-directed and stimulus-driven attention. *Nature Neuroscience, 13*(4), 507-512.

Barry, R.J., Clarke, A.R., Johnstone, S.J., Magee, C.a., & Rushby, J.A. (2007). EEG differences between eyes-closed and eyes-open resting conditions. *Clinical Neurophysiology, 118*, 2765-2773.

Beckmann, C.F., DeLuca, M., Devlin, J.T., & Smith, S.M. (2005). Investigations into resting-state connectivity using independent component analysis. *Philosophical Transactions of the Royal Society B: Biological Sciences, 360*, 1001-1013

Benoit, R., Gilbert, S., Volle, E., & Burgess, P. (2010). When I think about me and simulate you: medial rostral prefrontal cortex and self-referential processes. *NeuroImage, 50*, 1340-1349.

Berger, H. (1931/1969). On the electroencephalogram of man: third report. *Electroencephalography and Clinical Neurophysiology, 28,* 95-132.

Binder, J. R., Frost, J. A., Hammeke, T. A., Bellgowan, P. S., Rao, S. M., & Cox, R. W. (1999). Conceptual processing during the conscious resting state. A functional MRI study. *Journal of Cognitive Neuroscience, 11,* 80-95.

Biswal, B.B., Yetkin, F.Z., Haughton, V.M., & Hyde, J.S., (1995). Functional connectivity in the motor cortex of resting human brain using echo-planar MRI. *Magnetic Resonance in Medicine, 34*, 537-541.

Bledowski, C., Prvulovic, D., Goebel, R., Zanella, F.E., & Linden, D.E. (2004). Attentional systems in target and distractor processing: a combined ERP and fMRI study. *NeuroImage, 22,* 530-540.

Bluhm, R.L., Osuch, E.A., Lanius, R.A., Boksman, K., Neufeld, R.W.J., Theberge, J., & Williamson, P. (2008). Default mode network connectivity: effects of age, sex, and analytic approach. *NeuroReport, 19*, 887-891.

Bonnellea, V., Hama, T.E., Leecha, R., Kinnunenc, K.M., Mehtad, M.A., Greenwoode, R.J., & Sharpa, D.J. (2012). Salience network integrity predicts default mode network function after traumatic brain injury. *Proceedings of the National Academy of Sciences of the United States of America, 109*(12), 4690-4695.

Botvinick, M.M., Cohen, J.D., & Carter, C.S. (2004). Conflict monitoring and anterior cingulate cortex: an update. *Trends in Cognitive Sciences, 8*(12), 539-546.

Botvinick, M.M., Nystrom, L.E., Fissell, K., Carter, C.S., & Cohen, J.D. (1999). Conflict monitoring versus selection-for-action in anterior cingulate cortex. *Nature, 402*(6758), 179-181.

Brazdil, M., Dobsik, M., Mikl, M., Hlustik, P., Daniel, P., Pazourkova, M., Krupa, P., & Rektor, I. (2005). Combined event-related fMRI and intracerebral ERP study of an auditory oddball task. *NeuroImage, 26*, 285-293.

Brodbeck, V., Kuhn, A., von Wegner, F., Morzelewski, A., Tagliazucchi, E., Borisov, S., Michel, C.M., & Laufs, H. (2012). EEG microstates of wakefulness and NREM sleep. *NeuroImage, 62*(3), 2129-2139.

Broyd, S.J., Demanuele, C., Debener, S., Helps, S.K., James, C.J., & Sonuga-Barke, E.J. (2008). Default-mode brain dysfunction in mental disorders: a systematic review. *Neuroscience and Behavioural Reviews, 33*(3), 279-296.

Buckner, R.L. (2003). Functional-anatomic correlates of control processes in memory. *Journal of Neuroscience, 23*, 3999-4004.

Buckner, R.L., Andrews-Hanna, J.R., & Schacter, D.L. (2008). The brain's default network: anatomy, function and relevance to disease. *Annals of the New York Academy of Sciences, 1124*, 1-38.

Buckner, R.L, & Carroll, D.C. (2007). Self-projection and the brain. *Trends in Cognitive Sciences 11*, 49-57.

Buckner, R. L., Raichle, M. E., Miezin, F. M., & Petersen, S. E. (1996). Functional anatomic studies of memory retrieval for auditory words and visual pictures. *Journal of Neuroscience, 16,* 6219-6235.

Buckner, R.L., Sepulcre, J., Talukdar, T., Krienen, F.M., Liu, H., Hedden, T., Andrews-Hanna,

J.R., Sperling, R.A., & Johnson, K.A. (2009). Cortical hubs revealed by intrinsic functional connectivity: mapping, assessment of stability, and relation to Alzheimer's disease. *Journal of Neuroscience, 29,* 1860-1873.

Buckner, R. L., & Vincent, J. L. (2007). Unrest at rest: default activity and spontaneous network correlations. *NeuroImage, 37,* 1091-1096.

Buxton, R.B. (2009). *Introduction to Functional Magnetic Resonance Imaging: Principles and Techniques.* Cambridge University Press, Cambridge, UK.

Cabeza, R., Ciaramelli, E., Olson, I.R., & Moscovitch, M. (2008). The parietal cortex and episodic memory: an attentional account. *Nature Reviews Neuroscience, 9*, 613-625.

Carter, A.R., Astafiev, S.V., Lang, C.E., Connor, L.T., Rengachary, J., Strube, M.J., Pope, D.L., Shulman, G.L., & Corbetta, M. (2010). Resting interhemispheric functional magnetic resonance imaging connectivity predicts performance after stroke. *Annals of Neurology, 67*(3), 365-375.

Cavanna, A.E., & Trimble, M.R. (2006). The precuneus: a review of its functional anatomy and behavioural correlates. *Brain, 129*(3), 564-583.

Chadick, J.Z., & Gazzaley, A. (2011). Differential coupling of visual cortex with default or frontal-parietal network based on goals. *Nature Neuroscience, 14*, 830-832.

Chai, X.J., Nieto-Castanon, A., Ongur, D., & Whitfield-Gabrieli, S. (2012). Anticorrelations in resting state networks without global signal regression. *NeuroImage, 59*, 1420-1428.

Chang, C., Liu, Z., Chen, M.C., Liu, X., & Duyn, J.H. (2013). EEG correlates of time-varying BOLD functional connectivity. *NeuroImage, 72,* 227-236

Chen, A.C.N., Feng, W., Zhao, H., Yin, Y., & Wang, P. (2008). EEG default mode network in the human brain: Spectral regional field powers. *NeuroImage, 41*, 561-574

Chen, A.C.N., Zhao, H.X., & Feng, W.J. (2008). EEG default mode network: Gender consistency and difference. *International Journal of Psychophysiology*, 69(3), 184.

Christoff, K., Gordon, A., Smallwood, J., Smith, R., & Schooler, J. (2009). Experience sampling during fMRI reveals default network and executive system contributions to mind wandering. *Proceedings of the National Academy of Sciences of the United States of America, 106*, 8719-8724

Connolly, J.D., Goodale, M.A., Menon, R.S., & Munoz, D.P. (2002). Human fMRI evidence for the neural correlates of preparatory set. *Nature Neuroscience*, *5,* 1345-1352.

Corbetta, M., Kincade, J. M., Ollinger, J. M., McAvoy, M. P., & Shulman, G. L. (2000). Voluntary orienting is dissociated from target detection in human posterior parietal cortex. *Nature Neuroscience, 3*(3), 292-297.

Corbetta, M., Patel, G., & Shulman, G.L. (2008). The reorienting system of the human brain: from environment to theory of mind, *Neuron,* 58(3), 306-324.

Corbetta, M., & Shulman, G. L. (2002). Control of goal-directed and stimulus-driven attention in the brain. *Nature Reviews Neuroscience, 3*(3), 201-215.

Coull, J.T., Frith, C.D., Frackowiak, R.S.J., & Grasby, P.M. (1996). A fronto-parietal network for rapid visual information processing : a PET study of sustained attention and working memory. *Neuropsychologia, 34*, 1085-1095.

Coull, J.T., Nobre, A.C. & Frith, C.D. (2001). The noradrenergic alpha2 agonist clonidine modulates behavioural and neuroanatomical correlates of human attentional orienting and alerting. *Cerebral Cortex, 11*, 73-84.

D'Argembeau A, Stawarczyk D, Majerus S, Collette F, Van der Linden M, Feyers D, Maquet, P., & Salmon, E. (2010). The neural basis of personal goal processing when envisioning

future events. *Journal of Cognitive Neuroscience, 22*(8), 1701-1703.

D'Argembeau, A., & Van der Linden, M. (2004). Phenomenal characteristics associated with projecting oneself back into the past and forward into the future: Influence of valence and temporal distance. *Consciousness and Cognition, 13*(4), 844-858.

Damoiseaux, J.S., Beckmann, C.F., Arigita, E., Barkhof, F., Scheltens, P., Stam, C.J., Smith, S.M., & Rombouts, S.A.R.B. (2008). Reduced resting-state brain activity in the "default network" in normal aging. *Cerebral Cortex 18*(8),1856-1854.

Damoiseaux, J.S., Rombouts, S.A., Barkhof, F., Scheltens, P., Stan, C.J., Smith, S.M., & Beckman, C.F. (2006). Consistent resting-state networks across healthy subjects. *Proceedings of the National Academy of Sciences of the United States of America, 103*, 13848-13853.

Daselaar, S.M., Prince, S.E., & Cabeza, R. (2004). When less means more: deactivations during encoding that predict subsequent memory. *NeuroImage 23*, 921-927.

De Luca, M., Beckmann, C.F., De Stefano, N., Matthews, P.M., & Smith, S.M. (2006). fMRI resting state networks define distinct modes of long-distance interactions in the human brain. *NeuroImage, 29*, 1359-1367.

Delamillieure, P., Doucet, G., Mazoyer, P., Turbelin, M-R., Delcroix, N., Mellet E., Zago, L., Crivello, F., Petit, L., Tzourio-Mazoyer, N., & Joliot, M. (2010). The resting state questionnaire: an introspective questionnaire for evaluation of inner experience during the conscious resting state. *Brain Research Bulletin, 81*, 565-573.

Dodell-Feder, D., Koster-Hale, J., Bedny, M., & Saxe, R. (2011). fMRI item analysis in a theory of mind task. *NeuroImage 55*(2), 705-712.

Drevets ,W.C., Burton, H., Videen, T.O., Snyder, A.Z., Simpson, J.R.J., & Raichle, M.E. (1995).

Blood flow changes in human somatosensory cortex during anticipated stimulation. *Nature, 373*, 249-252.

Elliott, R. (2003). Executive functions and their disorders. *British Medical Bulletin, 65*(1), 49-59.

Fair, D.A., Cohen, A.L., Dosenbach, N.U.F., Church, J.A., Miezin, F.M., Barch, D.M., Raichle, M.E., Petersen, S.E., & Schlaggar, B.L. (2007). The maturing architecture of the brain's default network. *Proceedings of the National Academy of Sciences of the United States of America, 105*(10), 4028-4032.

Fan, J., Flombaum, J. I., McCandliss, B. D., Thomas, K. M., & Posner, M. I. (2003). Cognitive and brain consequences of conflict. *NeuroImage, 18*(1), 42-57.

Fan, J., Gu, X., Guise, K.G., Xun Liu, X., Fossella, J., Wang, H., & Posner, M.I. (2009). Testing the behavioral interaction and integration of attentional networks . *Brain and Cognition, 70*, 209-220.

Fan, J., McCandliss, B.D., Fossella, J., Flombaum, J.I., & Posner, M.I. (2005). The activation of attentional networks. *NeuroImage, 26*, 471-479.

Fichtenholtz, H., Dean, H., Dillon, D., Yamasaki, H., McCarthy, G., & LaBar, K. (2004). Emotion-attention network interactions during a visual oddball task. *Cognitive Brain Research, 20*, 67-80.

Fox, M.D., Corbetta, M., Snyder, A.Z., Vincent, J.L., & Raichle, M.E. (2006b). Spontaneous neuronal activity distinguishes human dorsal and ventral attention systems. *Proceedings of the National Academy of Sciences of the United States of America, 103,* 10046-10051.

Fox, M.D., Raichle, M.E., (2007). Spontaneous fluctuations in brain activity observed with functional magnetic resonance imaging. *Nature Reviews Neuroscience, 8*, 700-711.

Fox, M.D., Snyder, A.Z., Vincent, J.L., Corbetta, M., Van Essen, D.C., & Raichle, M.E. (2005). The human brain is intrinsically organised into dynamic, anticorrelated functional networks. *Proceedings of the National Academy of Sciences of the United States of America, 102,* 9673-9678.

Fox, M.D., Snyder, A.Z., Zacks, J.M., Raichle, M.E., (2006a). Coherent spontaneous activity accounts for trial-to-trial variability in human evoked brain responses. *Nature Neuroscience, 9*, 23-25.

Fox, M.D., Zhang, D., Snyder, A.Z., & Raichle, M.E. (2009). The global signal and observed anticorrelated resting state brain networks. *Journal of Neurophysiology, 101*, 3270-3283.

Fransson, P. (2005). Spontaneous low-frequency BOLD signal fluctuations: An fMRI investigation of the resting-state default mode of brain function hypothesis. *Human Brain Mapping, 26*, 15-29.

Fransson, P. (2006). How default is the default mode of brain function? Further evidence from intrinsic BOLD signal fluctuations. *Neuropsychologia, 44,* 2836-2845.

Fransson, P., & Marrelec, G. (2008). The precuneus/posterior cingulate cortex plays a pivotal role in the default mode network: Evidence from a partial correlation network analysis. *NeuroImage, 42*, 1178-1184.

Friston, K.J., Frith, C.D., Liddle, P.F., & Frackowiak, R.S. (1993). Functional connectivity: the principal-component analysis of large (PET) data sets. *Journal of Cerebral Blood Flow And Metabolism, 13*, 5-14.

Gaab, N., Gabrieli, J.D., & Glover, G.H. (2007). Assessing the influence of scanner background noise on auditory processing. II. An fMRI study comparing auditory processing in the absence and presence of recorded scanner noise using a sparse design. *Human Brain*

Mapping, 28(8), 721-732.

Gallagher, S. (2000). Philosophical conceptions of the self: implications for cognitive science. *Trends in Cognitive Sciences, 4*(1), 14-21.

Ganzetti, M., & Mantini, D. (2013). Functional connectivity and oscillatory neuronal activity in the resting human brain. *Neuroscience, 240*, 297-309.

Gerlach, K.D., Spreng, R.N., Gilmore, A.W., & Schacter, D.L. (2011). Solving future problems: Default network and executive activity associated with goal-directed mental simulations. *NeuroImage, 55*, 1816-1824.

Ghatan, P. H., Hsieh, J. C., Wirsen-Meurling, A., Wredling, R., Eriksson, L., Stone-Elander, D., Levander, S., & Ingvar, M. (1995). Brain activation induced by the perceptual maze test: a PET study of cognitive performance. *NeuroImage, 2,* 112–24.

Giambra, L.M. (1995). A laboratory method for investigating influences on switching attention to task-unrelated imagery and thought. *Consciousness and Cognition, 4*(1), 1-21.

Giambra, L.M. (1989). Task-unrelated-thought frequency as a function of age: a laboratory study. *Psychology and Aging, 4*(2), 136-143.

Gilbert, S.J., Frith, C.D., & Burgess, P.W. (2005). Involvement of rostral prefrontal cortex in selection between stimulus-oriented and stimulus-independent thought. *European Journal of Neuroscience, 21*(5), 1423-1431.

Gilbert, S. J., Dumontheil, I., Simons, J. S., Frith, C. D., & Burgess, P. W. (2007). Comment on "Wandering minds: the default network and stimulus-independent thought". *Science, 317,* 43.

Gilbert, S. J., Simons, J. S., Frith, C. D., & Burgess, P. W. (2006). Performance-related activity in medial rostral prefrontal cortex (area 10) during low-demand tasks. *Journal of*

Experimental Psychology: Human Perception and Performance, 32, 45–58.

Gillebert, C.R., & Mantini, D. (2013). Functional connectivity in the normal and injured brain. *Neuroscientist*, http://dx.doi.org/10.1177/ 1073858412463168.

Grady, C.L., Springer, M.V., Hongwanishkul, D., McIntosh, A.R., & Winocur, G. (2006). Age-related changes in brain activity across the adult lifespan. *Journal of Cognitive Neuroscience, 18*(2), 227-241

Greene, J. D., Sommerville, R. B., Nystrom, L. E., Darley, J. M., & Cohen, J. D. (2001). An fMRI investigation of emotional engagement in moral judgment. *Science, 293,* 2105-2108.

Greene, J., & Haidt, J. (2002). How (and where) does moral judgment work? *Trends in Cognitive Sciences, 6,* 517-523.

Greicius, M.D., Krasnow, B., Reiss, A.L., & Menon, V. (2003). Functional connectivity in the resting brain: a network analysis of the default mode hypothesis. *Proceedings of the National Academy of Sciences of the United States of America, 100*, 253-258.

Greicius, M.D., & Menon, V. (2004). Default-mode activity during a passive sensory task: uncoupled from deactivation but impacting activation. *Journal of Cognitive Neuroscience, 16*, 1484-1492.

Greicius, M.D., Srivastava, G., Reiss, A.L., & Menon, V. (2004). Default-mode network activity distinguishes Alzheimer's disease from healthy aging: evidence from functional MRI. *Proceedings of the National Academy of Sciences of the United States of America, 101*, 4637-4642.

Gusnard, D. A., & Raichle, M. E. (2001). Searching for a baseline: functional imaging and the resting human brain. *Nature Reviews Neuroscience, 2,* 685-694.

Gusnard, D. A., Akbudak, E., Shulman, G. L., & Raichle, M. E. (2001). Medial prefrontal cortex and self-referential mental activity: relation to a default mode of brain function. *Proceedings of the National Academy of Sciences of the United States of America, 98,* 4259-4264.

Hagmann, P., Cammoun, L., Gigandet, X., Meuli, R., Honey, C.J., Wedeen, V.J., & Sporns, O. (2008). Mapping the structural core of human cerebral cortex. *PLoS BIOLOGY, 6*(7), e159. doi:10.1371/journal.pbio.0060159

Hahn, B., Ross, T. J., & Stein, E. A. (2007). Cingulate activation increases dynamically with response speed under stimulus unpredictability. *Cerebral Cortex, 17,* 1664-1671.

Haxby, J. V., Horwitz, B., Ungerleider, L. G., Maisog, J. M., Pietrini, P., & Grady, C. L. (1994). The functional organization of human extrastriate cortex: a PET-rCBF study of selective attention to faces and locations. *Journal of Neuroscience, 14,* 6336-6353.

Hayden, B.Y., Smith, D.V., & Platt, M.L. (2010). Cognitive control signals in posterior cingulate cortex. *Frontiers in Human Neuroscience, 4*(223), doi:10.3389/fnhum.2010.00223.

Hayes, S.M., Salat, D.H., & Verfaellie, M. (2012). Default network connectivity in medial temporal lobe amnesia. *Journal of Neuroscience, 32*(42),14622-14629.

He, B.J., Snyder, A.Z., Vincent, J.L., Epstein, A., Shulman, G.L., & Corbetta, M. (2007). Breakdown of functional connectivity in frontoparietal networks underlies behavioral deficits in spatial neglect. *Neuron, 53,* 905-918.

Helps, S., James, C., Debener, S., Karl1, A., & Sonuga-Barke, E.J.S. (2008). Very low frequency EEG oscillations and the resting brain in young adults: a preliminary study of localisation, stability and association with symptoms of inattention. *Journal of Neural Transmission, 115*, 279-285.

Hlinka, J., Alexakis, C., Diukova, A., Liddle, P.F., & Auer, D.P. (2010). Slow EEG pattern predicts reduced intrinsic functional connectivity in the default mode network: an inter-subject analysis. *NeuroImage, 53*, 239-246.

Ingvar, D. H. (1979). "Hyperfrontal" distribution of the cerebral grey matter flow in resting wakefulness: on the functional anatomy of the conscious state. *Acta Neurologica Scandinavia, 60,* 12-25.

Ingvar, D. H. (1985). "Memory of the future": an essay on the temporal organization of conscious awareness. *Hum. Neurobiology, 4,* 127-36.

Ino, T., Nakai, R., Azuma, T., Kimura, T., Fukuyama, H. (2011). Brain Activation During Autobiographical Memory Retrieval with Special Reference to Default Mode Network. *The Open Neuroimaging Journal, 5*, 14-23.

Jann, K., Dierks, T., Boesch, C., Kottlowa, M., Strik, W., & Koenig, T. (2009). BOLD correlates of EEG alpha phase-locking and the fMRI default mode network. *NeuroImage, 45*, 903-916.

Jann, K., Kottlow, M., Dierks, T., Boesch, C., & Koenig, T. (2010). Topographic electrophysiological signatures of fMRI resting state networks. *PLoS ONE, 5*(9), e12945. doi: 10.1371/journal.pone.0012945.

Jorge, J., van der Zwaag, W., & Figueiredo, P. (2013). EEG–fMRI integration for the study of human brain function, *NeuroImage*, http://dx.doi.org/ 10.1016/j.neuroimage.2013.05.114

Kane, M.J., & Engle, R.W. (2002). The role of prefrontal cortex in working-memory capacity, executive attention, and general fluid intelligence: An individual-differences perspective. *Psychonomic Bulletin & Review, 9*(4), 637-671.

Kawashima, R., O'Sullivan, B., & Roland, P. (1995). Positron-emission tomography studies of

cross-modality inhibition in selective attention tasks: Closing the “minds eye’. *Proceedings of the National Academy of Sciences of the United States of America,* 92, 5969-5972.

Kedzior, K.K., Koch, M., & Basar-Eroglu, C. (2007). Auditory-evoked EEG oscillations associated with prepulse inhibition (PPI) of auditory startle reflex in healthy humans. *Brain Research, 1163*, 111-118.

Killingsworth M, & Gilbert D. (2010). A wandering mind is an unhappy mind. *Science, 330*, 932.

Kim, D.I., Mathalon, D.H., Ford, J.M., Mannell, M., Turner, J.A., Brown, G.G., Belger, A., Gollub, R., Lauriello, J., Wible, C., O'Leary, D., Lim, K., Toga, A., Potkin, S.G., Birn, F., & Calhoun, V.D. (2009). Auditory oddball deficits in schizophrenia: an independent component analysis of the fMRI multisite function BIRN study. *Schizophrenia Bulletin, 35*(1), 67-81.

Kim, D.Y., & Lee, J.H. (2011). Are posterior default-mode networks more robust than anterior default-mode networks? Evidence from resting-state fMRI data analysis. *Neuroscience Letters, 498*(1), 57-62.

Kim, H. (2012). A dual-subsystem model of the brain's default network: Self-referential processing, memory retrieval processes, and autobiographical memory retrieval, *NeuroImage, 61*, 966-977.

Kincade, J.M., Abrams, R.A., Astafiev, S.V., Shulman, G.L., & Corbetta, M. (2005). An event-related functional magnetic resonance imaging study of voluntary and stimulus-driven orienting of attention. *Journal of Neuroscience, 25,* 4593-4604.

Klinger, E., & Cox, W. (1987). Dimensions of thought flow in every-day life. *Imagination*

Cognition and Personality, 7(2), 105-128.

Knyazev, G.G. (2013). EEG correlates of self-referential processing. *Frontiers in Human Neuroscience, 7*, 264, doi: 10.3389/fnhum.2013.00264.

Knyazev, G.G., Bocharov, A.V., & Pylkova, L.V. (2012). Extraversion and fronto-posterior EEG spectral power gradient: an independent component analysis. *Biological Psychology, 89*(2), 515-524.

Knyazev, G.G., Slobodskoj-Plusnin, J.Y., Bocharov, A.V., & Pylkova, L.V. (2011). The default mode network and EEG alpha oscillations: An independent component analysis. *Brain Research, 1402*, 67-79.

Koechlin, R., & Summerfield, C. (2007). An information theoretical approach to prefrontal executive function. *Trends in Cognitive Sciences, 11*(6), 229-235.

Laufs, H., Holt, J.L., Elfont, R., Krams, M., Paul, J.S., Krakow, K., & Kleinschmidt, A. (2006). Where the BOLD signal goes when alpha EEG leaves. *NeuroImage, 31*, 1408-1418.

Laufs, H., Kleinschmidt, A., Beyerle, A., Eger, E., Salek-Haddadi, A., Preibisch, C., Krakow, K. (2003a). EEG-correlated fMRI of human alpha activity. *NeuroImage, 19*, 1463-1476.

Laufs, H., Krakow, K., Sterzer, P., Eger, E., Beyerle, A., Salek- Haddadi, A., & Kleinschmidt, A. (2003b). Electroencephalographic signatures of attentional and cognitive default modes in spontaneous brain activity at rest. *Proceedings of the National Academy of Sciences of the United States of America, 100*, 11053-11058.

Lee, M.H., Hacker, C.D., Snyder, A.Z., Corbetta, M., Zhang, D., Leuthardt, E.C., & Shimony, J.S. (2012a). Clustering of Resting State Networks. *PLoS ONE, 7*(7), doi:10.1371/journal.pone.0040370.

Lee, M.H., Smyser, C.D., Shimony, J.S. (2012b). Resting-State fMRI: A Review of Methods and

Clinical Applications. *American Society of Neuroradiology*, http://dx.doi.org/10.3174/ajnr.A3263.

Leech, R., Braga, R., & Sharp, D.J. (2012). Echoes of the Brain within the Posterior Cingulate Cortex. *The Journal of Neuroscience, 31*(1), 215-222.

Leech, R., & Sharp, D.J. (2013). The role of the posterior cingulate cortex in cognition and disease. *Brain*, doi:10.1093/brain/awt162.

Li, H. (2009). EEG Default Mode Network: Laterality Index of Spectral and Regional alpha EEG Asymmetry. *NeuroImage, 47*(1), 82.

Li, C.S. Yan, P., Bergquist, K. L., & Sinha, R. (2007). Greater activation of the "default" brain regions predicts stop signal errors. *NeuroImage, 38,* 640-648.

Linden, D.E.J., Prvulovic, D., Formisano, E., Vollinger, M., Zanella, F.E., Goebel, R., & Dierks, T. (1999). The functional neuroanatomy of target detection: An fMRI study of visual and auditory oddball tasks. *Cerebral Cortex, 9*, 815-823.

Liu, X., Banich, M. T., Jacobson, B. L., & Tanabe, J. L. (2004). Common and distinct neural substrates of attentional control in an integrated Simon and spatial Stroop task as assessed by event-related fMRI. *NeuroImage, 22*(3), 1097-1106.

Lombardo M, Chakrabarti B, Bullmore E, Wheelwright S, Sadek S, Suckling J., MRC AIMS Consortium, & Baron-Cohen, S. (2010). Shared neural circuits for mentalizing about the self and others. *Journal of Cognitive Neuroscience, 22*, 1623-1635.

Long, X.-Y., Zuo, X.-N., Kiviniemi, V., Yang, Y., Zou, Q., Zhu, C.-Z., Jiang, T., Yang, H., Gong, Q.-Y., Wang, L., Li, K., Xie, S., & Zang, Y. (2008). Default mode network as revealed with multiple methods for resting-state functional MRI analysis. *Journal of Neuroscience Methods, 171*, 349-355.

Mantini, D., Perrucci, M.G., Del Gratta, D., Romani, G.L., & Corbetta, M. (2007). Electrophysiological signatures of resting state networks in the human brain. *Proceedings of the National Academy of Sciences of the United States of America, 104*, 13170-13175.

Mars, R.B., Neubert, F-Z., Noonan, A.P., Sallet, J., Toni, I., Rushworth, F.S. (2012). On the relationship between the "default mode network" and the "social brain'. *Frontiers in Human Neuroscience*, doi: 10.3389/fnhum.2012.00189.

Martuzzi, R., Ramani, R., Qiu, M., Rajeevan, N., & Constable, R.T. (2010). Functional connectivity and alterations in baseline brain state in humans. *NeuroImage, 49*, 823-834.

Mason, M. F., Norton, M. I., Van Horn, J. D., Wegner, D. M., Grafton, S. T., & Macrae, C. N. (2007). Wandering minds: the default network and stimulus-independent thought. *Science, 315,* 393-395.

Mazoyer, B., Zago, L., Mellet, E., Bricogne, S., Etard, O., Houde, O., Crivello, F., Joliot, M., Petit, L., & Tzourio-Mazoyer, N. (2001). Cortical networks for working memory and executive functions sustain the conscious resting state in man. *Brain Research Bulletin, 54,* 287-298.

McGuire, P.K., Paulesu, E., Frackowiak, R.S., & Frith, C.D. (1996). Brain activity during stimulus independent thought. *NeuroReport, 7*(13), 2095-2099.

McKiernan, K.A., D'Angelo, B.R., Kaufman, J.N., Binder, J.R. (2006). Interrupting the "stream of consciousness": an fMRI investigation. *NeuroImage, 29*, 1185-1191.

McKiernan, K.A., Kaufman, J.N., Kucera-Thompson, J., & Binder, J.R. (2003). A parametric manipulation of factors affecting task-induced deactivation in functional neuroimaging. *Journal of Cognitive Neuroscience, 15,* 394-408.

Meltzer, J.A., Negishi, M., Mayes, L.C., & Constable, R.T. (2007). Individual differences in

EEG theta and alpha dynamics during working memory correlate with fMRI responses across subjects. *Clinical Neurophysiology, 118*, 2419-2436.

Menon, V., & Uddin, L.Q. (2010). Saliency, switching, attention and control: a network model of insula function. *Brain Structure and Function, 214*(5-6), 655-667.

Mevel, K., Chetelat, G., Eustache, F., & Desgranges, B. (2011). The Default Mode Network in Healthy Aging and Alzheimer's Disease. *International Journal of Alzheimer's Disease,* http://dx.doi.org/10.4061/2011/535816.

Miller, S.J., Celone, K., DePeau, K., Diamond, E., Dickerson, B.C., Rentz, D., Pihlajamäki, M., & Sperling, R.A. (2008). Age-related memory impairment associated with loss of parietal deactivation but preserved hippocampal activation. *Proceedings of the National Academy of Sciences of the United States of America, 105(*6), 2181-2186.

Moll, J., Zahn, R., de Oliveira-Souza, R., Krueger, F., & Grafman, J. (2005). Opinion: the neural basis of human moral cognition. *Nature Reviews Neuroscience, 6,* 799-809.

Morcom, A. M., & Fletcher, P. C. (2007). Does the brain have a baseline? Why we should be resisting a rest. *NeuroImage, 37,* 1073-82.

Murphy, K., Birn, R.M., Bandettini, P.A. (2013). Resting-state fMRI confounds and cleanup. *NeuroImage, 80*, 349-359.

Mutschler, I., Wieckhorst, B., Speck, O., Schulze-Bonhage, A., Hennig, J., Seifritz, E., & Ball, T. (2010). Time scales of auditory habituation in the amygdala and cerebral cortex. *Cerebral Cortex, 20*(11), 2531-2539.

Northoff, G., Heinzel, A., de Greck, M., Bermpohl, G., Dobrowolny, H., & Panksepp, J. (2006). Self-referential processing in our brain - a meta-analysis of imaging studies on the self. *NeuroImage, 31*, 440-457.

Okuda, J., Fujii, T., Ohtake, H., Tsukiura, T., Tanji, K., Suzuki, K., Kawashima, R., Fukuda, H., Itoh, M., & Yamadori, A. (2003). Thinking of the future and past: the roles of the frontal pole and the medial temporal lobes. *NeuroImage, 19,* 1369-1380.

Ongur, D. & Price, J.L. (2000). The Organization of Networks within the Orbital and Medial Prefrontal Cortex of Rats, Monkeys and Humans. *Cerebral cortex, 10*(3), 206-219.

Pascual-Marqui, R.D. (2002). Standardized low-resolution brain electromagnetic tomography (sLORETA): technical details. *Methods and Findings in Experimental and Clinical Pharmacology, 24*(Suppl. D), 5-12.

Pessoa, L., Gutierrez, E., Bandettini, P., & Ungerleider, L. (2002). Neural correlates of visual working memory: fMRI amplitude predicts task performance. *Neuron, 35,* 975-987.

Petersen, S.E., & Dubis, J.W. (2012). The mixed block/event-related design. *NeuroImage, 62(2)*, 1177-1184.

Posner, M.I. (2008). Measuring Alertness. *Annals of the New York Academy of Sciences, 1129*, 193-199.

Posner, M.I., & Cohen, Y. (1984). Components of visual orienting. In H. Bouma & K. Kenison (Eds.), *Attention and Performance X: Control of Language Processes* (pp. 531-556). Hillsdale, NJ: Erlbaum.

Posner, M.I., & Rothbart, M.K. (2007). Research on Attention Networks as a Model for the Integration of Psychological Science. *Annual Review of Psychology, 58*, 1-23.

Posner, M.I., Walker, J.A., Friedrich, F.J., & Rafal, R.D. (1984). Effects of parietal injury on covert orienting of attention. *Journal of Neuroscience, 4*(7), 1863-1874.

Power, J.D., Barnes, K.A., Snyder, A.Z., Schlaggar, B.L., & Petersen, S.E. (2012). Spurious but systematic correlations in functional connectivity MRI networks arise from subject

motion. *NeuroImage, 59*, 2142–2154.

Power, J., Fair, D., Schlaggar, B., & Petersen, S. (2010). The development of human functional brain networks. *Neuron* 67, 735-748.

Preminger, S., Harmelech, T., & Malach, R. (2011). Stimulus-free thoughts induce differential activation in the human default network. *NeuroImage, 54*, 1692-1702.

Rabin, J.S., Gilboa, A., Stuss, D,T., Mar, R.A., & Rosenbaum, R.S. (2010). Common and unique neural correlates of autobiographical memory and theory of mind. *Journal of Cognitive Neuroscience, 22*(6), 1095-1111.

Race, E., Keane, M.M., & Verfaellie, M. (2011). Medial temporal lobe damage causes deficits in episodic memory and episodic future thinking not attributable to deficits in narrative construction. *Journal of Neuroscience, 31*(28), 10262-10269.

Raichle, M. E., & Snyder, A. Z. (2007). A default mode of brain function: a brief history of an evolving idea. *NeuroImage, 37,* 1083-1090.

Raichle, M. E., MacLeod, A. M., Snyder, A. Z., Powers, W. J., Gusnard, D. A., & Shulman, G.L. (2001). A default mode of brain function. *Proceedings of the National Academy of Sciences of the United States of America, 98,* 676–82.

Ramnani, N., Owen, A.M. (2004). Anterior prefrontal cortex: insights into function from anatomy and neuroimaging. *Nature Reviews Neuroscience,* 5, 184-194.

Reniers, R.L., Corcoran, R., Völlm, B.A., Mashru, A., Howard, R., & Liddle, P.F. (2012). Moral decision-making, ToM, empathy and the default mode network. *Biological Psychology, 90*(3), 202-210.

Rosazza, C., Minati, L., Ghielmetti, F., Mandelli, M.L., & Bruzzone, M.G. (2012). Functional connectivity during resting-state functional MR imaging: study of the correspondence

between independent component analysis and region-of-interest-based methods. *American Journal of Neuroradiology, 33*, 180-187.

Sajonz, B., Kahnt, T., Margulies, D., Park, S., Whittmann, A., Stoy, M., Strohle, A., Heinz, A., Northoff, G., & Bermpohl, F. (2010). Delineating self-referential processing from episodic memory retrieval: common and dissociable networks. *NeuroImage, 50*, 1606-1617.

Sambataro, F., Murty, V.P., Callicott, J.H., Tan, H.Y., Das, S., Weinberger, D.R., & Mattay, V.S. (2010). Age-related alterations in default mode network: impact on working memory performance. *Neurobiology of Aging, 31*(5), 839-852.

Saxe, R., & Kanwisher, N. (2003). People thinking about thinking people: the role of the temporo-parietal junction in "theory of mind". *NeuroImage, 19,* 1835-1842.

Saxe, R., & Powell, L. J. (2006). It's the thought that counts: specific brain regions for one component of theory of mind. *Psychological Science, 17,* 692-699.

Saxe, R., Carey, S., & Kanwisher, N. (2004). Understanding other minds: linking developmental psychology and functional neuroimaging. *Annual Review of Psychology, 55,* 87-124.

Schacter, D.L., & Addis, D.R. (2009). On the nature of medial temporal lobe contributions to the constructive simulation of future events. *Philosophical Transactions of the Royal Society (B), 364,* 1245-1253.

Scheeringa, R., Bastiaansen, M.C.M., Petersson, K.M., Oostenveld, R., Norris, D.G., Hagoort, P. (2008). Frontal theta EEG activity correlates negatively with the default mode network in resting state. *International Journal of Psychophysiology, 67*, 242-251.

Schooler, J., & Schreiber, C.A. (2004). Experience, Meta-consciousness, and the Paradox of Introspection. *Journal of Consciousness Studies, 11*(7-8), 17-39.

Seeley, W.W., Menon, V., Schatzberg, A.F., Keller, J., Glover, G.H., Kenna, H., Reiss, A.L., & Greicius, M.D., (2007). Dissociable intrinsic connectivity networks for salience processing and executive control. *Journal of Neuroscience, 27*(9), 2349-2356.

Sestieri, C., Corbetta, M., Romani, G.L., & Shulman, G.L. (2011). Episodic memory retrieval, parietal cortex, and the default mode network: functional and topographic analyses. *Journal of Neuroscience, 31*(12), 4407-4420.

Shulman, G.L., Astafiev, S.V., McAvoy, M.P., d'Avossa, G., & Corbetta, M. (2007). Right TPJ deactivation during visual search: functional significance and support for a filter hypothesis. *Cerebral Cortex, 17*, 2625-2633.

Shulman, G. L., Fiez, J. A., Corbetta, M., Buckner, R. L., Miezin, F. M., Raichle, M.E., & Petersen, S.E. (1997). Common blood flow changes across visual tasks: II.: decreases in cerebral cortex. *Journal of Cognitive Neuroscience, 9,* 648-663.

Shulman, G.L., Ollinger, J.M., Akbudak, E., Conturo, T.E., Snyder, A.Z., Petersen, S.E., & Corbetta, M. (1999). Areas involved in encoding and applying directional expectations to moving objects. *Journal of Neuroscience, 19,* 9480-9496.

Smallwood, J.M., Baracaia, S.F., Lowe, M., & Obonsawinb, M. (2003). Task unrelated thought whilst encoding information. *Consciousness and Cognition, 12*, 452-484.

Smallwood, J., Brown, K., Baird, B., & Schooler, J.W. (2012). Cooperation between the default mode network and the frontal–parietal network in the production of an internal train of thought. *Brain Research, 1428*, 60-70.

Smallwood, J., & Schooler, J.W. (2006). The restless mind. *Psychological Bulletin, 132*, 946-958.

Smith, S.M., Fox, P.T., Miller, K.L., Glahn, D.C., Fox, P.M., Mackay, C.E., Filippini, N.,

Watkins, K.E., Toro, R., Laird, A.R., & Beckmann, C.F. (2009). Correspondence of the brain's functional architecture during activation and rest. *Proceedings of the National Academy of Sciences of the United States of America, 106*, 13040-13045.

Sokoloff, L., Mangold, R., Wechsler, R. L., Kenney, C., & Kety, S. S. (1955). The effect of mental arithmetic on cerebral circulation and metabolism. *Journal of Clinical Investigation, 34,* 1101-1108.

Somers, D.C., Dale, A.M., Seiffert, A.E., Tootell, R.B. (1999). Functional MRI reveals spatially specific attentional modulation in human primary visual cortex. *Proceedings of the National Academy of Sciences of the United States of America, 96*, 1663-1668.

Sonuga-Barke, E.J.S., & Castellanos, F.X. (2007). Spontaneous attentional fluctuations in impaired states and pathological conditions: a neurobiological hypothesis. *Neurosciences and Biobehavioral Reviews, 31*, 977-986.

Spreng, N. (2012). The fallacy of a "task-negative" network. *Frontiers in Psychology*, doi: 10.3389/fpsyg.2012.00145.

Spreng, R.N., Mar, R.A., & Kim, A.S. (2009). The common neural basis of autobiographical memory, prospection, navigation, theory of mind, and the default mode: a quantitative meta-analysis. *Journal of Cognitive Neuroscience, 21*, 489-510.

Spreng, R.N., Stevens, W.D., Chamberlain, J.P., Gilmore, A.W., & Schacter, D.L. (2010). Default network activity, coupled with the frontoparietal control network, supports goal-directed cognition. *NeuroImage, 53*, 303-317.

Sridharan, D., Levitin, D.J., & Menon, V (2008). A critical role for the right fronto-insular cortex in switching between central-executive and default-mode networks. *Proceedings of the National Academy of Sciences of the United States of America, 105*(34), 12569-12574.

Stawarczyk, D., Majerus, S., Maquet, P., & D'Argembeau, A. (2011). Neural correlates of ongoing conscious experience: both task-unrelatedness and stimulus-independence are related to default network activity. *PLoS ONE 6*(2), e16997. doi:10.1371/journal.pone.0016997.

Sturm, W., & Willmes, K. (2001). On the functional neuroanatomy of intrinsic and phasic alertness. *NeuroImage, 14*, 76-84.

Svoboda, E., McKinnon, M. C., & Levine, B. (2006). The functional neuroanatomy of autobiographical memory: a meta-analysis. *Neuropsychologia, 44,* 2189-2208.

Szpunar, K. K., Watson, J. M., & McDermott, K. B. (2007). Neural substrates of envisioning the future. *Proceedings of the National Academy of Sciences of the United States of America, 104,* 642-647.

Teasdale, J.D., Dritschel, B.H., Taylor, M.J., Proctor, L., Lloyd, C.A., Nimmo-Smith, I., Baddeley, A.D. (1995). Stimulus-independent thought depends on central executive resources. *Memory and Cognition, 23*(5), 551-559.

Teasdale, J.D., Proctor, L., Lloyd, C.A., & Baddley, A.D. (1993). Working memory and stimulus independent thought: effects of memory load and presentation rate. *European Journal of Cognitive Psychology, 5*, 417-433.

Tulving, E. (1985). Memory and consciousness. *Canadian Psychology, 26*, 1-12.

Todd, J.J., Fougnie, D., & Marois, R. (2005). Visual short-term memory load suppresses temporo-parietal junction activity and induces inattentional blindness. Psychological Science, *16,* 965-972.

Uddin, L.Q., Kelly, A.M.C., Biswal, B.B., Castellanos, F.X., & Milham, M.P. (2009). Functional connectivity of default mode network components: correlation,

anticorrelation, and causality. *Human Brain Mapping, 30*(2), 625-637.

Van de Ven, V.G., Formisano, E., Prvulovic, D., Roeder, C.H., & Linden, D.E. (2004). Functional connectivity as revealed by spatial independent component analysis of fMRI measurements during rest. *Human Brain Mapping 22*(3), 165-178.

Van Dijk, K.R., Hedden, T., Venkataraman, A., Evans, K.C., Lazar, S.W., & Buckner, R.L. (2010). Intrinsic functional connectivity as a tool for human connectomics: theory, properties, and optimization. *Journal of Neurophysiology, 103*, 297-321.

Vanhatalo, S., Palva, J.M., Holmes, M.D., Miller, J.W., Voipio, J., & Kaila, K. (2004). Infraslow oscillations modulate excitability and interictal epileptic activity in the human cortex during sleep. *Proceedings of the National Academy of Sciences of the United States of America, 101(14)*, 5053-5057.

Vanhaudenhuyse, A., Noirhomme, Q., Tshibanda, L.J., Bruno, M.A., Boveroux, P., Schnakers, C., Soddu, A., Perlbarg, V., Ledoux, D., Brichant, J.F., Moonen, G., Maquet, O., Greicius, MD., Laureys, S., & Boly, M. (2010). Default network connectivity reflects the level of consciousness in non-communicative brain-damaged patients. *Brain, 133*, 161-171.

Verfaellie, M., Race, E., & Keane, M.M. (2012). Medial Temporal Lobe contributions to Future thinking: Evidence from Neuroimaging and Amnesia. *Psychology in Belgium, 52*(2-3), 77-94.

Verhaeghen, P., & Cerella, J. (2002). Aging, executive control, and attention: a review of meta-analyses. *Neuroscience & Biobehavioural Reviews, 26*(7), 849-857.

Vincent, J.L., Kahn, I., Snyder, A.Z., Raichle, M.E., Buckner, R.L., 2008. Evidence for a frontoparietal control system revealed by intrinsic functional connectivity. *Journal of*

Neurophysiology, 100, 3328-3342.

Vincent, J.L., Snyder, A.Z., Fox, M.D., Shannon, B.J., Andrews, J.R., Raichle, M.E. & Buckner, R.I. (2006). Coherent spontaneous activity identifies a hippocampal–parietal memory network. *Journal of Neurophysiology, 96*(6), 3517-3531.

Vossel, S., Thiel, C.M., & Fink, G.R. (2006). Cue validity modulates the neural correlates of covert endogenous orienting of attention in parietal and frontal cortex. *NeuroImage, 32,* 1257-1264.

Vossel, S., Weidner, R., Thiel, C.M., & Fink, G.R. (2009). What is "Odd" in Posner's Location-cueing Paradigm? Neural Responses to Unexpected Location and Feature Changes Compared. *Journal of Cognitive Neuroscience, 21*(1), 30-41.

Weissman-Fogel, I**.**, Moayedi, M., Taylor, K.S., Pope, G., & Davis, K.D. (2010). Cognitive and default-mode resting state networks: do male and female brains "rest" differently? *Human Brain Mapping, 11*, 1713-1726.

Weissman, D. H., Roberts, K. C., Visscher, K. M., & Woldorff, M. G. (2006). The neural bases of momentary lapses in attention. *Nature Neuroscience, 9,* 971-978.

Whitfield-Gabrieli, S., Moran, J.M., Nieto-Castanon, A., Triantafyllou, C., Saxe, R., & Gabrieli, J.D.E. (2011). Associations and dissociations between default and self-reference networks in the human brain. *NeuroImage, 55*, 225-32.

Whitfield-Gabrieli, S., & Nieto-Castanon, A. (2012). Conn: a functional connectivity toolbox for correlated and anticorrelated brain networks. *Brain Connect, 2*(3), 125-141.

Wojciulik, E., & Kanwisher, N. (1999). The Generality of Parietal Involvement in Visual Attention. *Neuron, 23*(4), 747-764.

Woodward, N.D., Rogers, B., & Heckers, S. (2011). Functional resting-state networks are differentially affected in schizophrenia. *Schizophrenia Research, 130*(1-3), 86-93.

Wolf, D.H., Turetsky, B.I., Loughead, J., Elliott, M.A., Pratiwadi, R., Gur, R.E., & Gur, R.C. (2008). Auditory Oddball fMRI in Schizophrenia: Association of Negative Symptoms with Regional Hypoactivation to Novel Distractors. *Brain Imaging and Behaviour, 2*(2), 132-145.

Yeo, B.T., Krienen, F.M., Sepulcre, J., Sabuncu, M.R., Lashkari, D., Holinshead, M., Roffman, J.L., Smoller, J.W., Zollei, L., Polimeni, J.R., Fischl, B., Liu, H., & Buckner, R.L. (2011). The organization of the human cerebral cortex estimated by intrinsic functional connectivity. *Journal of Neurophysiology, 106,* 1125-1165

Yuan, H., Zotev, V., Phillips, R., Drevets, W.C., & Bodurka, J. (2012). Spatiotemporal dynamics of the brain at rest - Exploring EEG microstates as electrophysiological signatures of BOLD resting state networks. *NeuroImage, 60,* 2062-2072.

Zhang, D., & Raichle, M.E. (2010). Disease and the brain's dark energy. *Nature Reviews Neuroscience, 6*, 15-28.

Zhou, J., Greicius, M.D., Gennatas, E.D., Growdon, M.E., Jang, J.Y., Rabinovici, G.D., Kramer, J.H., Weiner, M., Miller, B.L., & Seeley, W.W. (2010). Divergent network connectivity changes in behavioural variant frontotemporal dementia and Alzheimer's disease. *Brain, 133*, 1352-1367.

APPENDIX A

Key electroencephalographic preprocessing steps

This appendix presents examples of the outcome from key electroencephalographic preprocessing steps (outlined in section 4.2.5, chapter 4) that were conducted in experiment 1, analysis 2. Data presented are from a participant who produced both good EEG and fMRI data.

Step 1: Scanner Artifact Correction:

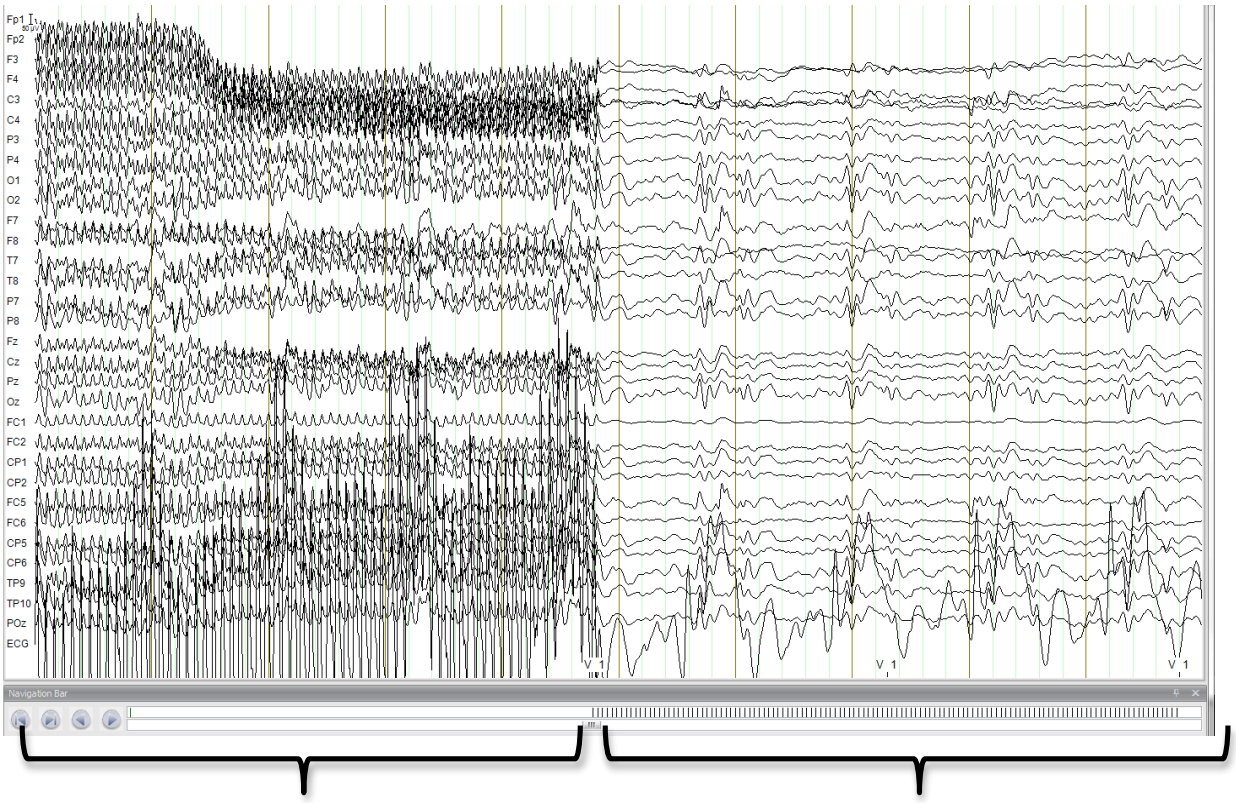

Figure A.1. EEG data before and after scanner artifact correction

Step 3: Segmentation of cardioballistic artifact: Illustrating how well *Pulse Artifact Correction* (step 2) corrected for cardioballistic effects (example illustrates frontal electrode *F7* (top image) and *ECG* electrode (bottom image):

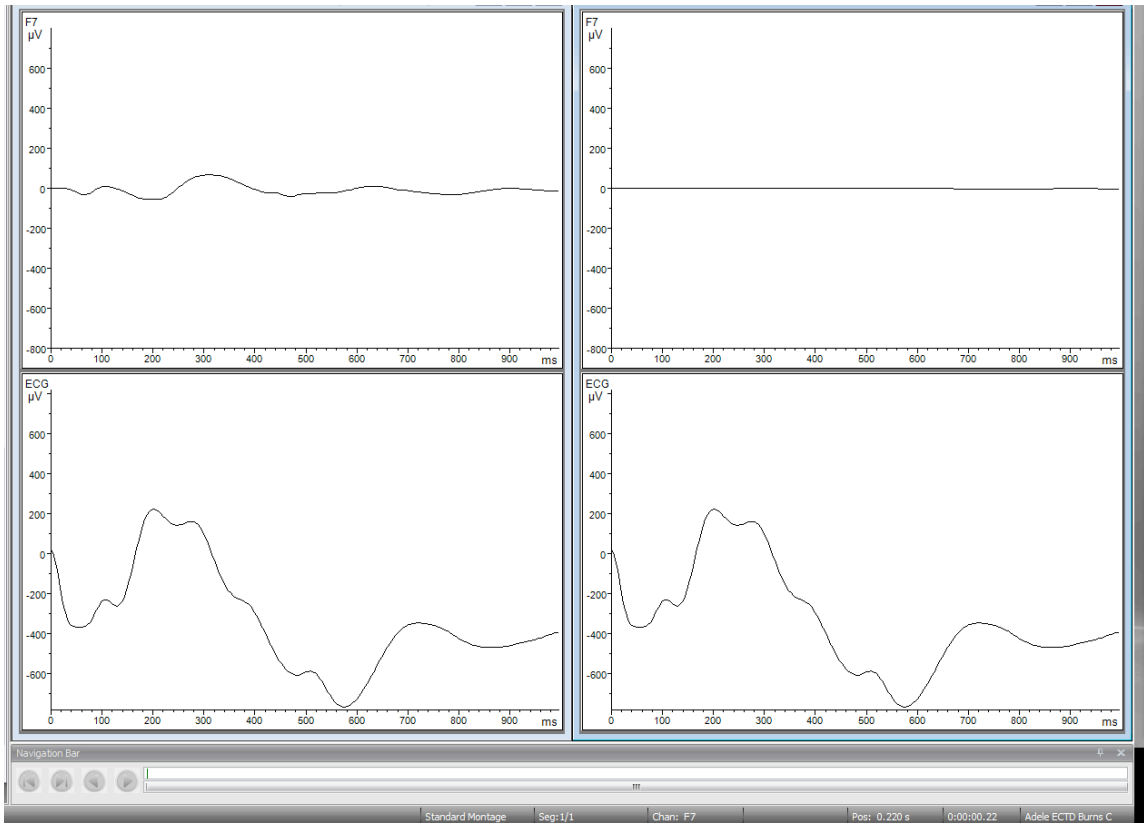

Figure A.2. Segmentation of cardioballistic artifact

Step 8: Filters: Application of a 1Hz Butterworth Zero Phase filter to data in order to filter out high frequency fluctuations in the beta frequency power calculations. Note that this varied between 1-5 Hz across participants. Channels illustrated here are Fz, Cz and Pz, which were most representative of the power signals across all other channels across the complete task duration:

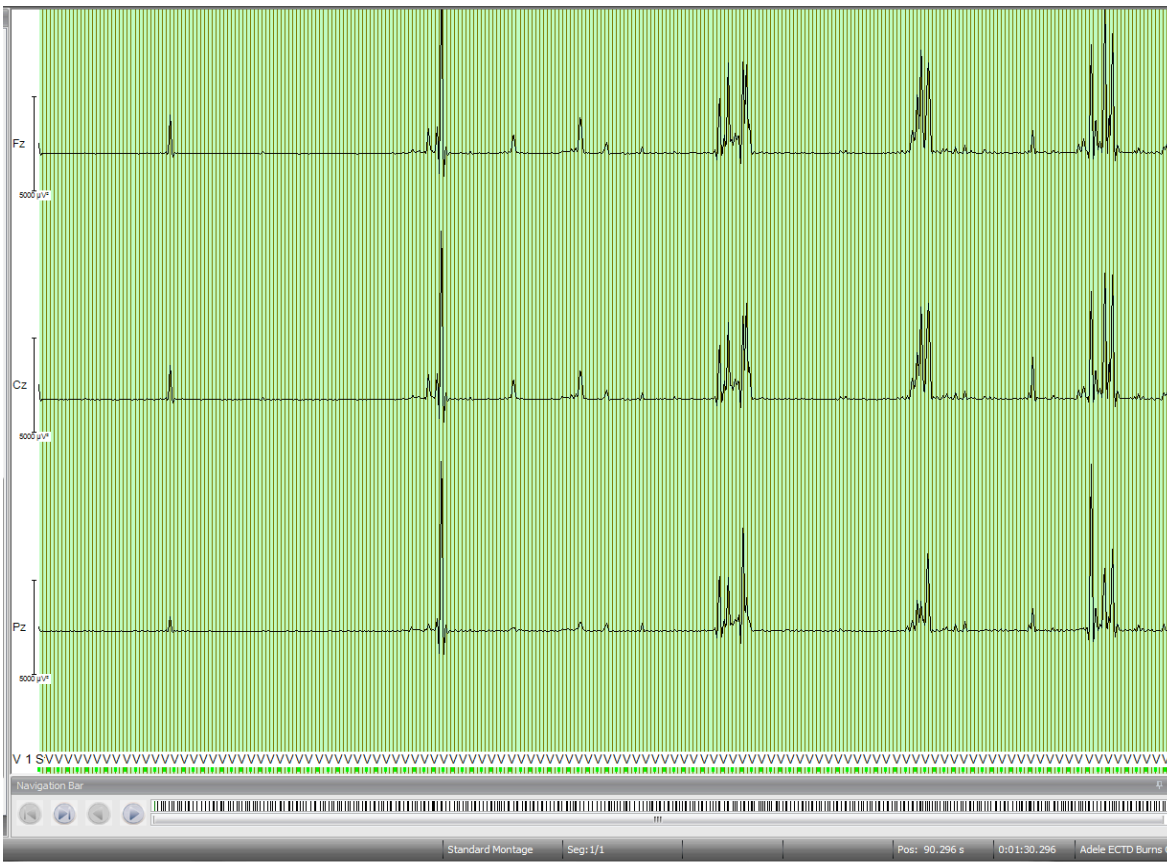

Figure A.3. Channels Fz, Cz and Pz following the application of 1Hz Butterworth Zero Phase Filter

APPENDIX B

CONN setup steps and information relating to experiment 1

This appendix outlines CONN related information for experiment 1, analysis 1: Resting-state functional connectivity and electrophysiological investigation of the Default Mode Network.

CONN: setup:

Basic Setup: Number of Subjects: 10
Repetition Time (seconds): 2.5
Number of sessions: 1

Functional: Functional Data Setup:
Subjects = 10
Sessions = 1 1 1 1 1 1 1 1 1 1
Select functional data files: 120 SPM preprocessed files for each subject were included.

Structural: The anatomical image set by default in conn was used (spm8\canonical\avg152T1.nii)

ROI: ROI mask .img files were loaded for each participant; these included grey matter, white matter and CSF. All files were coregistered to the normalized structural of the appropriate subject.

Condition: Condition name: Resting
Onset: 0
Duration: 310s

Covariates: N/A

Preprocessing:

GLM – Define possible confounds: Confounds included white matter, CSF and whole brain.

Preview Results: Results of BOLD % variance explained for each of confound for each subject was previewed before moving on to first-level ANALYSES.

First-level results: GLM connectivity sources (ROIs) were defined, bivariate correlations selected, Hrf within-conditions weights selected, and connectivity measures previewed before moving on to second-level results.

APPENDIX C

CONN setup steps and information relating to experiment 2, analysis 1

This appendix outlines CONN related information for experiment 2, analysis 1: Is DMN activity observed in an active auditory attention task designed to induce activity in the goal- and stimulus-driven attention networks?

CONN: setup:

Basic Setup: Number of Subjects: 9
Repetition Time (seconds): 2.5
Number of sessions: 1

Functional: Functional Data Setup:
Subjects = 9
Sessions = 1 1 1 1 1 1 1 1 1
Select functional data files: 336 SPM preprocessed files for each participant were included.

Structural: The anatomical image set by default in conn was used (spm8\canonical\avg152T1.nii)

ROI: ROI mask .img files were loaded for each participant; these included grey matter, white matter and CSF. All files were coregistered to the normalized structural of the appropriate participant.

Conditions: One condition was created in order to assess functional connectivity of the DMN across task duration (840s)
Condition name: default_auditory
Onset: 0
Duration: 840s

Covariates: N/A

Preprocessing:
GLM – Define possible confounds: Confounds included white matter, CSF and whole brain.

Preview Results: Results of BOLD % variance explained for each of confound for each participant was previewed before moving on to first-level ANALYSES.

First-level results: GLM connectivity sources (ROIs) were defined, bivariate correlations selected, Hrf within-conditions weights selected, and connectivity measures previewed before moving on to second-level results.

APPENDIX D

CONN setup steps and information relating to experiment 2, analysis 2b

This appendix outlines CONN related information for experiment 2, analysis 2b: Given that reaction times suggest that there is no change in DMN activity over time, there will be no significant change in functional connectivity of the DMN across conditions.

CONN setup:

Basic Setup: Number of Subjects: 9
Repetition Time (seconds): 2.5
Number of sessions: 1

Functional: Functional Data Setup:
Subjects = 9
Sessions = 1 1 1 1 1 1 1 1 1
Select functional data files: 336 SPM preprocessed files for each participant were included.

Structural: The anatomical image set by default in conn was used (spm8\canonical\avg152T1.nii)

ROI: ROI mask .img files were loaded for each participant; these included grey matter, white matter and CSF. All files were coregistered to the normalized structural of the appropriate participant.

Conditions: Three conditions were included in order to assess functional connectivity over the task duration:

Condition name: default_auditory1
Onset: 0
Duration: 280s
Condition name: default_auditory2
Onset: 280s
Duration: 280s
Condition name: default_auditory3
Onset: 560s
Duration: 280s

Covariates: N/A

Preprocessing:
GLM – Define possible confounds: Confounds included white matter, CSF and whole brain.

Preview Results: Results of BOLD % variance explained for each of confound for each participant was previewed before moving on to first-level ANALYSES.

First-level results: GLM connectivity sources (ROIs) were defined, bivariate correlations selected, Hrf within-conditions weights selected, and connectivity measures previewed before moving on to second-level results.

Second-level Results:
Between-conditions contrast: In between-contrasts window the following was entered:
-1 1 0: predicting default_auditory2 > default_auditory1
0 -1 1: predicting default_auditory 3 > default_auditory2
1 0 -1: predicting default_auditory 1 > default auditory3

APPENDIX E

CONN setup steps and information relating to experiment 3, analyses 1-4

This appendix outlines CONN related information for experiment 3, analyses 1-4: Functional connectivity of the attention reorienting, executive/frontoparietal control and salience networks, and their relationship to the default mode network.

CONN: setup:

Basic Setup: Number of Subjects: 9
Repetition Time (seconds): 2.5
Number of sessions: 1

Functional: Functional Data Setup:
Subjects = 9
Sessions = 1 1 1 1 1 1 1 1 1
Select functional data files: 336 SPM preprocessed files for each participant were included.

Structural: The anatomical image set by default in conn was used (spm8\canonical\avg152T1.nii)

ROI: ROI mask .img files were loaded for each participant; these included grey matter, white matter and CSF. All files were coregistered to the normalized structural of the appropriate participant.

Analysis 1: Functional connectivity of the goal-driven network (GDS) in an active auditory attention task

Conditions: One condition was created in order to assess functional connectivity of the dorsal frontoparietal network across task duration (840s). This also allowed for the exploration of the interaction between this network and DMN seed regions.

Condition name: auditory_GDN
Onset: 0
Duration: 840s

Analysis 2: Functional connectivity of the stimulus-driven network (SDN) in an active auditory attention task

Conditions: One condition was created in order to assess functional connectivity of the ventral frontoparietal network across task duration (840s). This also allowed for the exploration of the interaction between this network and DMN seed regions.
Condition name: auditory_SDN
Onset: 0
Duration: 840s

Analysis 3: Functional connectivity of the executive/frontoparietal control network (ECN) in an active auditory attention task
Conditions: One condition was created in order to assess functional connectivity of executive network over 840s. This also allowed for the exploration of the interaction between this network and DMN seed regions.
Condition name: auditory_executivecontrol
Onset: 0
Duration: 840s
Analysis 4: Functional connectivity of the salience network (SN) in an active auditory attention task
Conditions: One condition was created in order to assess functional connectivity of salience network over 840s. This also allowed for the exploration of the interaction between this network and DMN seed regions.
Condition name: auditory_salience
Onset: 0
Duration: 840s

Covariates: N/A

Preprocessing in CONN:
GLM – Define possible confounds: Confounds included white matter, CSF and whole brain.

Preview Results: Results of BOLD % variance explained for each of confound for each subject was previewed before moving on to first-level ANALYSES.

First-level results: GLM connectivity sources (ROIs) were defined, bivariate correlations selected, Hrf within-conditions weights selected, and connectivity measures previewed before moving on to second-level results.